# ASPECTS OF ANALYSIS AND PROCESSING OF ELECTROMYOGRAPHIC SIGNALS

# ASPECTS OF ANALYSIS AND PROCESSING OF ELECTROMYOGRAPHIC SIGNALS

by

HUIBREGT de BRUIN, B.Eng., M.Eng.

A Thesis

Submitted to the Faculty of Graduate Studies

in Partial Fulfilment of the Requirements

for the Degree

Doctor of Philosophy

McMaster University

July 1976

DOCTOR OF PHILOSOPHY (1976)
(Electrical Engineering)

MCMASTER UNIVERSITY
Hamilton, Ontario

| | | |
|---|---|---|
| TITLE | : | Aspects of Analysis and Processing of Electromyographic Signals |
| AUTHOR | : | Huibregt de Bruin, B.Eng. (McMaster University)<br>M.Eng. (McMaster University) |
| SUPERVISOR | : | Professor E. Della Torre |
| NUMBER OF PAGES | : | xiii, 231 |

## ABSTRACT

Skeletal muscles produce detectable electrical currents and voltages when they contract from any cause. The electrical potentials or electromyographic (EMG) signal is recorded from the muscle using suitable electrodes. The research presented in this thesis is concerned with the analysis and processing of electromyographic signals with a view to their use as a source of control for environmental control or other rehabilitation devices. An application of myo-electric control of a simple communication device for a cerebral palsied patient is presented. A model of the myo-electric source which can be used to simulate EMG signals in real-time is proposed. The model algorithm has been tested for two different electrode systems and the results compared with real signals recorded using these electrode systems. A number of statistical parameters of the surface recorded EMG signal have been examined to determine which parameter is most suitable for myo-electric control. Finally, a pattern recognition algorithm is proposed which attempts to extract the motor unit recruitment and discharge frequency information present in the surface recorded EMG signal. The statistical parameters and the algorithm have been tested for six normal subjects, under isometric conditions.

TO JOANNE AND TABITHA

## ACKNOWLEDGEMENTS

First and foremost I would like to express my gratitude to Dr. E. Della Torre for his encouragement and support during this work. My special thanks go to Dr. M. Milner for his helpful advice and discussions during the latter stages of the work.

I would like to thank Dr. N.K. Sinha and Dr. M.E. Brandstater for discussions concerning some of the aspects of this work. I would also like to thank my friends among the bioengineering graduate students for the many stimulating discussions.

Appreciation is expressed to the National Research Council of Canada and McMaster University for their financial support.

Finally, I am grateful to my wife, Joanne, who typed this manuscript, for her constant patience and encouragement during the course of the work.

TABLE OF CONTENTS

TABLE OF CONTENTS - continued

## LIST OF ILLUSTRATIONS

# CHAPTER 1

## INTRODUCTION

Toward the end of the eighteenth century Galvani discovered that skeletal muscles will contract when stimulated electrically and, conversely, that they produce detectable electrical currents or voltages when they contract from any cause. The latter phenomenon proved to be largely a scientific curiosity until the twentieth century when improved methods of detecting and recording minute electrical discharges became widely available. From the late 1920's on, neurophysiologists began to use the technique of recording and studying the electrical potentials produced by muscle - or electromyography - for clinical and diagnostic purposes to detect neuromuscular disorders. Toward the end of the Second World War, with the great improvement in electronic instrumentation, anatomists, kinesiologists and others began to make increasing use of electromyography in studying muscle function. Today, electromyography is a standard diagnostic technique and is widely used by researchers involved in the many aspects of normal and abnormal muscle function.

The electrical potentials or electromyographic (EMG) signal is recorded from the muscle using suitable electrodes. It has been well established that the amplitude of the electromyographic signal increases with increasing muscle force or tension. Consequently, in the last two

decades many researchers working in the area of rehabilitation have begun to use this signal as a control source for powered prosthetic and orthotic devices. Only amplitude parameters, mainly the mean absolute value, of the EMG signal are currently employed in these myo-electric control applications to detect muscle force. Other parameters of the EMG signal may give a more reliable estimate of the muscle force and also be less sensitive to measurement noise. Although much work has been accomplished in the design and fabrication of these rehabilitation devices, relatively little research has been carried out in the processing of electromyographic signals to extract suitable alternate force detection parameters.

The research presented in this thesis is concerned with the analysis and processing of electromyographic signals with a view to their use as a source of control for environmental control or other rehabilitation devices. An application of myo-electric control of a simple communication device for a cerebral palsied patient is presented. A model of the myo-electric source is proposed which can be used to simulate EMG signals in real-time. Finally, a number of parameters of the EMG signal are examined as possible detectors of muscle force under isometric conditions.

Chapter 2 describes a pilot study performed by the author to examine the feasibility of providing an EMG-controlled communication device for a severely-afflicted cerebral palsied patient. It also serves as an introduction to the myo-electric control of rehabilitation devices. An electromyographic trainer is described which can serve as a simple

communication device or as a device for training cerebral palsied patients to produce controlled electromyographic signals. Promising results have been obtained with the patient and indications are that the electromyographic signals from a minimally controllable muscle can serve as a control source for communication devices.

A knowledge of the basic structural and functional units in striated muscle is required in order to effectively use the electromyographic signal as an information source. Chapter 3 gives a review of the physiology and anatomy of skeletal muscle. The functional unit of the motor system, the motor unit, is described including some of the properties of its constituent muscle fibres. The recorded electromyographic signal is the temporal and spatial summation of the electrical activities of all those motor units located near the recording electrode(s). Emphasis is therefore placed on the electrical response of the muscle fibre, the fibre action potential, and on the recorded motor unit action potential. Part of the research presented in this thesis concerns the formulation of suitable EMG muscle force detection strategies. The mechanisms by which muscle tension can be increased or decreased during voluntary contraction : motor unit recruitment and changes in the discharge patterns of active units, are therefore also described. A brief description of some of the neuromuscular controls is also included.

The statistical characteristics of motor unit recruitment and discharge patterns make the theoretical determination of new EMG force detection strategies extremely difficult. A model of the myo-electric

source will aid in determining relevant parameters used in new detection strategies. Analysis of such a model may also facilitate an understanding of the physiological system involved. In addition, a model which can simulate EMG signals in real-time under operator control can be used to quickly test different computer-implemented detection strategies or hardware detectors. Chapter 4 describes such a model which is based on the motor unit and its recorded action potential. The model algorithm can be used to simulate electromyographic signals recorded from different electrode configurations. The algorithm has been tested for two different electrode systems, pasteless surface electrodes and coaxial needle electrodes, and the results compared with real signals recorded using these electrodes. There is good agreement between simulated and real signal autocorrelation and power spectral density plots especially for surface recorded signals, but analysis of these plots points out the necessity of a more force-sensitive comparison criterion.

The surface recorded EMG signal contains both amplitude and frequency information. Alternate force detection strategies may therefore involve amplitude parameters, spectral parameters or a combination of both. Chapter 5 describes a number of parameters of the EMG signal which may be used to provide suitable force detection strategies. Since the EMG signal is the result of a stochastic process, some of the statistical functions of the signal can be examined as possible suitable parameters. In addition to the commonly used mean absolute value, the chapter also considers other statistical functions such as higher-order moments, the autocorrelation function, and the power spectral density of

the raw EMG signal. Possible hardware or software implementations of the force detector based on each parameter are also described. Finally, a detection strategy using simple pattern recognition is presented which attempts to extract the motor unit recruitment and discharge frequency information present in surface recorded EMG signals.

The computation algorithms for the different EMG parameters or force detection strategies described in Chapter 5 can be implemented on a minicomputer. The surface recorded EMG signal parameters or detector responses can then be calculated for a range of constant isometric contractions of a selected muscle. Chapter 6 presents the results of these calculations for a range of low to moderate contractions of the biceps brachii of six normal adult male subjects. Each parameter or detector is evaluated according to its sensitivity to the force range in question and the reliability of its estimate of each force level. The results show that the autocorrelation and power spectral density of surface EMG signals cannot be used as indicators of muscle force. In addition, the mean absolute value and the r.m.s. value of the signal are virtually equivalent for this range of contractions, and all amplitude parameters considered are equally effective as muscle force detectors. The pattern recognition algorithm provides equivalent results to the amplitude detectors using the same algorithm parameters for each subject. Better results can therefore be achieved for the algorithm by matching its parameters to each subject tested.

Finally, the conclusions drawn from the research presented in

this thesis are stated in greater detail in Chapter 7. Recommendations for further research are also included in this chapter.

# CHAPTER 2

# AN ELECTROMYOGRAPHIC TRAINER FOR A CEREBRAL PALSIED PATIENT

## 2.0 Introduction

As stated in Chapter 1, the research presented in this thesis is concerned with the processing and analysis of electromyographic signals with a view to their use as a source of control for environmental control or other rehabilitation devices. Before advancing to this research, it was first necessary to gain some clinical experience and a greater understanding of some of the problems involved in using these signals in this context. A pilot study was therefore performed by the author to examine the feasibility of providing an EMG-controlled electronic communication device for a severely-afflicted cerebral palsied teenager. This young male, who was confined to a wheelchair, lacked an effective means of communication. Due to the severity of his affliction he possessed no means of verbal communication. In addition, the communication aids available at the Cerebral Palsy Centre at Chedoke Hospitals, Hamilton, where he was being trained, and those available commercially were inadequate for his case since their activation required much greater muscular control than he was capable of. This study would therefore not only provide the needed practical experience but might also produce a useful rehabilitation aid.

This chapter describes an electromyographic trainer which can

serve as a communication device or as a device for training cerebral palsied patients to produce controlled electromyographic signals. Test results are presented and a number of possible improvements to the basic device suggested.

### 2.0.1 Capabilities of the Patient

The patient in question was severely disabled with cerebral palsy. It was difficult to assess the mental status of the patient, but subjective impressions of the staff, reinforced by clinical observations, indicated that he was attentive, alert, orientated and cooperative in all aspects of the study. Although his comprehension of verbal speech and visual displays was good, he was incapable of verbal speech and was only able to signify "yes" or "no" by gross, poorly coordinated movements which often were difficult to interpret.

As regards motor skills, the patient was spastic and athetoid. In attempting any movement, his performance was severely compromised by a profusion of unwanted activity which interfered with the task performance. From clinical observations, his best control was flexion of the right elbow, and therefore this was selected as the most likely trainable movement. However, even this task was poorly controlled and subject to frequent overshoot.

The first phase of the project should perhaps have been a thorough study of the patient to determine if there existed muscles other than the biceps brachii of the right arm, which were minimally control-

lable at low or very low force levels. This study would involve training periods conducted by physiotherapists, of potentially controllable muscles. However, such a study was not undertaken since considerable time and personnel resources could be spent without finding a suitable alternate source. Since the patient exhibited some control over the above-mentioned biceps brachii, it was decided to use the action of this muscle as the control input to the communication device.

Although the patient could track well with his eyes, it was decided not to use an optically-activated device such as a NASA Sight Switch (NASA) to provide the control input signals. Since the communication device would include a display such as selected lights or messages, it was felt that using eye position as a control would severely restrict his visual feedback and hamper his concentration during generation of a message.

### 2.0.2 Design Criteria for the Communication Device

A communication device, or more generally, an environmental control device can be separated into several functional blocks as shown in Fig. 2.1. For this particular patient the controllable source will be the biceps brachii and only a display system will be implemented.

The design criteria for the communication device fall into two categories. The first category includes those concerned with general equipment design such as those relating to patient safety, the selection of a suitable display system, portability of the device, ease of handling and adjustment by therapists, and finally, cost. The second category includes those criteria relating to the control input from the

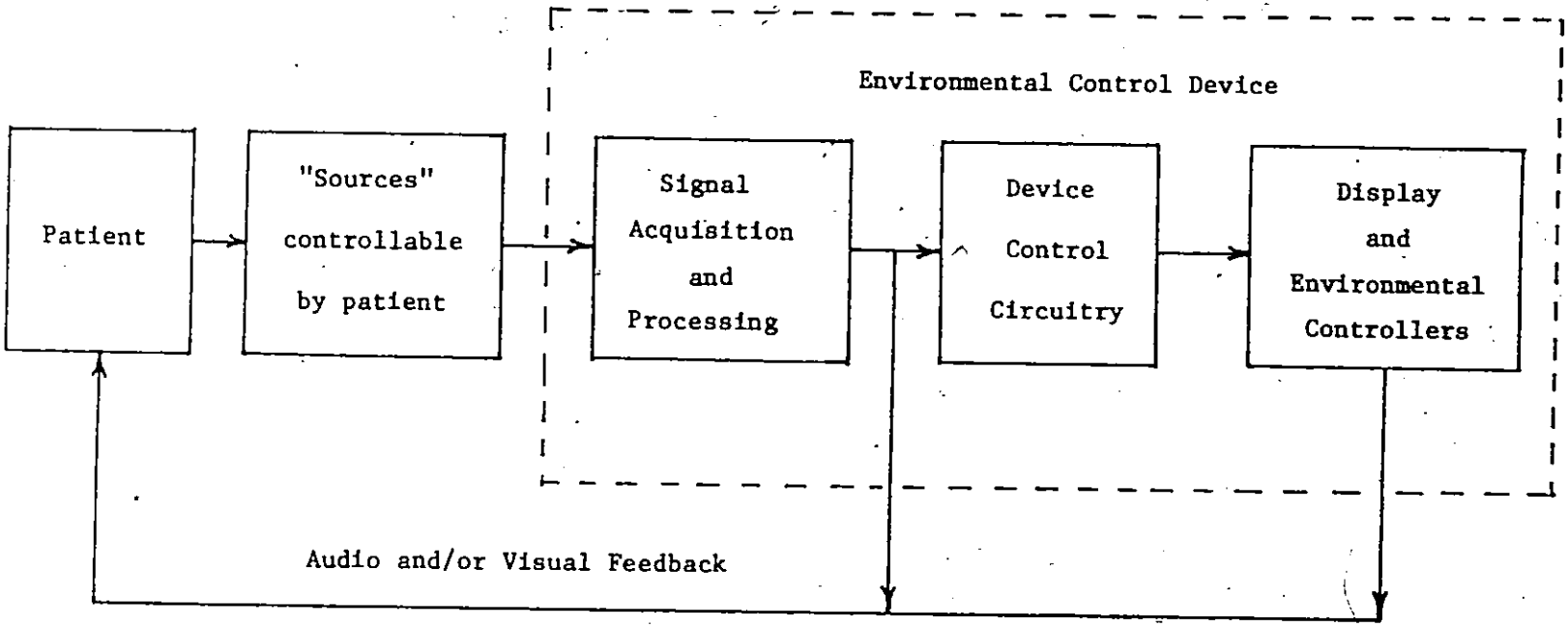


Figure 2.1 The General Environmental Control System

patient such as force levels to be considered, minimization of errors due to spasms and poor control and patient comfort and effort required to generate a control decision. The following is a description of some of the above-mentioned design requirements.

## A Patient Safety

There should be no possibility of electric shock to the patient from electronic circuitry or any connected electric display system. The biological effects of electricity are primarily a function of the current - not the voltage - applied. For this particular prosthetic application only macroshock or the shocks due to surface electrodes or contact need be considered. The accepted maximum harmless current intensity is 5 ma. if applied at the surface for a maximum period of 1 second (Friedlander, 1971). However, even low current intensities will produce burns or blisters if contact is maintained for longer periods.

Electric shock hazards can be reduced if any electrodes or electrically driven sensors connected to, or near the patient's skin, are isolated from both the power line and ground, and low supply voltages are used wherever possible. All electrodes should be situated so that the heart region is not included in any possible current path. Since the skin/electrode impedance determines the impedance of any current path, it should be kept as high as possible from a safety point of view. If the device is battery-operated with low supply voltages (e.g. $\pm$10 V), most of the electrical hazards will be eliminated even for low impedance (2 kohm.) paste surface electrodes. Finally, if the device is to be located near the patient (i.e. on his wheelchair table), it should be en-

capsulated in a non-conducting box with rounded edges to avoid injury due to sudden uncontrolled movements of his limbs.

B The Display System

The final display system could include any of the following: an electronically controlled typewriter, a display of messages which will light up when selected, other indicator lights and buzzers or tone generators. An initial training display of indicator lights and buzzers would provide auditory and visual feedback to the patient and serve as a simple message generator. The device control circuitry must therefore be able to supply "error-free" discrete-level input signals to the selected display system using binary or other multi-level codes. These signals, when decoded, will determine the state of the display system. Finally, due to the mental and physical limitations of the teenager, all displays should be relatively simple, large and well-positioned for ease of viewing.

C Portability of the Device

Ideally, the device should be battery-operated and small enough to mount on the patient's wheelchair with the display system fixed to the wheelchair table. In addition to being electrically safer, it would then also be completely portable and independent of the availability of wall outlets. Using rechargeable batteries would lower long-term operating costs. The requirement that the device be portable does not limit its complexity. Very complex processing and control circuits can be physically quite small due to the sophistication of modern electronic

circuits (e.g. microprocessor). However, complex circuits may require more power necessitating larger batteries or having part of the circuit powered from the line voltage.

D Device Adjustments and Interfacing

Controls requiring skilled adjustment should be kept to a minimum and any sensors should be easily applied to the patient. If interfacing the patient to the device and initial adjustments are too lengthy or complicated, therapists will be unwilling to use it. Therefore, the device must be made as reliable and simple as possible from the therapist's point of view.

E Patient Force Level and Movement Constraints

Cerebral Palsy is a disease which causes loss of inhibitory inputs to the lower motoneurons, resulting in "underdamped or positive feedback" from the proprioceptive receptors of the muscle - hence a sensory loss of movement. Neuromuscular control and some aspects of cerebral palsy are more fully described in Section 3.7. To minimize uncontrolled contractions resulting from proprioceptive afferents, only low level forces should be considered and the forearm should be restrained so that the biceps contracts isometrically. If different levels of force are to be used as control inputs, they must be sufficiently separated so that the patient can generate them with minimum error. These force levels should also be kept as low as possible to avoid fatigue since the communication device will be used continually by the patient. Although only isometric contractions are to be used, the arm

should not be fixed so rigidly as to cause the patient long term discomfort.

F Minimization of Control Errors

For this individual it is impossible to avoid sudden spasms during a contraction-relaxation cycle or during periods of relaxation. The device control circuitry should therefore be able to accommodate these spasms without changing the state of the display system. It is envisaged that after a period of training, the controllability of the patient's biceps will improve. This will allow either a decreased control decision time (an increased information rate) and/or a decrease in the effort required per decision. The processing and control circuitry should therefore be sufficiently flexible to allow minimization of both decision effort and time concurrent with a reasonable error rate. However, as in most real systems, a compromise will have to be made between information rate and error rate.

## 2.1 Myo-Electric Control of Rehabilitation Devices

### 2.1.1 Existing Communication Aids for Cerebral Palsied Patients

By 1971 (when the project was initiated) several communication devices for cerebral palsied children had been implemented and were available. The least expensive devices were simple message boards through which the child could communicate by pointing to the appropriate message or alphanumeric characters. In order to facilitate more rapid responses, a variety of pointing aids can be fitted as dictated by each

child's capabilities. If the child has insufficient control of an extremity, a light beam mounted on his forehead can be used to illuminate the selected response (Micheelsen, 1966). Micheelsen (1966) has developed an electric typewriter with a specially designed large, separate keyboard which can be activated by a pointer attached to the forehead or any controllable extremity. Another example of a more complex system is the POSSUM device developed in England, which consists of a controllable illuminated alphanumeric display coupled to an electric typewriter. By operating a single suitable patient interface such as a control lever, a "suck and blow" tube, or a microswitch, any character can be illuminated and typed.

In order to use any of these devices (with the exception of the "suck and blow" activated POSSUM device), the user must have sufficient motor control of an extremity. Unfortunately, the patient in question did not have the necessary control as outlined in Section 2.0.1. Although a microswitch interface requires little effort and movement, spasms will cause too many errors. Even if a large control lever were used to accommodate spasms, the time and effort required to move it would prohibit a reasonable information rate. Using Bliss symbols for cerebral palsied patients (Ontario Crippled Children's Centre, 1974) rather than alphanumeric characters would increase this rate. Even though communication devices are commercially available, the more complex devices are very expensive and the patient interfaces (signal acquisition and control block of Fig. 2.1) were considered unsuitable for this patient.

### 2.1.2 Selection of the Patient Interface

The selection of the input signals or patient interface is the most important decision in the design of the communication device. If one considers the constraints outlined in Section 2.0.2, only a few interfaces can be considered which depend on low force levels and little limb movement. As mentioned above, microswitches are unsuitable because the frequent uncontrolled spasms would trigger the switch and cause errors. The signals from strain gauges or other force transducers could be processed to remove the effects of these spasms. However, using such transducers requires careful calibration and once a limb position is chosen, it cannot be easily changed without providing new mechanical linkages. This approach was rejected because the most comfortable (and most controllable) position had not yet been determined and may change from day to day. It was therefore decided not to use a mechanical or electromechanical interface.

The novel approach of using muscle electrical impedance as a control source has been suggested by Kadefors and Olson (1972). However, if the contraction is constrained to being isometric, the geometry changes very little and the variation in impedance is very small. The results reported by Nirenberg et al. (1971), of using motor artifacts in the EEG as a prosthetic control source show that this method is unreliable.

A possible input signal which requires neither limb movement nor an electromechanical interface with the patient is the electromyographic signal (E.M.G.) of the controllable muscle. The EMG signal, as indicated by its name, is the temporal and spatial summation of the electrical

activity of the muscle or part of the muscle. Since the amplitude of the EMG signal increases as the contraction of the muscle increases, it can be used as a control signal. The electrical activity of the muscle and its relation to contraction levels is more fully described in Chapter 3. By using suitable electrodes positioned over the selected muscle, this signal can be recorded and processed to provide the input to the device control circuitry of Fig. 2.1. With proper design of the acquisition and processing circuits, changes in limb position and spasms can be accommodated. It was therefore decided to use the EMG signal of the right biceps brachii as the input signal.

### 2.1.3 Electromyographic Signals used as a Control Source

A wide-ranging literature search failed to reveal any previous applications of EMG signals for environmental control for cerebral palsy victims. The only applications of EMG signals in this context were for clinical and research diagnostic procedures (for example: Ashby and Burke, 1971; Burke et al., 1972). However, extensive research has been carried out in various research centres around the world (for example: Bottomley et al., 1963; Vodovnik et al., 1965; Furnée and Wijnschenk, 1968; Kadefors, 1970; Long, 1970; Bousso and Ishai, 1969; Scott [Principal Author], 1969-1971; Dorcas et al., 1970; and Horn, 1972) on the use of EMG signals for communication purposes and to control powered prostheses and orthoses for amputees, quadriplegics, paraplegics, Thalidomide victims, etc. With the exception of the controller proposed by Horn (1972), these all rely on amplitude discrimination of the rectified and filtered EMG signal for "on-off" , or, sometimes, multi-level control purposes. Horn

(1972) uses the rise of the raw EMG above a threshold to trigger the control, but this method is completely unsuitable for cerebral palsy applications since any spasm, however brief, would generate a control decision. Other researchers (for example: Basmajian, 1974; Scott [Principal Author], 1969-1971; Milner et al., 1969-1970 ; and Magnusson and Petersén, 1971) have used EMG signals to study muscle function and for gait analysis. The above references are only a sample of the numerous papers dealing with the prosthetic and orthotic control applications of EMG which have appeared in the last decade.

The most successful applications of EMG control appear to be in providing prostheses for amputees. Varying degrees of success with these devices are reported ranging from success [e.g. lower arm prostheses (Scott [Principal Author], 1969-1971) and forequarter prosthesis (Dorcas et al., 1970)], to failure [long term acceptance of complicated upper arm prostheses (Long, 1970)]. Reasonable facility and versatility have been obtained in the majority of cases, especially when normal functional muscle groups can be used as EMG sources.

It is generally accepted that there is a rough inverse relationship between the degree of complexity of a prosthetic/orthotic device (measured by the length of time required for a user to master its operation) and its long term acceptance (Long, 1970; NASA, 1970). From studies carried out with normal and quadriplegic subjects, Long (1970) concludes it is not practicable to utilize more than two EMG sources concurrently in any control application. However, Basmajian (1974) reports considerable success in training subjects to isolate an individual motor unit (basic functional unit of the motor system -see Section 3.1) and

vary its rate of firing at will. He reports that with proper auditory or visual feedback, most subjects can isolate one or two units readily while some can master even six or more in the same muscle. These results indicate that with suitable biofeedback during training, sufficient neuromuscular control may be readily achieved, to adequately control more complex prosthetic/orthotic devices.

In the case of cerebral palsy, it is anticipated that nowhere near the same degree of success will be achieved, due to the complicating presence of spasticity, rigidity and athetosis. However, even a reliable, relatively fast "on-off" switch will be a considerable improvement over existing patient interfaces.

### 2.1.4 Selection of the Electrode System

To record EMG signals, percutaneous or intramuscular (needle or wire) electrodes, surface electrodes or implanted biotelemetry units (Scott [Principal Author], 1969-1971; Fryer, 1970; Herberts et al., 1970) could be used. Percutaneous electrodes are used widely for short-term experimental or clinical purposes. However, they are unsuitable for long-term use in myo-electric control systems because of possible inflammation and electrode migration during movement. In addition, the pain resulting from the insertion process makes them unattractive for daily use on cerebral palsied children. The processing circuit would also have to be recalibrated after each insertion of the electrodes. Finally, if percutaneous rather than surface electrodes are used, there is a greater risk of tissue damage or severe shock resulting from high current densities in the event of electrical malfunction.

Surface electrodes are suitable for measuring the gross myoelectric activity of large superficial muscles and are widely used in myo-electric control systems. With most high-performance electrodes, an electrolytic paste or gel is required to establish contact between the electrode and the skin. To avoid skin problems during chronic use, skin preparation should be minimal and the paste should not be irritating. However, problems such as movement artifacts (voltage errors caused by electrode movement on the skin or relative to the underlying muscle), large common mode interference signals (especially when electrode impedances become unbalanced due to electrolyte degeneration or an electrode coming loose), a low amount of high frequency power in the EMG power spectrum, and crosstalk from other muscles all result from the use of surface electrodes. Biocompatible transdermal electrodes (vitreous carbon implants) and biotelemetry implants which are under investigation at several centres avoid most of these problems. Although they cannot be considered for this project, these electrodes may eventually be the most suitable ones for long-term use in these applications.

Surface electrodes with paste were chosen for the patient interface because of their ease of application, low electrode impedance and the fact that the position and size of the biceps brachii reduces the possibility of crosstalk from other active muscles of the upper arm.

## 2.2 A Preliminary Electromyographic Trainer

An inexpensive electromyographic trainer was designed and constructed by the author to serve as both a training unit and initial com-

munication device. The EMG processing strategy used for this preliminary trainer consists of full-wave rectification followed by a smoothing filter. This strategy was used because it is most widely accepted for myo-electric control systems (see Section 2.1.3). The control circuit following this processor consists of two parallel voltage threshold detectors which generate "on-off" control signals for the display system. Improvements to this preliminary design would probably be suggested by the results of laboratory and clinical tests of the trainer.

In order to avoid a lengthy design and debugging phase, it was decided to use integrated circuits wherever possible in the electronic circuitry. Nickel-cadmium batteries were chosen for the trainer power supply. A battery charger was therefore constructed to allow recharging by any clinical personnel. The first trainer unit employed two LED's as display so that the entire system could be enclosed in one small box located on the wheelchair table. However, in addition to being positioned too close to the patient, these early LED's (1971) were not bright enough or large enough for easy viewing by the patient. A separate display system was therefore constructed using a buzzer and jewelled lights and powered from the line voltage. The hardware system is shown in Fig. 2.2. A complete description of the electromyographic trainer including the performance characteristics of its differential amplifier are given in Appendix A.

The signal electrodes shown in Fig. 2.2 are Rochester Medical 6 mm. pure tin discs and are placed longitudinally over the belly of the biceps brachii using elastic tape and Ingram & Bell Cardio-Cream electrolytic paste. The reference electrode is a 2.5 x 3.8 cm. lead plate

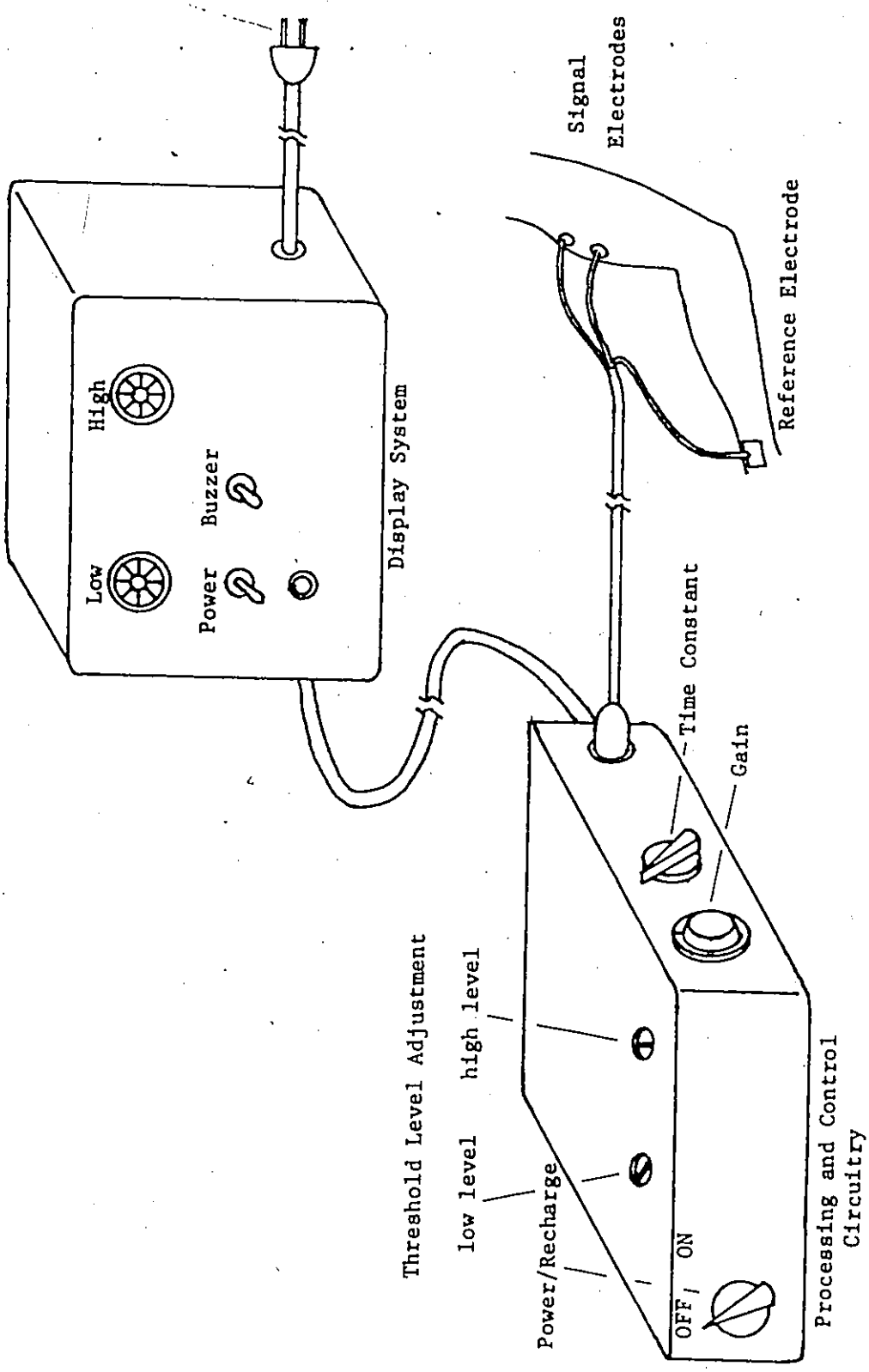


Figure 2.2 The Electromyographic Trainer

and is applied with paste and tape on the wrist. These electrodes and paste were chosen because of their ready availability from Chedoke Hospitals, and the fact that the small discs being more selective than large ones, will record less crosstalk from other muscles.

### 2.2.1 Performance Characteristics of the Trainer

As stated in Appendix A, the differential amplifier input impedance, bandwidth, and common mode rejection ratio meet the requirements of surface recorded EMG signals. The trainer was also tested by normal subjects to determine suitable averaging time constants and evaluate its performance as a display controller. The range of suitable time constants is naturally dependent on the muscle (and its normal anatomical function) used as a control source and the contraction levels required from that muscle. Larger muscles used in the movement of large limb segments such as the biceps brachii cannot be voluntarily contracted and relaxed as quickly, without additional training, as smaller muscles such as the abductor pollicis brevis. The minimum period required for a strong contraction-relaxation cycle also seems longer than that for low to moderate contraction-relaxation cycles. The averaging time constant should therefore be increased for large muscles and higher contraction levels. The time constants of .25, .6 and 1.2 seconds were found to be a suitable range for weak to moderate contractions of the biceps brachii.

Harvard Apparatus #321 silver disc electrodes were used in the trainer tests rather than the electrodes mentioned above because their adhesive collars facilitated attachment over different muscles. Figure 2.3 shows the response of the control circuit to moderate contractions

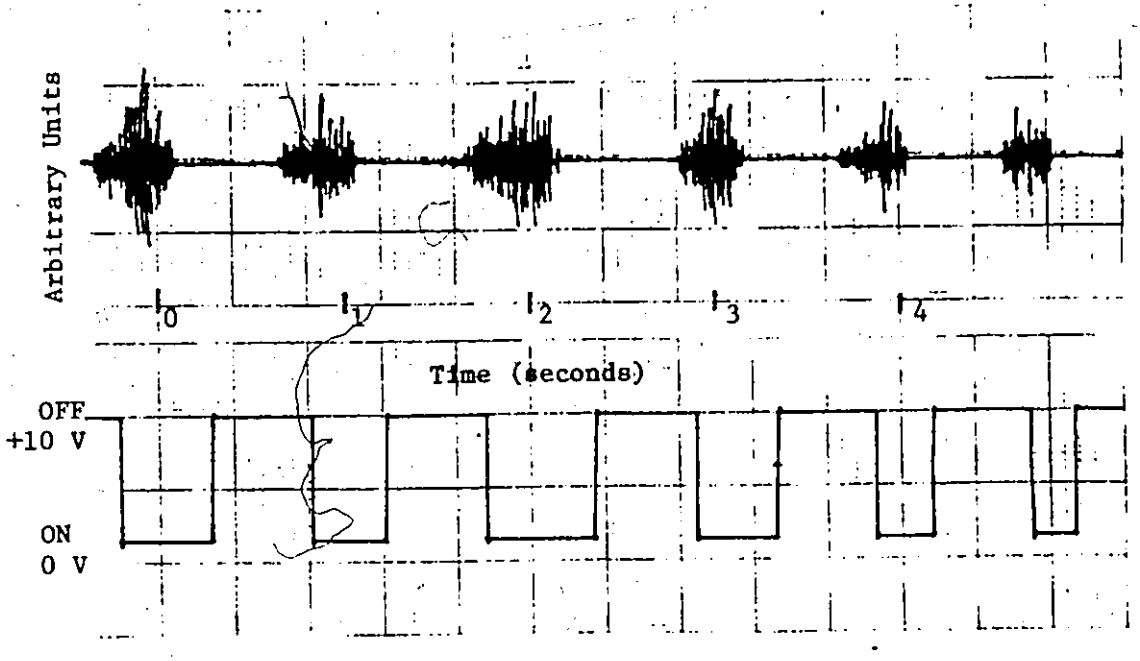


(a) Averaging Time Constant = 1.2 sec.

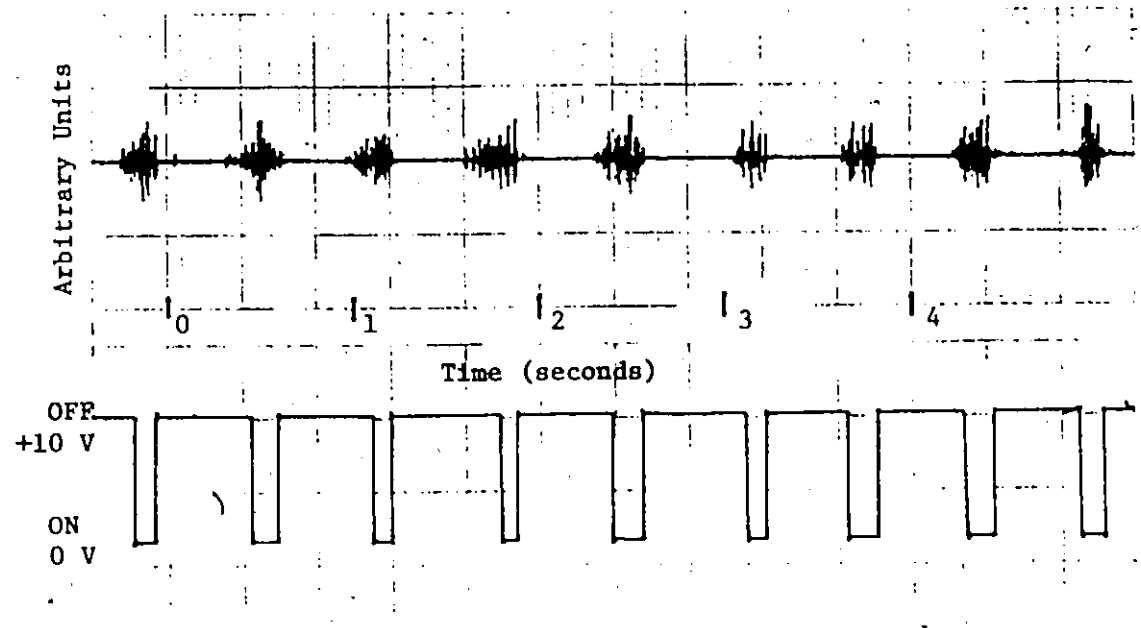


(b) Averaging Time Constant = .25 sec.

Figure 2.3 Response of the Control Circuit to Contractions of the Biceps Brachii

of the biceps for .25 and 1.2 second time constants. The control signal is that appearing at the collector of the switching transistor shown in Fig. A.2. A Watanabe 2-channel strip chart recorder was used to generate these displays. Although it is a pen recorder, it has sufficient bandwidth to display the EMG activity since it can reproduce 80 Hz full-deflection sine waves. As can be seen, the delay between initiation of EMG activity and a change of state of the control signal is longer for the 1.2 sec. time constant - hence requiring more effort to control the display. The shortest time constant should therefore be used whenever possible.

Figure 2.4 shows the response of the trainer to moderate contractions of the flexor carpi radialis of a normal volunteer for a .25 second time constant. As can be seen, this time constant is suitable for detecting rapid contractions of this muscle and the trainer generates up to 6 control pulses per second in this test. Since such rapid contraction rates would not be used for communication purposes, a .25 second averaging time constant is a suitable minimum for normal subjects. The trainer performed well as a display control for the three normal subjects tested.

## 2.3 Clinical Testing of the Trainer

The electromyographic trainer was tested as a communication device for the cerebral palsied patient. He was trained in its control during a number of clinical sessions conducted first by the author, and later by therapists at the Cerebral Palsy Centre. It was found that lightly restraining the forearm at the wrist by a cloth sling provided

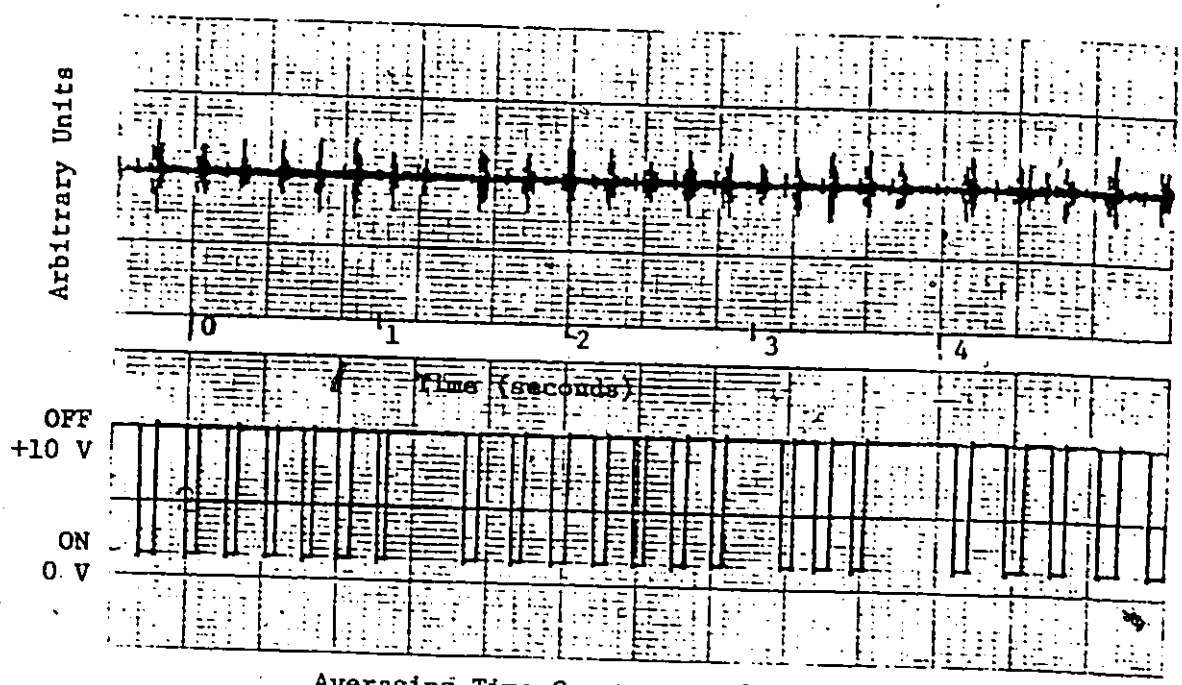


Figure 2.4 Response of the Control Circuit to Contractions of the Flexor Carpi Radialis

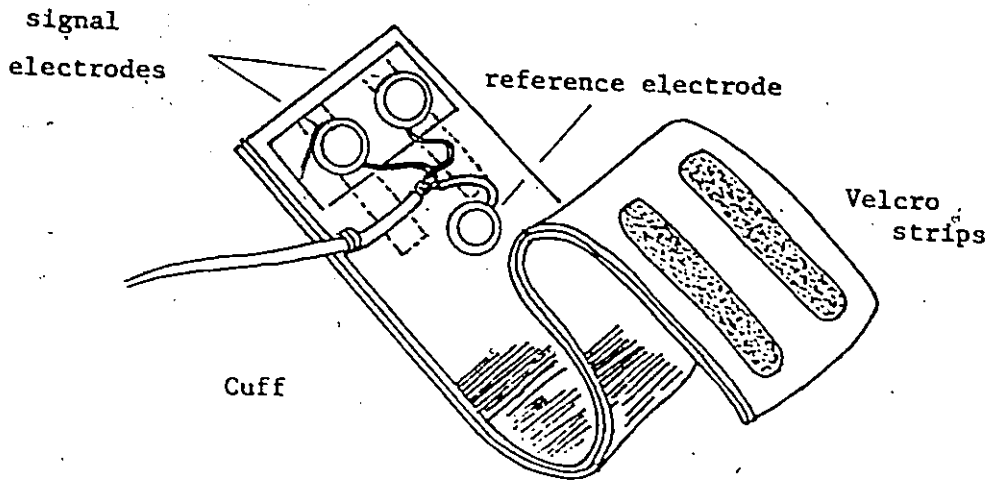


Figure 2.5 A Dry Electrode System

sufficient immobilization and also tactile sensory feedback. A rigid total arm splint with a 90 degree elbow angle, made of the thermoplastic Sansplint, was also used. However, no improvement in control could be detected and the splint was consequently rejected because its use increased patient discomfort.

Within two or three sessions, the patient demonstrated some control of the device and by the end of the author's sessions, could turn the low level light on and off up to six times successively without error. As expected, the best results were achieved when the patient was relaxed, allowing the threshold level to be adjusted as low as possible - hence requiring only light contractions to control the device. The patient had no difficulty in initiating a contraction but even when generally relaxed, experienced spasms when trying to relax the muscle. When only light contractions were used, these spasms were minimized and consequently the contraction-relaxation period during successive "on-off" cycles of the light was as brief as 2 to 3 seconds. The 1.2 second averaging time constant was found to be most suitable since shorter time constants resulted in errors caused by spasms and poor control even when the patient was relaxed. He could sometimes control two levels but this occurred only under the best conditions and the two levels set for light and medium contractions. However, the medium contraction required a longer relaxation period and resulted in stronger spasms which could cause errors in the low level control signal.

Problems Encountered during Training Sessions

Although the patient was well-motivated at first; there was con-

siderable day-to-day variability in his concentration and control. In order to be sufficiently relaxed he had to be isolated from all distractions since any disturbance excited him, resulting in a subsequent loss of control. Even when relaxed, his short attention span and perhaps fatigue, limited training sessions to a maximum of 15 minutes. The threshold level usually had to be adjusted several times during a training session to accommodate periods of rigidity and incomplete relaxation. That is, during these periods the level had to be set so that only a small additional voluntary contraction would turn the light on. As a result of these problems, considerable patience and constant encouragement were required during each training session. Finally, once the boy became successful in controlling the light, he lost interest and showed little improvement after that. A series of display systems (of increasing complexity) should therefore be used in order to provide sufficient stimulation for later training sessions.

The small electrode used, tended to move and eventually lose contact because of the electrode paste working into the adhesive. In addition, the therapists found the combination of gain and threshold level adjustments required for minimum contraction levels, too complicated. The hysteresis offset, although partially determined by the threshold level itself, was too large for very low levels resulting in an inability to turn the light off once it had been turned on.

### 2.3.1 The Use of Auditory Feedback

The buzzer was found to be useful in providing auditory feedback and also an additional stimulus during training sessions. However, it

is only activated when a threshold level is crossed and provides no information about interlevel activity.

An auditory feedback which provides continuous information about the contraction level would be most useful in training in the control of a muscle. The output of the averager (Block B of Fig. A.1) was connected to a voltage controlled oscillator which provided an audio signal to a loudspeaker. The result is a tone whose pitch rises or falls as the contraction level increases or decreases. This audio feedback was tested for normal subjects and found to be a much better indicator of contraction level than raw EMG fed to a loudspeaker. It can indicate the full range of contractions by adjusting the sensitivity of the VCO. By increasing the sensitivity, the audio signal becomes a very effective indicator of variations in low-level contractions.

This method of feedback seems well suited to the training of cerebral palsied patients in the control of light contractions and hence in the control of the communication device. It may also be useful to therapists involved in the general area of muscle training and especially in the training of muscle relaxation.

## 2.4 Suggested Improvements to the EMG Trainer

In addition to the above-mentioned VCO derived audio feedback, other improvements can be made to the trainer to eliminate some of the problems mentioned in Section 2.3.

Since the patient can initiate a contraction quickly but has difficulty in relaxing without attendant spasms, the control circuit should be "locked out" for a short time (i.e. 1 sec.) once the average

has first decreased below threshold. That is, once the control signal ($E_{ci}$ of Figures A.1 and A.2) has turned off (0 volts) it stays off for the set period regardless of the amplitude of the EMG average. The control circuit would therefore be immune to spasms generated during attempted relaxation of the muscle. This noise immunity could be provided by having the output of a monostable multivibrator which is triggered by the negative slope of the control signal, add a large offset to the threshold level.

Although the hysteresis offset is determined partially by the threshold level itself, it should also be made externally adjustable by replacing one of the hysteresis loop resistors by a potentiometer. A technician could then set the offset during initial adjustment to a value determined by the anticipated range of amplitudes of the EMG average. Once the control signal is turned on, the threshold offset should be zeroed after a set time (i.e. .2 sec.) so that the threshold level is the same for "turn on" and "turn off". This can be accomplished by again having the output of a monostable multivibrator, which is triggered by the positive slope of the control signal, provide the negative offset rather than the circuit shown in Figure A.1. The positive offset would be supplied by the above "lock-out" circuit.

The display system can also be expanded so that the trainer can become a useful communication device. Existing commercial display systems can also be connected to the trainer processing and control circuits through appropriate interfacing.

### 2.4.1 A Dry Electrode System

As mentioned in Section 2.3, the wet or paste electrodes used were found to be unsuitable for prolonged use because of i) method of application and ii) eventual loosening and loss of contact. Although application of the paste and electrodes is relatively easy, even with minimal skin preparation (alcohol swab) the process becomes tedious if it has to be repeated several times a day. This occurs when a number of training periods are required in a day and the electrodes have to be removed between sessions. Once the patient is trained to use the communication device, he will be using it constantly, requiring the electrodes to remain affixed for long periods of time. The long-term effect of even a mild electrode paste on the skin could be tissue breakdown and irritation. An electrode system is therefore required which can be quickly applied, has no harmful long-term skin effects, and keeps the electrodes in place and in contact over long periods of time.

A dry electrode system which meets these requirements was constructed by the author. This system, which is shown in Figure 2.5, is based on the dry electrodes used for electro-oculography by Geddes et al. (1973). The electrodes employed consist of coin-silver discs (silver dimes ground smooth on one side, 1.7 cm. diameter) and they are connected to the amplifier by a two-wire flexible shielded cable. The signal electrodes are spaced 3.5 cm. centre to centre apart and the reference electrode is connected to the shield. The electrode assembly is mounted on a cuff made of a stretch jersey-knit material. This cuff can be quickly fastened about the upper arm by overlapping sewn-on Velcro strips. Although the cuff fastening arrangement allows for a range of

adult arm diameters, it is too large to be used for children. A scaled down version (including smaller electrodes) would have to be made for cerebral palsied children applications.

The cuff has been tested on a number of normal subjects and found to be comfortable over the entire range of contractions. The cuff material is sufficiently flexible to accommodate changes in muscle geometry during contraction without constriction and the electrodes are always kept in contact with the skin.

Dry electrodes depend on perspiration under the electrode to lower the electrode impedance. The impedance of a dry electrode placed on dry human skin, decreases exponentially with the passage of time and stabilizes to a minimum value after a certain time interval. Geddes et al. (1973) have measured the impedance of this size electrode and found it to decrease within 10 minutes from an initial high of 1.4 MΩ to a stabilized minimum of 100 KΩ. In our tests it was found to be stabilized within approximately 5 to 10 minutes, depending on the subject's skin properties. For best results, the cuff should be applied to the arm approximately 10 minutes before connecting it to the amplifier.

Since these are high impedance electrodes (100 KΩ), they cannot be connected directly to the differential amplifier of Fig. A.1 which has a minimum input impedance of 300 KΩ. To test the electrode system, a PAR 113 preamplifier was used which has a 100MΩ input impedance. In addition, cable movement artifact had to be removed by high-pass filtering the signal (3 Hz 3 db. point). In order to use the dry electrode system with the trainer, the input stage operational amplifiers of the differential amplifier would have to be replaced by a junction field

effect transistor (J.F.E.T.) operational amplifier which has a moderately high input impedance, and a band-pass filter added. However, the band-pass filter can be avoided by mounting the J.F.E.T. operational amplifier directly on the cuff - thus eliminating cable movement artifact entirely. Since inexpensive J.F.E.T. operational amplifiers are now available, this circuit change will add little to the overall cost of the device.

## 2.5 Summary

A simple communication device, which uses the electromyographic signal from a selected muscle as control input, has been designed and constructed. This device has been tested for both normal subjects and a cerebral palsied patient. Normal subjects can control the device with little effort after a short training period. Very promising results have been obtained with the cerebral palsied teenager and indications are that the electromyographic signal from a minimally controllable muscle can serve as an effective control source for communication devices. Although the simple display system of the present device limits its usefulness as a communication medium, it can be used to train cerebral palsied patients to generate controlled EMG signals. An effective communication device can be realized by just adding a more complex display system to the present device.

Several modifications, including a dry electrode system, have been suggested for the device. These modifications will make the device more clinically acceptable and also improve its controllability by cerebral palsied patients. Since inexpensive integrated circuits have been

used, the hardware cost of the device is relatively low (under $60) - its most expensive part being the Nicad battery power supply ($32).

Finally, it is suggested that the processed EMG signal can be used as an effective feedback in low-level muscle training and muscle relaxation training of cerebral palsied patients.

# CHAPTER 3

## REVIEW OF THE PHYSIOLOGY AND ANATOMY OF SKELETAL MUSCLE

The electromyographic signal obtained from an active muscle is usually the summation of the activities of a great number of physiological units. To effectively use this signal as an information source, a knowledge of the basic structural and functional units in striated muscle is required.

This chapter briefly reviews the salient characteristics of each physiological unit. In addition to giving a brief description of the electrical activity or action potential of the muscle fibre itself, this chapter also considers the characteristics of the potential waveforms resulting from externally recording the action potentials of a number of "synchronously" discharging fibres. The last section also briefly describes some disorders of the neuromuscular system specifically related to cerebral palsy. A more comprehensive treatment of the various facets covered in this chapter can be obtained from the references given. The references relating to the physiology of skeletal muscle are only representative of the many publications in this field.

### 3.1 The Motor Unit

The functional unit of the motor system is neither the entire muscle, nor the individual muscle fibre but the "motor unit". Just before or just after entering the muscle, the axon or nerve fibre from

each motoneuron (located in the anterior horn of the spinal grey matter) branches many times and innervates a number of muscle fibres. Therefore the motor unit, shown schematically in Figure 3.1, consists of a single motoneuron, its axon and the group of muscle fibres innervated by this single axon. The motor unit represents the minimum or quantum basis of normal muscular activity, since an impulse descending the nerve axon causes all the muscle fibres in one motor unit to contract almost synchronously.

The number of muscle fibres in a motor unit is generally determined by the function of the muscle. Usually muscles controlling fine movements and adjustments (such as those attached to the eyeball and larynx) have the smallest number of muscle fibres per motor unit. On the other hand, large muscles producing gross movement e.g. those in the limbs, have larger motor units. The number of fibres per motor unit can vary from 3 in extrinsic eye muscles to 150 in some leg muscles (Ruch and Patton, 1965). In the human biceps brachii, the fibres in a motor unit are localized to an approximately circular region, with an average diameter of 5 mm. (Basmajian, 1974). However, this area includes many overlapping motor units. Hence the fibres in a motor unit may be scattered and intermingled with fibres of other units.

There can be considerable variation in the size of the motor units in the same muscle. Norris and Gasteiger (1955) have demonstrated that the electrical responses from different motor units in the gastrocnemius and the rectus femoris muscles can vary by greater than 4:1. The increased electrical response is associated with larger motor units since these units are only recruited when higher contraction levels are required.

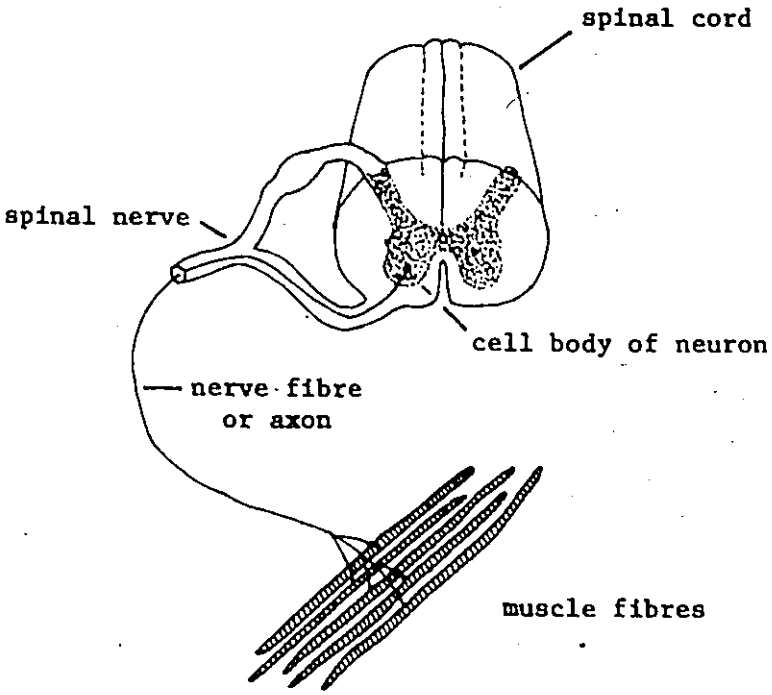


Figure 3.1 Scheme of a motor unit.

(Basmajian, 1974)

Person and Kudina (1972), in their study of recruitment patterns of motor units in the rectus femoris essentially confirmed these findings. The larger motor units may consist of a larger number of fibres, or the muscle fibres themselves may be larger.(Buchthal et al. (1955) report a threefold variation in fibre diameter within the muscle).

From the above it is apparent that even the larger motor units are quite small and a large limb muscle can contain hundreds of these units. A fundamental principle governing muscle contractions is that there must be a complete asynchrony of the active motor unit twitches imposed by asynchronous volleys of impulses coming down the many axons. The summation of a continuous shower of twitches with different frequencies within a muscle is a smooth pull. In certain disturbances, however, the contractions become synchronized, resulting in a visible tremor.

## 3.2 The Muscle Fibre

The basic structural unit of contraction is the muscle cell or muscle fibre. It can be described as a fine thread which has a length of up to 30 cm. and a diameter that can range between 10 and 100μ. When a muscle fibre contracts it contracts with all the force of which it is capable at that particular moment (Hollinshead, 1963). The tension developed depends upon the concentration of certain ions ($Ca^{++}$), the previous history of contraction, and the initial muscle length at the time of stimulation as given by the well-known isometric length-tension curves. The muscle fibre is capable of contraction to about 57% of its resting length.

A number of distinct events intervene between the synaptic initiation of an impulse in a spinal motoneuron and the contractions of the muscle fibres it innervates:

i) The impulse is conducted along the motoneuron axon, to its terminations on the muscle fibre motor end-plates.

ii) The impulse causes the liberation of a chemical transmitter substance, acetylcholine, from the axon terminals.

iii) By inducing a greater than threshold depolarization of the muscle fibre membrane, acetylcholine initiates a self-propagating impulse or "action potential" in it.

iv) The depolarization of the muscle membrane by the conducted impulse is followed by a brief phasic contraction of the muscle fibre - a twitch, followed by a rapid and complete relaxation.

The molecular basis of contraction is beyond the scope of this chapter but some description of the twitch time constants, and the summation of twitches resulting from repeated impulses is necessary.

The duration of the twitch and relaxation varies almost two orders of magnitude from a few msec. to as much as .2 sec., depending on the type of fibre involved. Although there are fast and slow twitch muscle fibres present in vertebrates, in mammals, fibres are always of the same type morphologically (and apparently physiologically) within any one motor unit. This is true even with the highly mixed muscles of man (Basmajian, 1974). For a typical fibre twitch the contractile tension rises to a peak in about 30 - 50 msec. and then declines more slowly to the initial or resting tension (Ruch and Patton, 1965). The electrical impulse which produced this twitch travels a few meters per sec.

along the fibre in both directions from the myoneural junction to produce sufficiently quick "mobilization" of the contractile apparatus in the interior of the cell. If the fibre is 5 cm. long the delay between the middle of the fibre and its two ends is only 5 msec. This results in only a slight phase lag in the tension development and does not seriously reduce the force exerted at the tendon (Katz, 1966).

When all the fibres in a muscle are stimulated synchronously by a single impulse the maximum twitch tension is developed. If a second impulse arrives before the contraction cycle is over, the response will increase further. The tension increases as the interpulse interval decreases, to a maximum of more than twice the tension of a single twitch. If the muscle receives a periodic impulse train, and the repetition rate is sufficiently high, the tension increases in diminishing increments until subsequent impulses add no more tension but do maintain the contraction. This response is called a tetanus and occurs when all the contractile elements in the fibres are maximally activated and elastic elements have attained a fixed length. The tension developed in a tetanus is usually about four times that of a single twitch (Ruch and Patton, 1965).

The repetition rate required for complete tetanus is naturally higher for fast muscles with their relatively brief contraction times and lower for slow muscles with their longer contraction times. A frequency of about 100 Hz is required for complete tetanus in a fast limb muscle. In contrast to the mechanical fusion of responses to repetitive impulses, the "action potentials" accompanying such contractions are always discrete and discontinuous. This emphasizes the fact that the

time constants associated with the contractile mechanism are much longer than those for the membrane mechanism. The above description of mechanical fusion of contractions of a muscle is also valid for a single muscle fibre - the whole muscle twitch being the temporal and spatial summation of the twitches of its individual fibres.

## 3.3 Membrane Properties of Skeletal Muscle

### 3.3.1 The Membrane Concept

Both nerve and muscle fibres are long cylindrical structures capable of propagating electrochemically-produced impulses over the whole surface. A nerve fibre is a long cell process far distant from its nucleus but surrounded by a myelin sheath interrupted at 1 mm. intervals and by a set of nucleated Schwann cells. A muscle fibre on the other hand, is a self-contained cell system with multiple nucleii distributed along its cytoplasm and virtually "bare" of any satellite cells. Their respective structures allow the nerve fibre to transmit signals rapidly between remote points and muscle fibre action potentials to rapidly initiate contraction over the whole fibre length.

Although the greater part of a nerve or muscle cell is taken up by water, which is in osmotic equilibrium with the surrounding tissue fluid, the chemical composition of the solutes, and in particular the electrolyte content of the cell, differs greatly from that of the interstitial fluid as shown in Table 3.1. The sign and size of the potential difference across the cell membrane is determined by its relative permeability to the principal inorganic ions, sodium, potassium

| Interstitial Fluid | | Intracellular Fluid | |
|---|---|---|---|
| [ION] | μM per $cm^3$ | [ION] | μM per $cm^3$ |
| $Na^+$ | 145 | $Na^+$ | 12 |
| $K^+$ | 4 | $K^+$ | 155 |
| $Cl^-$ | 120 | $Cl^-$ | 4 |
| $HCO_3^-$ | 27 | $HCO_3^-$ | 8 |
| Others | 7 | $A^-$ | 155 |
| Potential | 0 | | -90 mV |

Table 3.1 Approximate steady-state ion concentrations and potentials in mammalian muscle cells and interstitial fluid.

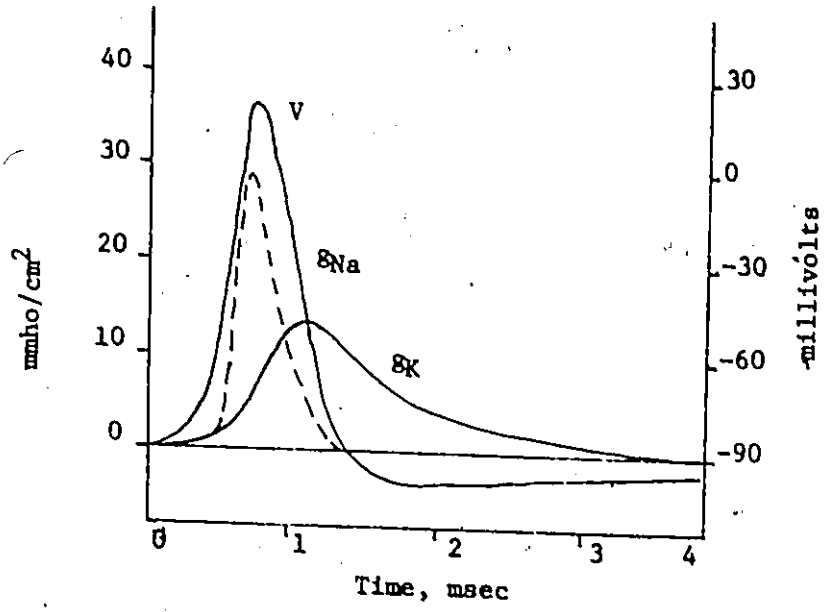


Figure 3.2 Calculated transmembrane action potential (Curve V) and sodium and potassium conductances from measured experimental data.

(Katz, 1966)

and chloride.

There exists a complex process, known as the sodium-potassium pump, which utilizes metabolic energy supplied by the cell to build up and maintain the concentration gradients across the cell membrane. This process simultaneously expels sodium ions which have diffused into the cell and helps accumulate potassium ions in the interior. The maintenance of the equilibrium potential or membrane resting potential is a secondary consequence of this; it results from the fact that the resting membrane has a much higher conductance for potassium (and for chloride in the case of muscle) than for sodium ions.

### 3.3.2 The Fibre Action Potential

Chemical and electrical stimuli are the most effective means of changing membrane permeability to sodium. It has been shown that membrane sodium conductance is a function of the membrane potential. The membrane behaves as a leaky capacitor with a time constant determined by its own capacitance and resistance. If a brief electrical stimulus causes sufficient current to pass out through the membrane, the membrane is depolarized and sodium conductance is increased. The increased flow of sodium ions into the cell further depolarizes the membrane, hence increasing sodium conductance. The restoring factor is the conductance of potassium and chloride ions which tends to return the potential to its resting value. If the membrane is sufficiently depolarized past the threshold potential, the mutual reinforcement of membrane depolarization and sodium permeability increase results in the spike or "action potential" shown in Fig. 3.2.

Because nerve and muscle fibres are long conductors, they exhibit cable properties and can conduct currents along the interior of the cell. The cable constants of the fibre (principally its surface capacity and the longitudinal resistances of the fibre core and external medium) are such that every 1 or 2 mm. the membrane depolarization is attenuated by 50 per cent. A sub-threshold depolarization is therefore not conducted along the fibre since nerve and muscle fibres can be 10's of cm. long. The shape of the membrane action potential, shown in Fig. 3.2, is determined by the dynamic conductances of sodium and potassium. Since at maximum amplitude, this potential is +50 mV with respect to the external fluid it can depolarize the adjacent membrane past threshold. Hence the action potential is propagated with constant amplitude and velocity along the whole length of the fibre in either direction from the stimulated region. This propagation velocity is a function of the cable constants and thus depends on the diameter of the fibre.

After an action potential has passed, it leaves the fibre in a refractory state for a few msec. During this time the fibre is unable to propagate another impulse. In addition, the fibres "accommodate" or adapt sooner or later to the change produced by an applied stimulus. For electric excitation this means that a constant current is effective only when it is initially applied. The action potential is then initiated by a sufficiently rapid change in the transmembrane current and not the magnitude of the current alone. Therefore nerve and muscle fibres can only conduct brief standard pulses with limited frequency because of their accommodation and refractory properties.

### 3.3.3 The Neuromuscular Junction

The interface between a motor nerve ending and a muscle fibre, is known as the neuromuscular junction or end plate. This myoneural junction in vertebrates serves as an impedance matching device - a physicochemical pulse transformer whose output provides sufficient electrical current to drive the low-impedance muscle fibre membrane beyond the threshold potential. Such a device is necessary because the diameter of the muscle fibre is much larger than that of the motor nerve ending.

The end plate is the region of the nerve fibre where the terminal branches of the motor axon lie on the muscle fibre and make synaptic contact with it. As the impulse travelling down the motor axon reaches the terminal branches on each of the muscle fibres in a motor unit, a complex physicochemical process is initiated. The impulse causes the release of a quantity of acetylcholine (called the chemical transmitter) from the terminal branch of the axon. The acetylcholine diffuses across the synaptic gap separating the nerve and muscle fibre membranes. This chemical then reacts with receptor molecules in the postsynaptic (muscle) membrane and makes it highly permeable to small cations such as sodium and potassium. The resultant influx of sodium ions depolarizes the post-synaptic membrane. This local depolarization, which is limited by a simultaneous efflux of potassium ions, is called the end plate potential. The e.p.p. does not reach the zero-potential level, but does cross the threshold of excitation so that an action potential is initiated in the adjacent muscle fibre which travels along the fibre in either direction from the end plate zone. In the above process there is a

total delay of 1.2 msec from the arrival of the impulse at the presynaptic site to the initiation of the action potential of which .7 msec is required for synaptic transmission (Katz, 1966).

Normally an impulse travelling down a motor nerve gives rise to an action potential in each of the muscle fibres in a motor unit without fail. Neuronal synapses on the other hand integrate different excitatory and inhibitory afferent signals to produce graded subthreshold potentials in the post-synaptic membrane. Transmission of impulses by the axon and its terminal branches is much faster than the propagation of an action potential along a muscle fibre. Hence impulses can be considered to have arrived almost synchronously at all the endplates of a motor unit (Buchthal et al., 1955). Finally, the myoneural junction also acts as a unilateral device in that only nerve to muscle transmission is possible.

## 3.4 The Motor Unit Action Potential

### 3.4.1 Externally Recorded Action Potentials

The action potential and potential changes described in previous sections and shown in Fig. 3.2 are transmembrane potentials. Measurement of these potentials is only possible in microbiological experiments using microelectrodes. However, in clinical or prosthetic measurements the external action potential is recorded whether surface or transcutaneous electrodes are used. For example, if two electrodes are placed longitudinally to the nerve or muscle fibre and external to it, the dynamic potential difference between them is a measure of the transmembrane action

potential propagating along the fibre. Figure 3.3 shows the local current paths as an action potential travels along the fibre. This figure also shows the resultant external and internal fibre potential changes $V_o$ and $V_i$ which result from the local currents flowing through mediums with finite conductances.

The total time duration of the action potential is longer in muscle than in nerve fibre. Although the depolarization phases of the two waves are similar, the time required for complete repolarization of the membrane is much longer in muscle fibre. In muscle, the rapid repolarization stops at 20 mV from resting potential, at which level the potassium conductance has returned to the resting condition. The membrane potential then approaches the resting level over a period determined by the cable constants of the muscle membrane (about 30 msec according to Ruch and Patton, 1965). Since there is little current flow outside the fibre during this period, the external potential is consequently negligible. The external action potential is then a brief monophasic wave of surface negativity (relative to the potential of the surrounding interstitial fluid) with a duration of about 2 to 4 msec.

While the current density arising from membrane activity is strongest in the immediate vicinity of the active region, there will be current everywhere in the surrounding medium. This medium can be called a volume conductor and is composed of the aggregate of passive tissue which supports current from active sources. Electrodes placed within such a volume conductor measure the net electric potential field (related to the current flow field) which is produced by the summation of all active surces. The external action potential described above is that

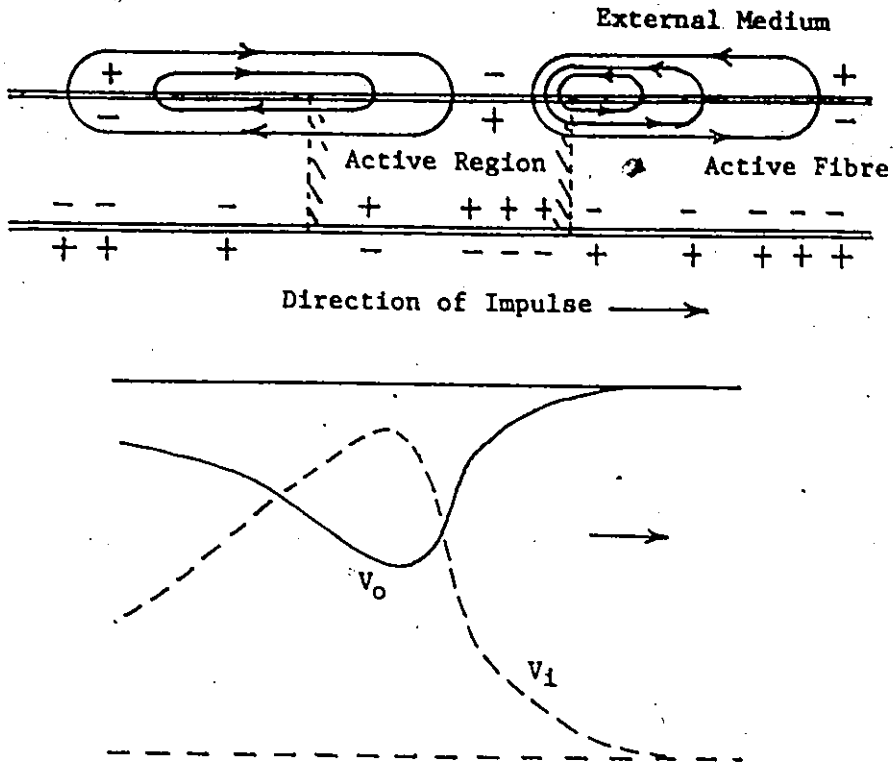


Figure 3.3 External potential change $V_o$ , internal potential change $V_i$ , and local currents (top diagram) as the action potential propagates along a fibre.

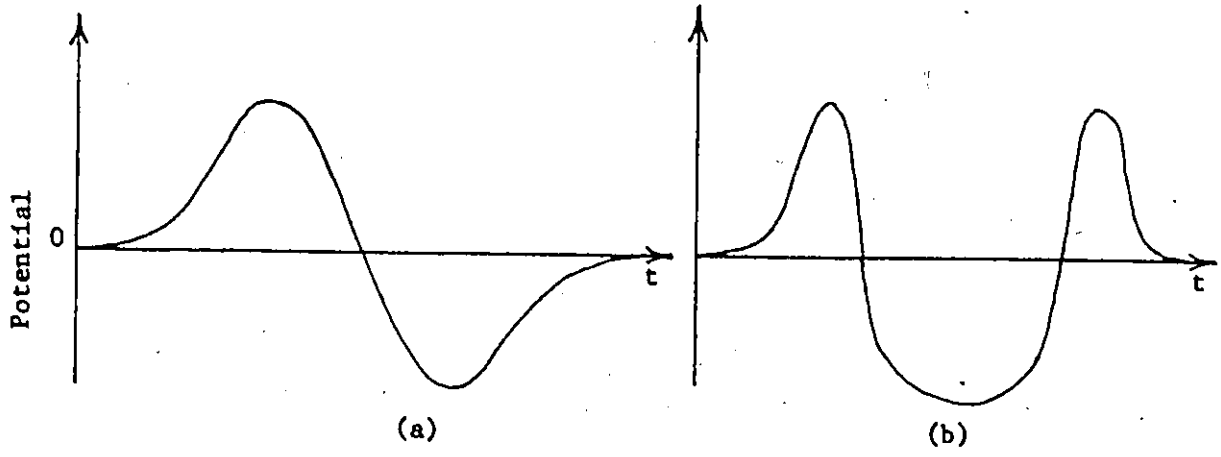


Figure 3.4 Externally recorded action potentials:
(a) diphasic (b) triphasic
(Plonsey, 1969)

found at the surface of the active fibre. In general, the action potential waveforms obtained clinically are very different from that described in Fig. 3.3. The waveform, duration and amplitude of an externally recorded action potential from a single active fibre depend on many factors such as the electrical properties of the volume conductor, the electrode configuration and spacings used, and their distances from the axis of the fibre.

### 3.4.2 Waveforms of Externally Recorded Action Potentials

In recording electromyographic signals for diagnostic or prosthetic purposes, many different electrode configurations are used. These fall into two broad categories, monopolar electrodes and bipolar electrodes. A monopolar electrode configuration measures the potential difference between an active and an inactive muscle region. The bipolar electrode configuration measures the potential difference between two active muscle regions. Examples of the former are unipolar needles and certain configurations of surface electrodes, while examples of the latter are bipolar needles, coaxial needles and flexible fine wire electrodes. Many workers have recorded and measured the action potential parameters using these different electrode configurations (for example: Basmajian, 1974; Norris and Gasteiger, 1955; Buchthal et al., 1955; Petersén and Kugelberg, 1949; Buchthal and Rosenfalck, 1955; and Brown, 1968). There is considerable variation in action potential waveforms recorded using the same electrode system. This variation results from the different distances of the active fibres from the electrodes and the end plate dispersion of motor units.

Monopolar Electrode Configuration

A rigorous theoretical derivation of the action potential recorded by both categories of electrode configurations is difficult due to the distributed nature of the time varying bioelectric sources and electrical properties of the volume conductor: nonlinear, inhomogeneous, and time varying. By making several assumptions Plonsey (1969) and Brown (1968) have developed the theoretical waveform as recorded by a monopolar electrode where the second electrode is distant and remains at essentially zero potential. They both use a simple dipole membrane model of the active fibre and assume that the regions of depolarization and repolarization are sharply defined. If only depolarization is considered, the resultant waveform at a point distant from the axis is that derived from a dipole moving along the fibre axis at a fixed velocity. This waveform, shown in Fig. 3.4 (a) is called a diphasic action potential. If both rapid depolarization and repolarization are considered, the resultant waveform at a distant point is that derived from two dipoles separated in space and 180° out of phase moving along the fibre axis. The derived waveform called a "triphasic" action potential is shown in Fig. 3.4 (b). Although the diphasic waveform of Fig. 3.4 (a) is observed frequently by workers recording action potentials from muscle fibres using monopolar electrodes, this particular shape of the triphasic action potential is not commonly reported. One explanation for the suitability of the derived diphasic waveform is that depolarization of the membrane is rapid and can be considered "sharply" defined. However, repolarization especially in muscle fibres is much slower and cannot be approximated by a single dipole.

Bipolar Electrode Configuration

In bipolar electrode systems, the electrodes are close together and the position of both in the potential field must be considered in the determination of the potential difference. If two electrodes are placed along the axis of an active fibre, close to the surface and a distance d apart, the recorded action potential will have a diphasic waveform. It is simply the difference between the monophasic external action potential $V_o$ shown in Fig. 3.3 propagating along the fibre with velocity v, and $V_o$ displaced $\Delta t$ where $\Delta t$ is simply d/v. The duration and amplitude of the diphasic waveform is dependent on the electrode spacing d. As d becomes very small the resulting diphasic waveform approaches the derivative with respect to time of $V_o$.

By considering the electrical properties of the physiological system, Plonsey (1969) has reduced the moving source, volume conductor field problem to a quasi-static one. That is, although the action potential is a moving source, at any instant of time steady-state conditions can be assumed corresponding to a stationary source. He presents a more accurate method (as given by Lorente de Nó) of calculating the potential field than the dipole depolarization-repolarization model mentioned above. This method depends on measuring or calculating the surface potential $\Phi_s$ of an excised nerve. The in situ potential at a point P can then be calculated from the simplified equation

$$\Phi(P) = \frac{-A}{4\pi}\int\left(\frac{\partial^2 \Phi_s}{\partial z^2}\right)\frac{1}{r}\,dz \qquad (3.4\text{-}1)$$

where A is the fibre cross sectional area and z and r are the axial and radial distances of P. Equation 3.4-1 is valid if P lies on a radius which exceeds five times the radius of the fibre.

Since the propagated action potential travels down the fibre without attenuation or dispersion and at constant velocity, the potential variation along a line parallel to the fibre axis can also be interpreted as the potential variation with respect to time of an arbitrary field point at the assumed distance from the axis. By using two closely spaced electrodes on a uniform portion of an excised nerve, Lorente de Nó (Plonsey, 1969) has measured the surface potential variation with respect to time $\frac{\partial \phi_s}{\partial t}$ and hence with respect to axial distance $\frac{\partial \phi_s}{\partial z}$. A typical record of the latter is shown in Fig. 3.5 along with its derivative and integral. The surface potential $\phi_s$ closely resembles that shown in Fig.3.3 except for the depolarization phase which is shorter in nerve than in muscle fibre as stated in Section 3.4.1. In addition, the time increments of the scale are larger for muscle due to the slower propagation velocity in muscle fibre. Lorente de Nó has then calculated the potential field surrounding the active fibre using Eqn. 3.4-1. The action potential recorded by bipolar electrodes at a point distant from the fibre axis can then be derived using the temporal-spatial relationship mentioned above. That is for a specific radius $\rho_o$, one can measure $\phi(t,\rho_o)$ and $\phi(t+z/v,\rho_o)$ and construct the required waveform. Figure 3.6 shows this triphasic action potential. The dependence of this waveform on $\frac{\partial^2 \phi_s}{\partial z^2}$ can be seen from their similarity of shape. The radial dependence of the recorded potential was examined by Lorente de Nó and although it was found to depend on z, its general character was that of

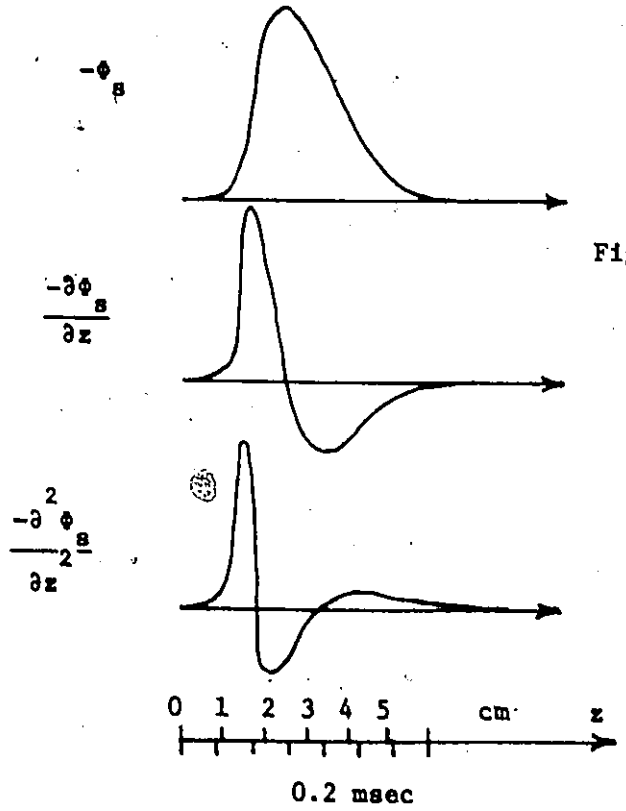


Figure 3.5 The external action potential $\phi_s$ of bullfrog alpha fibres, and its first and second derivatives.

(Plonsey, 1969)

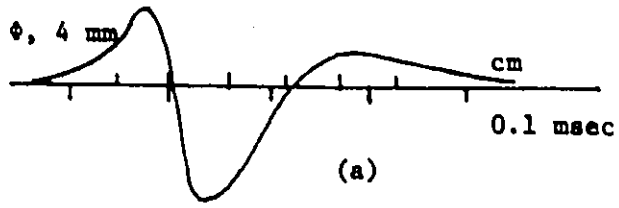


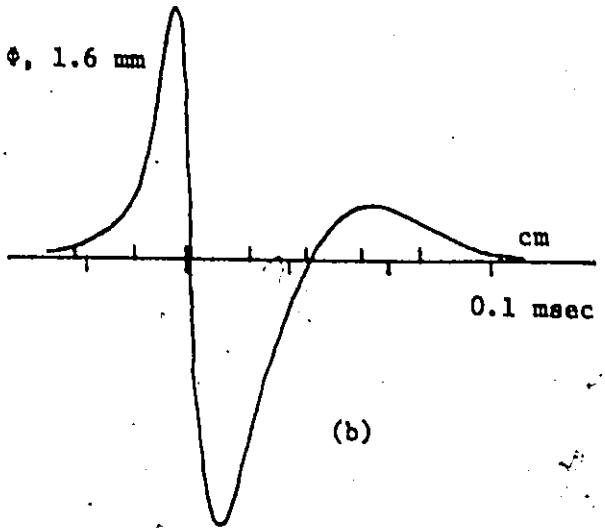


Figure 3.6 Computed action potentials of nerve in situ at points 4 and 1.6 mm from the axis of the nerve.

(Plonsey, 1969)

an exponential decay with increasing distance from the fibre. This derived triphasic waveform differs from that shown in Fig. 3.4 in that it does not depend on an idealized discontinuous transmembrane potential but rather utilizes the actual shape of $\phi_s$.

Comparison of Theoretical and Measured Waveforms

We shall now discuss how well the experimental action potentials recorded by different workers agree with these theoretical waveforms. Petersén and Kugelberg (1949) have recorded the diphasic waveform of Fig. 3.4 and the triphasic waveform of Fig. 3.6 using monopolar and bipolar electrodes. Norris and Gasteiger (1955) who used fine wire monopolar electrodes also report diphasic action potentials with the waveshape of Fig. 3.4. Brown (1968), using monopolar surface electrodes over a stimulated nerve, has also recorded only diphasic potentials with this waveshape.

Pollak (1971) has theoretically compared the waveshape of action potentials recorded with monopolar, bipolar and coaxial needle electrodes. He concludes that the waveshape recorded with monopolar and coaxial needles will be that of Fig. 3.4 (a) while bipolar needles will record a symmetric triphasic action potential which is the time derivative of the unipolar diphasic waveform. However, Buchthal et al. (1955) have recorded both the diphasic waveform of Fig. 3.4 and the triphasic waveform of Fig. 3.6 while using only coaxial electrodes in the biceps brachii. In their recordings of action potentials from different skeletal muscles of normal subjects, Buchthal and Rosenfalck (1955) most frequently observed diphasic and triphasic waveforms whether using coaxial or bipolar needle

electrodes. We have also observed both types of waveforms when using a coaxial electrode in the biceps brachii.

Buchthal and Rosenfalck (1955) also found that diphasic potentials had their lowest incidence (and triphasic the highest) in large leg muscles. In contrast, the small muscles of the hand and facial muscles gave the highest percentage of diphasic potentials. This may be explained by the fact that these muscles have smaller motor units - hence more motor units are in the immediate vicinity of the recording electrodes. The probability of the electrode being close to the surface of the fibres of the active motor unit is thus greater. For this case, the recorded action potential will approach the diphasic surface potential derivative $\frac{\partial \Phi_s}{\partial z}$ shown in Fig. 3.5. As can be seen, the diphasic waveform of Fig. 3.4 and the triphasic waveform of Fig. 3.6 can be considered typical action potentials as recorded respectively by monopolar and bipolar electrodes.

### 3.4.3 Motor Unit Action Potential Parameters

#### Time Duration

In their examination of propagation velocities in the biceps brachii of different normal subjects, Buchthal et al. (1955) observed a mean velocity of 4.7 m/sec with a maximum deviation of 1.3 m/sec in the same muscle. The theoretical propagation velocity increases with the square root of the fibre diameter if the fibres are immersed in a large conducting volume (Katz, 1966). The narrow range of propagation velocities is then inconsistent with the threefold variation in fibre diameter in the muscle. Buchthal et al. account for this range of veloci-

ties by assuming that the external resistance is localized mainly in the interstitial fluid and cannot be neglected. They have also found that 67 per cent of the motor end plates in the biceps brachii are situated within 10 per cent of the muscle length and the action potential is initiated almost synchronously in each fibre of the motor unit.

Although the fibre action potential lasts 2 to 3 msec, the motor unit action potential has a duration of 5 to 12 msec if recorded by needle electrodes. This results from the electrodes summing slightly dispersed fibre action potentials (due to fibre end plate dispersion). Buchthal and Rosenfalck (1955) report much shorter motor unit action potential durations for the small facial muscles than large limb muscles. These results are consistent with the above explanation since the larger motor units are assumed to have larger end plate regions. Petersén and Kugelberg (1949) found that action potentials recorded in the same muscle by monopolar and coaxial needles have a mean duration of 7.34 msec, while those recorded by fine wire shielded electrodes with the same dimensions have a mean duration of 2.28 msec. Norris and Gasteiger (1955) report mean durations of 4.0 to 4.8 msec for all motor units recorded from the same muscle while using very fine monopolar wires. This variation in duration can be explained by the fact that the fine wire electrodes have a smaller recording area and are therefore far more selective than the other needle electrodes and sum the potentials from only some of the fibres of an active motor unit. With surface electrodes the durations are prolonged even more as the potentials are "blurred" and rounded out due to dispersion effects.

Amplitude

Motor unit potential amplitudes are usually measured in microvolts with typical amplitudes being of the order of 500μV (Basmajian, 1974). The amplitude of the motor unit potential just as the duration also depends on the type and size of electrodes used. Larger motor units also produce larger potentials and potential variations greater than 4:1 have been reported for the same muscle (Norris and Gasteiger, 1955). The theoretical motor unit action potential derived by George (1970) is based on cylindrical arrays of dipoles representing action potentials moving along the fibres of an active motor unit. The resulting diphasic waveform, as would be recorded by a monopolar electrode, is the summation of the dipole fields as the arrays move synchronously or asynchronously (axially distributed) along the fibre axis. He has calculated that the amplitude of the potential from a very large assembly of dipoles will only be marginally greater than that from a small one - a result not observed by experiment (Norris and Gasteiger, 1955). He has also found that the spacing between the peaks of the diphasic potential increases with the size of the assembly especially if there is a small amount of axial scatter as would be due to end plate dispersion. The resulting diphasic waveform still resembles that of Fig. 3.4, demonstrating the validity of this waveform even for motor unit potentials. In contrast Katz (1966), using a very simple derivation, shows that the ratio of the change in external fibre potential $\Delta V_o$ to the change in transmembrane potential $\Delta(V_i-V_o)$ is:

$$\frac{\Delta V_o}{\Delta(V_i-V_o)} = \frac{-r_o}{r_o+r_i} \qquad (3.4-2)$$

where $r_o$ is the resistance per unit length of the external medium (including the shunt resistance presented by inactive fibres) and $r_i$ is the internal axoplasmic resistance of active fibres. If only one fibre is active $r_i >> r_o$, but as each additional fibre becomes synchronously active $r_i$ decreases and $r_o$ increases. One would therefore expect the external recorded potential to be proportional to the number of active fibres but never greater than the transmembrane action potential. Considering experimental observations (Norris and Gasteiger, 1955), this explanation of a variable external resistance seems more valid than the theoretical derivations using a constant external volume conductivity.

## 3.5 Motor Unit Recruitment

In Chapter 5 various processing strategies are presented which can be used to estimate the muscle tension from surface recorded EMG signals. It is therefore necessary to have an understanding of how muscle tension is increased or decreased during voluntary contraction. There are two mechanisms by which muscle tension can be increased during voluntary contraction : (i) the discharge frequency of active motor units can be increased; and (ii) more motor units can be activated (recruitment). The control process which utilizes these two mechanisms is very complex since the muscle is composed of hundreds of motor units of different sizes and the discharge frequency can be increased from 1 Hz to greater than 50 Hz. In addition, other factors such as those described below affect this process.

Henneman et al. (1965) in their investigation of motoneuron susceptibility to various types of reflex excitation and inhibition in

decerebrate cats found that the order of recruitment of motoneurons is in accord with cell size (the larger motor units have larger motoneurons). They also found that the larger the unit the more susceptible it is to inhibition. In their study of isometric contraction of a hand muscle, Freund et al. (1973) confirm this cell size principle. Grimby and Hannerz (1968) in their observation of motor unit recruitment on voluntary contraction in the anterior tibialis muscle, found that the recruitment order differed depending on the velocity of contraction. This dependency has also been found and studied by other authors mentioned by Basmajian (1974). Grimby and Hannerz also observed that simultaneous contraction of another lower leg muscle altered the recruitment order. They conclude that proprioceptive afferents, particularly from muscle spindles play a major role in the change in recruitment order of motor units of similar thresholds. Impairment of proprioceptive functions are essential factors in the development of spasticity and at least some types of rigidity.

Norris and Gasteiger (1955) in an extensive study of the rectus femoris and gastrocnemius muscles from different subjects have found that the population of different motor units is the same at all depths within the muscle. They have classified motor units into four groups corresponding to the four levels of isometric contraction (weak, moderate, strong, maximum) in which they first appeared. They have also observed the motor unit size principle of recruitment and in addition found that the active units discharge at higher frequencies as the contraction increased, with the smaller units reaching frequencies in excess of 50 Hz and the largest units discharging at less than 5 Hz. Per-

son and Kudina (1972) have recorded motor unit potentials during low to moderate isometric contractions of the rectus femoris muscle of different normal subjects. In their study of motor unit discharge frequency and recruitment during increases in contraction level, they have also found that the motor unit size principle of recruitment is generally followed. Figure 3.7 gives typical curves for discharge frequency and recruitment for a cycle of voluntary contraction. As can be seen, lower threshold units reach higher discharge frequencies than the higher threshold units. During prolonged constant contractions they observed a decrease in the discharge frequency of active motor units and recruitment of new units about 20 - 40 seconds after initiation of the contraction. A voluntary increase of tension was accompanied by a new increase in frequency. They conclude that recruitment is the main reserve of contraction strength increase because of the large number of motor units in a muscle and the low (4-10) tetanus-twitch tension ratio of skeletal muscle. However, the mechanism of frequency change is unsurpassed as far as precision and smoothness of contraction are concerned.

Although some general principles of recruitment have been accepted, there is still a great deal of controversy concerning the interaction of these two control mechanisms.

## 3.6 Discharge Pattern of Motor Units

If one examines the spike (action potential) train produced by a motor unit, it can be seen that the discharge of action potentials is not a periodic function. Since the amplitude and waveform of the

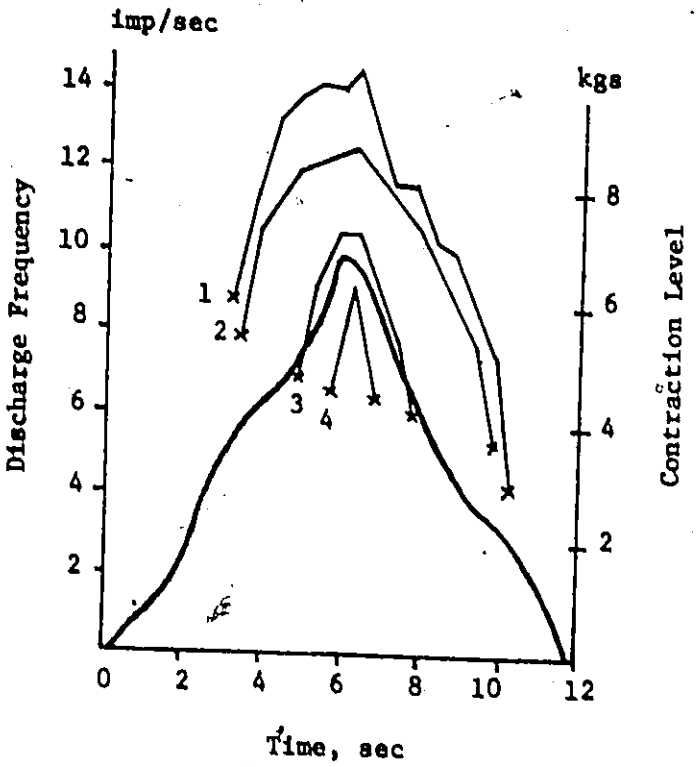


Figure 3.7 Recruitment pattern of motor units during a cycle of voluntary contraction. The numbers 1-4 on the curves indicate recruitment order and the x's indicate time of initiation and release of motor units. The solid line is the contraction level.

(Person and Kudina, 1972)

recorded action potential are constant for the unit (determined by the electrode configuration and electrode distance from the unit), only the discharge frequency provides information about the unit's activity. Each action potential in the spike train can be considered an event with the time of occurrence of each event (spike) being the only parameter that differentiates them. The spike train can therefore be treated as a stochastic point process with the interspike intervals (ISI) exhibiting the properties of random variables. If the interspike intervals are statistically independent the stochastic process is known as a renewal process. Since a population of such spike trains constitutes the EMG signal, a knowledge of the statistics of the spike train will aid in the interpretation of this signal.

Clamann (1969) has extensively studied motor unit spike trains recorded during stationary isometric contraction of the biceps brachii of different normal subjects. He has examined the spike trains which were stationary (no discharge frequency drift) and observed Gaussian ISI distributions for mean discharge rates of the order of 8 to 18 per second. Using joint interval density plots of adjacent intervals, he has determined that successive ISI's are uncorrelated and hence statistically independent. Freund et al. (1973) have also observed these results for stationary isometric contraction of the first dorsal interosseus muscle of normal subjects. Person and Kudina (1972) observed Gaussian ISI distributions for mean discharge frequencies of greater than 10.5 per sec. in the rectus femoris muscle, but found a slight negative correlation between successive intervals. However, considering the weight of the evidence, the spike train can be considered a stochas-

tic renewal point process.

On applying a stricter test to the ISI distribution, Clamann (1969) has found that this distribution is slightly skewed with very long intervals being marginally more likely than very short ones especially in units with low discharge frequency. Person and Kudina (1972) have found this skewness more pronounced for discharge frequencies less than 8 per sec. with the ISI distribution resembling a Poisson distribution for these frequencies. They have also observed no dependence between ISI parameters on the one hand and motoneuron threshold and duration of contraction on the other. However, the frequency dependence of the ISI distribution shape shows that the statistical characteristics are significantly affected by the range of discharge frequencies.

It has been observed by many authors that the standard deviation of the ISI's is dependent on the mean ISI or discharge frequency. Clamann (1969) has plotted the standard deviation vs. mean and obtained both a linear and parabolic fit to the data. The standard deviation increases monotonically with the mean as does the scatter in the data. He has therefore reduced the description of the motor unit to a one-parameter system since the standard deviation is a function of the mean. Person and Kudina (1972) have also plotted the standard deviation vs. mean but do not obtain a linear relationship. Instead they have observed that the standard deviation is relatively stable and not greater than 5 msec. for a mean less than 80 msec. ($f>12.5$Hz). For a mean between 80 and 105 msec., the standard deviation is in a transition region while for a mean greater than 105 msec. ($f<9.5$Hz) it increased until for a mean of 180 msec. it was 50 to 60 msec. Although they observed no

distinct groups of "tonic" and "kinetic" motoneurons, the transition region for different motor units was quite large. The observations of Stalberg and Thiele (1973) lend support to this conclusion of a definite region of higher discharge frequency where the standard deviation is small and stable. They have recorded spike trains from a voluntarily activated motor unit, using feedback techniques (see also Basmajian, 1974) in different muscles of the upper and lower limbs of normal subjects. After a training period of 10 to 15 minutes frequencies of 8 to 20 Hz could be achieved with good precision. However, a lower limit was observed below which the deviation became larger. This lower limit of regularity varied for different motor units in a muscle and varied even more for different muscles. The larger lower limb muscles had lower limits than those of the upper limb with the biceps brachii having a limit of 8 to 10 Hz. Hence the ISI standard deviation is not a simple linear function of the mean ISI but may be related to the function of the motor unit.

Freund et al. (1973) have observed that the discharge patterns of motor units of patients with supraspinal lesions of the motor system or with lower motoneuron diseases are significantly different from normal patterns. The joint interval density plots of adjacent intervals and the autocorrelation functions show serial correlation of the ISI's. In addition, the ISI distribution deviates from normal and even becomes bimodal for certain diseases. Therefore, motor unit recruitment and motor unit discharge patterns are both significantly altered by diseases of the motor system. The statistical characteristics of the EMG signal should then also be altered, and a processor based on normal EMG

signals may not necessarily be suitable for EMG signals from diseased patients.

## 3.7 Neuromuscular Control

Since we are recording the EMG signals from a voluntarily contracted muscle (i.e. during a voluntary movement or attempted movement) some knowledge of how the nervous system controls a movement is necessary. In addition, since neuromuscular disorders can affect any part of the control system from the motor cortex to the muscle itself, the EMG signal will be affected differently depending on the disorder (Freund et al., 1973).

The simplest movement is apt to require the coordinated contraction - coordinated both in time and in strength of contraction - of a number of muscles or muscle groups and it is the function of the nervous system to bring about this coordination. The motor centres and especially the movement centre in the cerebral cortex are organized not anatomically on the basis of muscles but physiologically on the basis of movements.

Protagonists are those muscles or parts of muscles that directly carry out the particular movement required. For instance, the biceps brachii is the protagonist when flexion of the supinated forearm is required. Synergists are muscles that contract at the same time as the protagonist in order to facilitate and potentiate its effect. Antagonists are muscles that have actions more or less directly opposed to the actions of the protagonist but can also be considered synergists in normal movements. For example, the triceps can act as an antagonist if

flexion of the forearm is considered the required movement. Smoothness of movement against low resistance also depends on proper contraction and relaxation of the antagonists which must provide the proper level of resistance.

Approximately 40 per cent of the nerve fibres innervating a muscle are sensory in character in contrast to the efferent motor axons of the nerve (Chusid, 1973). Most of these fibres are known as proprioceptive (kinesthetic) fibres and are concerned with registering contraction within the muscle and tension within a tendon and transmission of this information to the central nervous system. The majority of proprioceptive sensory impulses do not reach the level of consciousness but play an extremely important part in the subconscious regulation and coordination of muscular contraction. In addition, the proper learning of movements is primarily dependent upon the proprioceptive sensory fibres. The proprioceptive sensory fibres in a muscle end in complex spirals about the noncontractile middle portion of small specialized groups of muscle fibres to form "muscle spindles". These muscle spindles are in parallel with the other muscle fibres and serve as receptors for the stretch reflex. On either side of the complex spirals are "flower-spray endings", which are receptors of smaller myelinated fibres and are also responsive to stretch, producing increased flexor and decreased extensor motoneuron activity. Other proprioceptive fibres end in complex twistings about tendon fibres to form "Golgi tendon organs". These lie in series with muscle fibres and may serve to inhibit contractile responses evoked by the muscle spindles. Their sensory fibres are believed to end in the spinal cord on inhibitory interneurons which in turn ter-

minate directly on motoneurons to the same muscle. The threshold of the Golgi organs is considerably higher than that of the muscle spindles - hence they serve to inhibit the production of excessive tension in the tendon. Interaction of the two groups of sensory organs assures smoothness of muscle performance.

The least complicated of the controls over the motoneuron (called the lower motor neuron) is that of the incoming or afferent sensory fibres at the spinal level. These fibres, their connections with the lower motor neuron and this neuron itself, can be regarded as forming an anatomical and functional unit which is called "a simple spinal reflex arc". The simple spinal reflexes constitute the basis of all muscular activity, even though the response of the lower motor neuron (hence muscle activity) is determined by the summation of all the excitatory and inhibitory impulses reaching it from volitional centres and numerous other reflex arcs.

One of the most important of the fibre tracts of the spinal cord, ending in connection with lower motor neurons, is the corticospinal or pyramidal tract. The neurons of this tract together with their cell bodies in the motor area of the cerebral cortex are known as upper motor neurons. These neurons, together with other neurons closely associated with the pyramidal tract in both the brain and spinal cord, initiate voluntary movement. Injuries to neurons of the pyramidal tract typically result in paralysis of voluntary movement. However, these injuries also impair inhibitory impulses from reaching lower motor neurons - hence these motoneurons are excessively excited by the reflex arcs converging on them and general contraction of the muscle ensues.

Upper motor neuron paralysis is therefore a "spastic" paralysis in which muscles cannot be used voluntarily and at the same time their contraction and their resistance to passive movement are increased markedly above normal. Infantile cerebral palsy includes disorders of the upper motor neurons characterized by paralytic symptoms in infancy and childhood. This is a broad category which includes such clinical types as spastic, athetoid, ataxic and rigid. Infantile spastic hemiplegia, the most common form of cerebral palsy, usually involves the upper extremity more than the lower. Mental retardation is common and sensory handicap may be more disabling than the motor because proprioception and form discrimination are lost. It has been shown by Freund et al. (1973) that the discharge patterns of the motor units of a patient with spastic hemiplegia are radically altered from normal.

# CHAPTER 4

# REAL-TIME SIMULATION OF EMG SIGNALS

## 4.0 Introduction

As indicated in Chapter 1, the recorded EMG signal is the summation of the electrical activities of all those motor units located near the recording electrode(s). The number of action potential trains summed depends upon the level of contraction and the selectivity of the electrodes (i.e. electrodes with a small surface area will record the activity of a small volume of muscle tissue). This number is large for all levels of contraction if surface electrodes are used, but even for relatively selective coaxial needle electrodes it can become large especially during moderate to strong contractions. The statistical characteristics of motor unit recruitment and discharge patterns, mentioned in Chapter 3, make the theoretical determination of new detection strategies extremely difficult. Since the EMG signal is the result of a complex stochastic process, a model of the EMG source will aid in determining relevant parameters used in new detection strategies. Analysis of such a model may also facilitate an understanding of the physiological system involved. In order to have a feasible model, it should not include any part of the central nervous system or controls described in Section 3.7, but should be limited to the muscle itself.

Although much work has been done concerning the statistics of motor unit activation, very few models of the EMG source or signal have

been proposed. However, several authors have recently presented such models based on different approaches. Parker and Scott (1973) propose a model based on the summation of the weighted action potential trains of N active motor units. The action potential is given by an expression having a diphasic waveform similar to that shown in Fig. 3.5 and the resulting monopolar electrode EMG signal is used to derive the bipolar electrode signal. They use their model to derive the relationship between the autocorrelation function of the single motor unit action potential train and that of the monopolar and bipolar electrode EMG signals.

In their model Brody et al. (1974) assume that pooling of a large number of independent motor unit impulse trains produces a Poisson pulse train. This train is then passed through a linear time-invariant causal dynamic system whose transfer function is KH(s), and the output is considered to be the aggregate EMG as recorded by surface electrodes. The final model equation is given by:

$$EMG(t) = \int_{-\infty}^{\infty} Kh(t-v) \sum_{m=1}^{N} \sum_{i=-\infty}^{\infty} \delta(v-t_{mi})dv \qquad (4.0\text{-}1)$$

where h(t) is the inverse Fourier transform of H(s), $\delta$ is the Dirac delta function, N is the number of active motor units, and $t_{mi}$ is the initiation time of the i th impulse in the m th impulse train. The autocorrelation function and both second and fourth moments of the real signals have been computed and then by using the method of least squares fitting different parameters of the model have been obtained. This mo-

del was used to find the generalized firing rate and the number of active motor units at different force levels for different subjects. The major drawback of the model is the assumption of a single constant motor unit mean firing rate for all levels of contraction.

Wani and Guha (1974) use a biomechanical analysis of the motion of the forearm to calculate the parameters of their model. Although their model has the advantage of using two independent criteria (EMG signal and muscle biomechanics) to obtain the parameters, several of their assumptions such as a single constant motor unit discharge frequency and a muscle centre to muscle surface recruitment pattern contradict the measured motor unit recruitment and discharge patterns described in Sections 3.6 and 3.7.

Kreifeldt and Yao (1974) do not consider any physiological basis but propose a multiplicative mathematical model of surface EMG based on the amplitude modulation of noise. The modulating signal represents gross low-frequency (10 Hz) volitional activity while the carrier is considered to be white noise. They use this model to determine the suitability of different amplitude detection strategies. However, this model completely ignores the frequency modulation characteristics of surface EMG and can only be used for amplitude considerations.

The model suggested by Moore (Basmajian, 1974) is based on the summation of Q identical diphasic waveforms randomly distributed over a certain period. He uses this model to investigate the variation of Q as a function of force and suggests possible recruitment patterns of motor units. Although many assumptions are made, its extreme simplicity makes this model quite attractive. A similar graphical model suggested by

Person and Libkind (1970) is based on the random superposition of a motor unit diphasic action potential train. The mathematical form of the model includes both asynchronous and synchronous firing of different motor units. The model has been used to investigate the properties of the autocorrelation function, power spectral density, and integration of the gross EMG signal. However both of these models assume that action potentials all have the same amplitude and all recruited motor units the same discharge frequency.

The model proposed by Abdel Azim and Della Torre (1975) is quite different from those mentioned above and attempts to be as closely related to the physiological basis as possible. It is a digital model composed of independent blocks representing different motor units and some of their neuromuscular controls. However, application and modification of this model is difficult due to the large number of parameters involved.

Finally, the model proposed by de Bruin and Della Torre (1975) has as its principal function the real-time simulation of EMG signals. Although this model is based on physiological principles, several simplifying assumptions have been made because of the constraints of real-time computation. This model and its computation algorithm are described in this chapter.

## 4.1 Aspects of Real-Time Simulation

Different on-line detection algorithms can be easily implemented on minicomputers. Since the EMG signal is a stochastic process, a reproducible EMG signal will aid in testing the different algorithms.

This reproducible EMG signal could be obtained by recording EMG signals, storing them on tape and playing them back repeatedly. A simulated EMG signal would also aid in testing the different algorithms since the signal parameters are precisely known and the detector responses can be measured for different sets of parameters.

Although the models mentioned above produce simulated EMG signals, the complexity and computational organization of their algorithms makes them unsuitable for real-time applications. Real-time simulation means that the successive discrete values of the signal are calculated and output at a sample rate consistent with the bandwidth requirements of the signal. In other words, the computer replaces the subject as a source of the EMG signal and can output this signal indefinitely. Such a real-time simulated signal would be most useful for long term testing. In addition, a controllable real-time simulated signal can be used to test an external hardware detector.

To satisfy absolute minimum EMG bandwidth requirements real-time simulated signals must be calculated at a minimum sample rate of 200 Hz. For complex discrete-time EMG signal models, the computation time per sample is too long to achieve even this rate. However, real-time simulated signals can be generated by these models using several techniques. In one, the sample values can be calculated off-line (i.e. computation time per sample is independent of real-time), stored on a direct access storage device such as a magnetic disk and transferred into core when required. The samples can then be read and used under real-time clock control.

Another method is to generate and output the sample values through a D/A converter and low pass filter to a tape recorder at a low real-time sampling rate and tape speed, and to play it back at a higher speed. Only those algorithms which have a relatively constant and brief sample computation time can be used for this method. Available core and disk storage space limits the length of continuous signal produced by the first method. The requirement of a wide-range multi-speed tape recorder with precisely related carrier frequencies makes the second undesirable. Neither method allows real-time control of the simulated signal.

Since the detection algorithm is to provide control signals for a prosthetic or communication device, it must be able to detect dynamic force behaviour rather than just constant contractions. Such parameters as the time constants or control lag of the detector must be determined and kept to a minimum if the detector is to provide responsive rather than sluggish control of a device. Therefore, if a simulated EMG signal is used to test an algorithm or hardware detector, the testing can be more comprehensive if the signal parameters can be changed under real-time control to simulate force changes. The time lag between a change in the signal parameters and a corresponding change in the detector output can then be measured accurately since the times of both changes are known. Real-time control of the signal parameters provides a rapid method of simulating various force patterns under operator control.

The algorithm proposed in this chapter generates in real-time a simulated EMG signal. Certain aspects of the model show similarity to some of the models mentioned above but it is not based on any of them.

The algorithm allows on-line control of the signal to represent dynamic force behaviour and attempts to be as realistic as possible consistent with real-time computation.

## 4.2 Proposed Computer Model

### 4.2.1 Physical Basis

As for most of the other models mentioned in Section 4.0, the physical basis of the proposed model is the motor unit. Since it has been adequately described in Chapter 3, only certain features of the recorded motor unit action potential applicable to this model will be discussed.

As stated in Section 3.4, the waveshape of the recorded motor unit action potential is dependent on the type of electrodes used and their proximity to the active motor unit. Surface electrodes are used for most prosthetic applications including the particular applications presented in this thesis. In addition, coaxial needle electrodes are extensively used in clinical work. The model should therefore be able to simulate the EMG signals recorded by these two types of electrodes. The motor unit action potential recorded by a surface electrode can be considered to have the diphasic waveform of Fig. 3.4, while the coaxial needle records action potentials with diphasic waveforms or triphasic waveforms similar to that shown in Fig. 3.6. The two recorded waveforms are shown again for convenience in Fig. 4.1.

Although the model is sufficiently general to simulate the EMG signal recorded by different electrode configurations, each implementa-

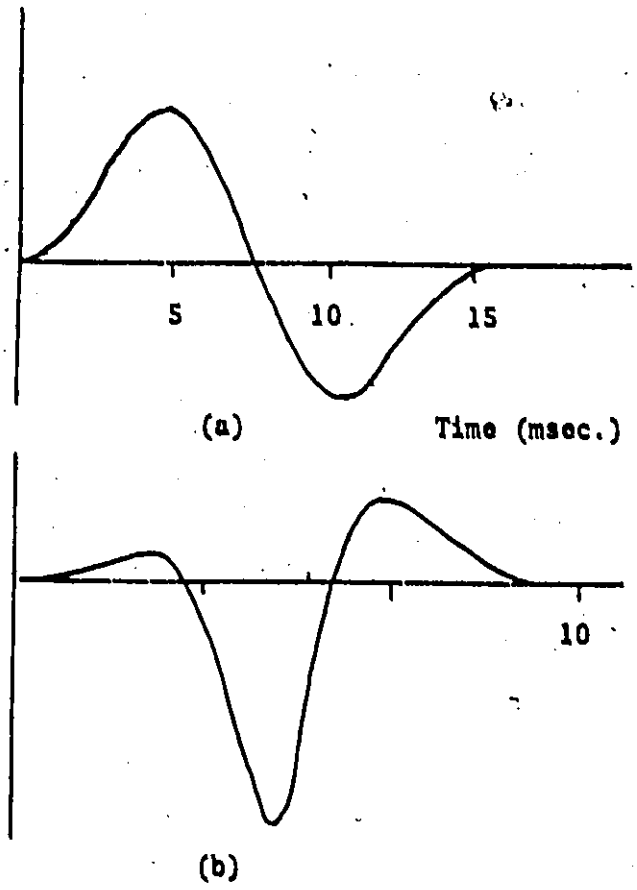


Figure 4.1 Typical motor unit action potentials:
a) diphasic b) triphasic

tion of the algorithm is valid only for the electrode configuration being considered. A more general approach would be to take the basic monophasic waveform of Fig. 3.5 as the motor unit action potential and include a transfer function in the model representing the required electrode configuration. This approach was not followed because of the additional computation time introduced by the electrode transfer function.

### 4.2.2 Formulation of the Model

The computer model attempts to approximate the EMG source described in Fig. 4.2. The model only considers the axon portion of the motoneuron of each motor unit and includes no part of the central nervous system or neuromuscular control mechanisms. For the model the following assumptions are made:

(a) all motor units are uncorrelated;

(b) all recorded motor unit action potentials have the same form and time duration;

(c) the conductive medium between the motor unit fibres and the recording site is purely resistive which allows simple addition of the motor unit potentials.

Assumption (a) can be considered valid especially for normal contractions of low to moderate force levels. As has been stated before, coaxial needles record both diphasic and triphasic action potentials. In addition, the time duration of the recorded action potential is dependent upon the motor unit size and action potential propagation velocity-both of which vary between motor units in a muscle. Assumption (b) will therefore introduce some error in the simulated EMG signal. Although

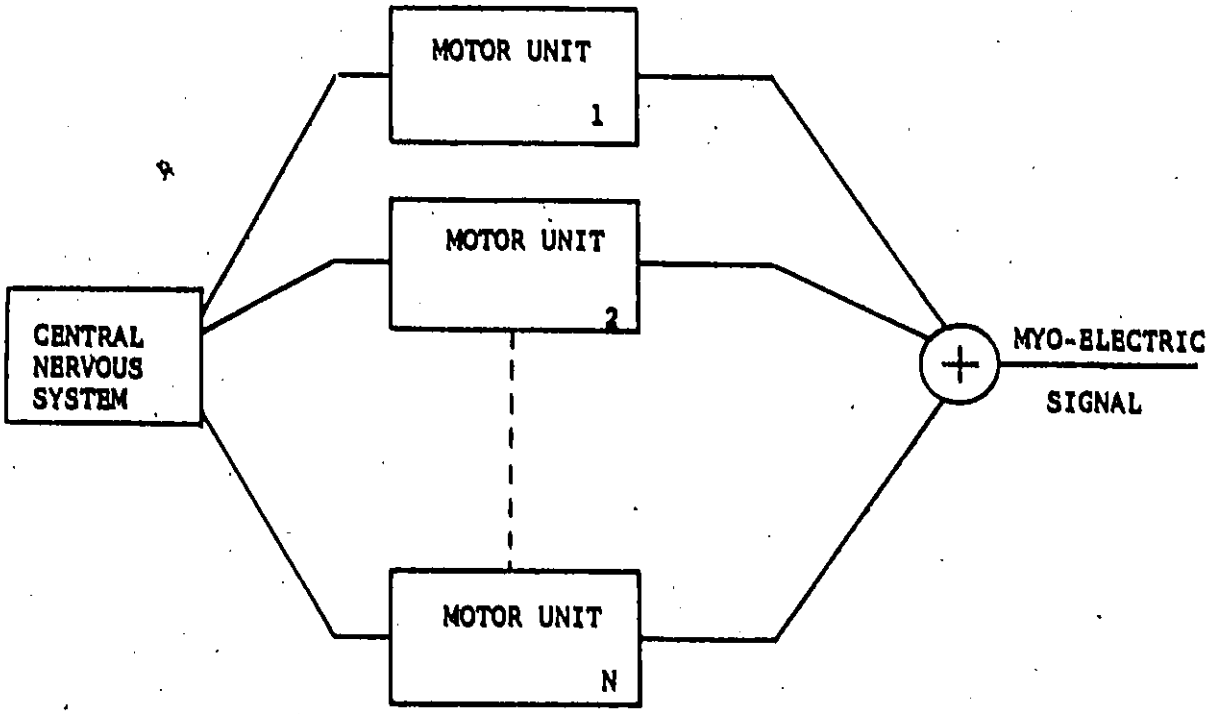


Figure 4.2 Schematic representation of myo-electric signal generation.

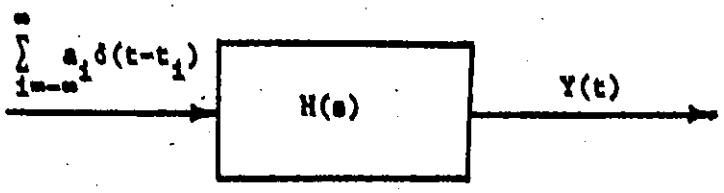


Figure 4.3 Simplified representation of the muscle.

there are capacitive elements in the conductive medium, assumption (c) should not introduce much error. Plonsey (1969) has presented experimental results which show that the action potential waveform remains fairly constant and is only reduced in amplitude as the recording electrodes are moved away from the active fibres.

Each motor unit can be considered a linear time-invariant causal dynamic system with the k th motor unit having as input a nerve impulse train

$$\sum_{i=-\infty}^{\infty} \delta(t-t_{ik}) \qquad (4.2\text{-}1)$$

and transfer function $a_k H(s)$. This impulse train is the stochastic point process described in Section 3.6. The interspike intervals are considered statistically independent and have a Gaussian distribution. Both coaxial needles and surface electrodes record the action potentials from many different motor units located at various distances from the electrodes. The variation in motor unit size and corresponding action potential amplitude preclude deduction of a motor unit distance from the recording site using its recorded action potential amplitude. The value of $a_k$, which is a positive constant for each motor unit, is therefore determined by the motor unit size and its distance from the recording site. In Eqn. 4.2-1, $\delta(t)$ is the Dirac delta function.

Let the electrical response of the motor unit to an impulse arriving at $t_i$ be

$$a_k h(t-t_i); \quad t>t_i \qquad (4.2\text{-}2)$$

The total electrical response of the motor unit to the nerve impulse train can be represented by

$$M(t) = \sum_{i=-\infty}^{\infty} a_k h(t-t_{ik}) \; ; \; h(\tau) = 0, \; \tau<0 \qquad (4.2\text{-}3)$$

This can also be written as

$$M(t) = \sum_{i=-\infty}^{\infty} \int_{-\infty}^{\infty} a_k h(t-u)\delta(u-t_{ik})du \qquad (4.2\text{-}4)$$

Interchanging the order of integration and summation and the position of $a_k$, one obtains

$$M(t) = \int_{-\infty}^{\infty} h(t-u) \sum_{i=-\infty}^{\infty} a_k \delta(u-t_{ik})du \qquad (4.2\text{-}5)$$

Equation 4.2-5 can easily be seen to be a convolution integral representing a stochastic process involving a train of impulses of area $a_k$ acting as input to a linear system (general motor unit) whose impulse response is $h(t)$.

Using Eqn. 4.2-5 the response of the entire muscle can be written as

$$Y(t) = \int_{-\infty}^{\infty} h(t-u) \sum_{k=1}^{N} \sum_{i=-\infty}^{\infty} a_k \delta(u-t_{ik})du \qquad (4.2\text{-}6)$$

where N is the number of motor units. The sum or pool of the individual impulse trains

$$\sum_{k=1}^{N} \sum_{i=-\infty}^{\infty} a_k \delta(u - t_{ik}) \qquad (4.2\text{-}7)$$

is a train of impulses having random areas. Cox and Smith (1954) have studied the pooling of N independent stochastic point processes and determined that a pooled input such as that given by 4.2-7 is completely random with the interpulse intervals approaching an exponential distribution as N approaches infinity. They state that this result may be expected to hold irrespective of the precise distribution of the individual processes. In addition, if the individual trains are renewal processes (interspike intervals are statistically independent) then the pooled input is a renewal process. Even though the interspike intervals of each impulse train given by 4.2-1 can be assumed to have a Gaussian distribution, in general the mean ISI and standard deviation are different for each motor unit. Although N can be considered large for surface recorded EMG, for coaxial needle electrodes it is small especially at low force levels. Therefore the precise nature of the inter-impulse interval distribution of the pooled input cannot be derived. The assumption of an exponential distribution is probably the best one from a theoretical point of view. However, this distribution is not the best choice if one considers the computational effort required to generate the random variable.

The pool of individual impulse trains given by 4.2-7 can also be written as

$$\sum_{j=-\infty}^{\infty} a_j \delta(t-t_j) \qquad (4.2\text{-}8)$$

where $a_j$ and $t_j$ are random variables. The response of the muscle can then be written as

$$Y(t) = \int_{-\infty}^{\infty} h(t-u) \sum_{j=-\infty}^{\infty} a_j \delta(u-t_j)\,du \qquad (4.2\text{-}9)$$

The relevant portion of Fig. 4.2 consequently reduces to the form shown in Fig. 4.3. Since the motor unit is a physical system $h(t-u) = 0, t<u$ (i.e. motor unit does not respond before an input pulse is applied at the neuromuscular junction). In addition, if the train of impulses given by 4.2-8 can be considered to start at t=0, the general convolution integral given by Eqn. 4.2-9 can be written as

$$Y(t) = \int_{0}^{t} h(t-u) \sum_{j=0}^{\infty} a_j \delta(u-t_j)\,du \qquad (4.2\text{-}10)$$

Equation 4.2-10 gives the general form of the EMG signal model proposed in this chapter.

### 4.2.3 Formulation of the Model Algorithm

Although Eqn. 4.2-10 gives a continuous-time EMG signal, a computer model must be a discrete-time or sampled-data system. This presents no restrictions on analysis of the signal since any real EMG signal acquired and stored by the computer is also a sampled-data sequence.

The output of the model algorithm must be a sequence of sample values with sample period $\Delta t$.

The general motor unit response or action potential h(t) will be assumed to have one of the forms shown in Fig. 4.1. Although the action potential decays exponentially, it can be considered essentially zero after a time duration $t_D$. The nth output sample can then be given by

$$Y(t) = EMG(n\Delta t) = \sum_{i=1}^{\infty} a_i h(t-t_i) \; ; \; h(\tau) = 0, t_D < \tau < 0 \qquad (4.2\text{-}11)$$

The algorithm must therefore generate a sequence of impulse arrival times $t_i$ and associated motor unit constants $a_i$. In the proposed algorithm an occurrence table composed of the pairs $(t_i, a_i)$ is continuously updated with new pairs while the output samples are being calculated. In order to calculate an output sample Y(t), it is necessary to generate only those pairs with $t_i \leq t$. In the calculation of this EMG sample Y(t), only those impulses occurring in the interval $[t-t_D, t]$ need be considered. Hence, for each sample Y(t), the occurrence table need contain only those pairs with $t-t_D < t_i \leq t$. Pairs with $t_i < t-t_D$ can therefore be deleted and the occurrence table remains arbitrarily small (dependent on mean interpulse interval) and requires little storage space even if the algorithm runs for hours. The method of deriving Y(t) using Eqn. 4.2-11 is shown in Fig. 4.4.

For each pair $(t_i, a_i)$, the impulse arrival time $t_i$ is calculated using the equation

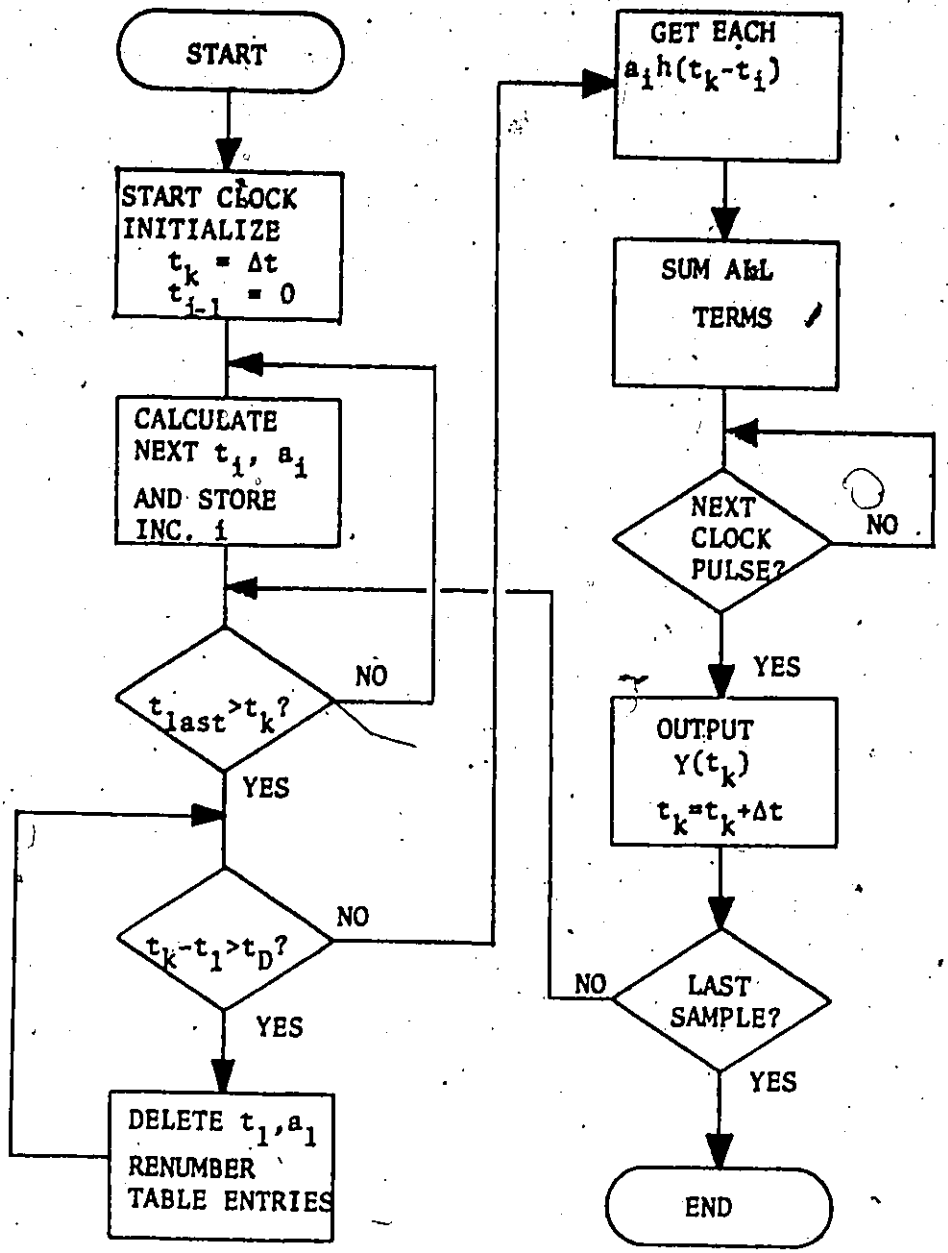


Figure 4.4 Flowchart of simulation algorithm.

$$t_i = C\Delta t_i + t_{i-1} \qquad (4.2\text{-}12)$$

where $C\Delta t_i$ is the interpulse interval and $\Delta t_i$ is a random variable. The constant C is determined by the required mean interpulse interval and hence decreases as the required force level increases. The motor unit constant $a_i$ is calculated by

$$a_i = Dm_i \qquad (4.2\text{-}13)$$

where D is a positive constant which varies as the required force level and $m_i$ is a random variable.

Although some authors (Brody et al., 1974) have assumed the pooled input given by 4.2-8 to be a Poisson pulse train (as far as the impulse arrival times are concerned), this is impossible to achieve in real-time simulation. The computation time required to derive a Poisson or Gaussian variable precludes the use of these distributions for the interpulse intervals. The random variables $\Delta t_i$ and $m_i$ are therefore assumed to have uniform distributions in the interval $[0,1]$ and are approximated by a multiplicative congruential pseudo-random number generator.

It is possible to derive the statistics of the impulse train generated by the algorithm. If the algorithm generates M impulse arrival times to simulate a constant force EMG signal Y(t), using Eqn. 4.2-10 the impulse train can be written as

$$P(t) = \sum_{i=1}^{M} a_i \delta(t-t_i) \qquad (4.2\text{-}14)$$

The i th pulse occurs at time $t_i$ which is a sum of i independent random variables (provided the pseudo-random number generator produces uncorrelated successive numbers).

$$t_i = C\Delta t_1 + C\Delta t_2 + \ldots + C\Delta t_i \qquad (4.2\text{-}15)$$

Since the $\Delta t_i$ and $m_i$ are random variables having a rectangular or uniform distribution over the interval $[0,1]$, $C\Delta t_i$ and $Dm_i$ have means $C/2$ and $D/2$, and variances $C^2/12$ and $D^2/12$ respectively. Thus the mean $E(t_i)$ and variance $V(t_i)$ of $t_i$ are given by

$$E(t_i) = E\sum_{j=1}^{i} C\Delta t_j$$

$$= \sum_{j=1}^{i} E(C\Delta t_j) = \frac{iC}{2} \qquad (4.2\text{-}16)$$

$$V(t_i) = V\sum_{j=1}^{i} C\Delta t_j$$

$$= \sum_{j=1}^{i} V(C\Delta t_j) = \frac{iC^2}{12} \qquad (4.2\text{-}17)$$

The central limit theorem states essentially that the distribution of the sum of a large number of independent random variables will approach the Gaussian distribution regardless of the probability distribution of the individual variables. The probability density function of $t_i$ is

therefore given by

$$f(t_i) = \frac{1}{\sqrt{\frac{\pi iC^2}{6}}} \exp\left[\frac{-\left(t_i - \frac{iC}{2}\right)^2}{\frac{iC^2}{6}}\right] \qquad (4.2\text{-}18)$$

This distribution is valid for all but the first few $t_i$ generated for the simulated signal. In the algorithm the first 200 $\Delta t_i$ are discarded to ensure independent successive random variables. If other distributions had been used for the generated interpulse intervals, only the variance of the distribution given by Eqn. 4.2-18 would have been affected.

In Eqn. 4.2-11 each motor unit action potential voltage $h(t-t_i)$ can be calculated from an analytical expression such as those used by some authors (Parker and Scott, 1973; Person and Libkind, 1970). In the proposed algorithm h(t) is a table of from 30 to 100 amplitudes (length depends on form of h(t)) of the action potential for the interval $[0,t_D]$ which can be calculated from an analytical expression or obtained directly from low-force real EMG signals. Earlier versions of the algorithm used linear interpolation to obtain voltage amplitudes $h(t-t_i)$ for $(t-t_i)$ falling between two table sample times. However, with a 30.- 100 sample action potential table and table sample period less than .5 msec, relatively little signal distortion was introduced (1 msec output sample period) if the amplitude values were read directly from the table. If $(t-t_i)$ falls between two table sample times $t_K$ and $t_{K+1}$, then $h(t-t_i)$ assumes the value of $h(t_K)$. This method of amplitude table look up was

used to minimize sample computation time.

## 4.3 Computer Implementation

### 4.3.1 General Remarks

A PDP 11/45 operating under the DOS Monitor system was used for real data acquisition, implementation of the simulation algorithm and analysis of the real and simulated EMG signals. A hardware and software system was therefore designed and implemented by the author to accomplish these various tasks. The hardware system allows the acquisition and display of analog data and real-time clock control of program execution. This system and some of the software written are described in Appendix B.

The simulation algorithm described in Fig. 4.4 was written in Fortran IV and made interactive with the computer keyboard. For each program run simulating constant force EMG signals, the action potential duration $t_D$, the interpulse multiplier C, the amplitude multiplier D, the output sample period $\Delta t$, and the choice of action potential waveform h(t) can be entered from the keyboard. The algorithm is synchronized with the real-time clock described in Section B.2 which is switched to run at a frequency $1/\Delta t$. This clock controls the running program through hardware interrupts and not only outputs each successive sample at $\Delta t$ intervals but also causes the algorithm to cease running if the sample computation time exceeds $\Delta t$ (i.e. synchronization is lost).

All the parameters mentioned above, and the $a_i$, $t_i$ and output samples are real or floating point numbers to avoid overflow and scaling

problems. The multiplicative congruential pseudo-random number generator used is that of the PDP 11 library, has the form

$$x_{i+1} = (2^{16}+3)\, x_i \bmod 2^{32} \qquad (4.3\text{-}1)$$

where $x_i$ and $x_{i+1}$ are successive random numbers, and uses double-precision integer arithmetic to calculate the pseudo-random number before scaling it to a floating point number in the interval $[0,1]$. The period of this pseudo-random number generator, which determines the period of the simulated signal is approximately $2^{29}$. Each 2048 samples of the simulated signal were displayed on a storage monitor for visual analysis and then stored in a file on disk for later signal processing.

The simulation algorithm written in Fortran IV runs at a maximum sample rate of 200 Hz when considering a realistic number of active motor units. This frequency limitation, which results mainly from the characteristics of the basic PDP 11 Fortran compiler, causes the Fortran version of the algorithm to be marginally suitable for only surface EMG signal simulation.

Since the minicomputer used has a floating point processor and semiconductor memory, it was decided to write the algorithm itself including the pseudo-random number generator in Pal 11R assembly language and store it in MOS memory (the clock routines were already written in assembly). All parameters were kept as floating point numbers as in the Fortran IV version. This version of the algorithm runs at a maximum rate of 2 kHz and requires approximately 550 words of storage.

The maximum output sample rate is determined by the action

potential duration $t_D$ and the mean interpulse interval $\overline{C\Delta t_i}$. At a 1 kHz sample rate, a maximum average of 3 motor unit action potentials can be contributing to the simulated EMG signal sample. For a time duration $t_D$ of 16 msec, this number of contributing action potentials corresponds to a mean interpulse interval $\overline{C\Delta t_i}$ of 6 msec. In Chapter 5 a force detection algorithm is proposed, one form of which is a positive peak detector (a positive peak being defined as a change in the sign of the slope of the EMG signal from +ve to -ve). If the model assumption that the surface EMG signal is composed of the superposition of diphasic action potentials is valid, then the number of positive peaks of the signal in a certain period should be a measure of the number of contributing action potentials in that period. Peak counts (for peaks greater than a minimum peak-to-peak amplitude) for typical surface EMG signals recorded for .45 kg. to 3.6 kg. force levels (presented in Chapter 6) vary from 32 to 86 for a .5 sec. window corresponding to mean interpulse intervals of from 15.6 to 5.8 msec. In addition, visual examination of needle recorded EMG signals indicates that the mean interpulse intervals of discernable spikes for the same force range have the same order of magnitude (i.e. 10 msec for 1.25 kg. force). Therefore, considering mean interpulse intervals, sufficiently realistic EMG signals can be simulated with a 1 kHz sample rate.

For the electrode configurations used, the measured bandwidth of needle and surface EMG signals was less than 500 Hz. For the needle recorded EMG signals there was some signal power above 500 Hz but it was very small. A sample rate of 1 kHz was therefore used to simulate both surface and needle EMG signals.

### 4.3.2 Derivation of the Action Potential Table

#### Measurement and Interpretation of Needle Recorded EMG Signals

Using .30 mm. coaxial needle electrodes, EMG signals for different force levels of isometric contraction (0-3.6 kg.in .45 kg. increments) were recorded from the biceps brachii of a normal subject at an elbow angle of approximately 120°. The amplifier was a.c.-coupled and its passband was set at 3 Hz to 10 kHz. The signals were then sampled at 10 kHz and stored on a magnetic disk in a file of ten 10,000 sample records. The system used for recording and processing the EMG signal is described in Section B.1. The signals were displayed on a storage monitor or incremental plotter using the programs mentioned in Section B.1. A 10 kHz sample rate was sufficient to give an accurate visual representation of the needle recorded signal.

Motor unit action potentials could be identified in each record for all force levels. These action potentials appeared as sharp negative spikes superimposed on a background of integrated smaller spikes and low frequency baseline fluctuations. For each force level, the spike amplitudes fell into distinct groups representing action potentials from the same motor unit or motor units of the same size and equidistant from the recording electrodes. As the force level increased, the average amplitude of the largest spikes in a record also increased indicating recruitment of higher threshold larger motor units. Spikes from low threshold motor units which appeared as the largest spikes in low force records also appeared in higher force records with amplitude unchanged indicating that these units were also still active at higher force levels.

Although coaxial needle electrodes are not sufficiently selective to allow precise measurements of motor unit activity, some general observations could be made. From the population of the largest spikes in a record, it could be seen that low threshold motor units discharge with higher frequency than higher threshold units. In typical record segments 9 of these spikes occurred in 200 msec of a .45 kg. record, while 2 occurred in a 2.7 kg. record of equal length. In addition, the ratio of amplitudes of the largest spikes in a 2.7 kg. record to those in a .45 kg. record was approximately 5:1. Although precise measurement of the time duration of each large spike was impossible due to the presence of noise (other much smaller action potentials superimposed on the large spikes) this duration can be considered to vary between 2 and 3 msec for all force levels considered. The above observations agree with the recruitment mechanism outlined in Section 3.5. The model assumption that all action potentials have the same waveform and time duration seems reasonable since most of the observed spikes had the same general shape and the variation in spike time durations was small.

Implementation of Triphasic Action Potential

Although isolated spikes could be observed in all records, isolated action potentials (negative spike plus one or more positive phases) only appeared in low force EMG signal records. A triphasic action potential with a time duration of 5 msec was chosen from a .45 kg. record and the 50 amplitude values read from the record. Power spectral density calculations using the FFT routine described in Chapter 5 showed

no d.c. component for EMG signals recorded with the coaxial needle electrodes and amplifier settings used. The a.c.-coupling and 3 Hz to 10 kHz passband of the amplifier ensures a zero-mean signal if the signal period is sufficiently long, but an EMG signal segment of 5 msec duration will not necessarily have a zero mean. The recorded action potential had a negative d.c. component due to the large negative spike.

In order to have a zero-mean simulated EMG signal, the action potential itself must have a zero mean. Therefore the recorded action potential had to be high-pass filtered before it could be used to construct a zero-mean action potential table h(t). A 2048 sample periodic signal composed of this action potential was constructed and its discrete Fourier transform calculated using the FFT routine mentioned above. Setting the first N coefficients equal to 0 and applying the inverse Fourier transform resulted in a periodic signal composed of zero-mean action potentials with a waveform similar to that shown in Fig. 4.1(b). For a signal composed of alternate 50 - sample action potentials and 50 - sample spaces, the best value for N was found to be 24. This zero-mean action potential was then used to construct a 50 or 100 sample amplitude table h(t). In the simulation of needle electrode signals the 100 sample table was used.

Measurement and Interpretation of Surface Recorded EMG Signals.

Surface EMG signals were recorded using the dry silver disc electrodes described in Section 2.4 placed over the belly of the biceps brachii. These signals were also recorded for force levels of 0 to 3.6 kg. of isometric contraction at an elbow angle of 120°. The ampli-

fier was a.c.-coupled and its passband was set at 3 Hz to 10 kHz to remove the low frequency cable motion artifact resulting from the use of high impedance electrodes. These signals were then sampled at 2 kHz and processed using the hardware and software system described in Section B.1.

Visual examination of the EMG signals from different force levels revealed that they were random signals with increasing r.m.s. amplitudes as the force level increased. However, diphasic waves similar to the waveform of Fig. 4.1(a) occurred frequently in the EMG signals recorded for all force levels. In addition, for each force level the amplitudes of these waves fell into distinct groups such that a diphasic wave of the same amplitude occurred frequently at random intervals in a particular record (as if they were produced by the same motor unit). The waveform remained constant for all force levels and only increased in amplitude as the force level increased. As for the needle electrode signals some properties of the recruitment mechanism could be inferred from these signals. As the force level increased, the average amplitude of the largest waves in a record also increased indicating recruitment of higher threshold larger motor units. The ratio of the amplitudes of the largest waves in a 3.6 kg. record to those in a .45 kg. record was approximately 5.4:1 which is similar to the ratio for the needle electrode signals.

Since there is more superposition of action potentials in a surface EMG signal, only the frequency of occurrence of the largest waves in a record could be determined - most smaller waves being distorted. It could be seen that once a larger motor unit is recruited its

discharge frequency increases as the force level is increased. In all the records the period of the diphasic waves varied 1 or 2 msec about an average of 15 msec which is of the same order as the time duration of surface recorded diphasic motor unit action potentials.

Implementation of Diphasic Action Potential

A diphasic wave of 15 msec duration (i.e. 31 samples) occurring in a .45 kg. force signal record was therefore taken as representative of the motor unit action potential and a 31 sample action potential table h(t) constructed using its amplitudes. Person and Libkind (1970) using simulation studies have shown that if an interference pattern (EMG signal) is constructed by the random superposition of a number of motor unit action potential trains, the mean period d of the diphasic waves in the interference pattern is given by

$$d \simeq .91c \qquad (4.3\text{-}2)$$

where c is the period of the diphasic action potentials of each motor unit train.

Therefore, even though surface recorded EMG does not show isolated motor unit action potentials, it may be used to derive some parameters of the action potential. It is only possible to consider the diphasic waves of the EMG signal as representative of action potentials if the EMG signal is not saturated (i.e. insufficient "equal" amplitude action potentials are superposed to distort all the motor unit potentials). Since only moderate forces were considered, all the records met this condition and repetitive diphasic waves could be observed even in 3.6 kg. records.

## 4.4 Simulation Results

The needle and surface electrode signals recorded for Section 4.3 were sampled at 1 kHz and stored on a disk using the system described in Section B.1. The records were then split into 2500 sample segments and the autocorrelation function calculated using the method described in Chapter 5. In addition, the normalized power spectral density was calculated for the first 2048 samples of each segment using the FFT routine described in Chapter 5. Simulated EMG signals were generated in real-time for both needle and surface electrode configurations in 2048 sample records. The autocorrelation functions and normalized power spectral densities were then calculated for these signals and compared with those obtained from real EMG signals. The simulated EMG signal visually resembled the real signal especially for surface electrode signals.

### 4.4.1 Autocorrelation Curves of Real and Simulated Signals

It was found that only the first 15-20 msec of the autocorrelation curve of a real EMG signal contains significant information. During simulation studies it was found that the time duration of the action potential (whether diphasic or triphasic) determined the first zero crossing $\tau_0$ of the autocorrelation curve. If the time duration $t_D$ and the action potential waveform is fixed, the variation in the next 8-12 msec of the curve is determined by the mean interpulse interval (i.e. the number of active motor units and their discharge frequencies). Figure 4.5 shows typical results of a simulation study of needle electrode signals using the triphasic action potential. The time duration $t_D$ was

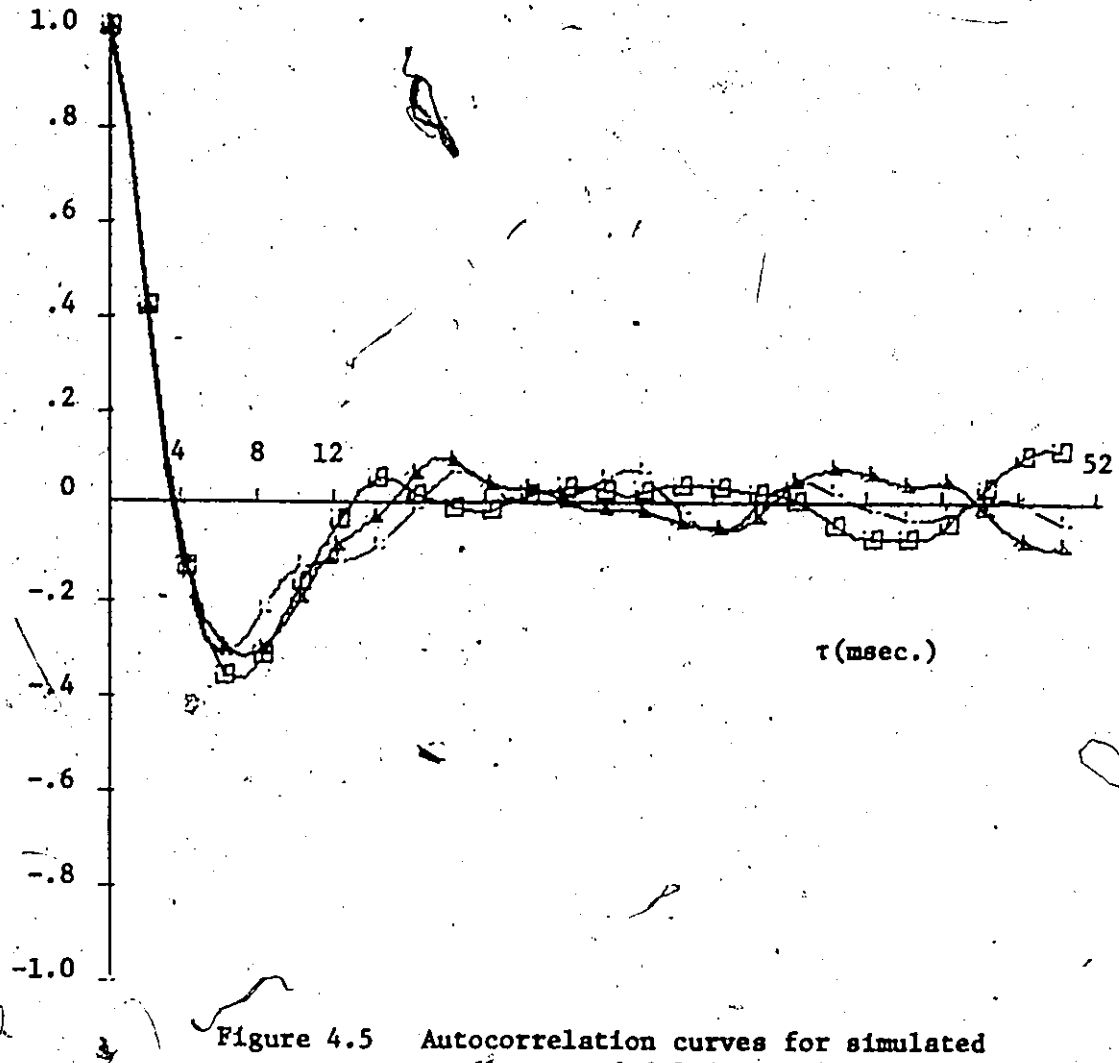


Figure 4.5 Autocorrelation curves for simulated needle recorded EMG signals. Action potential time duration is 45 msec.; average interpulse interval:

□ 18 msec.

Δ 23 msec.

L 35 msec.

fixed at 45 msec and the mean interpulse interval varied as shown). The next zero crossing $\tau_1$ of the autocorrelation curve decreases as the mean interpulse interval decreases which is expected since increased superposition of the action potentials results in greater randomness in the resulting EMG signal. Similar results were also obtained for surface simulated signals.

There is considerable variation after $\tau$=12 msec in the autocorrelation curves of real surface and subcutaneous EMG signals even for the same force levels as shown in Figures 4.6 and 4.7. A typical autocorrelation curve of a real EMG signal was therefore selected and the algorithm parameters $t_D$ and $\overline{C\Delta t}_i$ empirically determined by fitting the autocorrelation curve of the simulated signal to it. Figures 4.8 and 4.9 show a comparison of the autocorrelation curves for real and simulated EMG signals. A reasonable fit for simulated surface electrode EMG signals was obtained with an action potential duration of 16.5 msec and 15 msec average interpulse interval. For needle electrode simulated signals, a good fit was obtained with $t_D$ equal to 50 msec (corresponding to a negative spike duration of 6 msec) and $\overline{C\Delta t}_i$ equal to 25 msec.

As can be seen, the graphical autocorrelation curves for real needle signals are not smooth for the first 16 msec indicating that a sample rate higher than 1 kHz should really be used to achieve better fits (i.e. provide more points for the same time interval). However, a 2 kHz rate is outside the algorithm's limits of realistic simulation. The recorded surface EMG signals, on the other hand, have lower frequency content than the intramuscular signals and a 1 kHz sample rate is sufficient to achieve good fits of the autocorrelation curves. Since the first zero crossing $\tau_0$ of the autocorrelation curve is determined by the

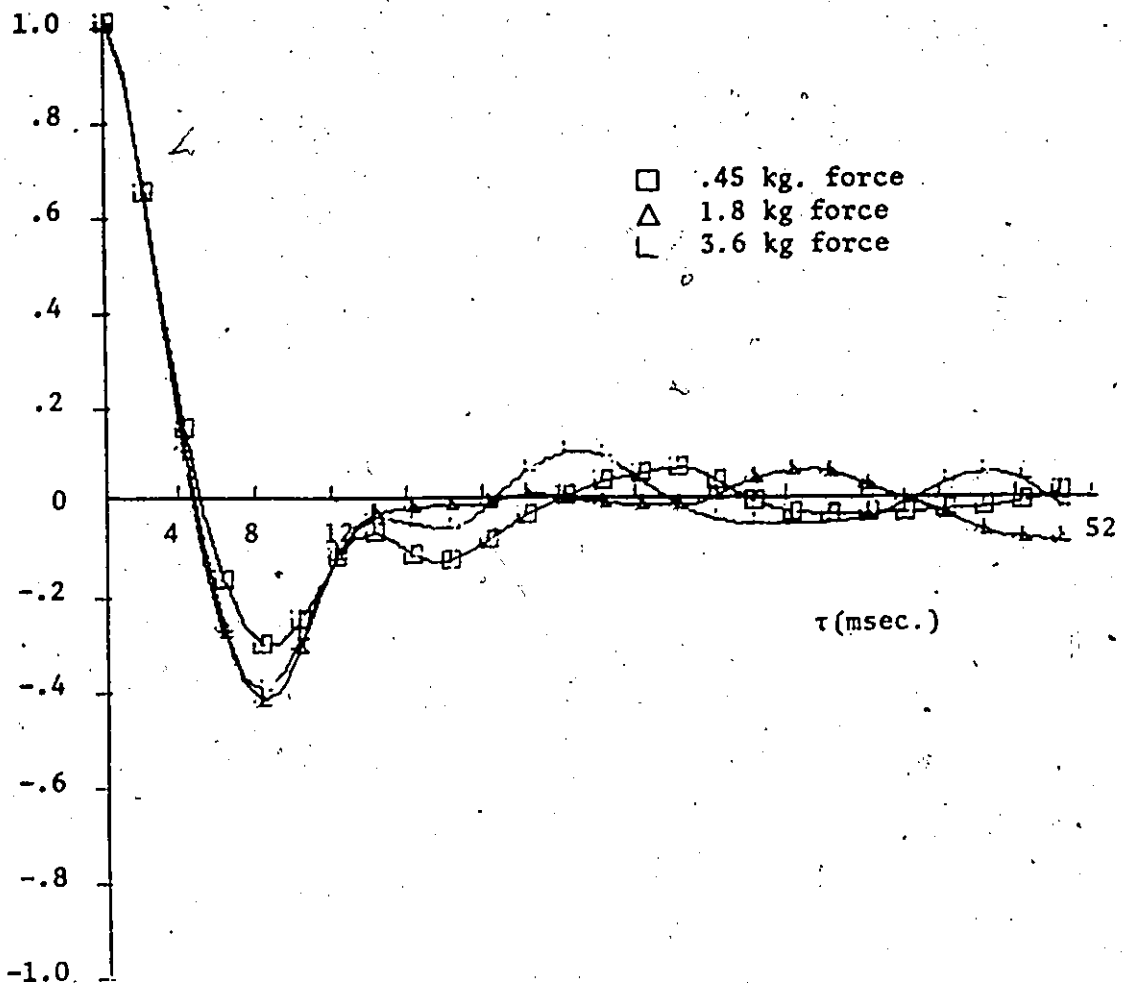


Figure 4.6 Autocorrelation curves for real surface electrode EMG signals. 1 kHz sampling rate.

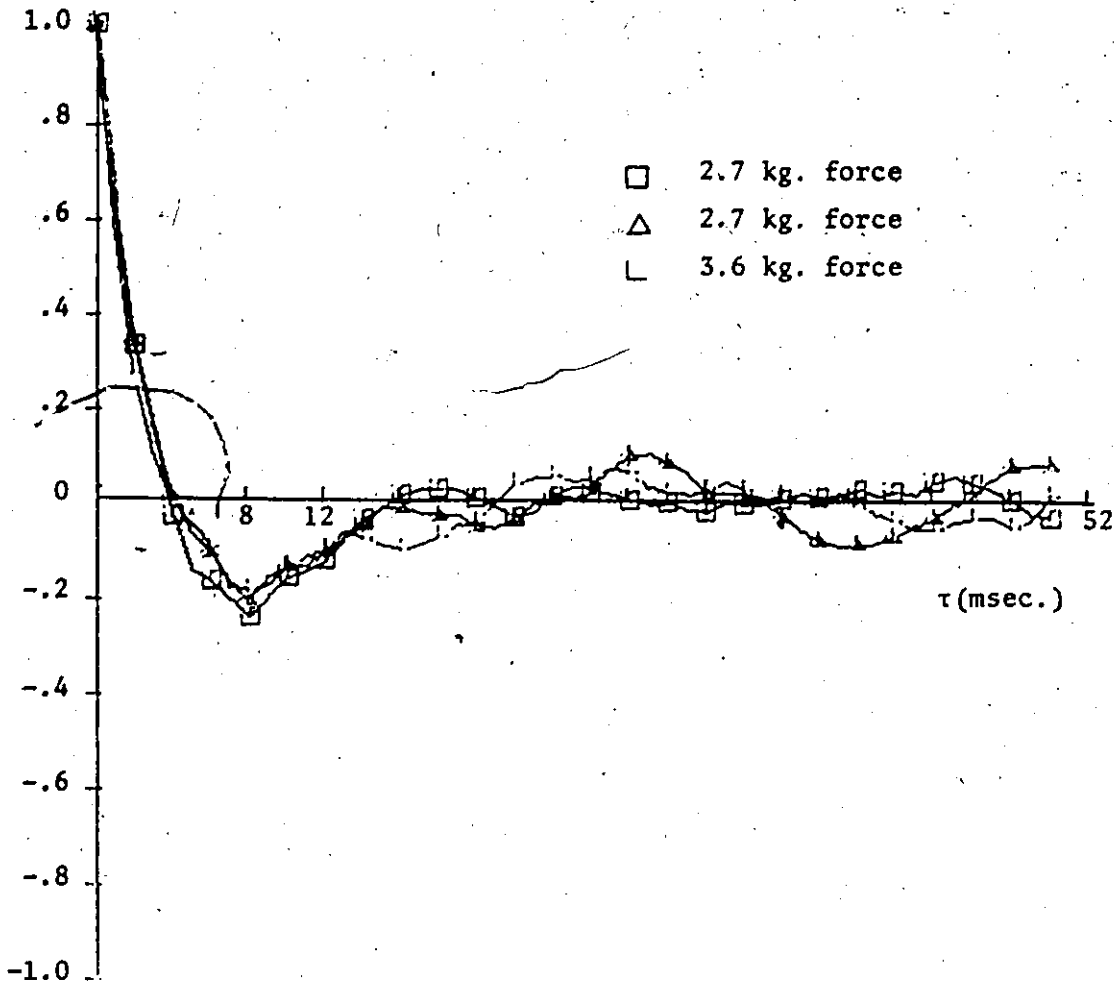


Figure 4.7 Autocorrelation curves for real needle electrode EMG signals. 1 kHz sampling rate.

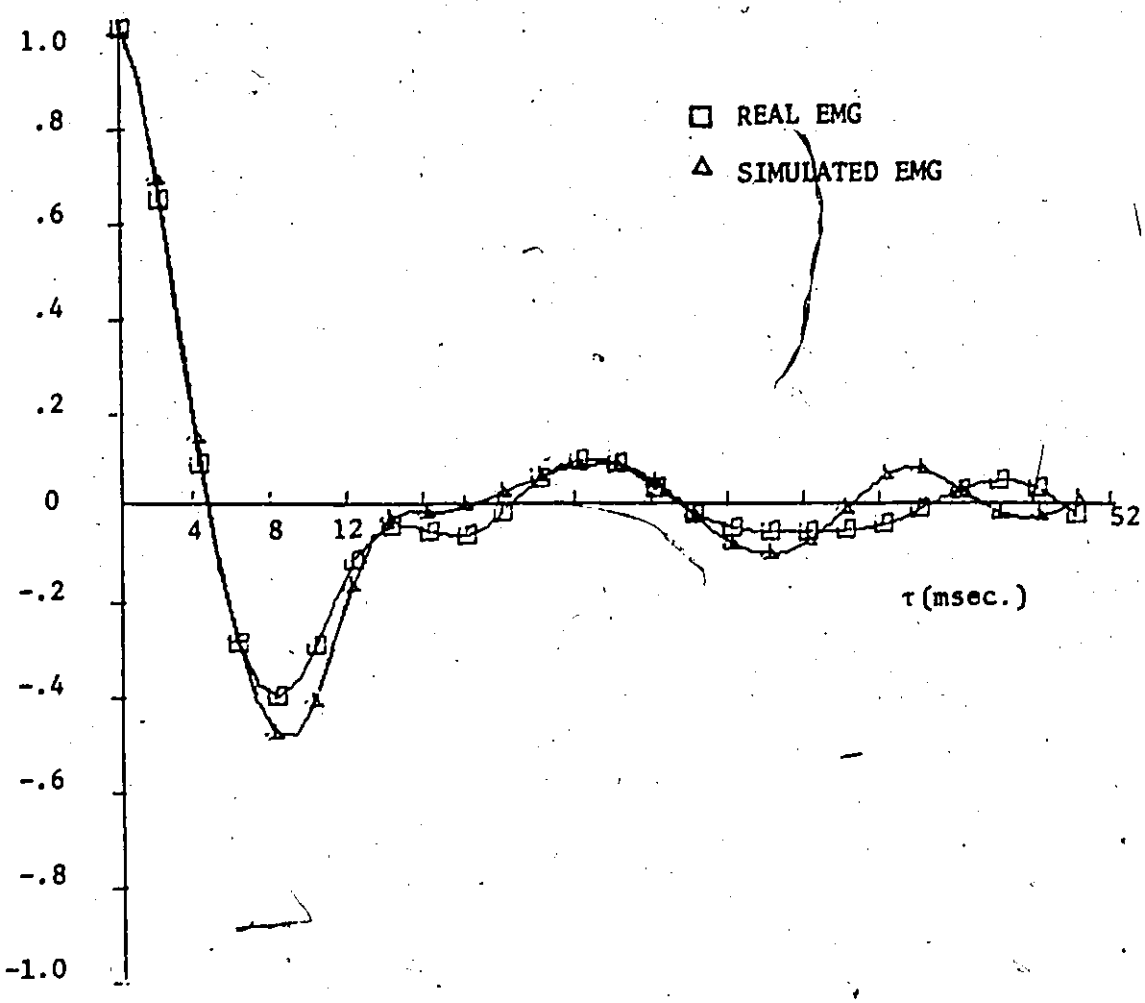


Figure 4.8 Autocorrelation curves for real and simulated surface EMG signals. 1 kHz sampling rate; 3.6 kg. force.

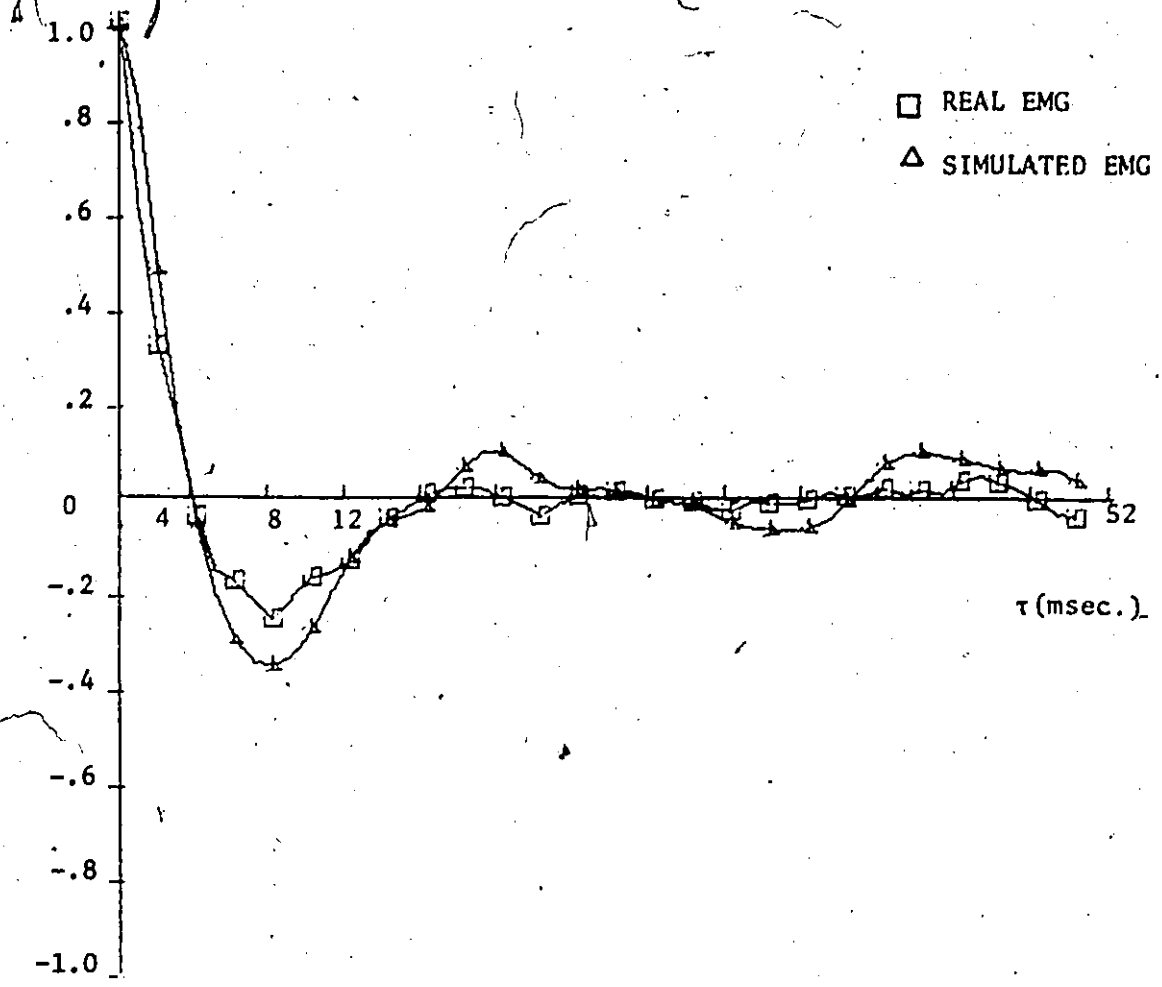


Figure 4.9 Autocorrelation curves for real and simulated needle electrode EMG signals. 1 kHz sampling rate; 2.7 kg. force.

action potential time duration, it can be related to the period of the diphasic waves of the surface EMG signal. As mentioned in Section 4.3.2, the average period of these waves ,d, is 15 msec. From Fig. 4.8, $\tau_0$ = 4.63 msec and $t_D$ = 16.5 msec. This relationship is then given by

$$\tau_0 = .27t_D = .31d \qquad (4.4\text{-}1)$$

These results agree closely with those of Person and Libkind (1970) even though they used a different simulation technique employing superposition of a Gaussian point process. Therefore, if the autocorrelation function of the surface EMG signal to be simulated is calculated, $\tau_0$ can be used to establish $t_D$ of the diphasic action potential. A fit of real and simulated signal autocorrelation curves can then be achieved by varying $\overline{C\Delta t}_1$.

### 4.4.2 Power Spectral Densities of Real and Simulated Signals

The normalized power spectral densities, for the surface EMG signals used to calculate the autocorrelation curves of Fig. 4.8, are shown in Fig. 4.10. Figure 4.11 shows the normalized power spectral densities for the subcutaneous EMG signals used to calculate the autocorrelation curves of Fig. 4.9. The power spectra are normalized with respect to the total spectral power in the signal. The "raw" power spectral density plot calculated for a signal of 2048 samples was too random in shape since it provided a power density for each .49 Hz frequency band. Therefore, in Fig. 4.10 each point represents the average spectral density for a band of 7.8 Hz and is plotted in the

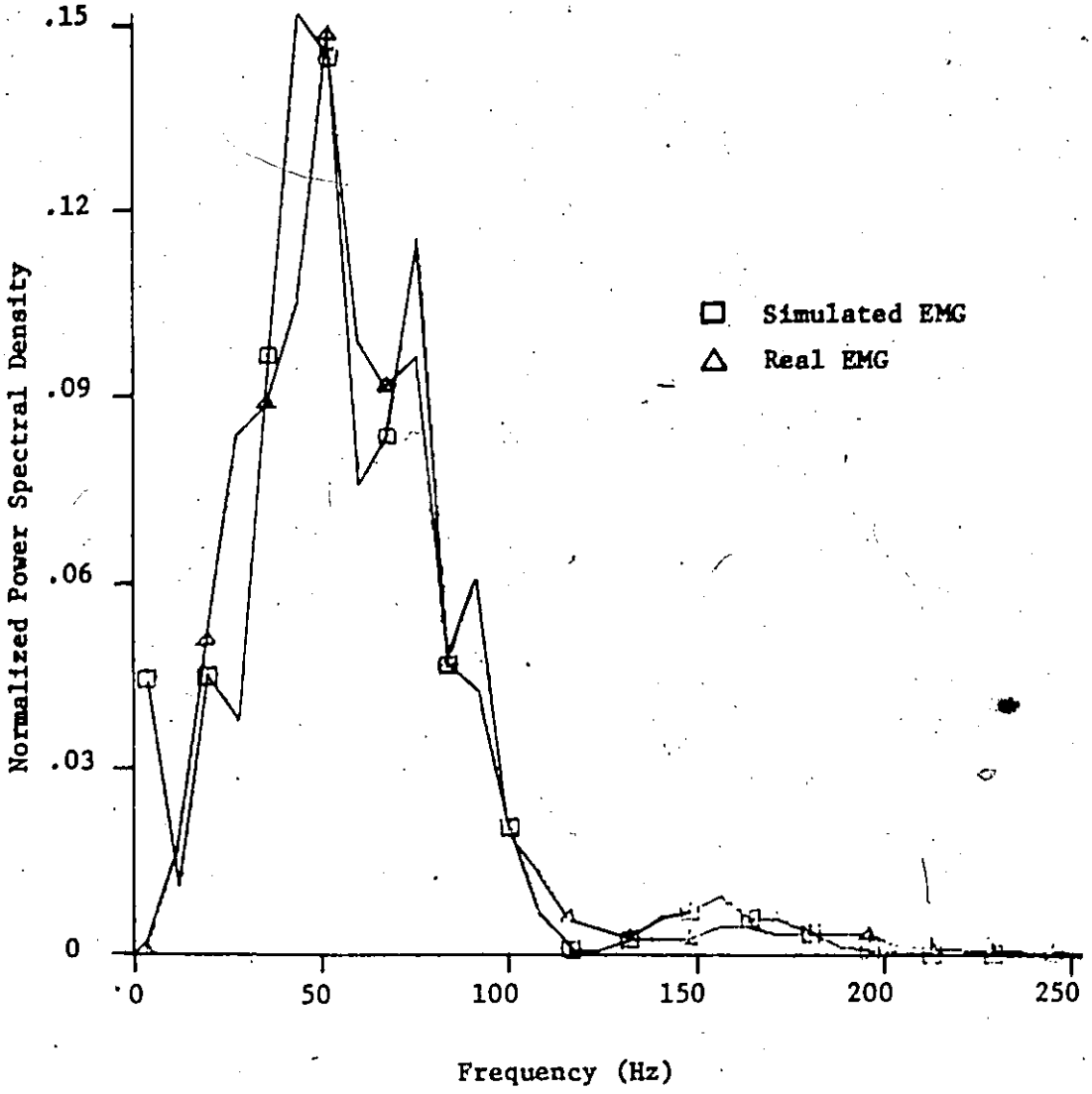


Figure 4.10 Normalized power spectra for real and simulated surface EMG signals. 1 kHz sampling rate; 3.6 kg. force. Power spectra are normalized with respect to the total spectral power. (symbols are plotted every other point)

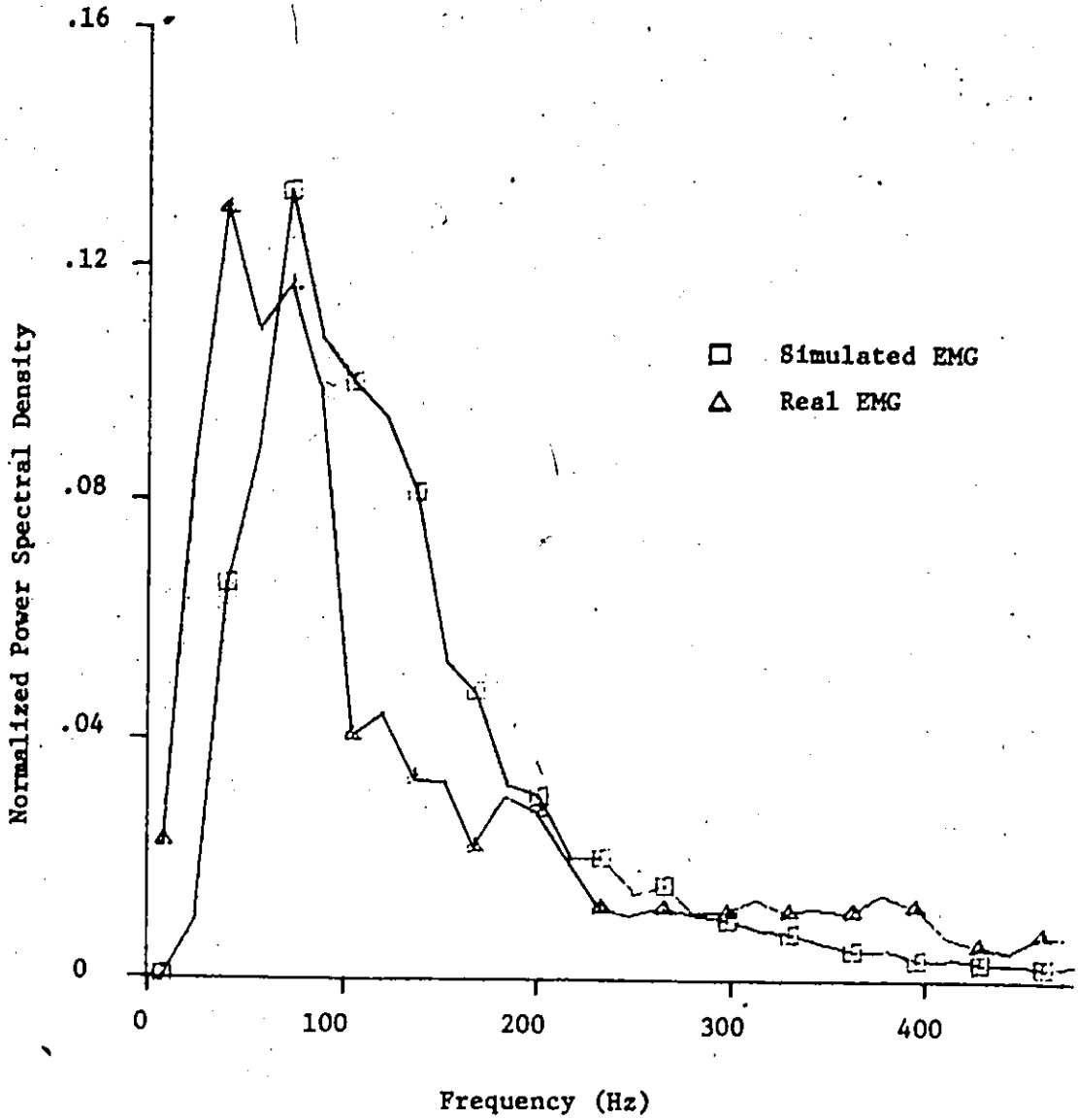


Figure 4.11 Normalized power spectra for real and simulated subcutaneous EMG signals. 1 kHz sampling rate; 2.7 kg. force. Power spectra are normalized with respect to the total spectral power. (symbols are plotted every other point)

centre of the band. Each point in Fig. 4.11 represents the average spectral density for a band of 15.6 Hz. Figure 4.10 shows good agreement between the spectral components of the simulated and real surface EMG signals, considering the stochastic nature of the EMG process. The agreement in Fig. 4.11 is not as good although both signals have the same approximate bandwidth. As stated in Section 4.4.1, a sample rate higher than 1 kHz should really be used to achieve better fits of the autocorrelation curves and hence of the power spectral densities for needle recorded EMG signals.

The significant power density in the 0-8 Hz band of the simulated signal spectrum of Fig. 4.10 can be explained by the fact that the action potential h(t) measured from the real surface EMG signal did not have a zero mean and hence produced a small d.c. component in the simulated signal. In contrast, the a.c.-coupling of the signal acquisition hardware of the real EMG signals ensured zero-mean real surface and subcutaneous signals. From Figures 4.10 and 4.11 it can also be seen that the bandwidth of subcutaneous needle recorded EMG signals is wider than that of surface recorded signals. These frequency plots provide information concerning the firing rate of motor units and as for the autocorrelation curves can also be used to determine the best average interpulse interval $\overline{C\Delta t}_i$ for the algorithm for different force levels.

## 4.5 Discussion

There has been no attempt made to fit the statistical function plots (autocorrelation and power spectral density) of the simulated and real signals in some rigid optimum sense since these plots are not unique

for real signals for the same force level. Although these plots are the most frequently used criteria for comparison of real and simulated EMG signals (Brody et al., 1974; Person and Libkind, 1970; Abdel Azim and Della Torre, 1975) they cannot be used to differentiate between signals representing different moderate force levels of isometric contraction. Although better results are achieved when force levels are far apart, these criteria are not always consistent even when the levels are 4 kg. apart. The average interpulse interval of the pooled impulse trains given by expression 4.2-8 should decrease as the required force level increases due to the recruitment of more motor units and an increase in the discharge frequency of active units (see Fig.3.7). Therefore the simulation results shown in Fig. 4.5 should represent successively higher force levels as $\overline{CAT}_1$ decreases.

However, the autocorrelation curves of real EMG signals do not behave in this prescribed manner. Figures 4.6 and 4.7 are representative of many autocorrelation curves calculated and plotted. In Fig. 4.6 the 1.8 kg. force curve approaches 0 again after the first zero-crossing sooner than the 3.6 kg. force curve contrary to expectations, while in Fig. 4.7 the two 2.7 kg. force curves are not identical and have a second zero-crossing sooner than the 3.6 kg. curve. Similar results are presented in Chapter 6 where the autocorrelation curves and power spectral density plots of surface recorded EMG signals are analyzed with a view to finding their suitability in force detection strategies.

These results may be explained by considering the recruitment and discharge frequency mechanisms explained in Chapter 3. As the required force increases to a certain level, large higher threshold units are

recruited with low initial discharge frequency. Their action potentials are much larger than those of the smaller units already active which are discharging at a higher frequency, and consequently "mask" many of these smaller action potentials, or action potentials from more distant units, contributing to the EMG signal. Hence the power spectrum of the recorded signal can be shifted towards the lower frequencies and the signal can have less apparent integration (i.e. less randomness) even though the force level is higher and more action potentials are contributing to the aggregate signal. As the force level increases again but not enough to recruit even larger units, the power spectrum shifts towards higher frequencies as the discharge frequencies of all active units increase. This effect is possible throughout the range of moderate force levels considered here because of the large number of different size motor units present in the biceps brachii. This effect was also noticed during the visual examination of the EMG signal described in Section 4.3.2 and is discussed further in Chapter 6.

A different criterion should therefore be found to adequately compare the simulated and real signals, which incorporates the recruitment and discharge frequency mechanisms of force control. However, because of real-time simulation limitations and the complex stochastic nature of these mechanisms, it is impossible to include them in the simulation algorithm.

It can be seen from Fig. 4.8 that the method of deriving the action potential h(t) for surface recorded signals is quite adequate since the first parts of the autocorrelation curves coincide. The two curves compare favourably considering the randomness of shape of the

autocorrelation curves of real EMG signals shown in Fig. 4.6. The choice of action potential for subcutaneous simulated signals is not as suitable, as shown by the first 6 msec. of the autocorrelation curves of Fig. 4.9 and the power spectral densities of Fig. 4.11. Perhaps a combination of diphasic and triphasic waveforms rather than just triphasic should be used to simulate these signals. This can be easily done in the present algorithm and requires some additional storage space but no increased computation time. However, the curves of Fig. 4.9 do compare favourably since the first and second zero crossings coincide and they both have the same general shape.

In Section 4.4 the real signals used for comparison were all obtained from one subject. The question therefore arises whether the algorithm using a particular action potential h(t), produces satisfactory results only for the subject whose EMG signal was used to derive h(t). Surface EMG signals were recorded from six adult male subjects using the same electrode configuration as for Section 4.3. The autocorrelation curves and power spectral density plots for these signals are described in Chapter 6. With the exception of one subject, all the autocorrelation curves have the same shape as that of Fig. 4.8 and the maximum variation in the first zero crossing $\tau_0$ is .5 msec. With the same exception, the power spectral density plots all have approximately the same bandwidth although not necessarily the same envelope shape. As stated in Section 4.4, the shape and time duration of h(t) determine the shape of the first part of the autocorrelation curve and the first zero crossing. Therefore, the same h(t) may be used to simulate surface EMG signals for different adult male subjects. However, the different recruitment patterns of the

subjects tested, means that the best mean interpulse interval for each force level will vary from subject to subject.

On-line control of the simulated signal can be easily implemented by connecting a variable voltage source to one of the input A/D channels of the computer to represent a dynamic force input. This channel could then be sampled every 100 msec. and the result used to modify C and D of Equations 4.2-12 and 4.2-13. Each floating point output sample $Y(t_k)$ of Fig. 4.4 can also be scaled to an integer number and output under clock control to a D/A converter rather than stored in 2048 sample files as done for Section 4.3. The output of the converter should then be passed through a 500 Hz low-pass filter (for surface EMG signals) to remove D/A switching noise and provide signal smoothing. The output of the filter can then be considered the analog simulated EMG signal. The above changes can be easily incorporated in both Fortran and assembly language versions of the algorithm if it is to be run on a minicomputer having A/D and D/A facilities.

As stated in Section 4.3.1, a 1 kHz output sample rate only allows simulation of moderate force level EMG signals due to a limit on the number of action potentials contributing to an output sample. This force limitation can be overcome by only increasing D as the required force level increases (i.e. $\overline{C\Delta t}_i$ remains constant). This method is quite adequate if only amplitude characteristics of the EMG signal are considered as is the case in most current EMG processors. A method of extending the lower limit of $\overline{C\Delta t}_i$ would be to make all parameters of the algorithm integers. This would allow simulation of higher force EMG signals and also a higher output sample rate for needle electrode signals.

Unfortunately,if the pseudo-random number generator outputs a random integer,its period is only $2^{15} - 1$ (vs. $2^{29}$ for floating point) severely restricting the period of the output signal. In addition, overflow and scaling problems may result. However, an integer algorithm could perhaps be implemented on other minicomputers less powerful than the PDP 11/45 used.

## 4.6 Summary

In summary, a model of the myo-electric source and its computation algorithm have been developed and implemented on a minicomputer. This algorithm performs real-time simulation of the myo-electric signals recorded from different electrode configurations. This algorithm has been tested for two different electrode systems, pasteless surface electrodes and coaxial needle electrodes and the results compared with real signals recorded using these electrodes. There is good agreement between simulated and real signal autocorrelation and power spectral density plots but analysis of these plots and visual examination of the EMG signal point out the necessity of a more force-sensitive comparison criterion. The algorithm can generate controllable simulated signals at a sufficiently high sample rate to test hardware EMG processors or software detection strategies. No precise physiological interpretation can be derived from the algorithm parameters since the model is too simplified to completely represent the myo-electric source. However, since the algorithm is based on physiological principles, analysis of these parameters can aid in determining better detection strategies.

A computer hardware and software system has also been developed and implemented to sample and convert multi-channel analog EMG signals

into digital records on a mass storage disk. These records can then be processed using Fortran or assembly language programs such as autocorrelation or fast Fourier transform routines. In addition, these signals can be rapidly examined visually and plotted on paper or photographed on polaroid film if required. This system therefore provides an accurate wide bandwidth (0 - 10 kHz) inexpensive method of obtaining graphical plots of EMG or other signals. It can also be used to provide biofeedback and control input information in such applications as the online testing of different EMG detection strategies.

# CHAPTER 5

# PROCESSING OF ELECTROMYOGRAPHIC SIGNALS USED AS A CONTROL SOURCE

## 5.0 Introduction

In Chapter 2 an electromyographic trainer has been described which can be used by a cerebral palsied patient as a simple communication device. Improvements to this trainer were suggested which would allow the control circuitry to make more effective use of the processed EMG signal in controlling the display system. However, a different detection or processing strategy may also result in better control of such devices.

The processing strategy used for the trainer consisted of full-wave rectification followed by low-pass filtering or averaging. This strategy was used because it is most widely accepted for myo-electric control systems (see Section 2.1.3) and is easy to implement using linear integrated circuits. The output of this processor may be considered as composed of the average of the rectified signal (the slowly changing or low-frequency component) that is representative of the contraction level and a ripple (or higher frequency component) partially obscuring the former. An improved processor of this type using a higher order filter would reduce the ripple. However, even for a constant isometric contraction, the "sliding-window" average varies from window to window if short windows are used (i.e. .25-.5 sec.). In addition, the amplitude of the EMG

signal is affected by electrode impedance, electrode and skin movement artifact (movement of muscle relative to skin), cable motion artifact if dry electrodes are used, and joint angle or degree of stretch of the muscle. Other parameters of the recorded EMG signal may be less sensitive to these sources of error and give a more reliable estimate of the contraction level of the muscle.

The surface recorded EMG signal contains both amplitude and frequency information. As outlined in Chapter 3, an increase in the contraction level of a muscle is caused by an increase in the discharge frequency of active motor units and the recruitment of additional motor units. In addition, successively larger motor units are recruited for larger force levels. These mechanisms were considered when developing the simulation algorithm described in Chapter 4. In this algorithm, an increase in force level can be simulated by decreasing the average interpulse interval and increasing the average action potential amplitude (see Section 4.2.3). Hence it is expected that an increase in force level should be accompanied by an increase in the r.m.s. amplitude or the average amplitude of the rectified EMG signal. However, spectral changes indicating increased motor unit activity may not be observable in the recorded EMG signal because of the frequency characteristics of the recording system and the fact that the surface EMG is the temporal and spatial integration of a large number of motor unit action potentials. Although an increase in motor unit activity may cause a shift to higher frequencies in the EMG power spectrum, integration of more action potentials may also result in more smoothing of the signal - hence a shift to lower frequencies in the power spectrum. Alternate detection strategies may therefore involve

amplitude parameters, spectral parameters, or a combination of both. If transient force levels are considered, the changes in EMG parameters will precede the change in force level because of the phase lag between the fibre action potential and the tension developed by the fibre.

Since the EMG signal is to be used as a control source for a communication device, the processor need consider only those signals recorded for light to moderate forces. This constraint on the input signals means that the processor should be able to detect smaller differences in force levels (i.e. 1 kg. in a 4 kg. range for an adult male biceps brachii) rather than gross differences such as 5 kg. in a 20 kg. range for this muscle. However, the exclusion of strong contractions allows one to tailor the processor to a limited range rather than the entire range of contractions and reduces the possible effects of fatigue on the subject's performance and hence facilitates calibration.

In determining suitable alternate detection strategies, it must be kept in mind that the processor should be capable of implementation by reasonably inexpensive hardware. A processor which does not meet this requirement, no matter how elegant or reliable, would have to be discarded. Fortunately, the advent of inexpensive microprocessors allows one to consider strategies which before could only be programmed as processing algorithms on minicomputers. Furthermore, it is envisaged that in the future, microprocessors will become the controllers of environmental control devices because of their continually reduced cost and increased sophistication. The same microprocessor could then provide both the signal processing and control functions. Hence, such methods as pattern recognition can also be considered for possible detection strategies.

Different strategies can be implemented and evaluated by programming suitable algorithms on the PDP 11/45 minicomputer described in Appendix B. This approach avoids the delay and expense of constructing and debugging a variety of hardware processors. In addition, modifications to a processor can be quickly incorporated as program changes to its algorithm rather than redesign of existing electronic circuits. The versatility and speed of such a minicomputer system allows one to test proposed strategies in real-time, hence determining their response to transient force inputs rather than just constant isometric forces.

This chapter describes different parameters of the EMG signal which may be used to provide suitable detection strategies. Since the EMG signal is the result of a stochastic process, some of the statistical functions of the signal can be calculated or measured, and examined as to their suitability in detecting changes in contraction level. The average of the rectified signal (mean absolute value), which has already been mentioned as a suitable processor is such a function. In addition, this chapter considers other statistical functions such as higher-order moments, the autocorrelation function and the power spectral density of the raw EMG signal. Finally, a detection strategy using simple pattern recognition is presented which attempts to extract the motor unit recruitment and discharge frequency information present in surface recorded EMG signals.

## 5.1 Stationarity and Ergodicity Considerations for Electromyographic Signals.

When considering the statistical functions of a stochastic process,

it is desirable that the process be stationary (i.e. its statistical properties are invariant with respect to time of observation). Ergodicity of a stationary stochastic process implies that the time-averaged statistical properties of a single sample function (or record) are equal to the corresponding ensemble-averaged values. Hence all the properties of an ergodic stochastic process can be determined by performing time averages over a single sample record. Therefore, if the statistical functions of the EMG process are to be considered as possible parameters for a detection strategy, the EMG process must be in some sense stationary and ergodic.

When a single time history record is referred to as being self-stationary, it is generally meant that the statistical properties computed over each of a sequence of short time intervals in the record do not vary significantly from one interval to the next. Weak self-stationarity means that only the mean and autocorrelation function need be invariant with respect to time. A sufficient condition for an arbitrary stochastic process to be weakly ergodic (Bendat and Piersol, 1968) is that a single sample record is weakly stationary. Therefore, if a typical single sample record of EMG signal is found to be weakly self-stationary, the EMG process can be assumed to be weakly stationary and ergodic.

Even for constant isometric contraction, EMG signals of long duration are probably non-stationary due to the physiology of the system. However, over a short enough observation time (e.g. 5-10 sec.), the EMG signal may be found to be weakly stationary. Most researchers assume stationarity and ergodicity of short term EMG signal for constant isometric contraction. A practical test for weak self-stationarity of a single sample record is given by Bendat and Piersol (1968). This test has been

used (Abdel Azim, 1975) to examine the stationarity of EMG signals for different levels of isometric contraction which were recorded using the dry electrodes described in Section 2.4.1 and the system described in Appendix B. As a consequence of these tests it can be assumed that the EMG process is weakly stationary and ergodic for a short term constant isometric contraction. The subsequent definitions in the chapter, of the statistical properties of the EMG signal, are based on this assumption.

## 5.2 Mean Absolute Value of the EMG Signal

Since the surface recorded EMG signal x(t) is usually a.c.-coupled, the mean $\bar{x}$ is constrained to be equal to zero and consequently contains no information about the contraction level. As stated before, some measure of the mean absolute value is most commonly used as the control parameter in myo-electric control systems. In general, this mean is given by

$$\overline{|x|} = \lim_{T\to\infty} \frac{1}{T} \int_0^T |x(t)|\,dt \qquad (5.2\text{-}1)$$

where T is the averaging period. In any practical application, however, T is limited to a finite time and only an estimated mean absolute value given by

$$\hat{\overline{|x|}} = \frac{1}{T} \int_0^T |x(t)|\,dt \qquad (5.2\text{-}2)$$

can be obtained. If the signal in the period T is sampled at a frequency greater than or equal to the Nyquist rate (i.e. twice the highest frequency component of x(t)), it can be represented by the train of N samples $x_i$, i = 1,2,3,...,N. The estimated mean absolute value can then also be given by

$$\hat{\overline{|x|}} = \frac{1}{N} \sum_{i=1}^{N} |x_i| \qquad (5.2\text{-}3)$$

The variance of $\hat{\overline{|x|}}$ given by Eqn. 5.2-2 may be large in EMG applications since T is usually limited to a short period (especially in myo-electric control systems). Equation 5.2-3 also gives an estimate of this mean but with the additional estimation error resulting from representing a continuous signal by N discrete samples. In addition, quantization error during analog-to-digital conversion may add to this error. However, with a 10-bit A/D converter, quantization error should be negligible.

Isometrically contracting muscle most certainly shows a direct relationship between the mechanical tension and the integrated (mean absolute value) of the surface recorded EMG signal. This has been demonstrated by many researchers working in the area of muscle mechanics and shown to be a monotonic relationship (see for example Basmajian, 1974). It is therefore the most commonly used property of the EMG signal, not only as a control parameter, but also in the study of muscle mechanics.

### 5.2.1 Analog Measurement of the Mean Absolute Value

The analog processor required to provide an estimate of the mean absolute value of the EMG consists of a rectifier followed by a smoothing

or averaging filter and is shown conceptually in Fig.5.1. As stated in Section 5.0, the output of this processor is composed of the mean absolute value representing the contraction level, and a higher frequency ripple caused by higher frequency components passed by the filter and the estimation error. Both the estimation error and high frequency components can be reduced by using a large filter time constant-hence averaging a longer sample record T. However, in a control situation this can produce a very sluggish and long system response time that reduces operator control. For a communication device this would reduce the maximum obtainable information rate and probably increase the effort required per decision.

The ripple can be reduced by employing a better smoothing filter which does not have a longer settling time. The simplest smoothing filter, the RC filter which is used in many myo-electric controls has frequency characteristics given by

$$F(j\omega) = \frac{1}{1 + j\frac{\omega}{\omega_c}} \qquad (5.2\text{-}4)$$

where $\omega_c = 1/RC$, the 3 db bandwidth. A perfect averaging filter, on the other hand, would have frequency characteristics given by

$$A(j\omega) = \frac{1 - e^{-j\omega T}}{j\omega T} \qquad (5.2\text{-}5)$$

where T is the time over which the filter averages its input. This filter produces a continuous output, each point of which represents the in-

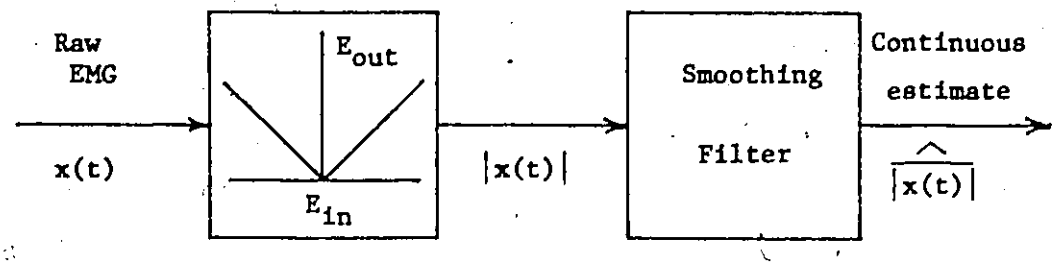


Figure 5.1 Conceptual processor for the mean absolute value of the EMG signal.

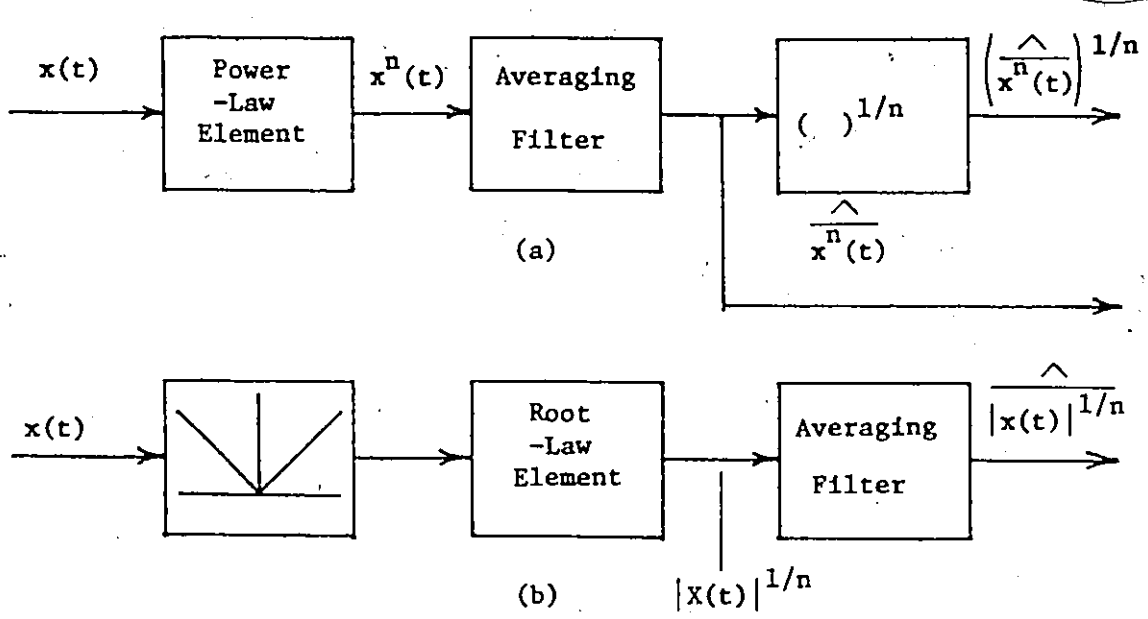


Figure 5.2 Conceptual mean function processors.
(a) Moments (b) Roots

put averaged over the last T seconds. The characteristics given by Eqn. 5.2-5 cannot be produced exactly by any analog device.

Kreifeldt (1971) has compared the effectiveness of three different linear low-pass filters in increasing the mean vs. ripple ratio of the processed EMG. These were a simple RC filter, a third-order Butterworth filter, and a third-order approximation to a perfect averaging filter. He has used common filter settling times of ¼, ½, and 1 second and considered different levels of isometric contraction. His results show that this ratio increases for all filters up to 25 per cent maximal contraction and then remains constant up to 50 per cent maximal. As expected, for all filters the ratio increased for longer filter time constants. The third-order Butterworth is only marginally better than the RC filter but the averaging filter is considerably better (40%) especially for longer settling times. These results confirm expectations since the averaging filter has a much sharper frequency roll-off for the same settling time than the other two and hence passes less high frequency components. It also obviously provides a better estimate of the mean absolute value since it is a closer approximation to Eqn. 5.2-5.

The processing circuit of the electromyographic trainer described in Chapter 2 uses a first-order approximation to the perfect averaging filter. Considering the increased circuitry (plus increased current consumption) for a typical third-order approximation (Garland et al., 1972) it seems that the processing circuit of the trainer is quite adequate if the estimated mean absolute value of the EMG signal is to be used as the control parameter. The third-order approximation would be useful in the laboratory processing of EMG signals, where its increased accuracy may be warranted and circuit cost and power consumption are not considered.

## 5.3 Higher-Order Moments and Mean Roots of the EMG Signal

A first-order statistic, the mean absolute value of the EMG signal, is most commonly used to detect the tension level of an isometric contraction. In addition, the best analog processor for this statistic seems to be a full-wave rectifier followed by an averaging filter - a processor already used for the trainer described in chapter 2. However, even with a perfect averaging filter, the output would not be constant for an averaging period T, even for constant isometric contraction, because of estimation error. The signal-to-noise ratio mentioned above, could then be defined in terms of a mean absolute value-to-variance of the estimated mean absolute value ratio. When T is short, this variance obviously increases and the estimated mean absolute value may no longer be a reliable detector of muscle tension. Perhaps a higher-order amplitude statistic (average of a function of the EMG signal) may have less variance in its estimate for the same averaging period T.

### 5.3.1 Higher-Order Moments of the EMG

The nth moment of the EMG signal x(t) is given by

$$m_n = \lim_{T\to\infty} \frac{1}{T}\int_0^T x^n(t)dt \qquad (5.3\text{-}1)$$

where T is the averaging period (Schwartz, 1959). Again, as for the mean absolute value only an estimate of the nth moment given by

$$\hat{m}_n = \frac{1}{T}\int_0^T x^n(t)dt \qquad (5.3\text{-}2)$$

can be obtained. If the signal in the period T is digitized into N samples $x_i$, i = 1,2,3, ... N, the estimated nth moment can also be given by

$$\hat{m}_n = \frac{1}{N} \sum_{i=1}^{N} (x_i)^n \quad . \qquad (5.3\text{-}3)$$

For Equations 5.3-2 and 5.3-3, the variance of the estimated moment decreases with increasing T.

The estimated second moment $\hat{m}_2$ or mean square value given by

$$\hat{m}_2 = \frac{1}{T} \int_0^T x^2(t)dt \qquad (5.3\text{-}4)$$

has special significance in signal processing and gives the average power of the time function x(t) in the period T. Since the mean of the EMG signal is equal to zero, the second moment is also the variance of the signal. The positive square root of the second moment, the r.m.s. voltage, is then also equal to the standard deviation. The r.m.s. amplitude of the surface recorded EMG signal therefore gives a measure of the spread of instantaneous amplitudes about 0. If the EMG signal x(t) is assumed to have a Gaussian amplitude probability density function, then the r.m.s. and mean absolute value are related by the constant $\sqrt{\pi/2}$ (Scott [Principal Author], 1969-1971). If this assumption is valid, then the choice between these two processors should be based on the variance of the estimates and circuit design. The r.m.s. amplitude of the EMG signal has also been used as a detector of muscle tension (e.g. Milner et al., 1969-1970) but these results show a general nonlinear relationship between the r.m.s. value of the EMG and muscle tension-the relationship being linear for

lower forces and the r.m.s. EMG rising more rapidly with higher forces. Therefore, the assumption of a Gaussian amplitude probability density function may be valid only for lower force levels.

It is, however, difficult to compare the relationships derived by different researchers between EMG parameters and muscle tension if different muscles have been studied. Even for the same muscle, the variation in surface electrode configurations (size and spacing) used by researchers seriously affects the amplitude-bandwidth characteristics of the recorded EMG. Comparisons of the relationships between different EMG parameters and muscle tension should be made only for the same muscle and electrode system.

### 5.3.2 Mean Root Values of the EMG

An estimate of the mean nth root value of the EMG signal x(t) is given by

$$\hat{\overline{x^{1/n}}} = \frac{1}{T}\int_0^T |x^{1/n}(t)|dt \qquad (5.3\text{-}5)$$

where T is the averaging period. The absolute value of x(t) must first be taken since the EMG is a bipolar signal. If the signal is digitized the mean nth root can also be given by

$$\hat{\overline{x^{1/n}}} = \frac{1}{N}\sum_{i=1}^{N} |x_i|^{1/n} \qquad (5.3\text{-}6)$$

As for the moments, the variance of the estimated mean root also decreases with increasing T.

Since the EMG process has been assumed to be only weakly or wide-sense stationary and ergodic, only the second moment can be considered invariant with respect to time. In addition, power and root functions are nonlinear transformations of the sample record. However, an assumption of strict stationarity is reasonable since random data representing actual physical phenomena will generally be strongly stationary if they are weakly stationary (Bendat and Piersol, 1968). Hence moments higher than the second may also be considered invariant with respect to time. This chapter is not a mathematical presentation of the statistics of the EMG signal and the variance of their estimates (only a definition of each statistic) since it is not possible to assume a general mathematical expression for the EMG process. Therefore an assumption of the time invariance of mean roots will not have later serious consequences. If this assumption is invalid, the measured variance for averaging periods T (see Chapter 6) will be large - hence causing the rejection of the mean root as a possible detection parameter.

### 5.3.3 Measurement of Higher-Order Moments and Mean Roots

The number of higher-order moments and mean roots of a random signal is infinite. Since the EMG signal is bipolar with zero mean, only even moments will be useful since odd moments will be close to zero. For the sake of practicality it was decided to examine only the second and fourth moments (power-law detectors) and the mean square and fourth roots (root-law detectors) as possible control parameters.

The analog processor required to provide an estimate of one of these function means resembles that shown conceptually in Fig. 5.1.

The nonlinear element of the mean absolute value detector, the full-wave rectifier, is just replaced by the appropriate nonlinear root or power processing element. The higher-order moment and mean root processors are shown conceptually in Fig. 5.2. The averaging filter has been chosen to provide smoothing for the reasons described in Section 5.2.1 and an optional post-averaging "linearization" element has been added to the moment processor in case such statistics as the estimated r.m.s. amplitude are to be examined.

Analog moment and mean root value processors can be constructed using logarithmic amplifiers to measure the powers and roots, and a full-wave rectifier and first-order approximation averaging filter similar to that described in Chapter 2 for the other processor elements. If the EMG signal is digitized and input to a computer, the moments and mean roots can be easily calculated using simple algorithms representing Equations 5.3-3 and 5.3-6. This approach avoids hardware approximations of these estimates, resulting in more accurate comparisons of the different parameters.

Kreifeldt and Yao (1974), using analog circuitry, have measured moments and roots of the EMG signal from one normal subject for 4 levels of isometric contraction (5 to 50% of maximal contraction). Their method of comparison of the different parameters is based on the mean estimate to variance of the estimate signal-to-noise ratio. They have concluded that only the mean fourth and second root values and the "linearized" mean square value (r.m.s.), in that order, are more suitable control parameters than the mean absolute value. However, their comparison based on the signal-to-noise ratio does not take into account the sensitivity or range of the EMG parameter to the range of contraction levels. The de-

creasing sensitivity of the mean roots to increasing contractions means that although their signal-to-noise ratios are best, they are not necessarily the best control parameters if parameter sensitivity to contraction level is considered. For these amplitude statistics, a ratio based on this signal-to-noise ratio and the statistic's sensitivity to the desired range of contraction levels, would be a more suitable basis of comparison.

## 5.4 Autocorrelation of the EMG Signal

The statistics defined above are all amplitude parameters of the EMG signal - hence subject to the amplitude errors mentioned in Section 5.0. A choice between them would therefore be based only on their relative estimation errors and circuit complexity. A statistic which furnishes information concerning properties of the EMG signal in the time domain may be useful in formulating an amplitude-independent force-detection strategy. The autocorrelation function of the EMG signal, which describes the general dependence of the signal amplitudes at one time on those at another time, is such a statistic. Because a sine wave, or any other deterministic data, will have an autocorrelation function which persists over all time displacements, as opposed to that of random data which diminishes to zero for large time displacements (assuming $\bar{x}=0$), an autocorrelation measurement clearly provides a powerful tool for detecting deterministic data which might be masked in a random background.

Since the EMG process is assumed to be ergodic, the autocorrelation between the values of $x(t)$ at time $t$ and $t + \tau$ is given by

$$R_x(\tau) = \lim_{T\to\infty} \int_0^T x(t)x(t+\tau)dt \qquad (5.4\text{-}1)$$

From Eqn. 5.4-1, it can be seen that $R_x(0)$ is the same as the mean squared value and $R_x(\infty)$ is the square of the mean. If the signal exists for time T, the (quasi-) autocorrelation function estimate $\hat{R}_x(\tau)$ can be defined by

$$\hat{R}_x(\tau) = \frac{1}{T-\tau} \int_0^{T-\tau} x(t)x(t+\tau)dt \quad 0<\tau<T \qquad (5.4\text{-}2)$$

$\hat{R}_x(\tau)$ is an unbiased estimate of $R_x(\tau)$, independent of T. As for the other statistics the variance of $\hat{R}_x(\tau)$ will decrease with increasing T.

If the EMG signal x(t) of duration T is sampled at greater than or equal to the Nyquist rate into N samples, $x_i$, i = 1,2,3, ... ,N, the estimated autocorrelation function for the lag rh is defined by

$$\hat{R}_r = \hat{R}_x(rh) = \frac{1}{N-r} \sum_{i=1}^{N-r} x_i\, x_{i+r} \quad r=0,1,2,\ldots,m \qquad (5.4\text{-}3)$$

where r is the lag number, m is the maximum lag number and h is the sampling interval. Although the EMG is assumed to have zero mean, this may not be true for the sample record of length T. Before calculating $\hat{R}_r$, the data can be transformed to zero mean by subtracting the sample record mean $\hat{\bar{x}}$. As a rule of thumb, it is desirable to keep the maximum lag m less than one-tenth of the sample size N to keep the error within tolerable limits (Bendat and Piersol, 1968). The sample autocorrelation

function may also be defined at lag r by

$$\hat{R}_r = \hat{R}_x(rh) = \frac{1}{N}\sum_{i=1}^{N-r} x_i x_{i+r} \qquad r = 0,1,2,\ldots,m \qquad (5.4\text{-}4)$$

Although this gives a biased estimate of $R_r$, for large N and relatively small m, the values obtained differ little from those obtained by Eqn. 5.4-3. A normalized value for the autocorrelation function is obtained by dividing $\hat{R}_r$ by $\hat{R}_0$ since this is always the largest value.

Autocorrelation curves have been used to describe the EMG signal recorded with both needles (for example: Freund et al., 1973; Parker and Scott, 1973) and surface electrodes (e.g. Person and Libkind, 1970). In Chapter 4, a method of simulating the EMG signal is described which is based on the linear superposition of randomly occurring, random amplitude action potentials. The autocorrelation curves for these simulated EMG signals showed that the first zero crossing of the curve $\tau_0$ was determined by the basic action potential time duration and the second zero crossing $\tau_1$ by the mean interpulse interval, decreasing as the interpulse interval decreases. Since a decreasing $\tau_1$ signifies increased muscle force (from increased motor unit discharge frequency and recruitment), it may be possible to detect muscle force from the autocorrelation of the EMG signal. An amplitude-independent detector may then be formulated which uses a ratio of autocorrelation values for lags in the interval $\tau_0$ to $\tau_1$.

It is possible to measure the autocorrelation for different lags for continuous EMG signals by using a variable length delay line, but

this requires complex and expensive circuitry. If the signal is digitized, the autocorrelation curves can be calculated by a minicomputer or microprocessor using a simple algorithm representing either Eqn. 5.4-3 or 5.4-4. For a detector which uses autocorrelation information, only the autocorrelation for the time lags of interest need be calculated - hence requiring much less calculation time than for even a short curve.

## 5.5 Power Spectral Density of the EMG Signal

### 5.5.1 The Power Spectral Density Function

A continuous random signal x(t) existing for a period T, $T\to\infty$ has the continuous Fourier transform (CFT) pair (giving frequency and time domain representations)

$$X(f) = \int_{-\infty}^{\infty} x(t)e^{-j2\pi ft}dt \qquad -\infty<f<\infty \qquad (5.5\text{-}1)$$

$$x(t) = \int_{-\infty}^{\infty} X(f)e^{j2\pi ft}df \qquad -\infty<t<\infty \qquad (5.5\text{-}2)$$

Although this random signal is not periodic over a finite measurement interval T, it may be expanded in a Fourier series of base period T. The time function is then made artificially periodic with the period T.

For this continuous signal of period T, the Fourier series may be written as

$$x(t) = \frac{1}{T} \sum_{n=-\infty}^{\infty} c_n e^{j\omega_n t} \qquad (5.5\text{-}3)$$

where $c_n$ is the complex Fourier coefficient for the frequency $f_n$ and is calculated using the transform of Eqn. 5.5-1 but with integration only over the signal period T. The power spectral density function (PSDF) for the signal is defined as the signal power density in the frequency interval $f_n$ to $f_n+\Delta f$ where $\Delta f = 1/T$. That is the two-sided PSDF $G_x(f_n)$ is given by

$$G_x(f_n) = \frac{1}{T}|c_n|^2 \qquad (5.5\text{-}4)$$

and the signal power in the frequency interval $f_n$ to $f_n+\Delta f$ is just $G_x(f_n)\Delta f$. Since $c_n^* = c_{-n}$, the one-sided PSDF is just twice $G_x(f_n)$. The PSDF defined by Eqn. 5.5-4 is really the estimated PSDF since T is a finite record length. The variance of this estimate again decreases as T increases.

The principal application for a PSDF measurement is to establish the frequency composition of the random data which, in turn, bears important relationships to the basic characteristics of the physical system involved. For the EMG signal, the PSDF envelope shape should change as muscle force increases since the increased discharge and motor unit recruitment should cause a shift in the spectral envelope to higher (or lower) frequencies as mentioned in Section 5.0. This shift however, may be obscured by the integration characteristics of the recording electrodes. If the PSDF envelope shape should change consistently as the muscle force changes, an amplitude-independent detector can be formulated using a ratio

composed of two or more affected power spectral densities. That is, if the PSDF envelope shifts with a force increase, a ratio of the PSD in a higher frequency band to the PSD in a lower frequency band would indicate this force increase.

If the signal $x(t)$ is filtered with a band-pass filter having a passband f to $f+k\Delta f$ and sharp cutoff characteristics and the output of the filter is $y(t)$, then the estimated power in that band is simply the estimated mean square value $\hat{\overline{y^2}}(t)$. The possible detector mentioned above would therefore consist of two parallel band-pass filters with passbands $f_L$ to $f_L+k\Delta f$ and $f_H$ to $f_H+k\Delta f$ followed by the mean square detectors described in Section 5.3. The ratio of the outputs of the two detectors would then provide an estimate of the muscle force.

This common method of parallel filtering has been used by Mortimer et al. (1970) and Magnusson and Petersén (1971) to determine the spectral densities for a few wide frequency bands, of surface EMG signals recorded during fatigue studies. Their results show that the power spectrum of the EMG signal shifts downwards for fatigue which they interpret as caused by decreased conduction velocities rather than just synchronous motor unit firing. Kwatny et al. (1970) have calculated the PSDF of the surface EMG signal recorded for two levels of isometric contraction and fatigued contraction. They also found that the PSDF also shifts downward for fatigue which they interpret as caused by synchronous motor unit firing. However, their results for the changes in the PSDF caused by normal force changes are inconclusive.

5.5.2 Measurement of the Power Spectral Density Function

As mentioned above the PSDF can be measured from analog signals by employing a bank of parallel filters, but this requires expensive instrumentation. In addition, the practical limitations on band-pass filter cutoff characteristics cause poorer estimates of the band power. If the signal over a period T is sampled at the Nyquist rate and digitized into N samples $x_i$ i=0,1,2,...,N-1, the PSDF can be computed using several different approaches. Since the EMG signal is stationary, the PSDF and autocorrelation function are Fourier transforms of each other (Wiener-Khintchine theorem). An estimate of the PSDF can therefore be calculated from the estimated autocorrelation function of the N samples. The PSDF can also be calculated by first computing the Fourier coefficients for the sampled signal and then using Eqn. 5.5-4. This approach is preferable since it involves one less set of calculations - hence less error in the PSD estimates.

The analogous discrete Fourier transform (DFT) pair that applies to sampled versions of the functions given by Eqns. 5.5-1 and 5.5-2 can be written in the form (Cochran et al., 1967)

$$X_r = \sum_{i=0}^{N-1} x_i \exp(-2\pi jri/N) \qquad r = 0, 1, \ldots, N-1 \qquad (5.5\text{-}5)$$

$$x_i = \frac{1}{N} \sum_{r=0}^{N-1} X_r \exp(2\pi jir/N) \qquad i = 0, 1, \ldots, N-1 \qquad (5.5\text{-}6)$$

where $X_r$ is the r th coefficient of the DFT, $x_i$ denotes the i th sample of

the N sample time series, and $j = \sqrt{-1}$. Since the signal x(t) has been assumed to be periodic in the period T, the sequences $X_r$ and $x_i$ are periodic functions of r and i respectively with period N.

The fundamental frequency $f_0$ or frequency increment $\Delta f$ and the sample period $\Delta t$ do not appear explicitly in Eqns. 5.5-5 and 5.5-6 but each r should still be interpreted as a harmonic number and each i as the sample period number. Therefore the DFT of the samples of x(t) with sample times 0, $\Delta t$, $2\Delta t$, ... , $N\Delta t$ is a series of Fourier coefficients for the frequencies 0, $f_0$, $2f_0$, ... , $f_s$ where $f_s$ is the sampling frequency. For the DFT transform pair $\Delta t$ and $f_0$ are related as follows

$$\left.\begin{aligned} T = N\Delta t &= \frac{1}{f_0} = \frac{1}{\Delta f} \\ f_s = Nf_0 &= \frac{1}{\Delta t} \end{aligned}\right\} \quad (5.5\text{-}7)$$

When the $x_i$ are real, as is the case for EMG signals, the real part of $X_r$ is symmetric about the folding frequency $f_f$ (where $f_f = f_{s/2}$) and the imaginary part is antisymmetric. This also means that the Fourier coefficients between N/2 and N-1 can be viewed as the "negative frequency" harmonics between -N/2 and -1 (Bergland, 1969). Likewise the last half of the time series can be interpreted as negative time. This is analogous to the CFT transform pair defined by Eqns. 5.5-1 and 5.5-2. The estimated PSDF of the EMG signal x(t) can therefore be calculated from the first N/2 Fourier coefficients of the DFT. That is

$$\hat{G}(rf_0) = |X_r|^2 \quad (5.5\text{-}8)$$

Since $\hat{G}(rf_0)$ will increase with increasing force, the spectral envelope shapes for different force levels can be more easily compared if the estimated PSDF is normalized with respect to a measure of the total power in the signal period T. That is, the normalized PSDF is given by

$$\hat{G}_n(rf_0) = \frac{\hat{G}(rf_0)}{\sum_{r=0}^{N/2-1} \hat{G}(rf_0)} \qquad (5.5\text{-}9)$$

The coefficients $X_r$ can be calculated directly using the DFT of Eqn. 5.5-5 but this requires $N^2$ operations for N coefficients. The Fast Fourier Transform or FFT (Cochran et al., 1967; Cooley et al.,1969), is a much more efficient method of computing the DFT especially if N is large. If the number of data points N is a power of 2, the FFT takes the form of the successive doubling algorithm (Cooley et al., 1969) which enables one to compute N coefficients in $N \log_2 N$ complex additions or subtractions and at most $1/2\ N \log_2 N$ complex multiplications (Cochran et al., 1967). For N = 1024 this represents a computational and round-off error reduction of more than 200 to 1 (Bergland, 1969). The FFT algorithm used for Chapters 4 and 6 has this form and is a standard subroutine (FFT2) available from the McMaster University Computer Centre. The coefficients calculated by this algorithm are in binary reversed order and must be unshuffled before calculating the PSDF.

Since the discrete Fourier transform is an approximation of the continuous Fourier transform, errors resulting from using the DFT are introduced into the computed PSDF in addition to the estimation error caused

by considering only a finite period of the EMG signal. The problem of "aliasing" refers to the fact that high-frequency components of a time function can impersonate lower frequencies if the sampling rate is too low. This problem has been avoided by sampling at a rate greater than or equal to twice the highest frequency component of the EMG signal (i.e. $f_s \geq$ the Nyquist rate).

The problem of "leakage" is inherent in the Fourier analysis of any finite record T of data. This signal truncation to a length T is equivalent in the time domain to multiplying the signal by a rectangular data window, or in the frequency domain, to convolving the frequency components of the signal by the Fourier transform of the rectangular data window (a (sin x)/x function). As a result, a single frequency component is represented by a (sin x)/x function rather than a single term, with some of the frequency energy "leaked" into the adjacent frequencies of the sidelobes. The contribution of a given frequency can be localized by selecting a data window in the time domain which has lower sidelobes in the frequency domain than the rectangular window (e.g. a Hanning window).

The width of the main lobe and the width $\Delta f$ of the side lobes of the rectangular window Fourier transform are inversely proportional to the window length T. If T is long (i.e. $\Delta f$ of Eqn. 5.5-7 small) the leakage of power from the main lobe frequency $f_i$ is into frequencies that are close to it (i.e. $f_i + k\Delta f$, $k = \pm 1$ etc.). As stated in Section 5.5.1, the PSDF envelope (smoothed) shapes will be compared for different force levels, not individual PSD's for each band $\Delta f$. If the envelope of the EMG PSDF is defined as just the PSD for a larger band $k\Delta f$, that is the

normalized PSD of the freqnency band $f_i$ to $f_i+(k-1)\Delta f$, using Eqn. 5.5-9, is given by

$$\hat{G}_e(f) = \frac{1}{k}\sum_{j=0}^{k-1}\hat{G}_n(f_{i+j}) \qquad (5.5\text{-}10)$$

then this value is a good estimate of the true PSD in that band, since most of the side lobes for the individual $\hat{G}_n(f)$ are included in the sum. Therefore, the effects of leakage can be reduced if the PSDF is first calculated for small $\Delta f$ and then averaged to produce the PSDF for a larger band $k\Delta f$. This is the approach used for Chapters 4 and 6. For further discussion of the problems associated with using the DFT see Bergland (1969). To reduce both estimation and DFT approximation error, the signal record to be analyzed should be as long as possible.

## 5.6 Pattern Recognition of EMG Signals

In Sections 5.2 to 5.5, various statistics of surface recorded EMG signal have been described and possible muscle force detectors based on these statistics suggested. With the exception of the possible autocorrelation-based detector, all the suggested detectors can be implemented by analog circuitry. However, the introduction of inexpensive microprocessors in recent years allows one to consider detection strategies which before could only be programmed as processing algorithms on minicomputers. Although the autocorrelation detector could be considered as such a strategy, it is a poor candidate for inexpensive microprocessor application since 2N additions and 2N multiplications are required to calculate the normalized autocorrelation for one lag for N samples. A force detector

based on simple pattern recognition of the EMG signal could also be implemented on a microprocessor since this would involve the calculation and combination of a number of signal parameters.

Before formulating possible pattern recognition algorithms, it is necessary to consider the limitations of current inexpensive microprocessors. Only integer arithmetic should be considered since floating point calculations (requiring large software routines) are not possible especially for real-time control applications. Calculated variables should be kept small (i.e. within the word length) to avoid overflow or excessive truncation errors. In addition, multiplications and divisions are to be avoided if possible, since they would have to be accomplished by software routines or special hardware. Finally, to avoid increased cost, writeable memory (variables and data arrays) and programmable-read-only-memory (the algorithm) must be kept to a minimum, especially the former. Therefore, the pattern recognition algorithm must be simple, require little data storage, and use only integer addition and subtraction if possible.

Simple pattern recognition has been used by some researchers (e.g. Hirose and Sobue, 1972) to quantify the electromyographic pattern recorded by needles for maximal contractions. By examining the time intervals of positive and negative phases and the amplitude of these phases, they attempt (with some success) to establish whether the electromyogram is normal, myopathic or neuropathic. It may be beneficial to examine the patterns of surface EMG recorded for different force levels and attempt to quantify these patterns (e.g. in terms of number of phases - hence a zero crossing detector etc.).

5.6.1 Visual Description of the EMG Signal.

For Section 4.3, the EMG signal for different force levels was recorded using the dry electrode system described in Section 2.4, and visually examined for the presence of possible motor unit action potentials. Figure 5.3 shows typical EMG signals recorded for .45, 1.8 and 3.6 kilograms of muscle force using dry electrodes and sampled at 2 kHz. The EMG pattern recorded using different surface electrode sizes and spacings may differ from those of Fig. 5.3. Since the dry electrodes were to be used for the final detector, it was decided to base any pattern recognition algorithm on EMG signals recorded with these electrodes and not consider any other electrode configurations.

In Fig. 5.3, the EMG appears to be a random signal with increasing r.m.s. amplitude for increasing muscle force. However, diphasic waves similar to the single motor unit action potential of Fig. 3.4(a) also appear frequently in the signal for all force levels. In addition, for each force level the amplitudes of these waves fall into distinct groups such that a diphasic wave of the same amplitude occurs (sometimes frequently) at random intervals as if they were produced by the same motor unit or similar motor units equidistant from the electrodes. As an example, see waves 1-4 of Fig. 5.3(a) and 1-5 of Fig. 5.3(c). For the different force levels, these waves have an average period of 15 msec. with a variation of at most 3 msec. Although one cannot say with absolute certainty that such a diphasic wave represents the surface recorded action potential of a single motor unit, they appear too invariant in shape and time duration and occur too frequently (especially in the .45 kg. signal) to be caused by the random

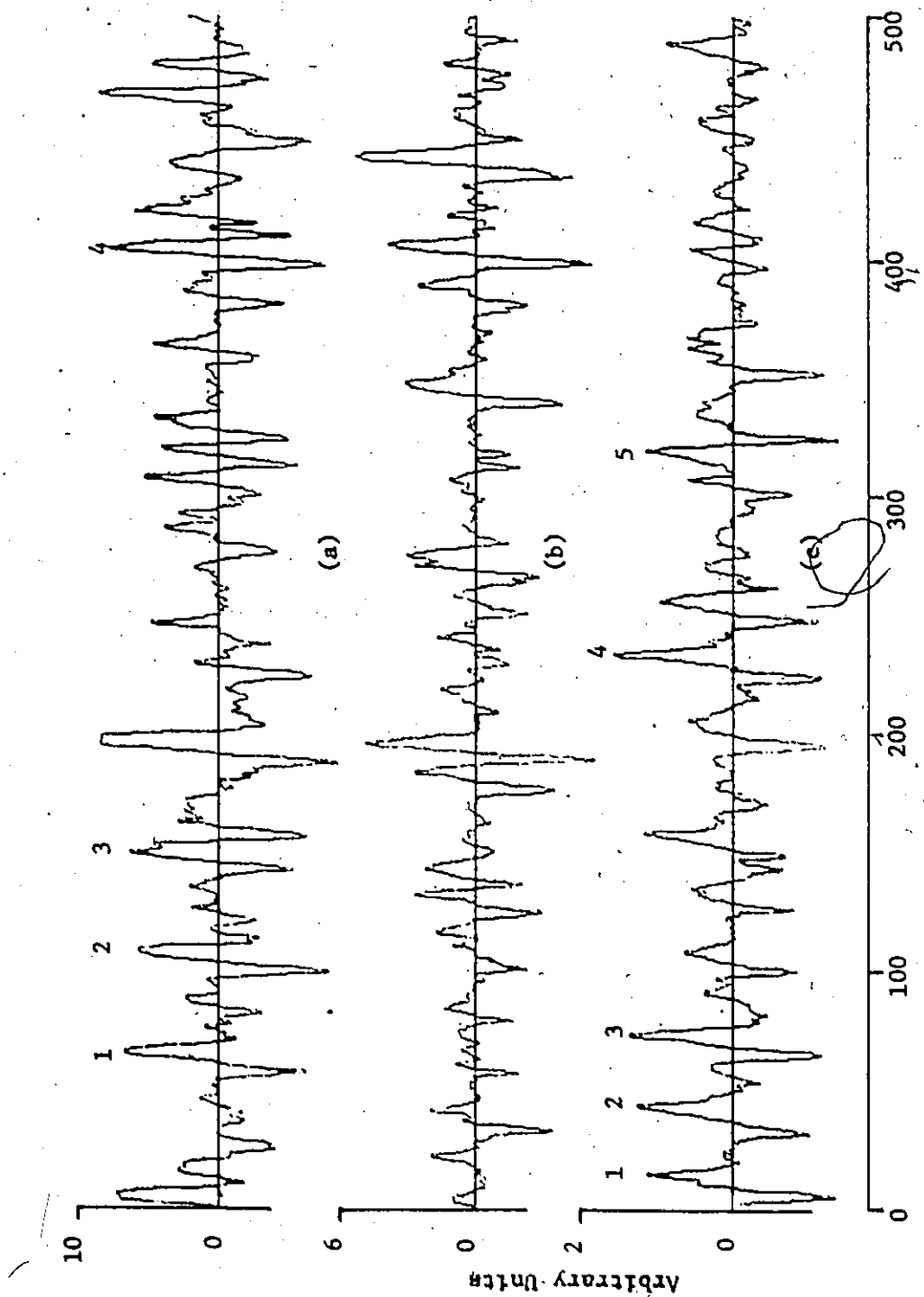


Figure 5.3 Surface EMG signals recorded for different muscle forces.
(a) 3.6 kg. (b) 1.8 kg. (c) .45 kg.
Sampling rate is 2 kHz. For the amplitude scale 1 unit = .091 mV.

superposition of a number of action potentials. At worst they may be the summed potentials of two or more synchronously firing motor units.

If one assumes that these diphasic waves represent single motor unit action potentials, it may be possible to extract some of the recruitment and discharge frequency information from these signals. As the force level increases, the average amplitude of the largest waves in a record also increases indicating recruitment of higher threshold larger motor units or smaller units closer to the electrodes. The latter interpretation is not as applicable if one considers the properties of recruitment described in Section 5.3 and the fact that no large waves (e.g. those for 1.8 kg.) appeared in any of the lower force (e.g. .45 kg.) records. The ratio of the amplitudes of the largest waves in a 3.6 kg. record to those in a .45 kg. record is approximately 5.4:1 which is similar to the ratio of spike amplitudes recorded with needle electrodes from the same subject and for the same force levels - reinforcing the assumption that the amplitudes of the diphasic waves indicate the relative sizes of the motor units involved. EMG signals recorded from other adult male subjects for the same force levels and using the same dry electrodes also contain these diphasic waves. The period of the diphasic waves in these signals is the same as for the EMG signals shown in Fig. 5.3. However, the amplitude ratio of the largest waves in a 3.6 kg. record to those in a .45 kg. record varies from subject to subject. This may be explained by the different recruitment patterns of the subjects tested and the fact that although they were all adult males, 3.6 kg. of force represents a different fraction of the maximal contraction for each subject.

Since there is considerable superposition of action potentials in

the surface EMG signal, only the frequency of occurrence of the largest waves in a record (i.e. indicating discharge frequency of the largest units) can be easily determined. Most of the smaller action potentials are either masked by these large waves or are superposed on each other or on larger waves. Therefore, to estimate the summed discharge frequency of all motor units contributing to the EMG signal, one must also consider the multi-peaked complexes of obviously superimposed action potentials.

Although the above discussion treats the diphasic waves as action potentials, this is only an attempt to link the changes in the gross signal with physiological principles for the purpose of formulating a pattern recognition algorithm. It must be stressed that no physiological interpretation should be made from the relative amplitudes of these waves or their frequencies of occurrence since the surface EMG signal is the sum of the electrical activities of many motor units which are situated at different distances from the recording electrodes.

### 5.6.2 Formulation of the Pattern Recognition Algorithm

An examination of the EMG signals shown in Fig. 5.3 reveals that the number of phases or zero-crossings of the signal for the .45, 1.8 and 3.6 kg. records is 74, 83 and 75 respectively. Although it is expected that the total discharge frequency (sum of active motor unit discharge frequencies) will increase as muscle force increases, this is not indicated by the number of zero-crossings. Therefore a zero-crossing detector will be an inadequate indicator of muscle force.

For the following discussion, a peak in the EMG signal refers to a change in the sign of the slope of the signal from positive to negative

(positive peak or "turn") or vice versa (negative peak or "turn"). The number of positive or negative peaks or "turns" in the record, greater than a minimum peak amplitude (determined by least significant bit noise of the A/D converter and background noise - e.g. residual 60 Hz. power line frequency), may be an indicator of the total discharge frequency - and hence of the muscle force. If one considers a single positive peak in the bipolar EMG signal to be caused by the positive phase of one action potential (or synchronous potentials), the amplitude value of the peak itself is not necessarily an indicator of this action potential amplitude. For example, a small action potential superimposed on a much larger potential may result in two large-amplitude value peaks. Better results may be achieved if peak-to-peak (e.g. -ve peak to +ve peak) amplitudes are assumed to be indicators of the associated action potential amplitudes. Although this assumption is valid for diphasic waves described in Section 5.6.1, it is not generally valid for the multi-peak signal complexes resulting from superimposed action potentials. However, if this assumption is to be used in formulating a pattern recognition algorithm, general validity is not necessary as long as the resultant errors remain sufficiently small. Using peak-to-peak amplitudes rather than the peak amplitude itself also makes the algorithm insensitive to large, low-frequency baseline fluctuations caused by movement artifact.

A detection algorithm based on pattern recognition of an EMG signal of period T has been developed which calculates the number of positive peaks in the signal and classifies these peaks into groups based on their peak-to-peak amplitudes.* The total number of peaks and the number occurring in each group are then used as parameters in quantifying

*(de Bruin and Della Torre, 1976)

the EMG pattern and hence estimating the muscle force. Figure 5.4 shows a representative segment of the EMG signal with the positive and negative peaks labelled as $TMAX_i$ and $TMIN_i$ respectively. Figure 5.5 shows the flow chart for that part of the algorithm which calculates the peak-to-peak amplitude for each acceptable positive peak.

For Figure 5.5, the signal samples X(I) are 10-bit (for a 10-bit A/D converter) two's-complement integers determined by sampling the EMG signal at a sufficiently high rate (e.g. 1-2 kHz). $\epsilon$ is an arbitrary number of binary states considered as background noise ($\geq 1$). PTP is the peak-to-peak amplitude for negative slopes and PSP is the peak-to-peak amplitude for positive slopes. For the signal shown in Fig. 5.4, the positive peak amplitudes would therefore be given by

$$TMAX_i - TMIN_i \qquad i = 1,2,\ldots,5 \qquad (5.6\text{-}1)$$

However, if $TMAX_1 - TMIN_2$ and $TMAX_4 - TMIN_4$ are less than the arbitrary noise value $\epsilon$, only the following positive peaks and their amplitudes will be accepted

$$TMAX_2 - TMIN_1$$

$$TMAX_3 - TMIN_3$$

$$TMAX_5 - TMIN_5$$

Since a diphasic action potential is characterized by one peak-to-peak amplitude, either positive or negative peaks should be considered but not both. Figure 5.3 shows that the amplitude of the diphasic waves is best measured by considering positive peaks but the reverse would apply if the electrodes were reversed (i.e. signal inverted). The first algorithm

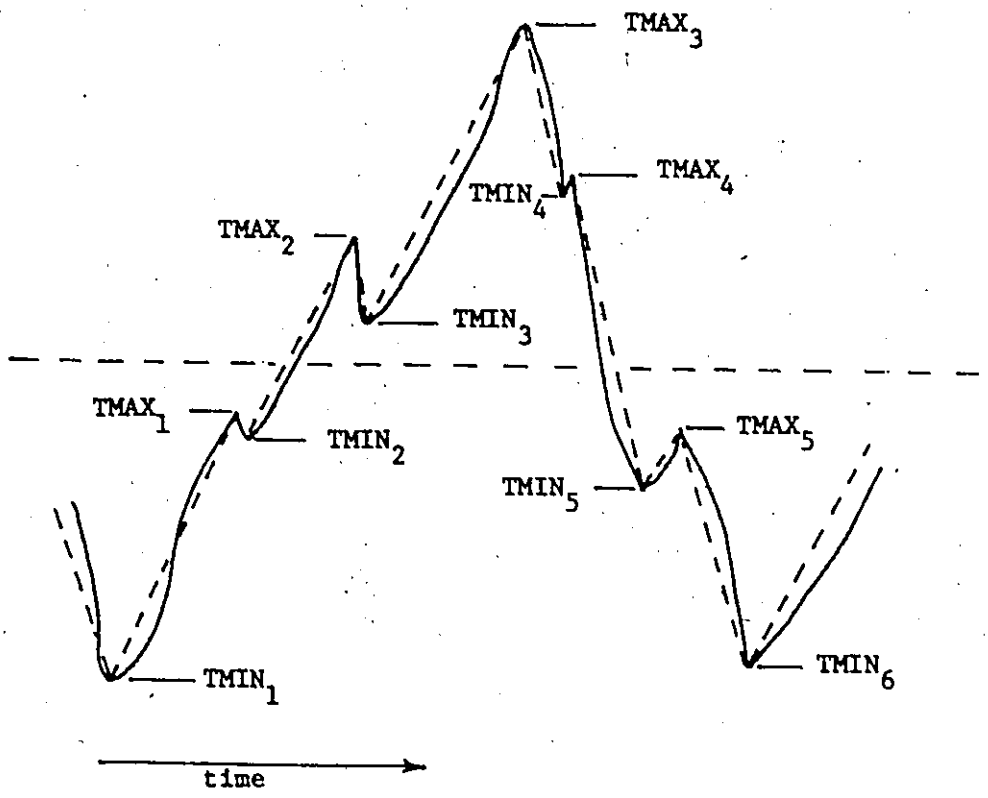


Figure 5.4 A segment of surface recorded EMG signal. The positive peaks ($TMAX_i$) and negative peaks ($TMIN_i$) are joined by dashed straight line segments.

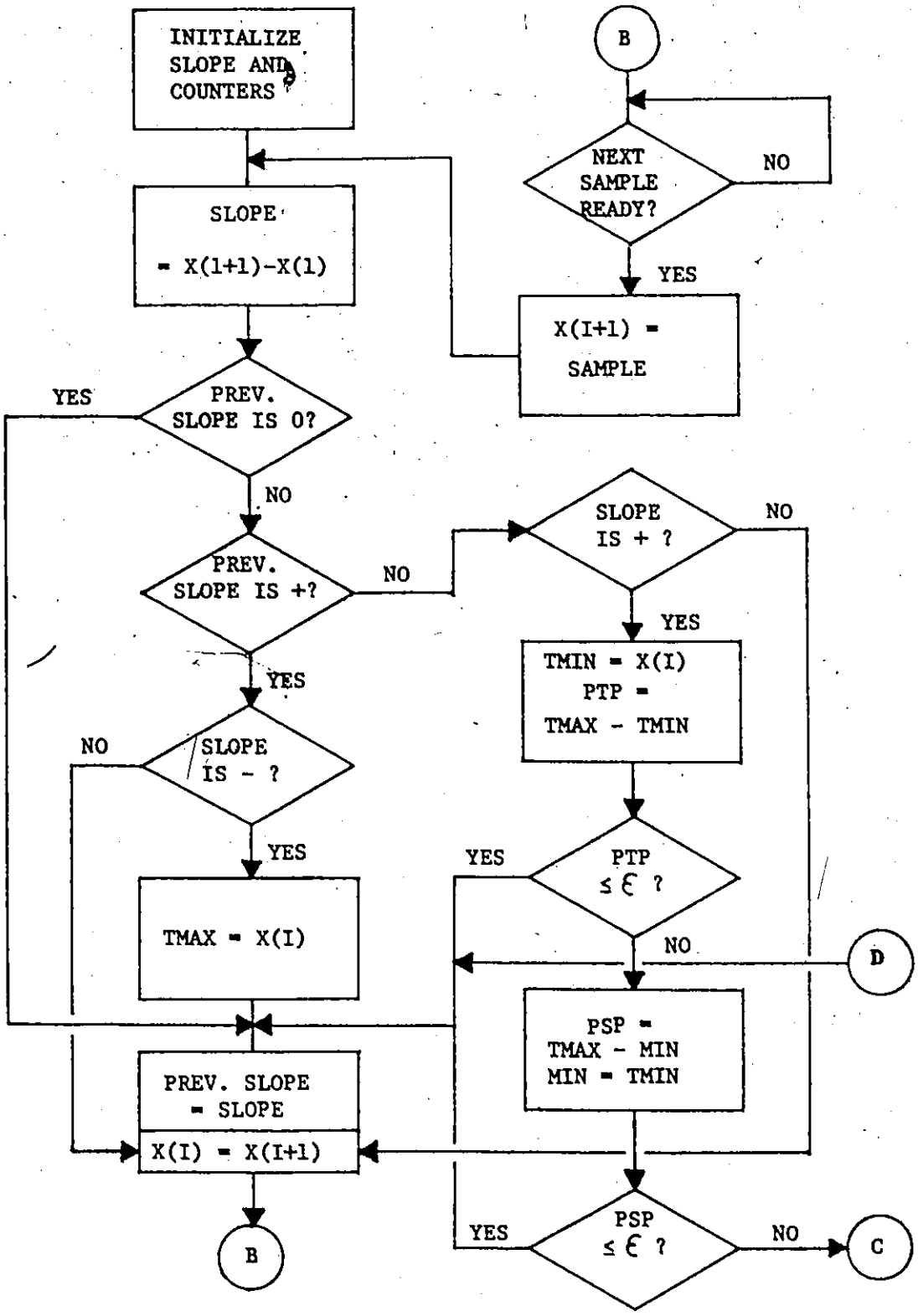


Figure 5.5 Flow chart for signal processing part of detection algorithm.

version is therefore based on positive peaks.

Figure 5.6 shows the flow chart for that part of the detection algorithm which classifies the peaks into groups according to their amplitudes. For this version, the peaks are classified into four groups or bins $B_1$ to $B_4$ whose respective amplitude boundaries in increasing order are: $\epsilon$ to M1, M1 to M2, M2 to M3, M3 to MAX, where MAX is the maximum peak-to-peak amplitude which has occurred for the force range of interest. M3 has been selected to be .8 MAX but the other boundary values M1 and M2 are variable (e.g. .25 MAX and .6 MAX respectively). The number of groups and their boundaries are arbitrary and the initial values were only selected to divide the amplitude range into approximate quarters so that the diphasic waves of the .45 kg. record of Fig. 5.3 would fall into the lowest group and those of the 3.6 kg. record would fall into the highest group. It is desirable to keep the number of groups to a minimum in order to keep the algorithm and the required data storage as small as possible - hence four was chosen as a reasonable minimum.

At the end of the signal period T, the pattern is quantified or the muscle force estimated from the calculated parameters by

$$y = m_p x PK + \sum_{i=1}^{4} m_i B_i \qquad (5.6\text{-}2)$$

where PK is the total number of peaks and $m_p$ and the $m_i$ are arbitrary constants which can be determined empirically for y having maximum sensitivity to the force range of interest and minimum variance for estimates of the same force level. If one proceeds with the assumption that the amplitude of the peak indicates the size of the motor unit, a reasonable

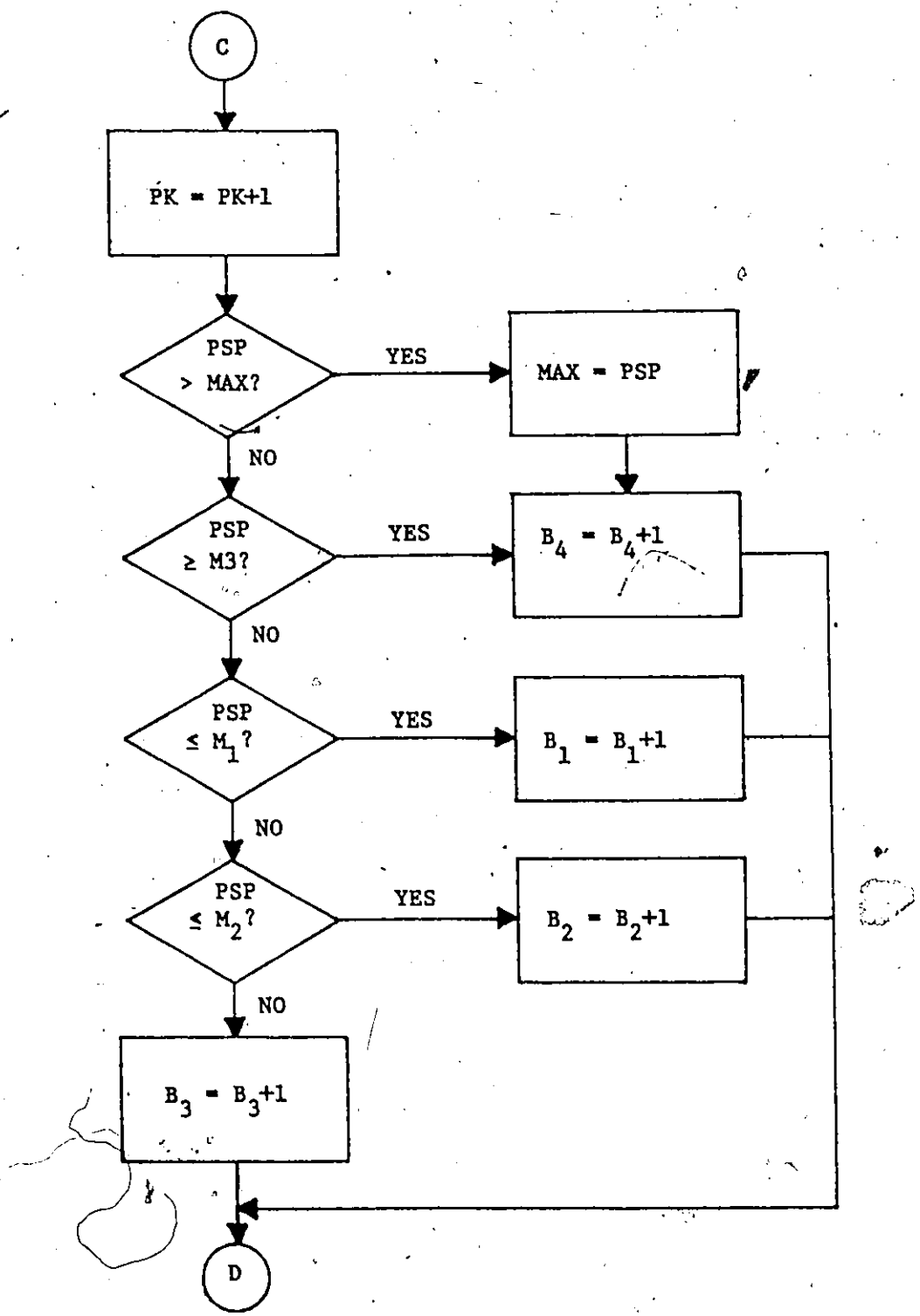


Figure 5.6 Flow chart for peak classification part of detection algorithm.

initial choice for the $m_i$ would be $m_i = i$ if each group represents one quarter of the entire amplitude range. If $m_p = 1$ and $m_i = 0$ $i = 1,..,4$, the algorithm would be a simple peak detector for peaks greater than $\mathcal{E}$ and would consequently be less sensitive to amplitude errors (e.g. changes in gain and electrode impedance). It is expected that "optimum" constants will be different for each subject since the recruitment pattern of motor units varies from subject to subject. It is also expected that the estimation error should decrease for increasing signal period T.

### 5.6.3 Implementation and Calibration of the Algorithm

A) Implementation

The pattern recognition algorithm described above lends itself readily to microprocessor implementation. As shown by Figures 5.5 and 5.6, the computation required per data sample is kept to a minimum. With the exception of the force estimate calculation using Eqn. 5.6-2, all arithmetic operations are subtractions and unit incrementation or clearing of counters - operations which are easily performed by a microprocessor. If the constants of Eqn. 5.6-2 are properly selected even this calculation can be accomplished with a minimum number of shifts and additions. Since the amplitude values themselves are not added, only the appropriate bin counter being incremented, there is no chance of variable overflow. Therefore an 8-bit A/D converter can be used with an 8-bit microprocessor without requiring any scaling of data. Finally, in addition to the algorithm being simple, it has few variables and only requires the storage of two data samples - hence requiring only a small writeable memory.

The peak classification part of the algorithm can be easily expanded to include more groups or bins if this should be necessary for some applications. The algorithm can give a discrete force estimate for successive T second periods of the EMG signal. However, a sliding window estimate such as those possible for the analog detectors described in Sections 5.2 and 5.3 is most desirable for control applications since this provides continuous estimates as the force changes. The detection algorithm can therefore be modified to approximate this sliding window estimation by calculating the signal parameter for successive T/2 or T/4 periods and using 2 or 4 sets of bins. The window, rather than moving by T second increments, therefore moves by T/2 or T/4 second increments - hence providing a force estimate every T/2 or T/4 seconds using

$$y = m_p \sum_{j=1}^{r} PK_j + \sum_{i=1}^{4} m_i \sum_{j=1}^{r} B_{ij} \qquad r = 2 \text{ or } 4 \qquad (5.6\text{-}3)$$

where the $PK_j$ and $B_{ij}$ are the peak and bin counters for each of the last r T/r second signal periods. This modification requires little extra computation and storage and should provide better control and operator feedback.

B) Calibration

As can be seen from Figure 5.6, this algorithm can be easily calibrated for the force range and resultant EMG amplitude range of interest. Since the bin amplitude boundaries M1, M2 and M3 are determined by the maximum peak-to-peak amplitude MAX, only MAX has to be determined during calibration. The algorithm calibrates itself (see Fig. 5.6) if

MAX is set to zero and a moderate contraction (approximate maximum force) is held for a few seconds. If this contraction is too low, MAX will be recalibrated upwards in any case during normal processing. Therefore one only has to ensure that this contraction is lower than the maximum force of interest. The algorithm can therefore be recalibrated periodically during the course of a control session without therapist intervention, simply by having the algorithm set MAX to zero periodically and indicating to the subject (e.g. by a light) that the detector is being calibrated.

## 5.7 Summary

A number of possible muscle force detection strategies have been described in this Chapter. Sections 5.2 to 5.5 describe strategies based on statistics of the EMG signal - the first of which, the mean absolute value, is the most commonly used strategy for both prosthetics control and muscle mechanics research. The amplitude statistics are obvious choices for muscle force detection since it is well known that the amplitude of the EMG signal increases with increasing muscle force. Although the autocorrelation and power spectral density statistics have been used to describe the EMG signal (e.g. see Chapter 4), they have not been used as the basis for muscle force detection.

Finally, a new detection strategy has been presented which attempts to extract the motor unit recruitment and discharge frequency information present in the surface EMG signal without using statistical mathematics. This strategy is based on the number of positive peaks (defined as a +ve to -ve change in the sign of the signal slope) occur-

ring in a short period of EMG signal and the distribution of their peak-to-peak amplitudes. In its simplest form, this strategy is a signal peak detector which may be less sensitive to amplitude errors in the EMG signal than other amplitude-dependent detection strategies. The resulting family of detection algorithms (using different levels of precision of peak classification) can be easily implemented on a microprocessor. In addition, the detection algorithm is self-calibrating during on-line processing. It is felt that this algorithm is a viable alternative to the amplitude strategies presently in use.

# CHAPTER 6

# EVALUATION OF EMG PROCESSING STRATEGIES

## 6.0 Introduction

Several parameters of the EMG signal which may be used to provide suitable muscle force detection strategies have been described in Chapter 5. These parameters have been calculated for the EMG signals recorded from six adult male subjects for a range of constant isometric contractions. The same signals have also been used to test the pattern recognition algorithm described in Chapter 5. The results of these tests and an evaluation of the different detection strategies are presented in this chapter.

### 6.0.1 Selection of the Biceps Brachii as the Test Muscle

The biceps brachii was chosen as the test muscle because it is a superficial muscle and functions as a flexor of the supine forearm. Consequently, the experimental procedure required to measure different levels of constant isometric contraction of this muscle is quite simple and consists of maintenance of elbow position with a supine forearm for a range of weights added to the forearm. In addition, its anatomical position and size facilitate application of surface electrodes and minimize crosstalk from other muscles.

A brief discussion of the function of the biceps brachii and its synergists is necessary in order to interpret the EMG-force relationships

presented in this chapter. Basmajian (1974) gives a more comprehensive treatment of this topic. There are three elbow flexor muscles, the biceps brachii, the brachialis, and the brachioradialis. In addition, the biceps brachii is composed of two heads and is a two-joint muscle. However, there is little difference between the activity of the two heads during isometric contraction and no evidence of separate contraction of distal and proximal regions of this muscle in normal subjects. Consequently, for the experimental conditions described in this chapter, the exact position of the electrodes over the belly of the biceps brachii does not affect results.

The biceps brachii is generally active during flexion of the supine forearm under all conditions. The brachioradialis can be ignored since it plays no appreciable role in the maintenance of elbow flexion with a supine forearm. However, the brachialis is active during maintenance of elbow flexion, i.e. isometric contraction, for all positions of the forearm. Therefore, the exact EMG-muscle tension relationship for isometric contraction of the biceps brachii cannot be derived by only considering the EMG signal from this muscle since two muscles are contributing to the maintenance of the force. In addition, there is considerable variation among normal subjects in the relative levels of activity of the two muscles. Since the research presented in this thesis is concerned with the use of surface EMG signals as a source of control, exact EMG-muscle tension relationships are not required. However, the presence of two active muscles can explain the variation in EMG-force relationships measured for different subjects.

### 6.0.2 Experimental Procedure

Surface EMG signals were recorded from six normal adult male subjects using the dry silver disc electrodes described in Section 2.4 placed over the belly of the biceps brachii. These signals were recorded for different force levels of isometric contraction (i.e. .5 to 5 kg. in .5 kg. increments) at an elbow angle of 90° with the forearm in a supine position. The experimental set-up described in Appendix B was used with the following modifications. Instead of using a scale, different weights were suspended from a strap attached to the wrist of the subject. The signals were also directly sampled at 1 kHz and stored by a PDP 11/10 minicomputer operating under the DOS Monitor system. Ten seconds of signal were recorded for each of the 10 force levels, resulting in a file of 100,000 data samples for each subject.

It is not possible to maintain a true constant isometric contraction by maintaining an elbow position. There will be some slight changes in the contraction level as the subject attempts to maintain a constant limb position. However, using a force signal as feedback will also result in small contraction level changes as the subject attempts to keep the force signal constant. The subjects were observed during signal acquisition and the data was rejected if limb movements were noticed. Since these force changes are small relative to the force increments considered here, the contraction can be considered constant within practical experimental limits.

The data was read, in 2500 sample records, and the different parameters and detection algorithm responses calculated for each record using the software system outlined in Section B.3. The results of these

calculations are presented in the following sections. It must be stressed that the term force or muscle force used in the following figures and discussion does not mean the muscle tension of the biceps brachii, but only the weight added to the forearm. Therefore zero force corresponds to the weight of the forearm itself. As stated in Section 6.0.1, the true muscle tension of the biceps brachii cannot be measured using the above experimental procedure.

## 6.1 Autocorrelation and Power Spectral Density of the EMG Signal

### 6.1.1 Experimental Results

Autocorrelation curves have been calculated for 2500 sample records (i.e. 2.5 sec.) of the EMG signals recorded for different force levels using Eqn. 5.4-4. Figures 6.1 and 6.2 show typical normalized curves calculated for 1.0, 2.5 and 5.0 kg. signal records. With the exception of one subject, all the autocorrelation curves have the same shape as that of Figures 6.1 and 6.2 and the maximum variation in the first zero-crossing $\tau_0$ is .5 msec. However, the curves calculated for EMG signal records representing both equal and different force levels for the same subject, show considerable variation for $\tau$ greater than 12-16 msec. As stated in Section 4.5, simulation results suggest that increased recruitment and discharge frequency, i.e. increased force level, should cause a decrease in $\tau_1$, the second zero-crossing. An examination of the autocorrelation results reveals no such change in the curves consistent with changes in the force level. For example, in Fig. 6.1 $\tau_1$ for the 1.0 kg. curve is greater than $\tau_1$ for the 2.5 kg. and

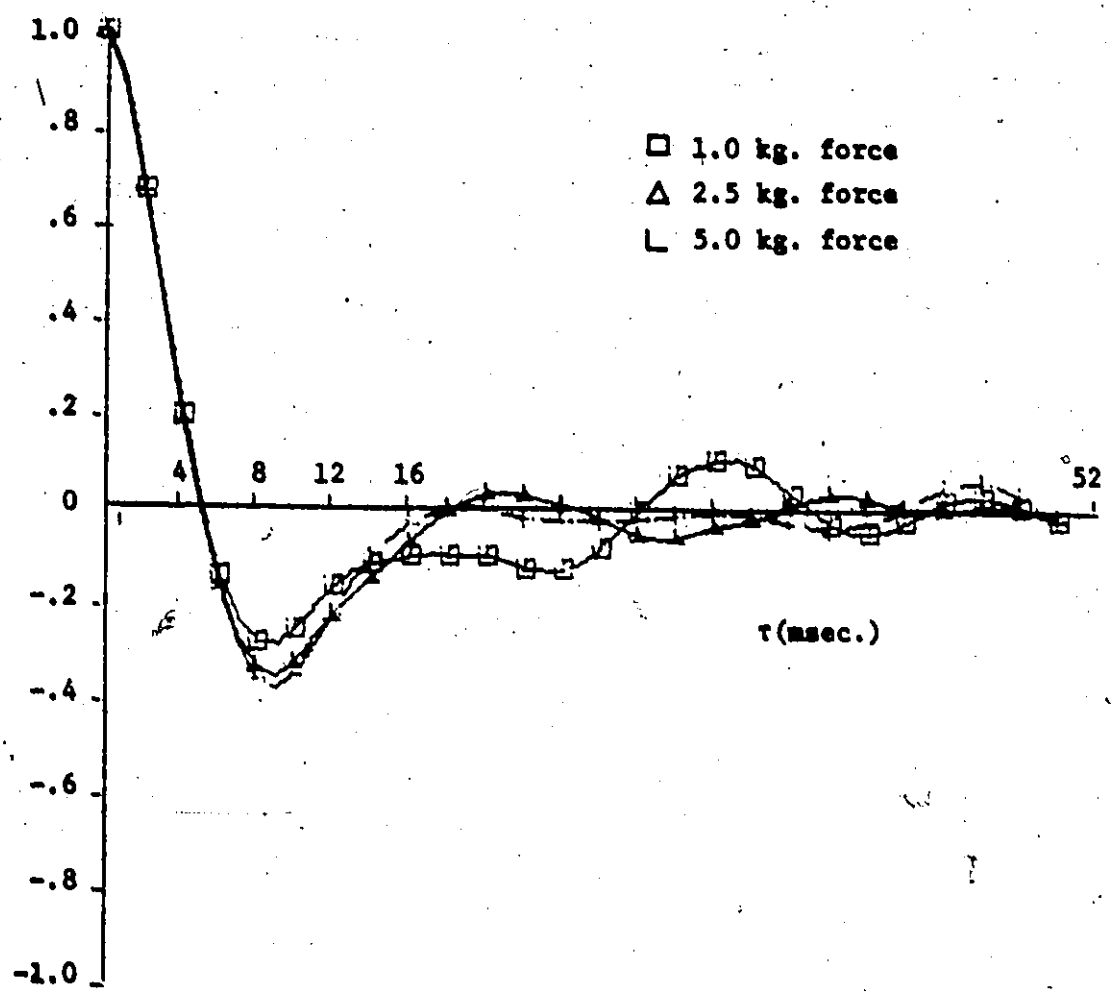


Figure 6.1 Autocorrelation curves for surface EMG signals. 1 kHz sampling rate; subject WB

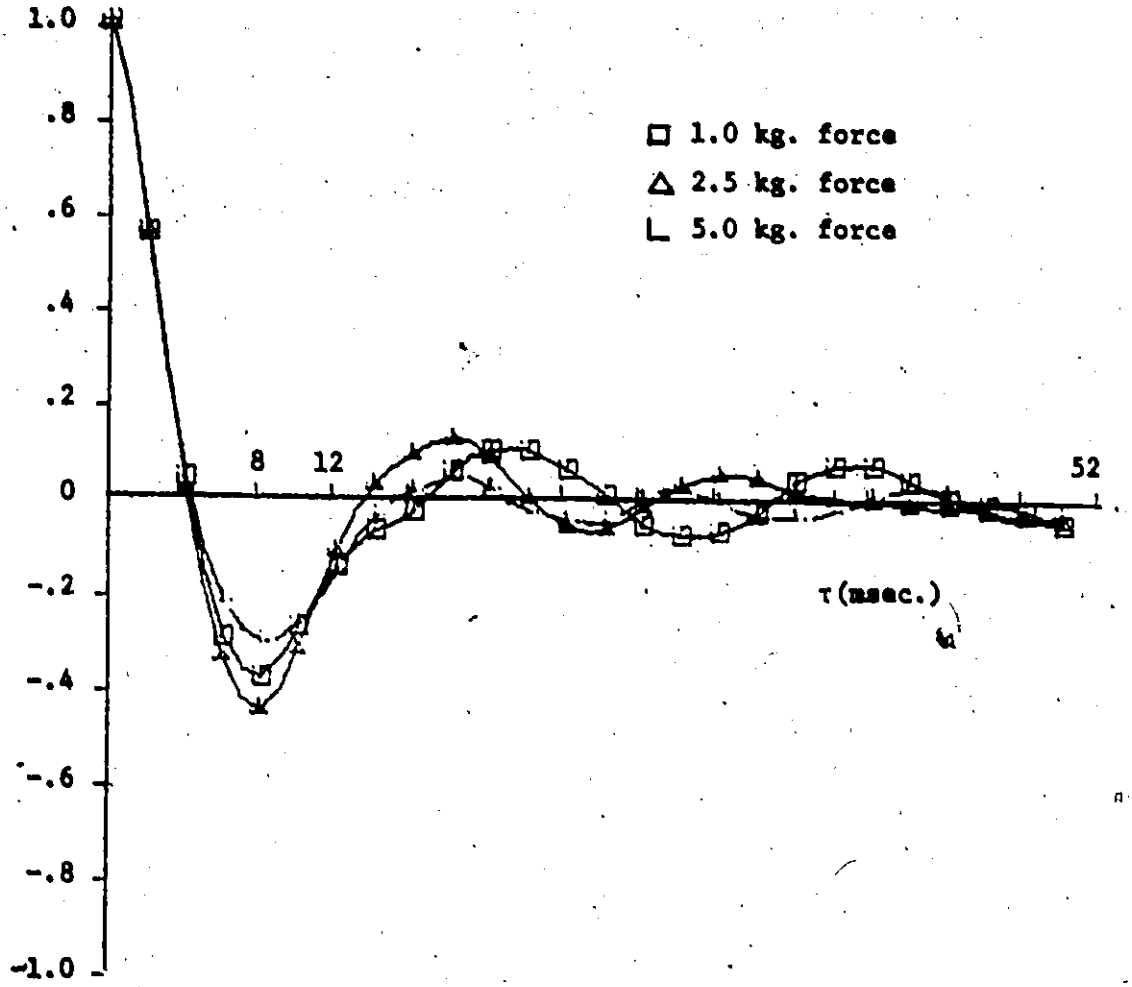


Figure 6.2 Autocorrelation curves for surface EMG signals.
1 kHz sampling rate; subject TW

5.0 kg. curves as expected, but the latter two zero-crossings are equal. In Fig. 6.2, the second zero-crossing, $\tau_1$, for the 2.5 kg. curve is less than that of the 5.0 kg. curve contrary to expectations. The autocorrelation curves for the EMG signals recorded from the other subjects all demonstrate such random variations.

Figures 6.3 and 6.4 show autocorrelation curves for two subjects calculated for different 2.5 sec. EMG records representing the same force level. As can be seen from these figures, there can be considerable variation in the autocorrelation of EMG signals recorded for the same force level even when 2.5 sec. signal windows are used. Generally, the results calculated for other subjects and for other force levels resemble those of Fig. 6.3. These results confirm that EMG signals recorded for constant isometric contractions are generally weakly stationary and that there is little useful information in the autocorrelation curves for $\tau$ greater than 12-16 msec., at least for the electrodes and force range considered here. However, the considerable variation in the curves of Fig. 6.4 indicate that the EMG signal can also sometimes be non-stationary if only a 2.5 sec. record is considered. It must be noted that although there is considerable variation in the autocorrelation curves of Fig. 6.4, there is no excessive variation in the estimates of the amplitude statistics for the same signal (see Fig. 6.10, etc.).

Normalized power spectral densities have been calculated for 2048 sample records (i.e. 2 sec.) of the EMG signals recorded for different force levels using Eqn. 5.5-9. Figures 6.5 and 6.6 show typical normalized power spectra calculated for 1.0, 2.5 and 5.0 kg. signal records. Figure 6.7 shows the normalized power spectra for three signal

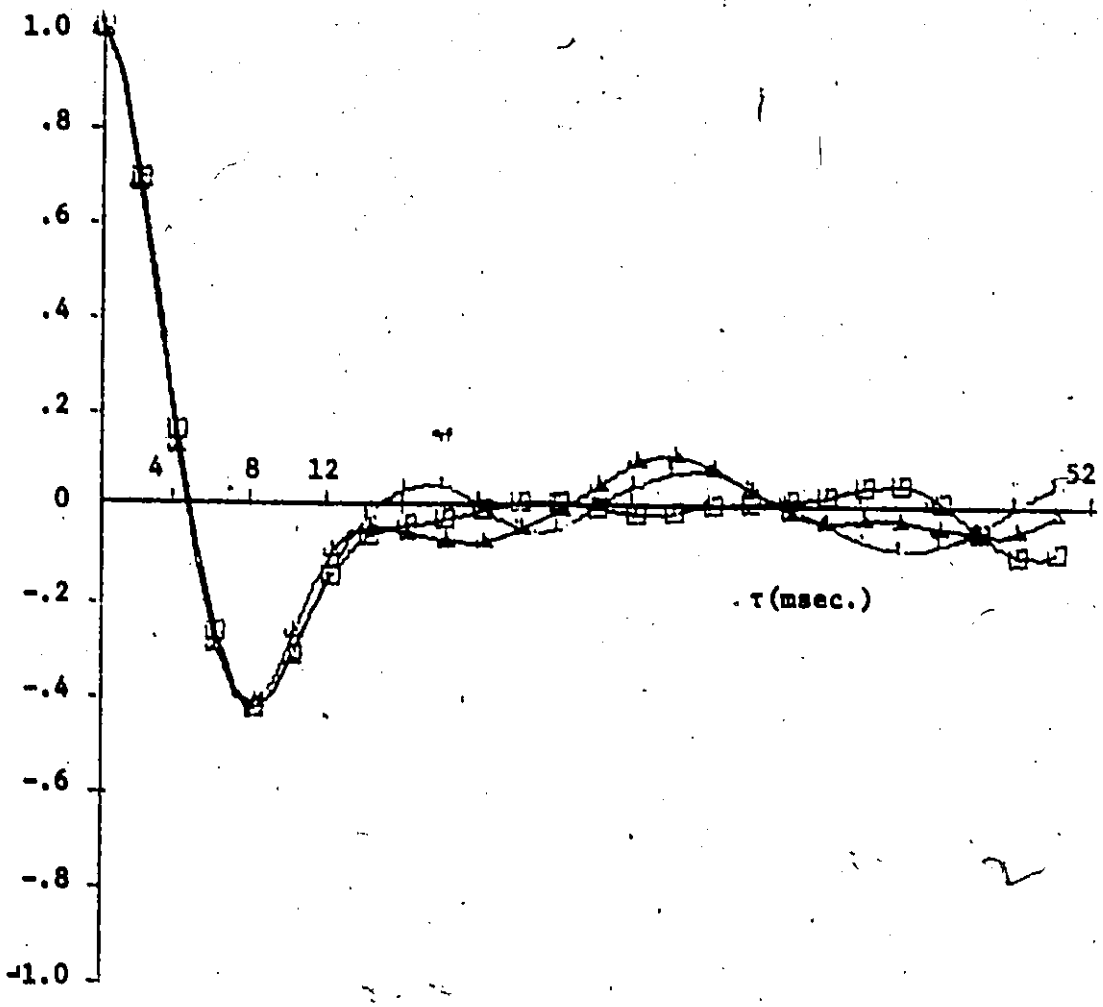


Figure 6.3 Autocorrelation curves for surface EMG signals recorded for the same force level. 1 kHz sampling rate; 4.0 kg. force; subject HD.

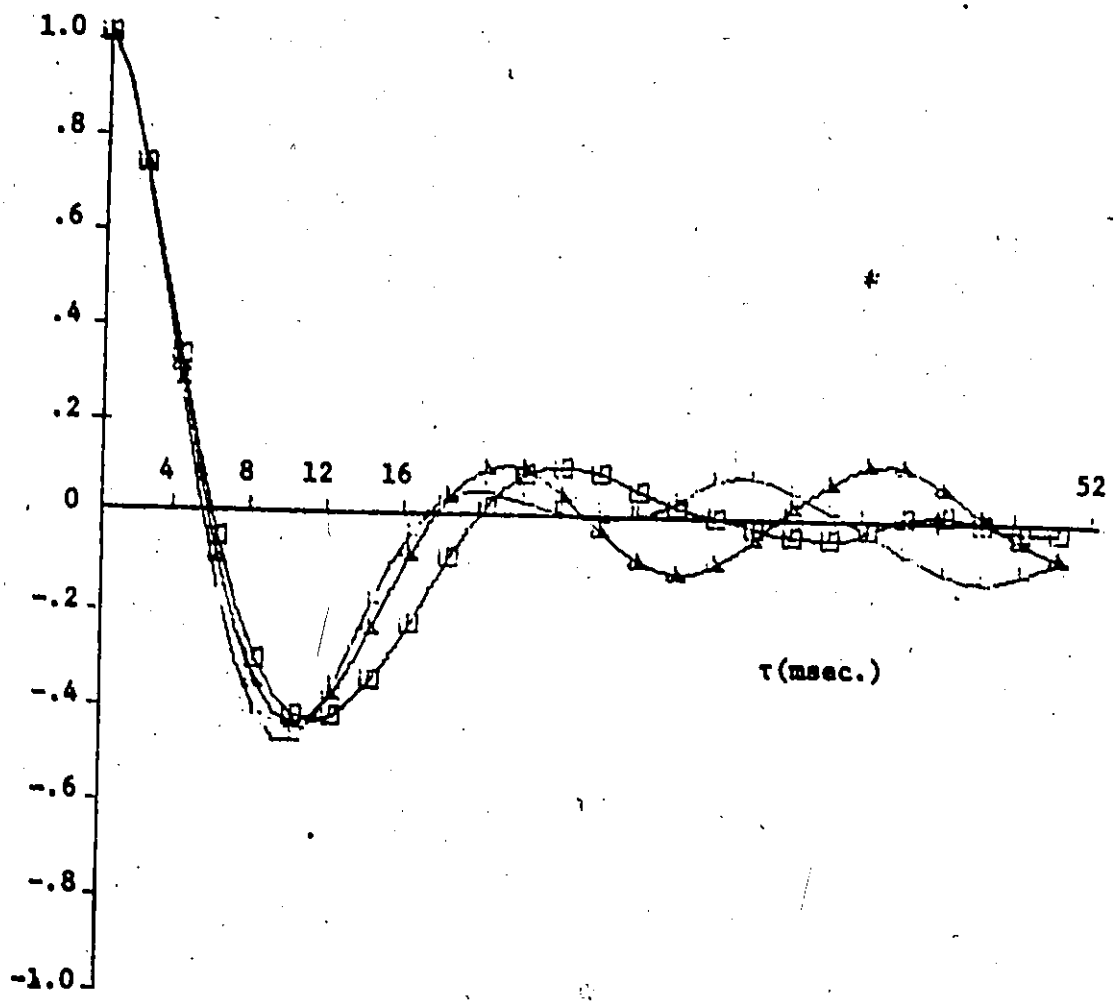


Figure 6.4 Autocorrelation curves for surface EMG signals recorded for the same force level. 1 kHz sampling rate; 2.0 kg. force; subject MM.

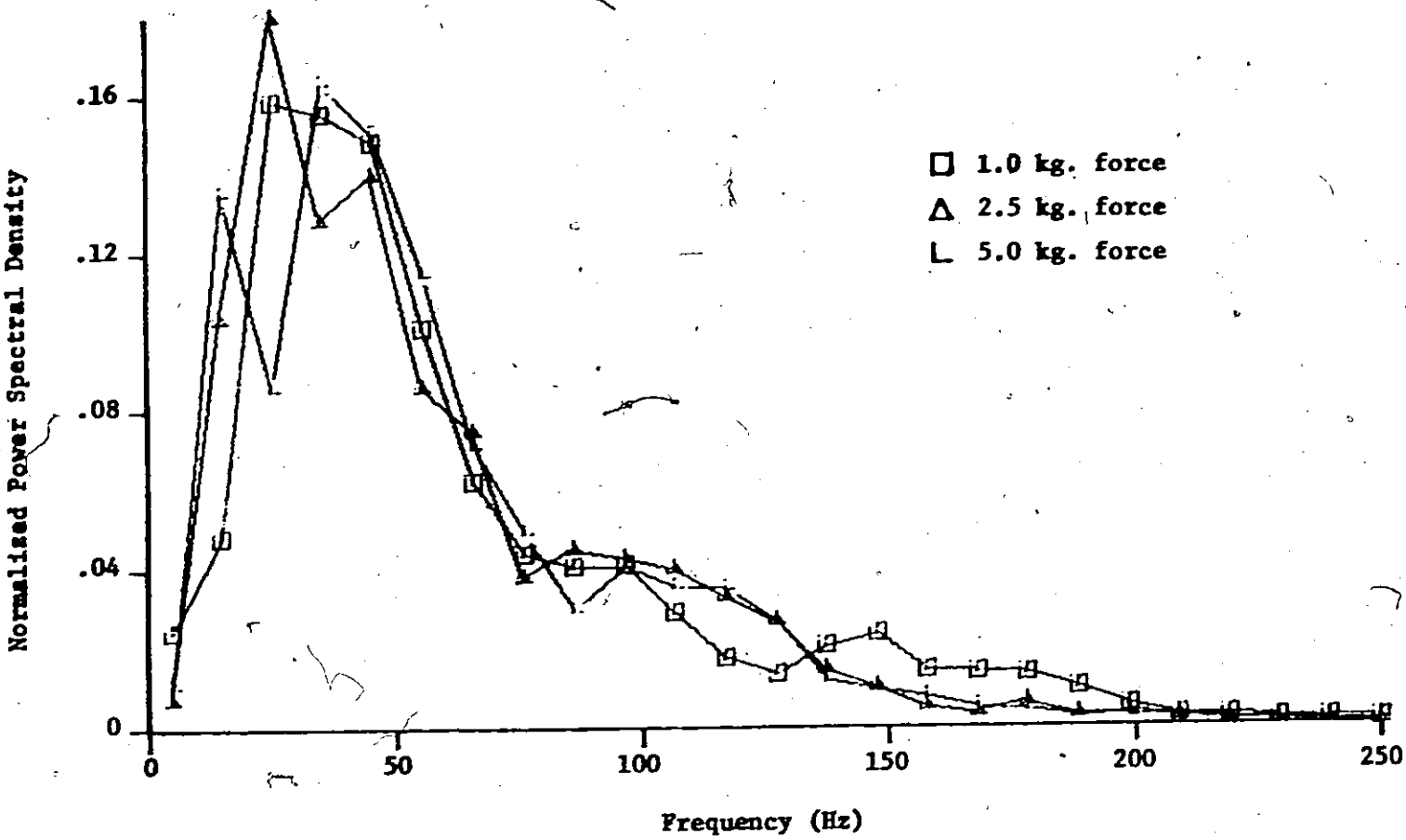


Figure 6.5 Normalized power spectra for surface EMG signals. 1 kHz sampling rate; subject SN. Power spectra are normalized with respect to the total spectral power.

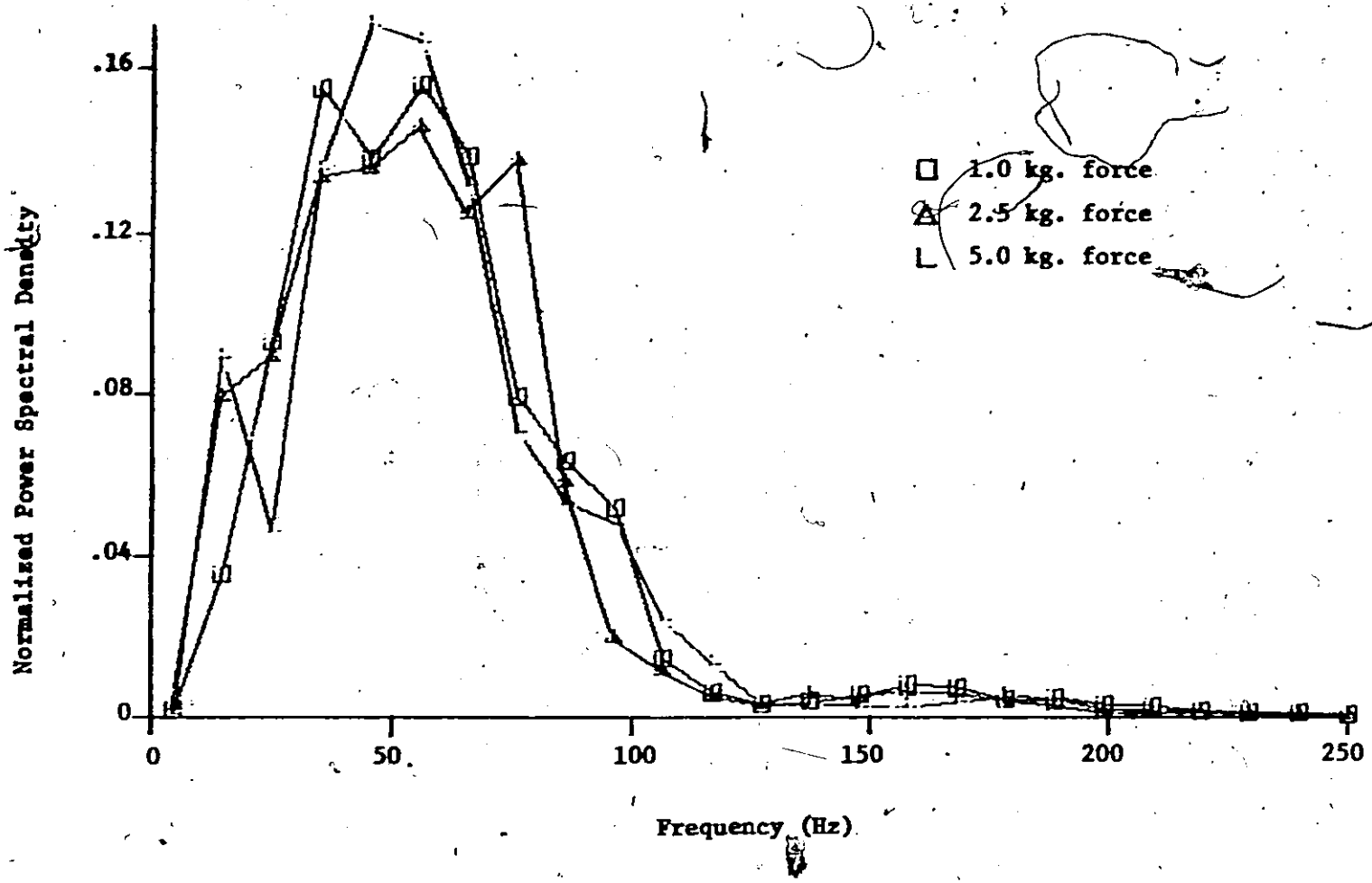


Figure 6.6 Normalized power spectra for surface EMG signals. 1 kHz sampling rate; subject HD. Power spectra are normalized with respect to the total spectral power.

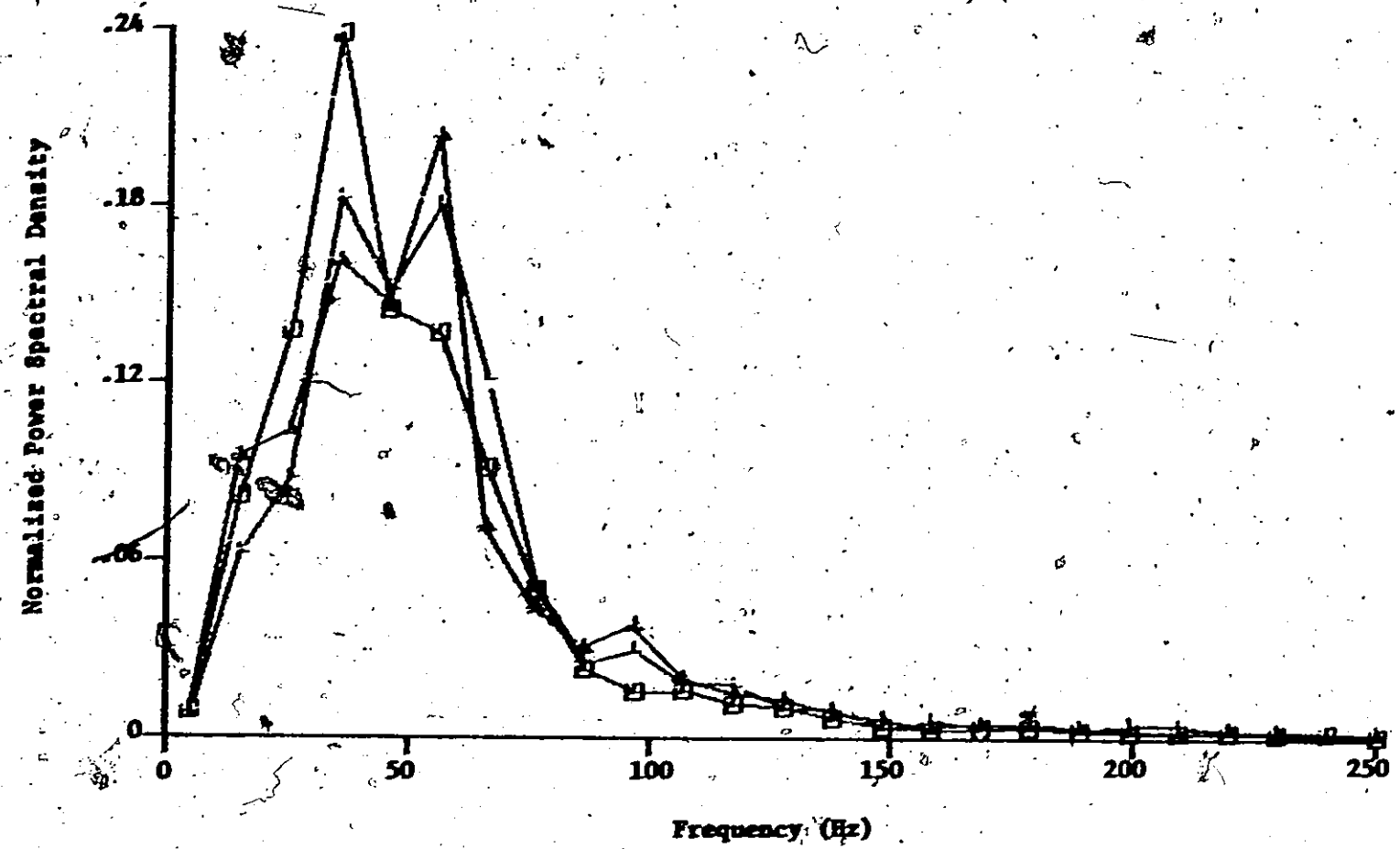


Figure 6.7 Normalized power spectra for surface EMG signals recorded for the same force level. 1 kHz sampling rate; subject KD; 4.0 kg. force. Power spectra are normalized with respect to the total spectral power.

records representing the same force level. In these figures each point represents the average normalized spectral density for a band of 10.4 Hz calculated using Eqn. 5.5-10, and is plotted in the centre of the band. Therefore, the spectral plot represents the power in each band as a fraction of the total signal power.

The power spectra of the signals recorded from the other subjects all have approximately the same bandwidth although not necessarily the same envelope shape as those shown in Fig. 6.6. The power spectra of Fig. 6.5 and the autocorrelation curves of the EMG signals recorded from this subject are markedly different from those calculated for the other subjects. The biceps brachii of this subject is significantly smaller in diameter, and hence the electrodes recorded the activity of a larger number of motor units (i.e. were relatively less selective). This fact may explain the higher bandwidth of the signals recorded from this subject.

As for the autocorrelation curves, an examination of the power spectra of signals recorded for different force levels revealed no changes in envelope shape consistent with changes in the force level. As can be seen, there are no major consistent shifts to higher or lower frequencies as the force level changes, only random variations in the spectral density of some bands. In addition, the power spectra of signal records representing the same force level also show an equivalent variation in envelope shape. The variation in the spectra shown in Fig. 6.7 is typical for all the subjects tested.

### 6.1.2 Discussion

If the surface recorded EMG signal is considered stationary the autocorrelation function and power spectral density function form a Fourier transform pair and hence both parameters can be considered simultaneously. As indicated above, there seems to be no force information present in the calculated autocorrelation and power spectral density plots. For some signal records, the variation in plots calculated for the same force level, is equal to the variation in plots calculated for a 4 kg. range of force levels. In addition, these plots were calculated for signal periods greater than 2 sec., while a reasonable signal period for control purposes should only be .5 sec. Therefore, these parameters cannot be used for EMG muscle force detection strategies.

In Section 4.5 a possible explanation is given for the lack of consistent change in the autocorrelation and power spectral density plots as the force level changes. As the required force increases to a certain level, large higher threshold motor units are recruited with low initial discharge frequency. Their action potentials are much larger than those of smaller units already active which are discharging at a higher frequency, and consequently "mask" many of these smaller action potentials, or action potentials from more distant units, contributing to the EMG signal. This recruitment of larger motor units can be readily seen in the signals of Fig. 5.3. Hence the power spectrum of the recorded signal can be shifted towards the lower frequencies and the signal can have less apparent integration (i.e. less randomness) even though the force level is higher and more action potentials are contributing to the aggregate signal. As the force level increases again but not enough to recruit even

larger units, the power spectrum shifts towards higher frequencies as the discharge frequencies of all active units increase. This effect is possible throughout the range of moderate force levels considered here because of the large number of different size motor units present in the biceps brachii. Hence the power spectrum of the EMG signal can shift up or down as the force level increases. The variation in the plots calculated for the same force level may be attributed to the stochastic nature of the EMG process.

## 6.2 Amplitude Parameters of the EMG Signal

### 6.2.1 Experimental Results

The amplitude parameters described in Sections 5.2 and 5.3 have been calculated for the EMG signals recorded for different force levels. The mean absolute values, second and fourth moments, and the mean second and fourth root values of the signals have been calculated for signal averaging periods, T, of 1.0, .5, and .25 sec. using Eqns. 5.2-3, 5.3-3, and 5.3-6 respectively. The r.m.s. values were calculated using Eqn. 5.3-3 and then taking the square root. These signal averaging periods were considered a reasonable range for control purposes since an averaging period longer than 1.0 sec. results in sluggish control, while periods less than .25 sec. result in excessive estimation error. Since 10 sec. of signal were recorded for each force level, discrete averaging periods of .25 sec. result in 40 estimates of each parameter for each force level.

The mean absolute values and the r.m.s. values of the EMG signal are virtually equivalent for all the subjects tested, at least for the range of contractions considered here. Figures 6.8, 6.9, 6.10 and 6.11

show typical comparisons of the mean absolute and r.m.s. values.

In Figures 6.8 and 6.10, the symbol points of each error bar indicate the lowest estimate, the mean of the estimates and the highest estimate of the parameter. In these figures the parameter values have been normalized with respect to the largest mean estimate calculated for the entire force range. This normalization is necessary for an adequate comparison of the different EMG signal parameters. In Figures 6.8 and 6.10, a polynomial has been fitted to the mean estimates of each parameter for the different force levels using the least-squares criterion. The order of the polynomial was determined by considering the least-squares error - the lower order polynomial being selected if only a 5-10% reduction in the error resulted from using the next higher order. In addition, polynomials which had a negative y-intercept or negative slopes in the interval were avoided if possible since it has been well established that the amplitude of the EMG signal increases with force.

Figures 6.9 and 6.11 show figures of merit for the parameters for each force level. An adequate figure of merit should consider both parameter sensitivity to changes in the contraction level and the estimation error at each force level. A ratio consisting of the slope of the polynomial at each force level, to the maximum estimate deviation from the polynomial value at this level is proposed as a figure of merit and used for these plots. For control applications, maximum deviation of the estimate should be considered rather than statistical parameters of the estimate such as the variance. Naturally, other ratios may also be considered which increase with increased sensitivity and

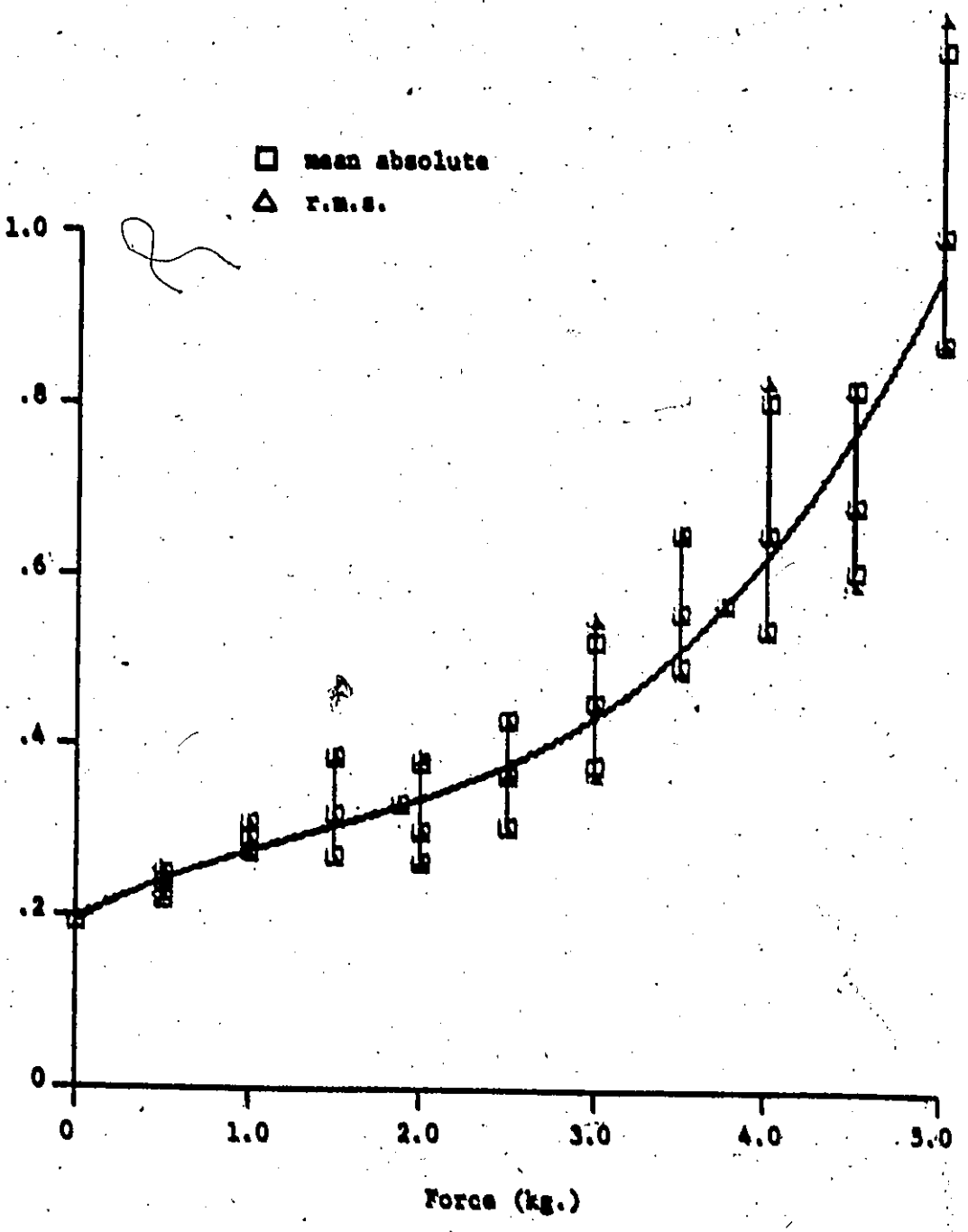


Figure 6.8 Mean absolute and r.m.s. values of EMG signals recorded for different force levels, T = 1.0 sec. Subject RD.

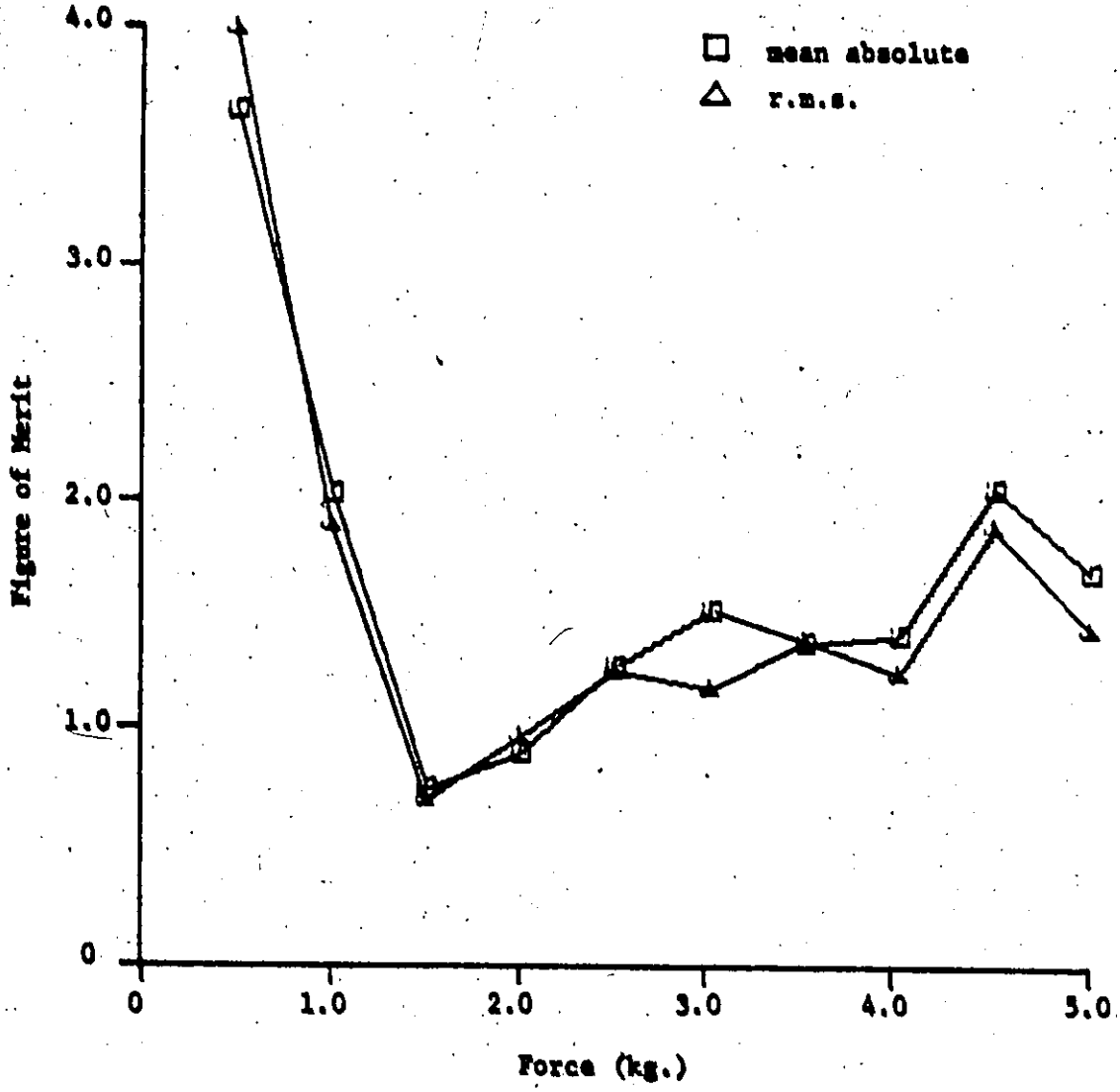


Figure 6.9 Figures of merit for the parameters of Fig. 6.8.

decrease with increased estimation error. The above discussion of error bars, normalization, curve fitting and figure of merit applies to all subsequent figures in this chapter.

It must be noted that Kreifeldt and Yao (1974) compare the amplitude parameters of the EMG signal using a mean estimate, to variance of the estimate, signal-to-noise ratio. However, this ratio favours such parameters as the mean root values which have a large mean estimate and relatively small variance over most of the force range, but are not very sensitive to changes in the force level.

Figures 6.8 and 6.10 show that the polynomials for the mean absolute and r.m.s. values are virtually the same indicating that the mean estimates of these parameters are identical. The small differences in the error bars cause the variation in the figures of merit shown in Figures 6.9 and 6.11. If the average figure of merit is calculated for the force range (see Table 5.1) it can be seen that these two parameters are equally effective as force detectors. Although different order polynomials were used for these parameters for the subjects tested, e.g. third-order for Fig. 6.8 and second-order for Fig. 6.10, the results are consistent.

The amplitude parameters and their figures of merit were plotted for each subject for the range of signal averaging periods. Although the order of polynomials and the figures of merit vary from subject to subject, they all demonstrate consistent results. In order to avoid an excessive number of figures for presentation in this thesis, the results from one subject were chosen. These are typical. Figures 6.10 to 6.25 show the amplitude parameters calculated for one subject. Table 5.1 presents the

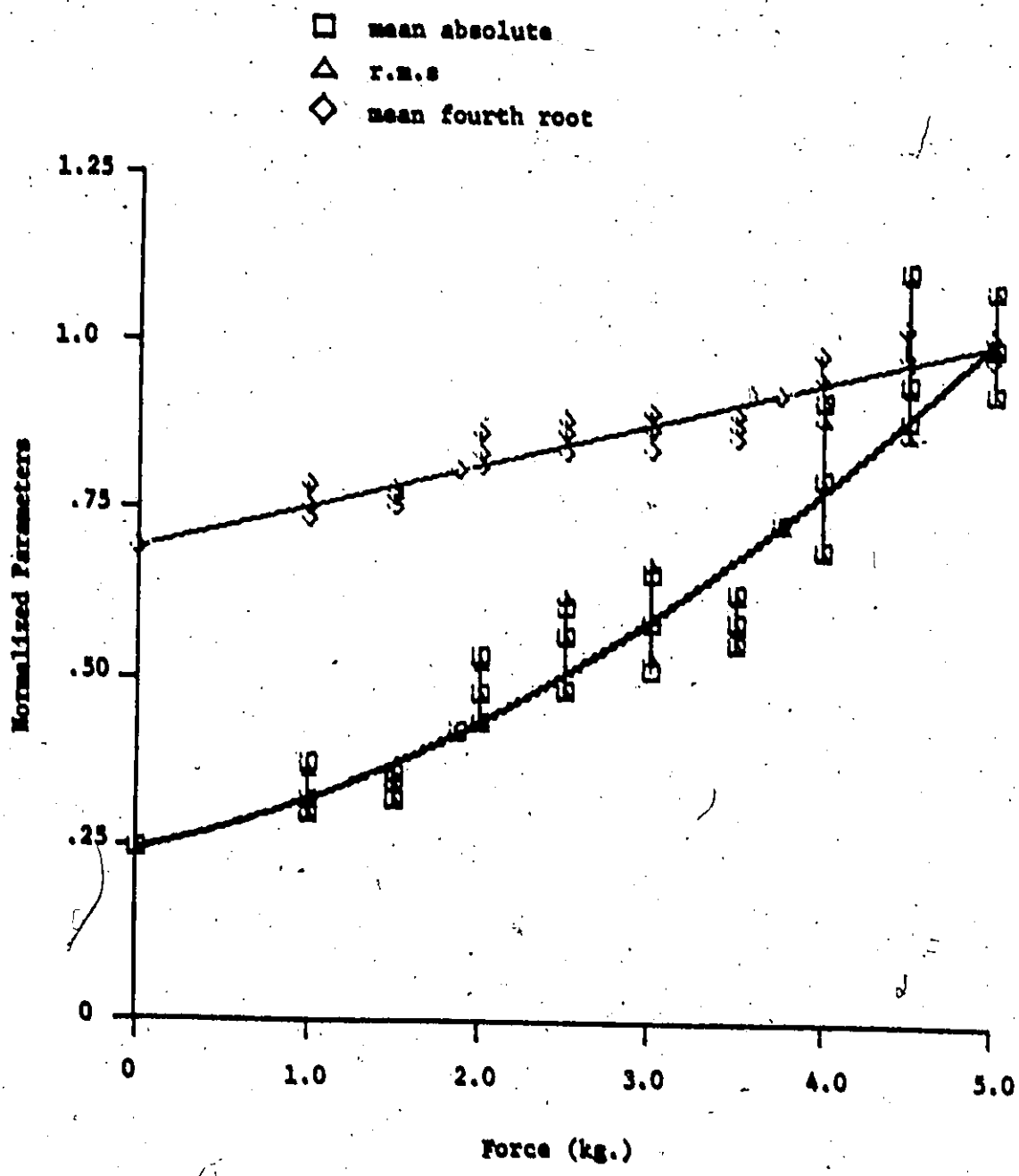


Figure 6.10 Mean absolute values, r.m.s., and mean fourth root values of EMG signals recorded for different force levels, T = 1.0 sec. Subject MM.

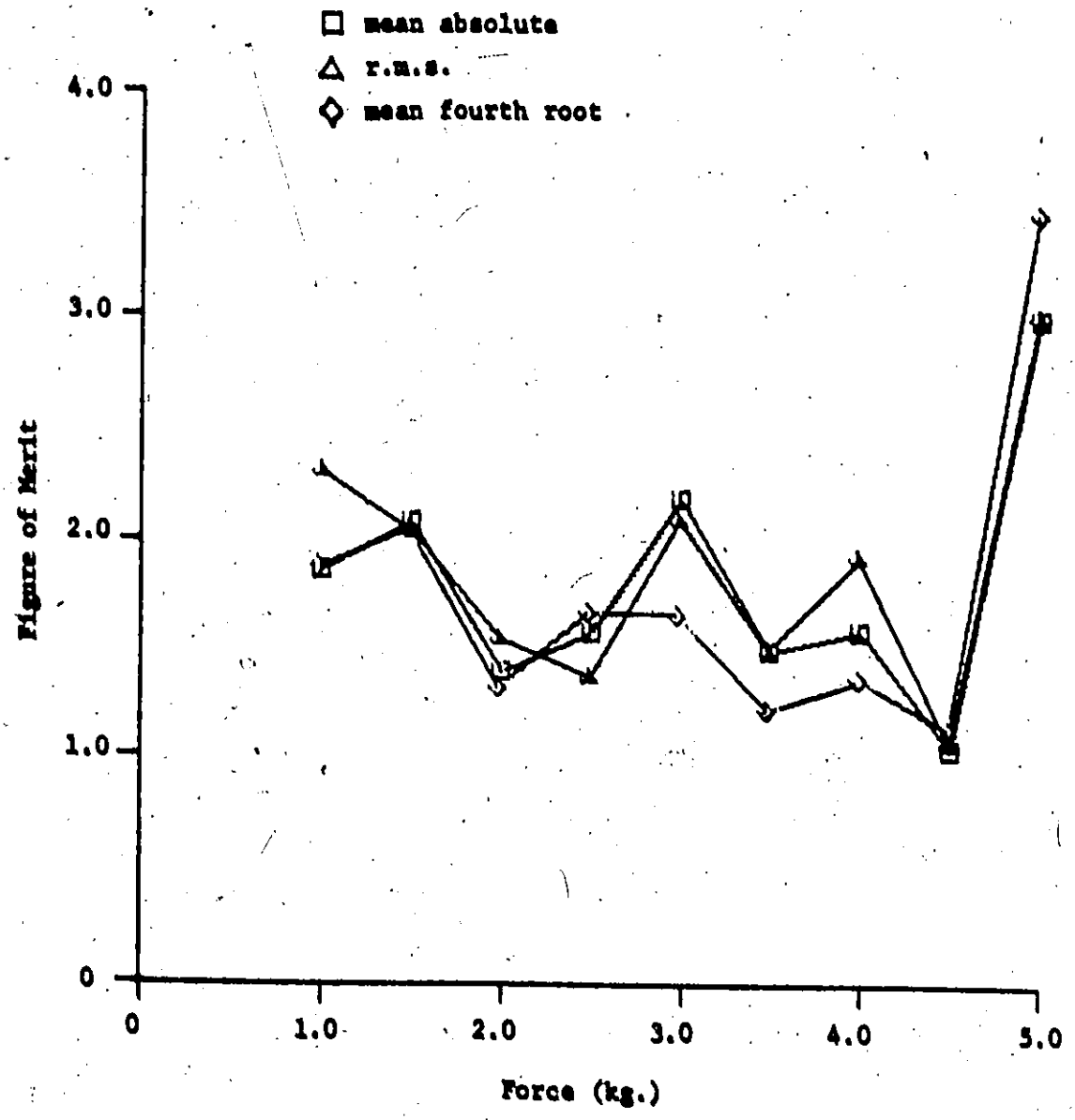


Figure 6.11 Figures of merit for the parameters of Fig. 6.10.

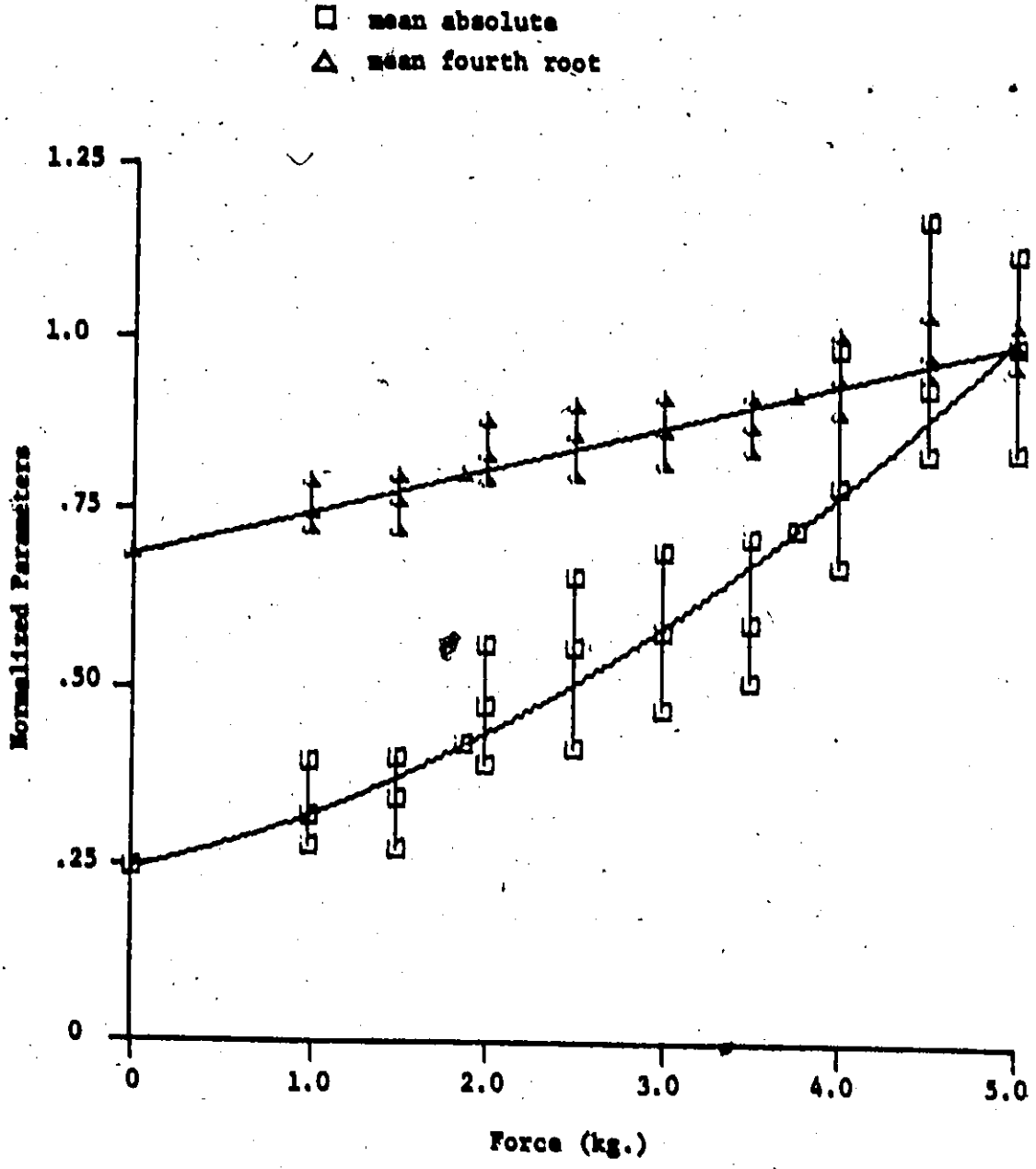


Figure 6.12 Mean absolute and mean fourth root values of EMG signals recorded for different force levels, T = .5 sec. Subject MM.

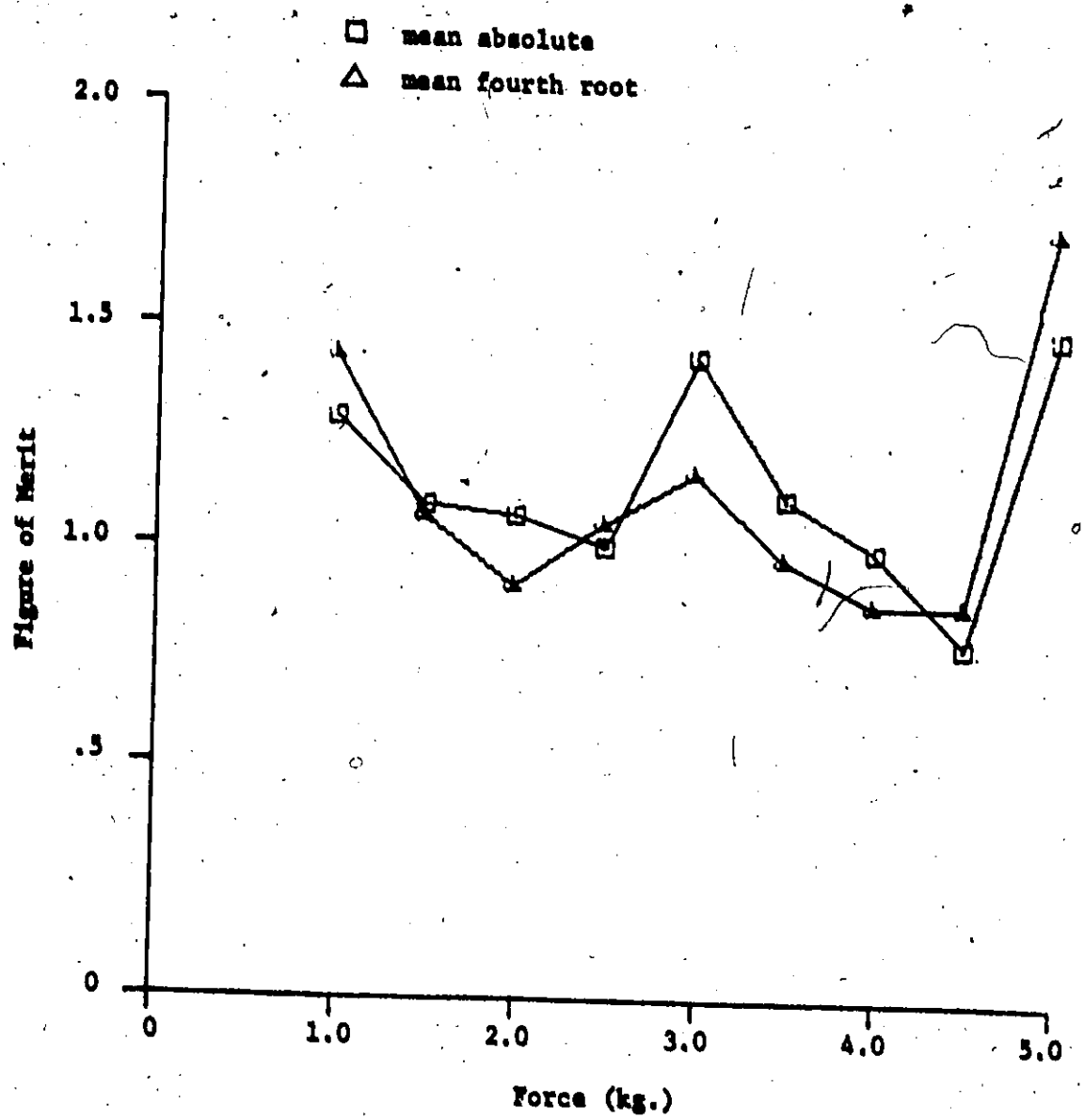


Figure 6.13 Figures of merit for the parameters of Fig. 6.12.

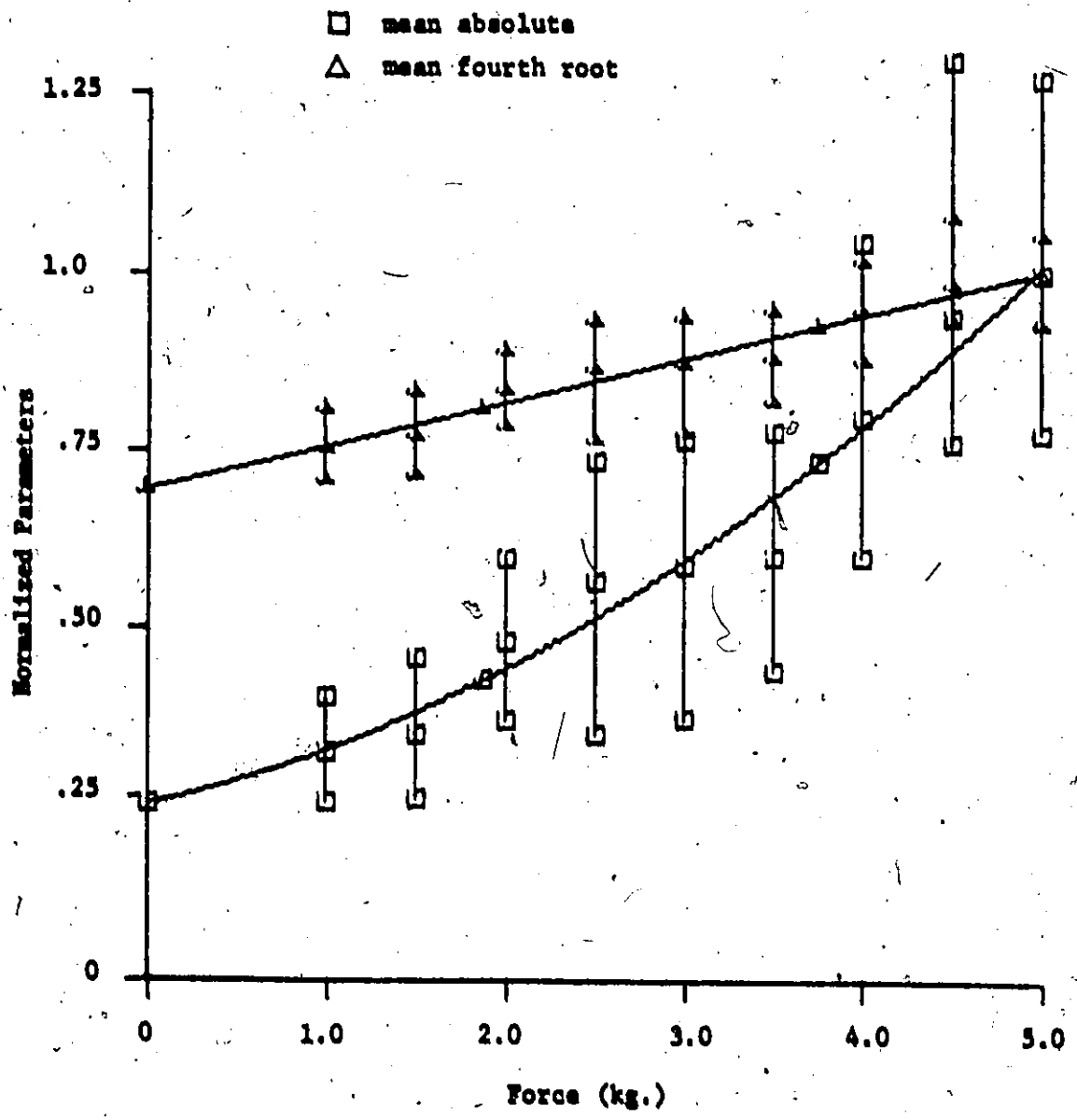


Figure 6.14 Mean absolute and mean fourth root values of EMG signals recorded for different force levels, T = .25 sec. Subject MM.

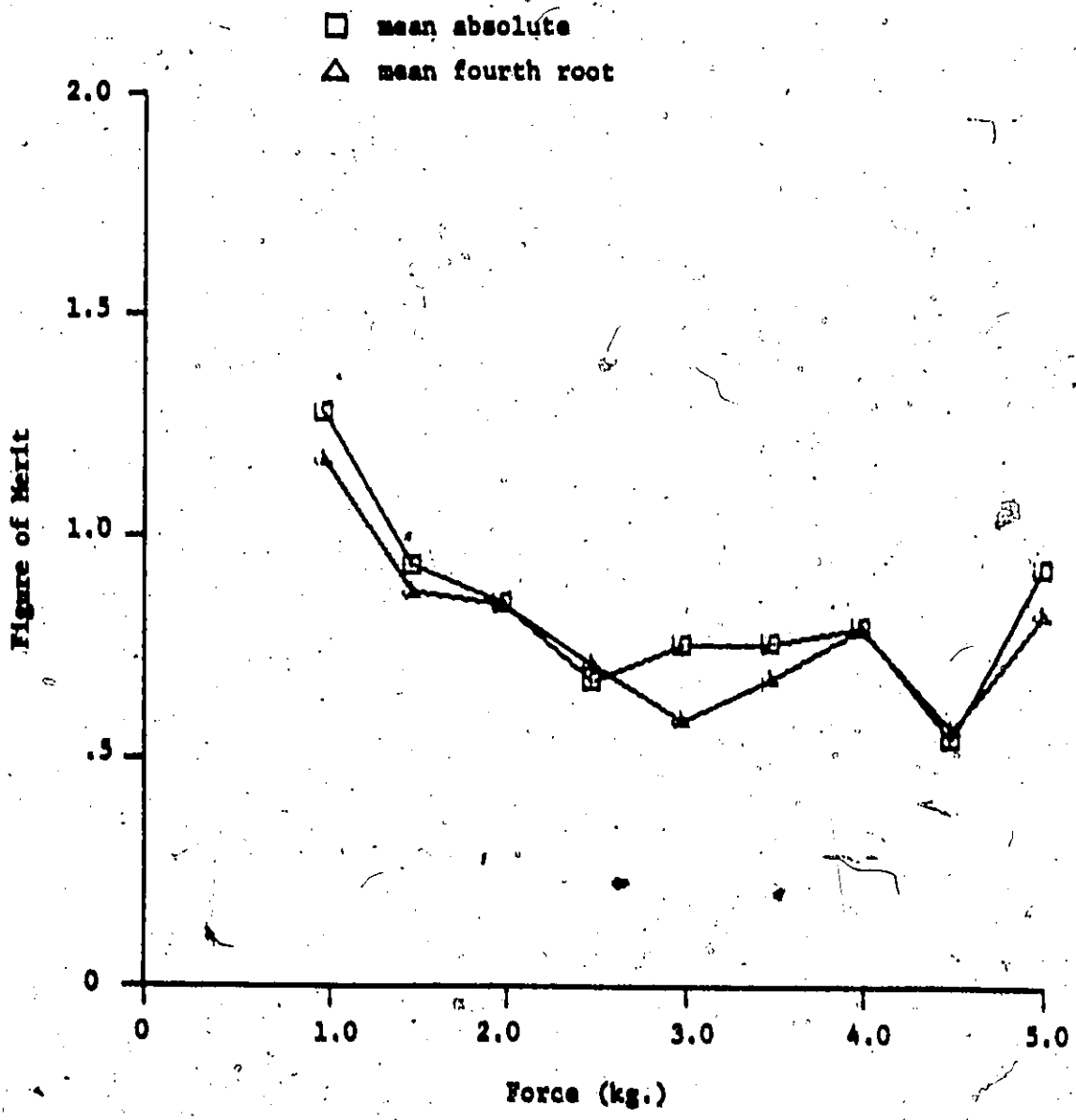


Figure 6.15 Figures of merit for the parameters of Fig. 6.14.

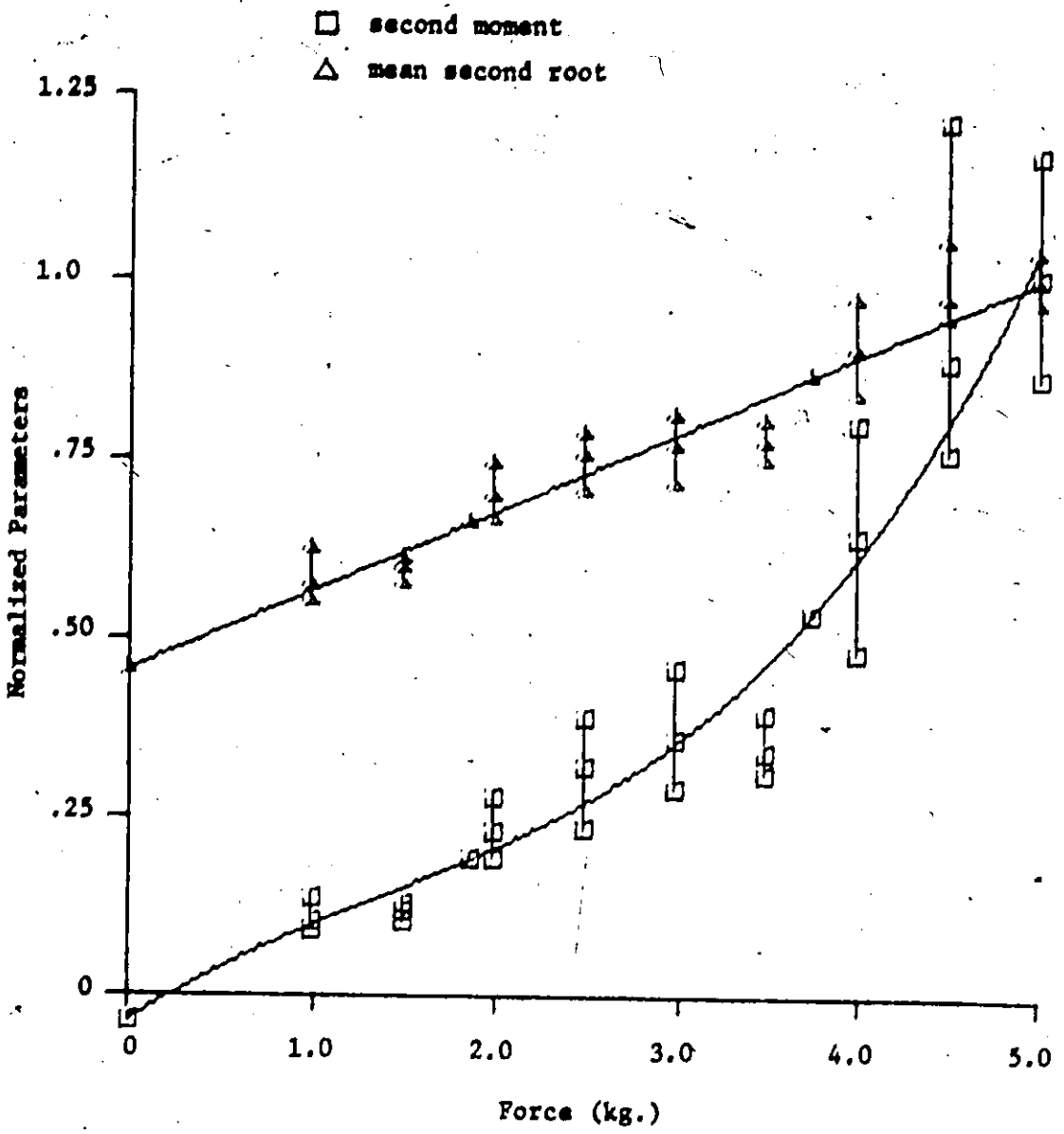


Figure 6.16 Second moments and mean second root values of EMG signals recorded for different force levels, T = 1.0 sec. Subject MM.

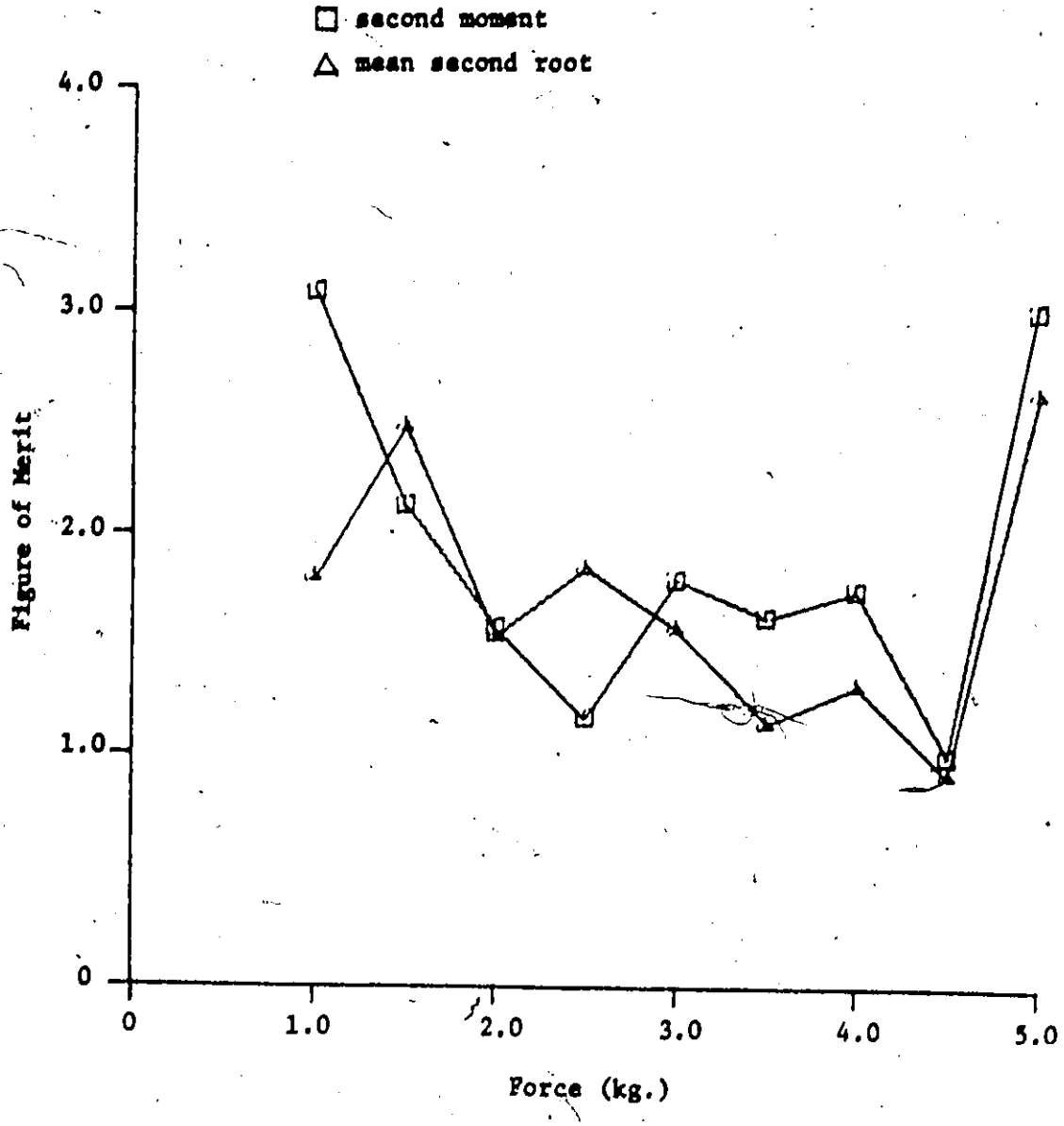


Figure 6.17 Figures of merit for the parameters of Fig. 6.16.

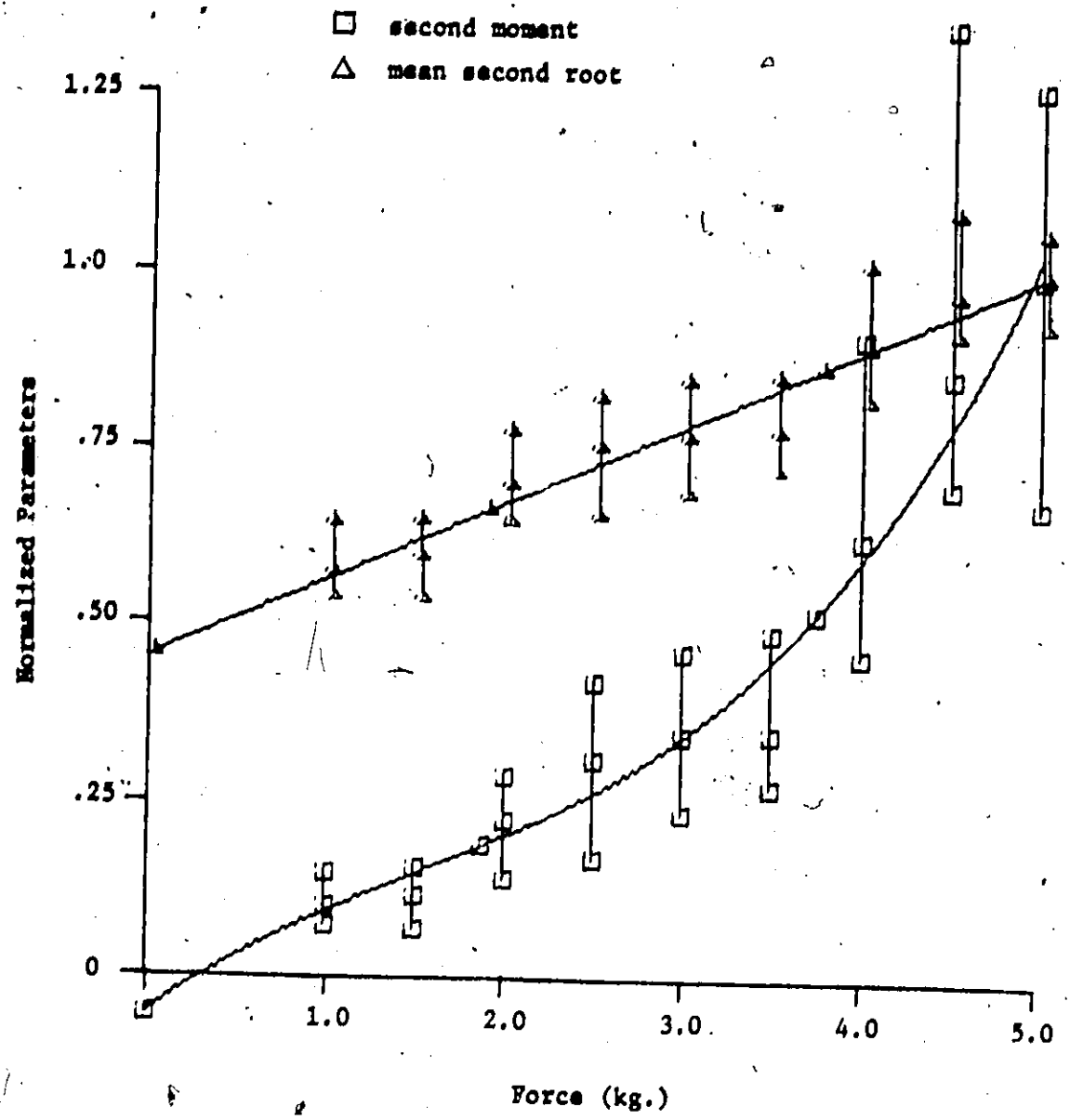


Figure 6.18 Second moments and mean second root values of EMG signals recorded for different force levels, T = .5 sec. Subject MM.

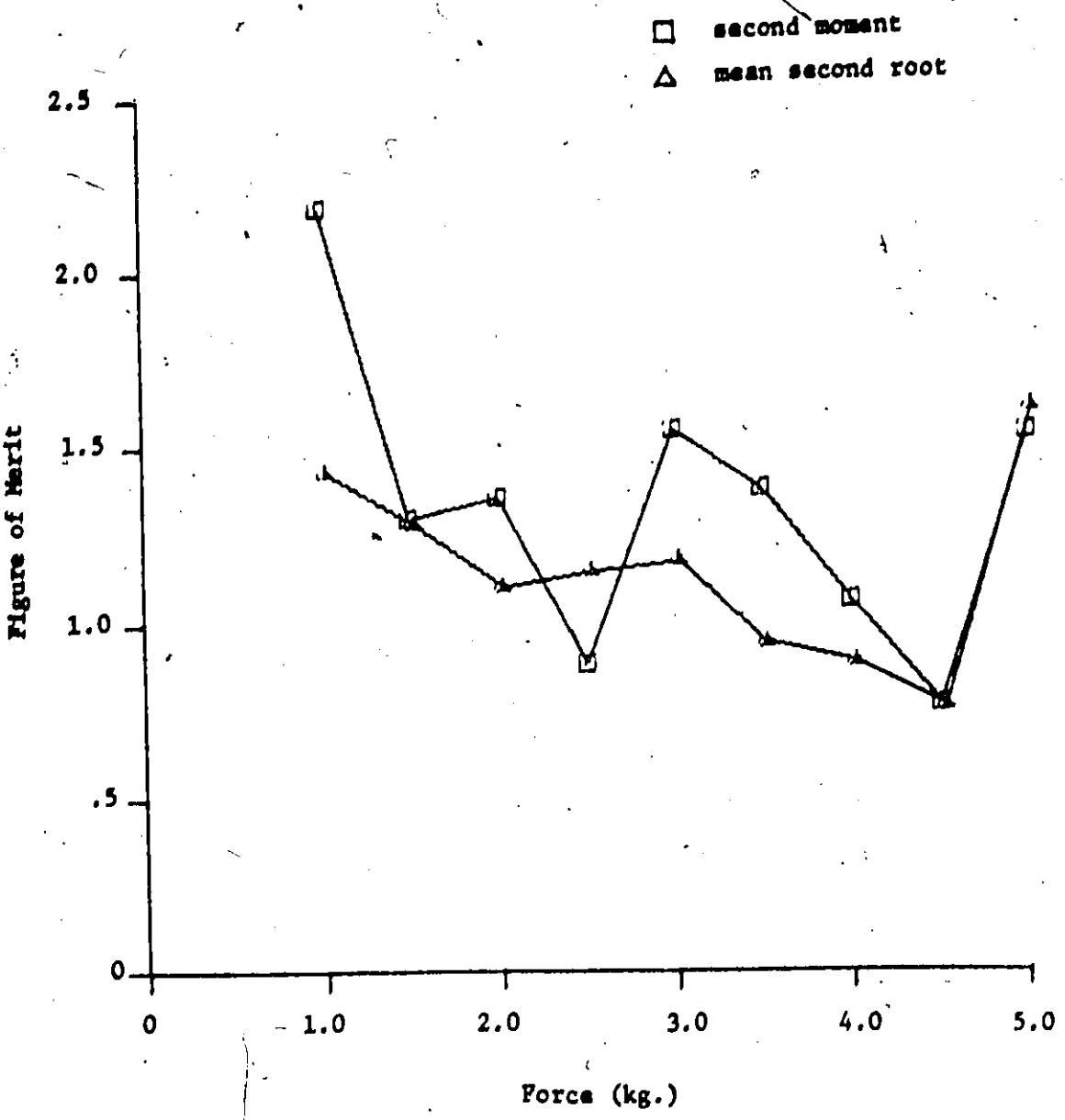


Figure 6.19 Figures of merit for the parameters of Fig. 6.18.

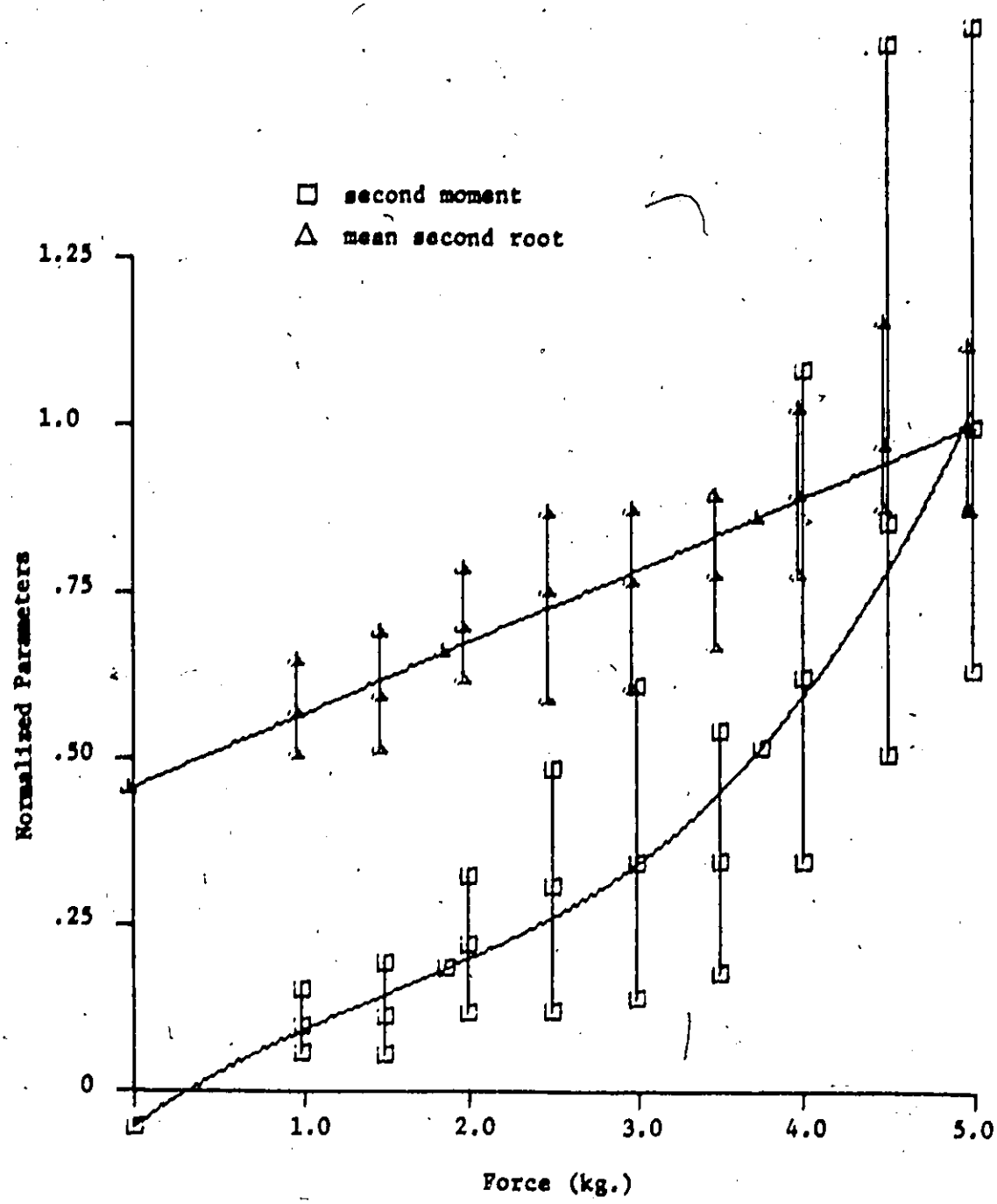


Figure 6.20 Second moments and mean second root values of EMG signals recorded for different force levels, T = .25 sec. Subject MM.

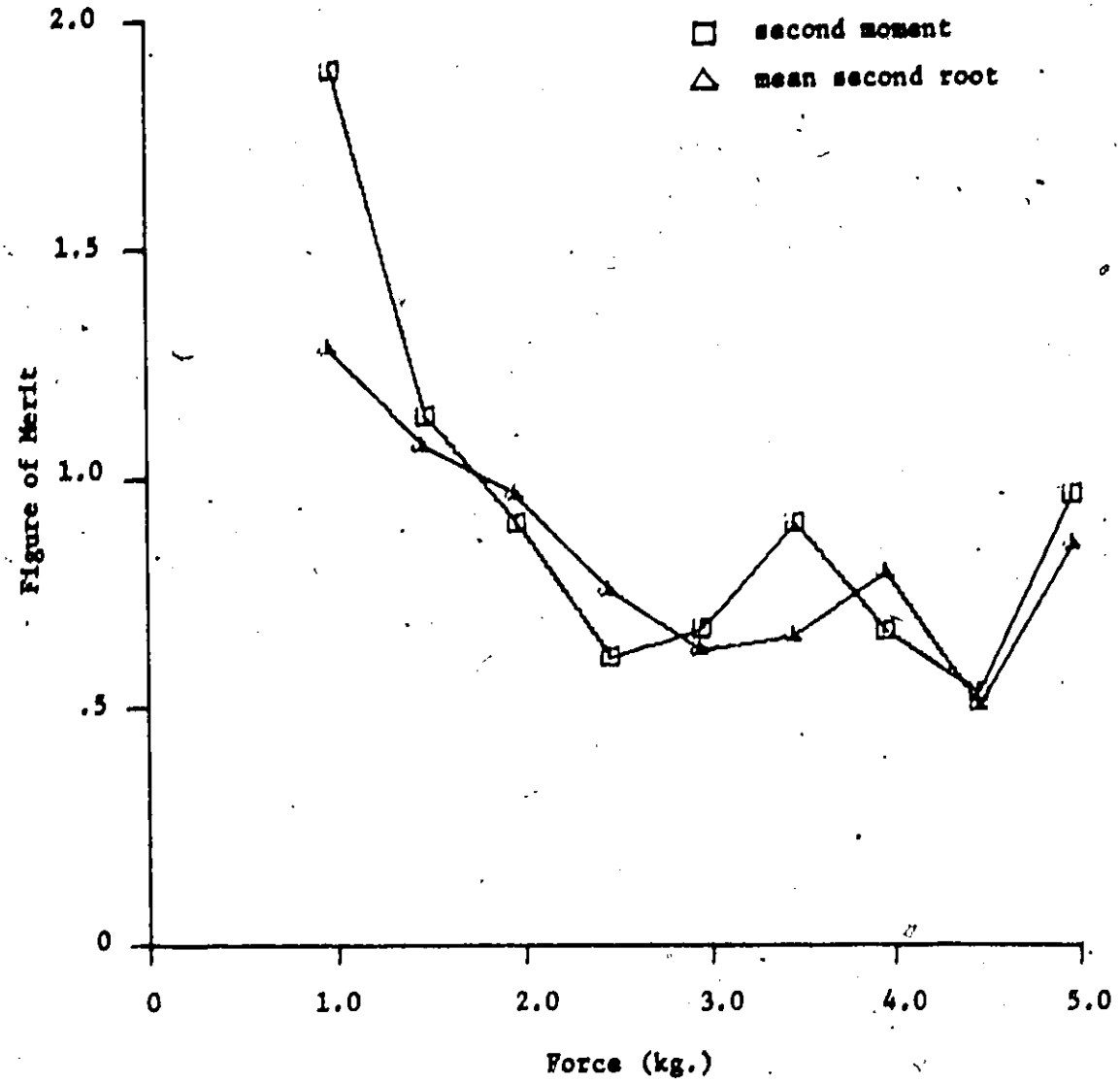


Figure 6.21 Figures of merit for the parameters of Fig. 6.20.

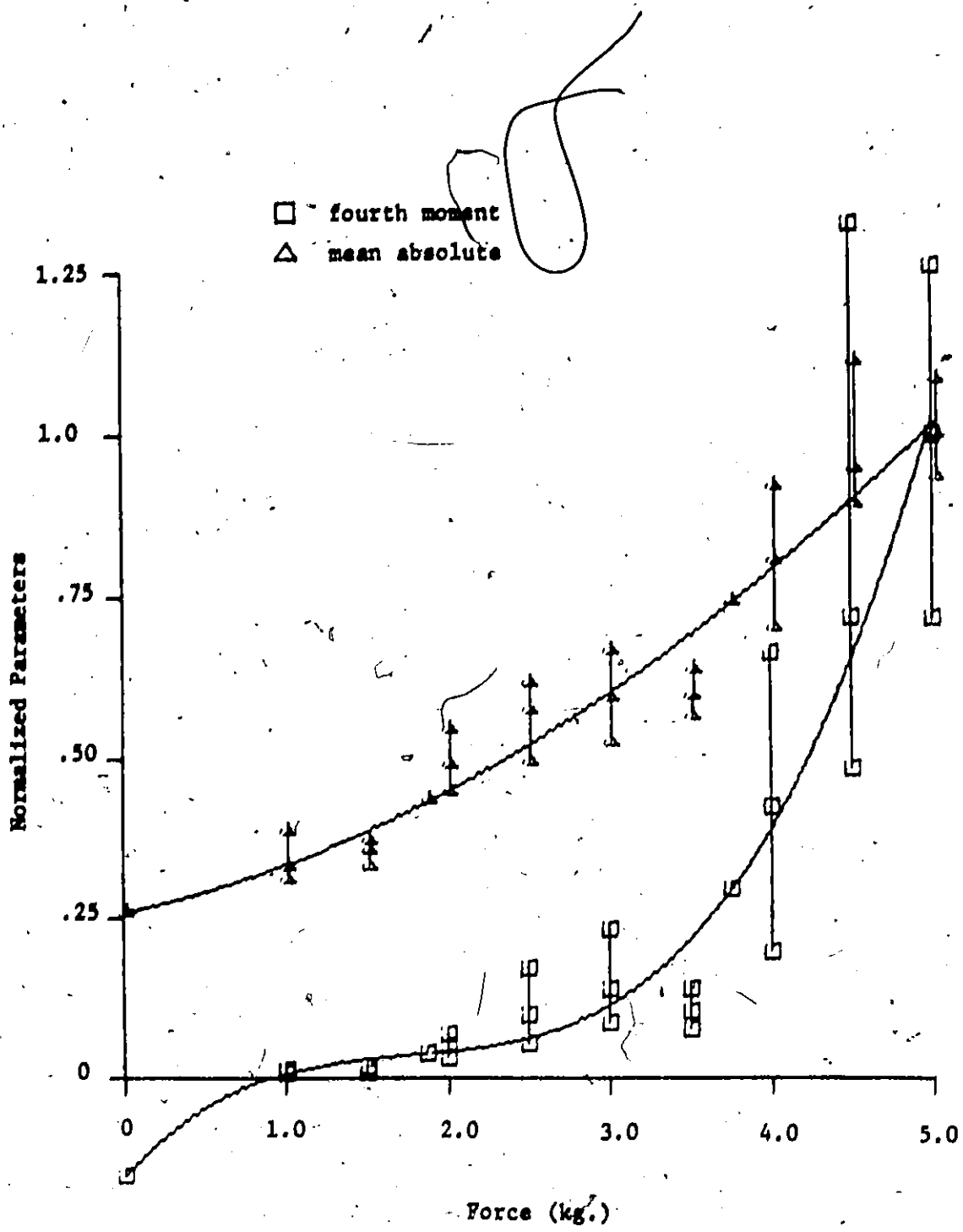


Figure 6.22 Fourth moments and mean absolute values of EMG signals recorded for different force levels, T = 1 sec. Subject MM.

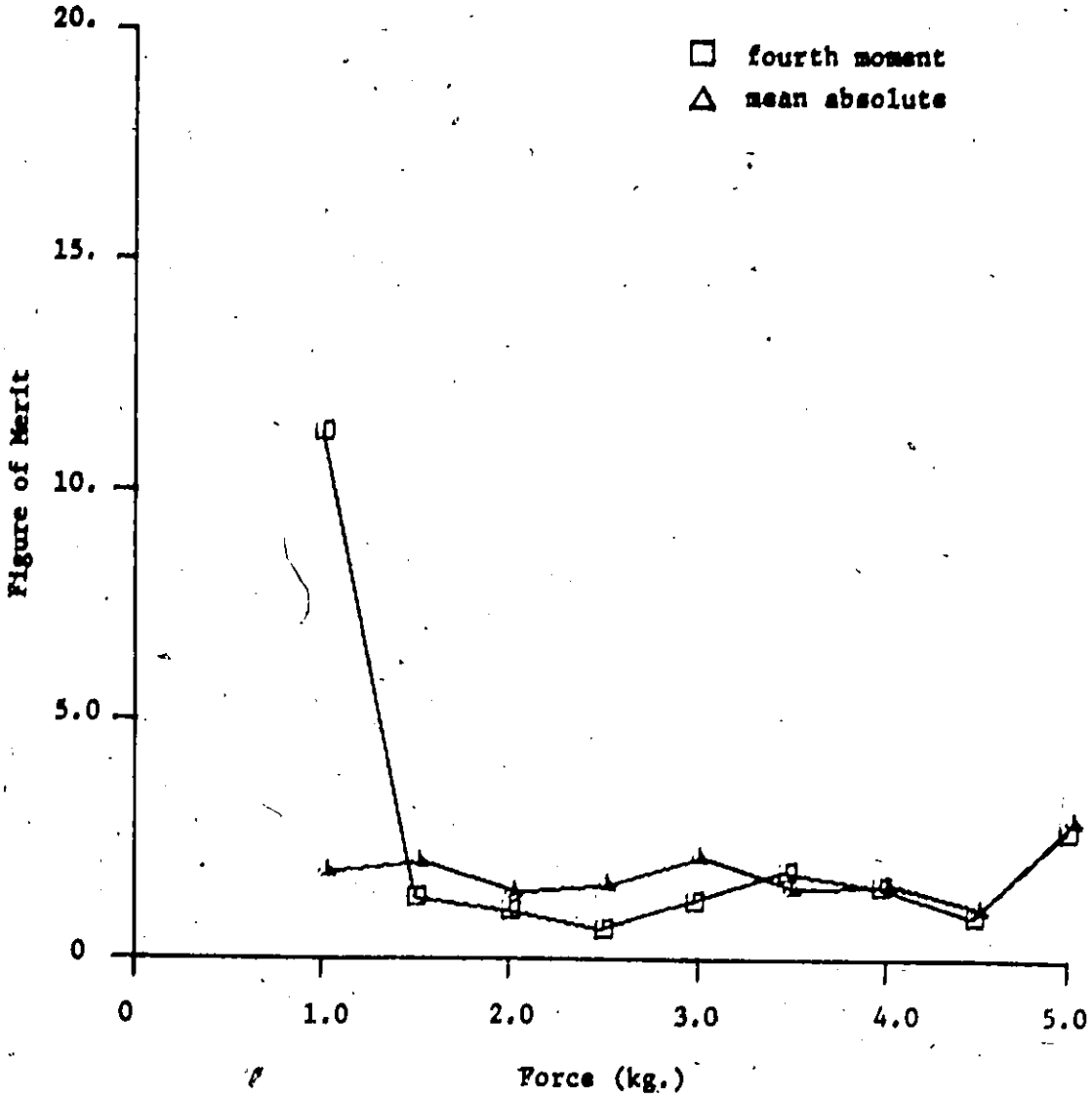


Figure 6.23 Figures of merit for the parameters of Fig. 6.22.

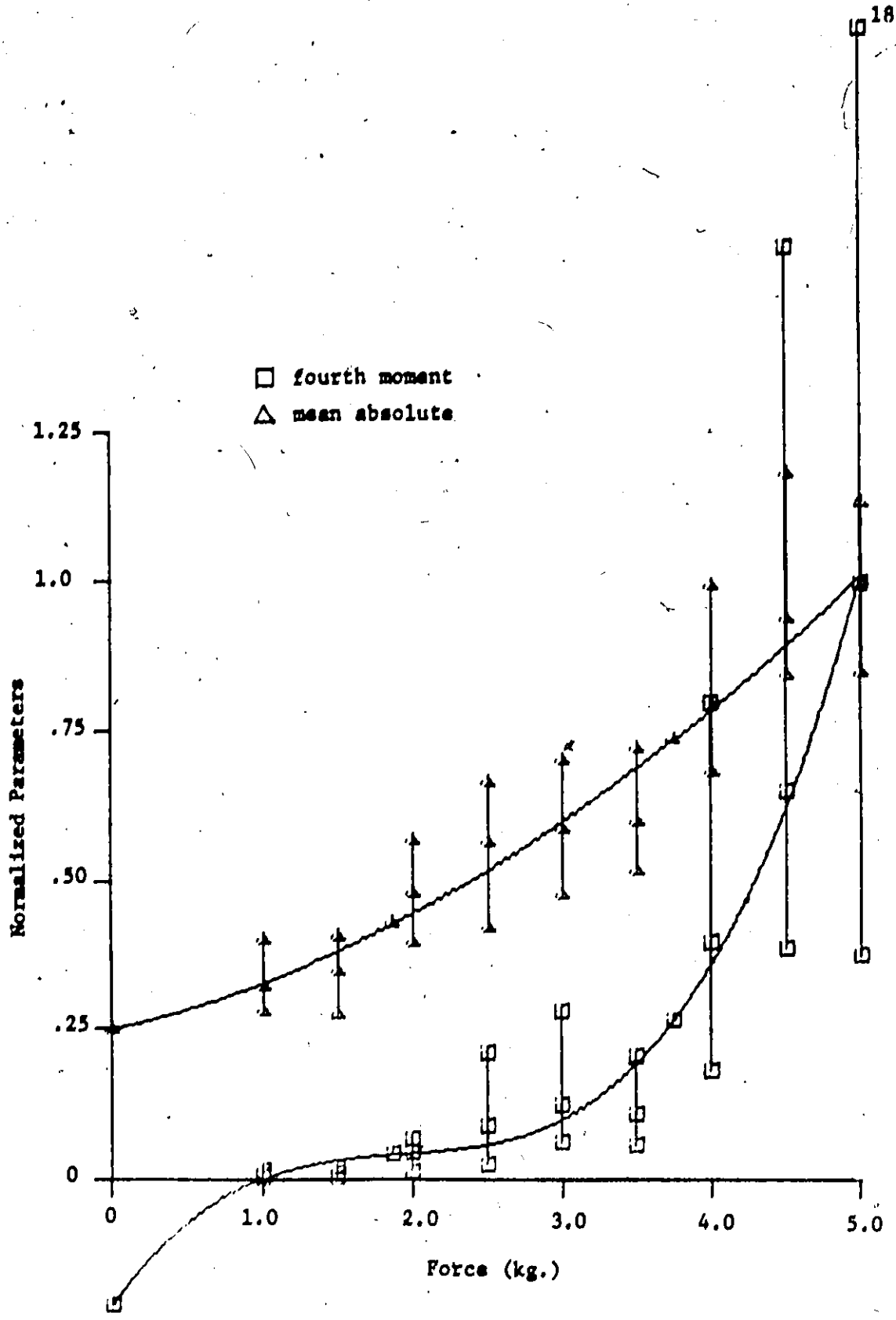


Figure 6.24 Fourth moments and mean absolute values of EMG signals recorded for different force levels, T = .5 sec. Subject MM.

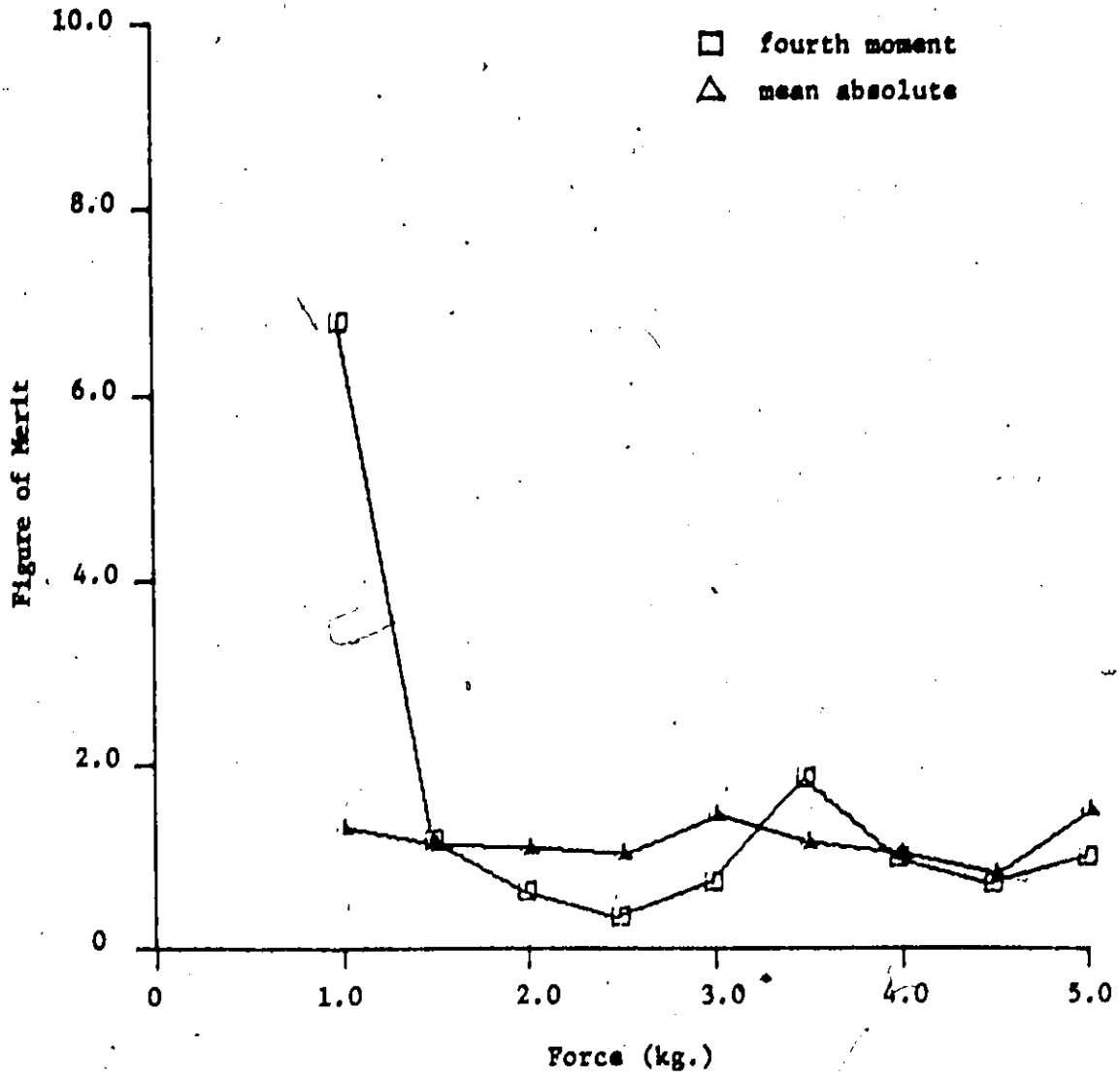


Figure 6.25 Figures of merit for the parameters of Fig. 6.24.

| Subject | HD | | | RD | | | SN | | | MM | | | WB | | | TW | | |
|---|---|---|---|---|---|---|---|---|---|---|---|---|---|---|---|---|---|---|
| T (sec.) | 1.0 | .5 | .25 | 1.0 | .5 | .25 | 1.0 | .5 | .25 | 1.0 | .5 | .25 | 1.0 | .5 | .25 | 1.0 | .5 | .25 |
| mean absolute value | 2.82 | 1 2.98 | 1.40 | 1.66 | 3 1.14 | .84 | 2.04 | 2 1.46 | 1.02 | 1.80 | 2 1.14 | .86 | 1.48 | 2 1.06 | .74 | 1.24 | 3 .88 | .60 |
| r.m.s. value | 2.62 | 1 1.80 | 1.30 | 1.60 | 3 1.04 | .74 | 1.88 | 2 1.40 | 1.04 | 1.86 | 2 1.24 | .86 | 1.50 | 2 1.08 | .70 | 1.36 | 3 .98 | .62 |
| second moment | 2.56 | 2 1.56 | 1.20 | 1.86 ** | 3 1.18 ** | .94 ** | 1.58 * | 2 1.18 * | .84 * | 1.92 ** | 3 1.34 ** | .94 ** | 1.48 ** | 1 1.08 ** | .72 ** | 1.40 | 3 .98 | .62 |
| mean second root | 2.40 | 1 1.72 | 1.24 | 1.50 | 3 1.08 | .80 | 2.06 | 1 1.50 | 1.0 | 1.74 | 1 1.14 | .84 | 1.42 | 2 1.0 | .70 | 1.12 | 3 .82 | .48 |
| mean fourth root | 2.30 | 2 1.74 | 1.22 | 1.46 | 3 1.06 | .80 | 2.18 | 1 1.36 | .94 | 1.76 | 1 1.12 | .80 | 1.36 | 2 .96 | .66 | 1.04 | 3 .76 | .52 |

Table 5.1 Average figures of merit for amplitude parameters of EMG signals recorded from different subjects. Single numeral in each box indicates polynomial order.

* negative slope at 1.0 kg.

** negative y-intercept.

average figures of merit and the polynomial order for each parameter for the six subjects tested. Although the order of the polynomial varies from parameter to parameter for each subject, the average figures of merit are approximately equal. As expected, the mean root values have small estimation errors while the moments have much larger errors. However, the increased sensitivity of the moments compensates for their large estimation errors and the average figures of merit remain approximately equal.

Figures 6.16 to 6.21 show the second moment and mean second root values for the different signal averaging periods. For these figures, a third-order polynomial which has a negative y-intercept is required to fit the moment mean estimates. A second-order fit was rejected since it has a negative slope in the interval. Similar problems were encountered for the moments calculated for the other subjects indicating that these parameters require an exponential fit. However, computer core limitations did not allow the additional programming required for exponential fitting. Consequently, the slope of the polynomial at 1.0 kg. is larger than it should be resulting in a large positive error for that level. Although the estimation errors for the moments shown in Figures 6.16 to 6.21 are much larger than the errors for the mean root values, their average figures of merit are approximately equal if the curve fitting problem is considered. Figure 6.21 demonstrates this quite effectively.

There was a similar problem in fitting curves to the fourth moment mean estimates as shown by Figures 6.22 to 6.25. As can be seen in Figures 6.23 and 6.25 a very large positive error is introduced into the figure of merit at 1.0 kg. resulting in much higher average figures of

merit. Fourth moment average figures of merit are therefore not included in Table 5.1. However, Figures 6.23 and 6.25 show that the fourth moment figures of merit are close to those for the mean absolute values for forces greater than 1.0 kg.

As can be seen in Figures 6.10 to 6.25, there is no significant change in the parameter polynomial (i.e. mean estimates) as the signal averaging period decreases. The decreased figures of merit as the signal period decreases result only from increased estimation error. The same result was observed for the parameters of all the subjects tested. Therefore, the mean estimate of the parameter is constant with changing signal averaging period.

### 6.2.2 Discussion

An examination of Table 5.1 shows that all the amplitude parameters of the EMG signal are equally effective as detectors of the muscle force. There is no significant variation in the average figures of merit for all the parameters calculated for each subject, if the errors introduced by poor polynomial fits are taken into account. As can be seen, the muscle force-EMG relationship is linear for the mean absolute value for only one subject. In addition, the polynomial order required to fit a parameter can vary from subject to subject. This variation in polynomial order can perhaps be explained by the activity of the brachialis muscle mentioned in Section 6.0.1. That is, the relative activities of the biceps and brachialis can vary from subject to subject as the load on the forearm increases. However, the object of the research presented in this chapter is a comparison of EMG amplitude parameters to determine

their relative suitability in myo-electric control applications, not an absolute determination of EMG-force relationships.

The results presented above contradict the conclusions of Kreifeldt and Yao (1974) that the mean fourth and second root values and the r.m.s. value, in that order, are more suitable control parameters than the mean absolute value. Their experimental method seems conceptually similar to that employed here and consists of recording processed EMG signals for four levels of isometric contraction (5% to 50% of maximal). However, their method of force indication consists of displaying the mean absolute value of the recorded signal, which the subject attempts to maintain at a preset level. Therefore the subject is not really attempting to maintain a constant force level but another parameter. In addition, their conclusions are obviously dictated by their selection of the signal-to-noise ratio as mentioned in Section 6.2.1. An examination of Fig. 6.10 shows that if their ratio were applied to the EMG signals recorded for this research, similar conclusions might be drawn (i.e. that the mean fourth root value is a better control parameter than the mean absolute value). It is felt that the figure of merit defined in Section 6.2.1 is a better indicator of parameter suitability since it also considers the parameter sensitivity to force level changes. It should also be recognized that results from only one subject have been presented in Kreifeldt and Yao's work. Since six subjects have been tested for 10 levels of contraction for the research presented in this chapter, it can be more generally concluded that all the EMG signal amplitude parameters considered here are appropriate as force detectors.

The choice of a suitable parameter should therefore be based on

economic and practical grounds. The mean absolute value or average of the rectified signal is the least expensive and simplest processor. Therefore, if a choice is to be made between amplitude parameters, the mean absolute value should be chosen.

## 6.3 Pattern Recognition of EMG Signals

### 6.3.1 Experimental Results

The pattern recognition detection algorithm described in Section 5.6 has been implemented and the detector responses calculated for the recorded EMG signals for 1.0, .5 and .25 sec. averaging periods using Eqn. 5.6-2. If such an algorithm is to be used for myo-electric control, it should be as simple as possible. Therefore, the simplest version of the algorithm which considers only four amplitude bins, was used. A successful test of this version should determine the validity of the pattern recognition concept outlined in Section 5.6.

The detection algorithm was tested for the four subjects whose amplitude parameters, calculated in Section 6.2, have the best average figures of merit. Even the simplest version of the algorithm requires the empirical determination of eight algorithm constants - the two lowest amplitude bin boundaries, M1 and M2, four bin multipliers, $m_i$, the peak count multiplier, PK, and the "noise" level, $\varepsilon$, (see page 148). No attempt was made to find the "optimum" algorithm constants for each subject, since the optimum set of constants for one subject may not produce good results for another subject as a result of variation in recruitment patterns. In addition, it is necessary to determine if the EMG signals

recorded from different subjects have common pattern characteristics. Therefore, a number of sets of constants were tested for each subject and the set chosen which produced the best results for all subjects. This approach also avoids closely matching the detector output to one set of experimental results which may include errors in the measured EMG-force relationship. For example, the mean estimate of the mean absolute value at 3.5 kg. of Fig. 6.10 is equal to that at 3.0 kg., where the expectation from the fitted curve is that it should be larger. In Fig. 6.8, the mean estimate of the mean absolute value at 2.0 kg. is less than that at 1.5 kg. Such errors in the amplitude parameter estimates occur for the signals recorded from all the subjects, but in general at different force levels as shown above. Consequently, if a common set of algorithm constants is determined, these errors will be given less weight.

Selection of Algorithm Constants

If one proceeds with the assumption that the peak-to-peak amplitude of the diphasic wave indicates the size of the motor unit, a reasonable choice for the amplitude bin multipliers, $m_i$, would be $m_i = i$ if each bin represents one quarter of the entire amplitude range. The peak count multiplier, PK, can be chosen such that the detector response is quite sensitive to force level changes. However, the detector response should have a small y-intercept since 0 kg. for these experiments does not correspond to 0 contraction level. The following algorithm constants were found to be suitable : bin boundaries $\mathcal{E}$ to .20MAX, .20MAX to .60MAX, .60MAX to .80MAX, and .80MAX to MAX; peak count multiplier, PK = .40;

bin multipliers, 4.0, 3.0, 2.0 and 0; and the noise level $\mathcal{E}$ = 63 binary states for MAX ≈ 2000 binary states. This choice of $\mathcal{E}$ ensures that the amplitude values of the signal can be represented by 8-bit binary numbers - hence an 8-bit microprocessor can be used to implement the algorithm. The detector output is then calculated using Eqn. 5.6-2 by

$$y = .40m_p + 2.0B_2 + 3.0B_3 + 4.0B_4 \qquad (6.3\text{-}1)$$

Figures 6.26 and 6.27 show the detector responses to the EMG signals used to calculate the amplitude parameters shown in Figures 6.10 to 6.25. These detector responses are typical. The average figures of merit for the four subjects tested are summarized in Table 5.2. An examination of this table shows that these figures of merit are equivalent to those of the amplitude parameters displayed in Table 5.1, with some being slightly better and others slightly worse than the corresponding figures in Table 5.1. It must be stressed that the algorithm constants used here are not optimum, but are only the best set of a few sets of constants tested.

Signal Sample Rate

If the algorithm is to be implemented using a microprocessor, it is necessary to determine the lowest suitable signal sample rate. The algorithm using the above constants was tested for 500 and 250 Hz sample rates by using every second or fourth sample of the 1 kHz-sampled EMG signals. There is no reduction in the figures of merit for two subjects and approximately 10% reduction in the figures of merit for the other

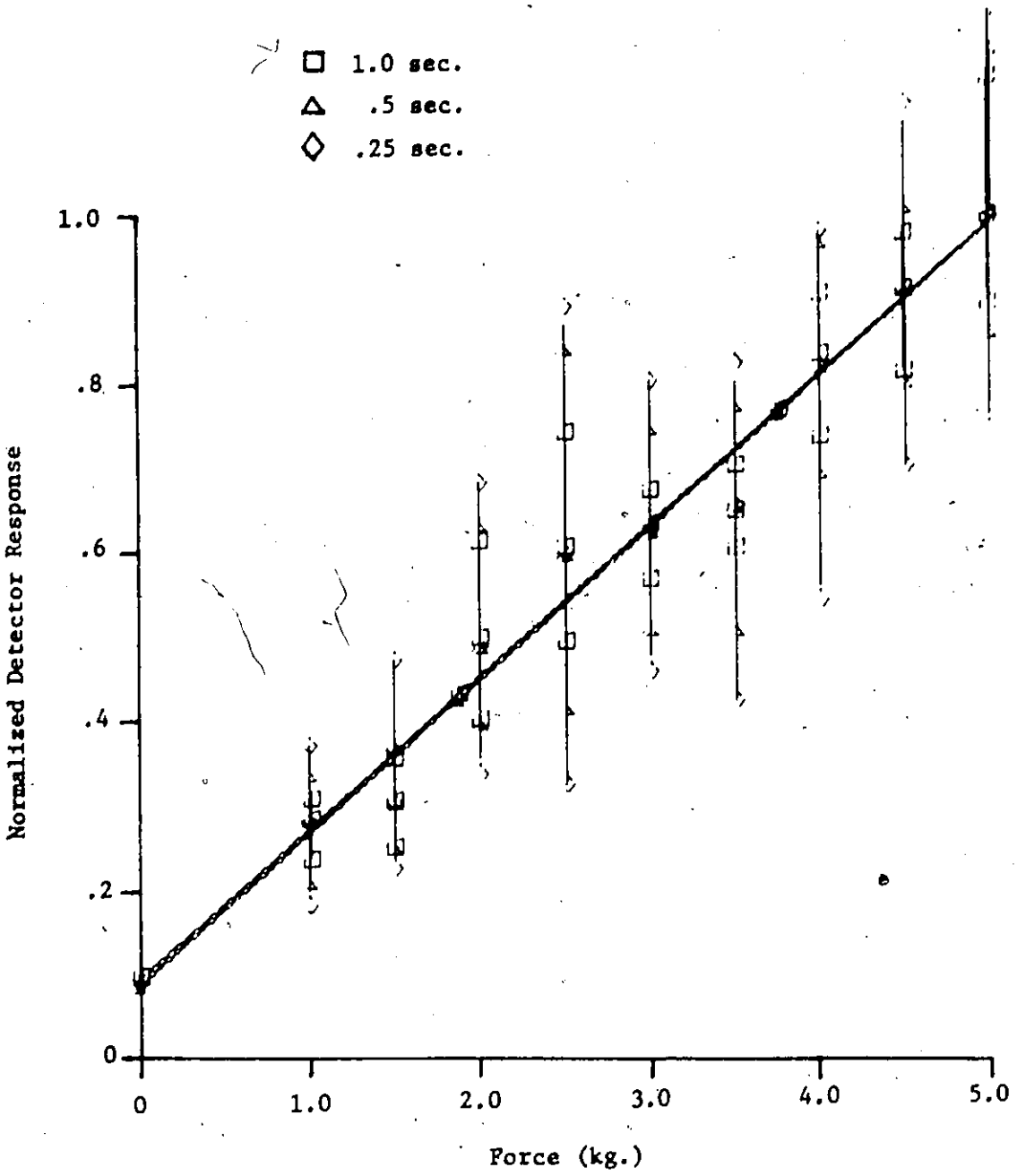


Figure 6.26 Detector responses for EMG signals recorded for different force levels. The responses are calculated for different signal periods, T. Subject MM.

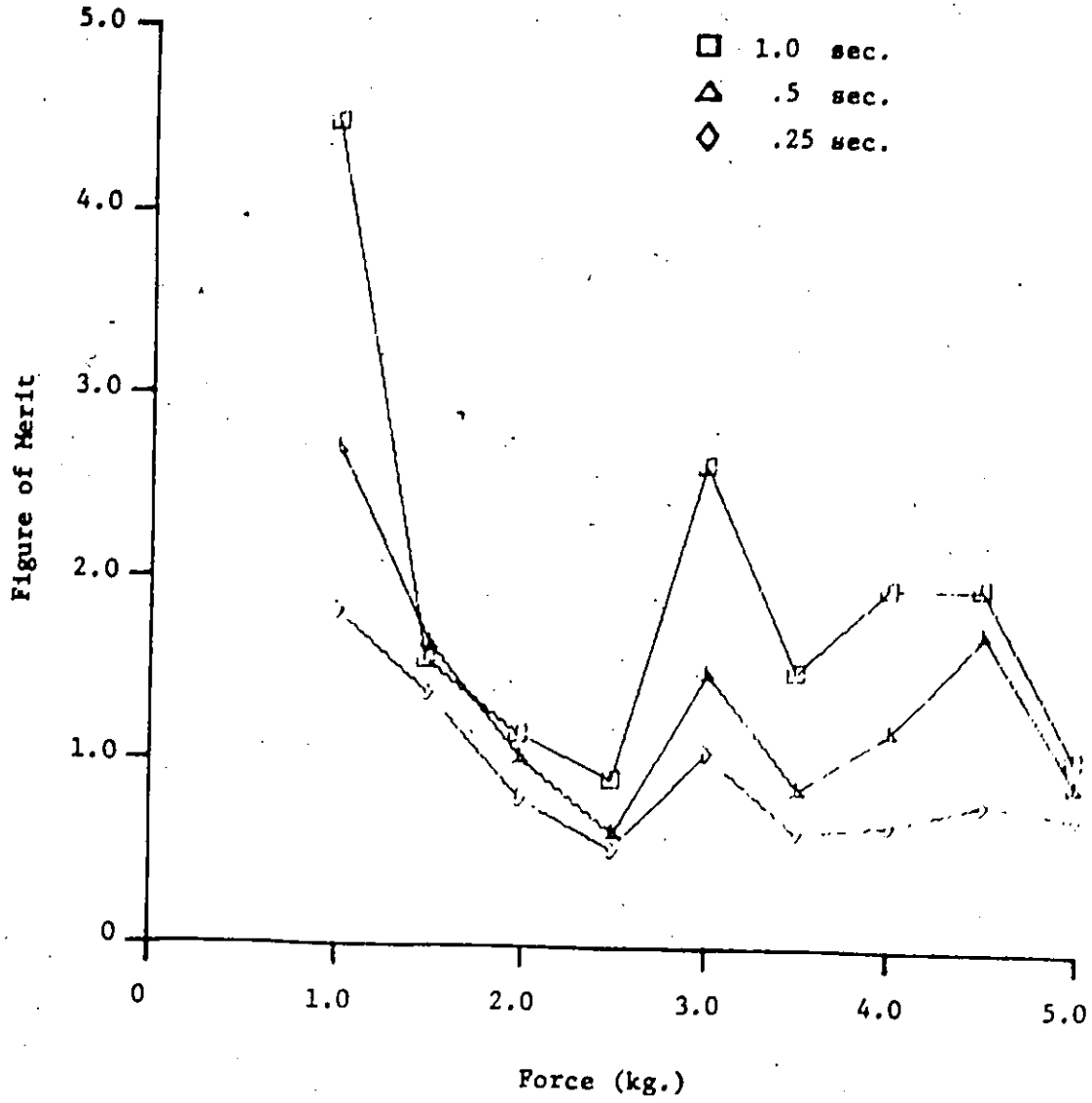


Figure 6.27 Figures of merit for the responses of Fig. 6.26.

| Subject<br>T (sec.) | HD | | | RD | | | SN | | | MM | | |
|---|---|---|---|---|---|---|---|---|---|---|---|---|
| | 1.0 | .5 | .25 | 1.0 | .5 | .25 | 1.0 | .5 | .25 | 1.0 | .5 | .25 |
| Bin Detector Response | | 1 | | | 3 | | | 1 | | | 1 | |
| | 2.60 | 1.58 | 1.24 | 1.84 | 1.16 | .80 | 2.10 | 1.38 | .94 | 1.92 | 1.38 | .92 |
| Peak Detector Response | | 2 | | | 2 | | | 2 | | | 2 | |
| | 1.86 | - | - | 1.34 | .76 | .52 | 1.68 | .94 | .58 | 1.24 | .74 | .46 |

Table 5.2 Average figures of merit for the responses of two versions of the pattern recognition algorithm. Single numeral in each box indicates polynomial order.

subjects. In addition, there is an average reduction of 22% in the figures of merit for all four subjects for a 250 Hz sample rate. Since the bandwidth of these signals is greater than 125 Hz as shown in Section 6.1, it is anticipated that there will be a deterioration in algorithm response for a 250 Hz sample rate. It may be concluded that a 1 kHz sample rate should be used for the detector. However, if necessary a 500 Hz rate may also be used with only a small reduction in performance.

Negative Peaks

The pattern recognition algorithm is described in Section 5.6.2 in terms of "positive" peaks or positive slopes of the EMG signal. The algorithm was tested to determine if "negative" peaks or slopes produced better results. That is, the same pattern recognition algorithm was used but with the signal inverted. Considerable variation could be observed in the figures of merit, i.e. up to 25%, in the positive and negative peak tests. However, a consistent test criterion was found which determined whether positive or negative peaks should be considered for best results. If the maximum peak-to-peak amplitude, MAX, for positive peaks is larger than that for negative peaks, positive peaks should be considered. If it is smaller the signal should be inverted. This test can be included in the algorithm calibration described in Section 5.6.3.

Simple Peak Detector

The simple peak detector version of the detection algorithm was also tested for the four subjects to determine if myo-electric control can be achieved by only considering the number of positive peaks occur-

ring in a period, T, of the EMG signal. The average figures of merit for this detector are shown in Table 5.2. As can be seen, these figures of merit are much lower than those measured for the amplitude bin detector. Figures 6.28 and 6.29 show peak detector responses for the EMG signals recorded from one subject. These results are typical for the four subjects tested. As can be seen from these figures, the number of peaks saturates as the force level increases resulting in a reduction of sensitivity and hence of the figure of merit. Close et al. (1960) have measured motor unit action potential counts for different levels of isometric contraction. Their results show no saturation in action potential counts at higher force levels but they used large needle electrodes. Since large surface electrodes are used here, the saturation effect may be explained by the integration of many action potentials, or the masking of smaller action potentials by large ones.

As for the EMG amplitude parameters of Section 6.2, the mean estimates of Figures 6.26 and 6.28 do not change with the signal period, T, and the decrease in the figures of merit is caused by increased estimation error. It may also be noted that the EMG-force relationships derived using the amplitude bin detector tend to be linear, where this relationship is linear for only one subject if the mean absolute value is used.

### 6.3.2 Discussion

It has been demonstrated that the pattern recognition algorithm using common algorithm constants is equally as effective in detecting muscle force level as the signal amplitude parameters described in

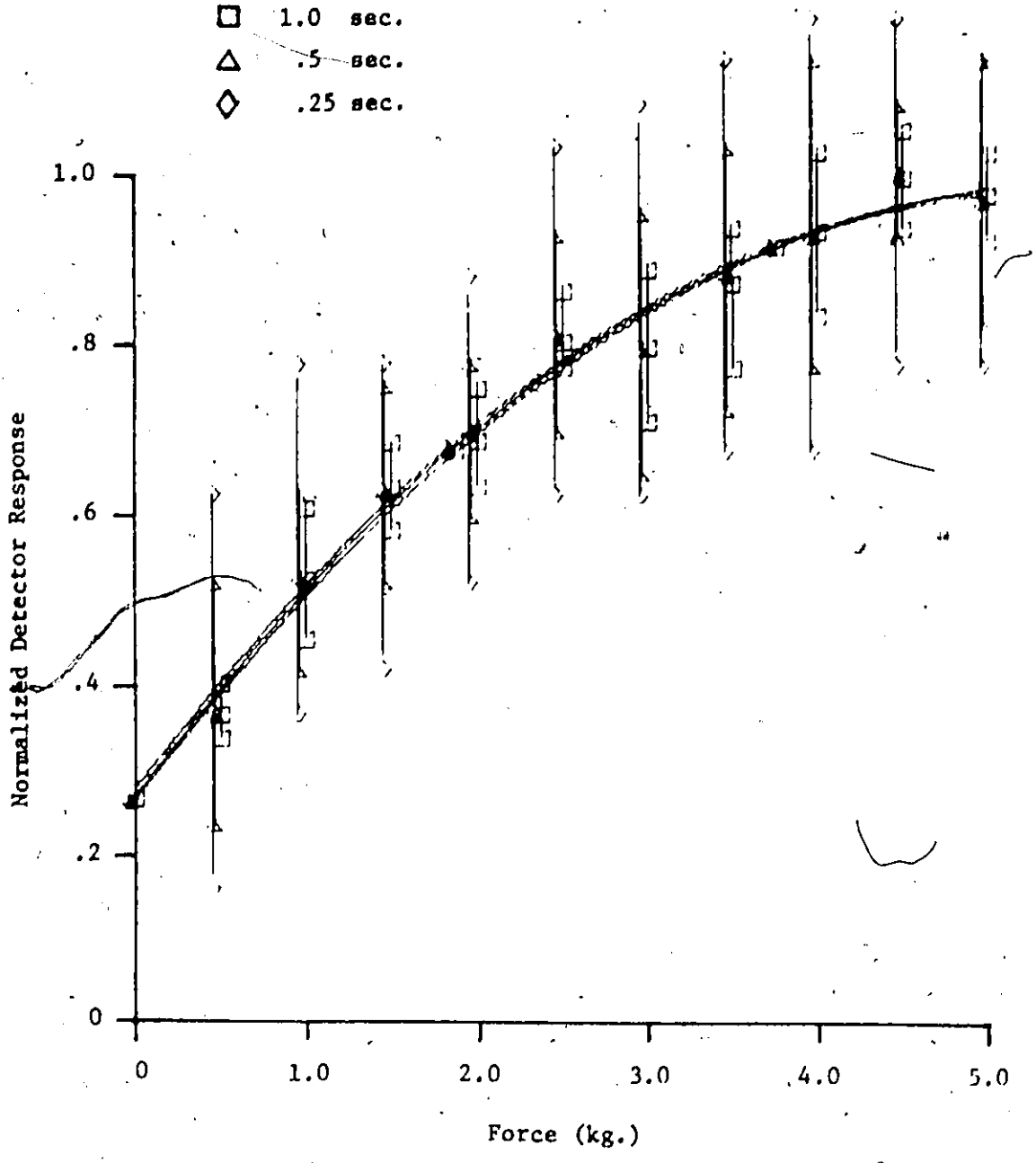


Figure 6.28 Peak detector responses for EMG signals recorded for different force levels. The responses are calculated for different signal periods, T. Subject SN.

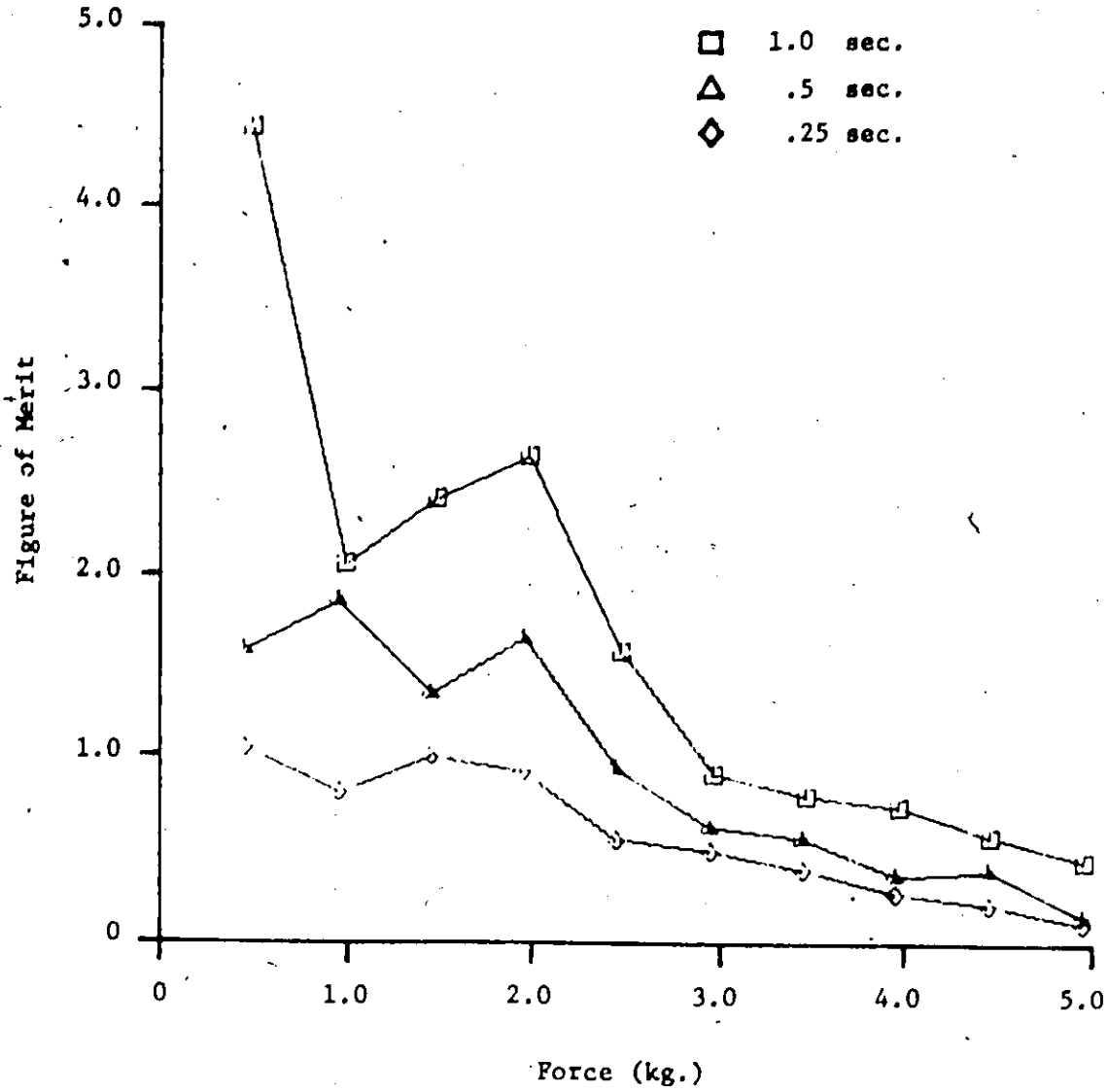


Figure 6.29 Figures of merit for the responses of Fig. 6.28.

Section 6.2. Although this detector does not use all the amplitude information in the EMG signal, i.e. by considering only four discrete peak-to-peak amplitude levels, it does use some of the frequency information by incorporating peak counts. The algorithm performance can be improved using three different techniques : an "optimum" common set of constants which will produce the best results for all the subjects can be determined; the algorithm constants can be matched to the signals for each subject; and a greater number of amplitude bins can be used. These techniques were not employed. It must be appreciated that the test results already validate the pattern recognition concept. It is to be expected that additional improvement in the detector performance can be achieved, and the pattern recognition algorithm can be considered at least as effective as the signal amplitude parameters in detecting different levels of constant isometric contraction.

Although the simple peak detector version of the algorithm is not as effective, its simplicity warrants further examination. Since the decrease in performance is caused by saturation of peak counts at higher force levels it can still be considered an appropriate processor of low force level EMG signals. Several real-time tests of the two versions of the detection algorithm show that the addition of visual feedback to the subject significantly improves the detector performance. This can be expected and naturally also applies to the amplitude parameter processors. In the real-time tests, subjects were required to maintain different levels of detector response. Most subjects could maintain three discrete levels using the simple peak detector.

## 6.4 Summary

Several parameters of the EMG signal have been evaluated as potential myo-electric control processors. These parameters have been calculated for the EMG signals recorded from six adult male subjects for a range of constant isometric contractions. The same signals have also been used to test a proposed pattern recognition algorithm. Recognizing that six subjects have been used in the tests, certain general conclusions can be stated.

There seems to be no force information present in the autocorrelation and power spectral densities of EMG signals recorded under the experimental conditions used in this work. No consistent changes in these plots can be discerned for changes in force level. In addition, random variations in the plots calculated for the same force level for the same subject can be as large as the random variations in the results calculated for different force levels. Therefore these statistical parameters cannot be used in EMG processing strategies.

A figure of merit has been proposed which considers both the sensitivity of a parameter to changes in the force level and the estimation error for the parameter at each force level. This figure of merit has been used to determine the relative suitability of the different amplitude parameters and the detection algorithm, in detecting muscle force. The mean absolute, r.m.s., and mean second and fourth root values, and the second and fourth moments are equally effective as detectors of muscle force. If economic and practical grounds are considered, the mean absolute value or the average of the rectified signal can be considered the most suitable amplitude processor.

The pattern recognition algorithm using a single preliminary set of algorithm constants is equally as effective as the above amplitude parameters in detecting muscle force. The performance of this detector can be improved by "optimizing" the algorithm constants or extending the algorithm to consider more amplitude bins. Finally, the simple peak detector version of this algorithm can be used as a processor of low force level EMG signals.

# CHAPTER 7

# CONCLUSIONS

The research presented in this thesis is concerned with the analysis and processing of electromyographic signals with a view to their use as a source of control for environmental control or other rehabilitation devices. Three different topics have been considered in this research. An application of myo-electric control of a simple communication device for a cerebral palsied patient has been presented. A model of the myo-electric source which can be used to simulate EMG signals in real-time has been proposed. Finally, a number of parameters of the EMG signal have been examined as possible detectors of muscle force under isometric conditions.

A simple communication device, which uses the electromyographic signal from a selected muscle of a patient as control input, has been designed and constructed. Very promising results have been obtained with the cerebral palsied patient and indications are that the electromyographic signal from a spastic, yet somewhat controllable muscle can serve as an effective control for communication devices. To our knowledge, this is one of the first applications of myo-electric control for a cerebral palsied patient.

A new model of the myo-electric source and its computation algorithm have been developed and implemented on a minicomputer. The algorithm per-

forms real-time simulation of the myo-electric signals recorded from different electrode configurations and can generate controllable simulated signals at a sufficiently high sample rate to test hardware EMG processors or software force detection strategies. The algorithm has been tested for two different electrode systems, pasteless surface electrodes and coaxial needle electrodes and the results compared with real signals recorded using these electrode systems. There is good agreement between simulated and real signal autocorrelation and power spectral density plots but analysis of these plots and visual examination of the EMG signal point out the necessity of a more force-sensitive comparison criterion. The studies presented in Chapter 6 reinforce this view. No precise physiological interpretation can be derived from the algorithm parameters since the model is too simplified to completely represent the myo-electric source. However, since the modelling process required the careful examination of both surface and intramuscular EMG signals, valuable insights were gained into the characteristics of EMG signals. For example, diphasic waves with certain discrete amplitudes, resembling motor unit action potentials, were observed in all surface EMG signals. Such observations led to the conclusion that simple pattern recognition can be applied to the EMG signal to detect changes in the muscle force.

A number of statistical parameters of the EMG signal were examined to determine which parameter is most suitable for myo-electric control. A figure of merit has been proposed which considers both parameter sensitivity to changes in the force level and the estimation error for the parameter at each force level. The parameters were tested for surface EMG signals recorded from six normal subjects for a range of low to moderate

constant isometric contractions of the biceps brachii. From these results, it can be concluded that the autocorrelation and power spectral densities of surface EMG signals recorded under these conditions reflect no muscle force information. In addition, the mean absolute, r.m.s., and mean second and fourth root values, and the second and fourth moments are equally effective as detectors of muscle force. If economic and practical grounds are considered, the mean absolute value or average of the rectified signal can be considered the most suitable amplitude processor.

A new pattern recognition algorithm capable of implementation on a microprocessor has been proposed which attempts to extract the motor unit recruitment and discharge frequency information present in the surface EMG signal without using statistical mathematics. In its simplest form, detection is accomplished by recognition of peak-to-peak signal excursions exceeding a predetermined or preset threshold. More sophistication follows from the classification of peak-to-peak excursions into discrete amplitude groups or bins. This detector has been tested for four subjects using the same method as for the statistical amplitude parameters. The algorithm constants employed were determined by trial and error and the detector was found to be equally as effective as the above mentioned amplitude parameters in detecting muscle force. It is to be expected that the detector performance can be improved by optimizing the algorithm constants or extending its number of amplitude bins. The simple peak detector version of this algorithm can also be used as a processor of low force level EMG signals. Therefore, it can be concluded that simple pattern recognition can be employed effectively to extract muscle force infor-

mation from surface recorded EMG signals under isometric conditions.

Future work should be directed towards the testing of algorithmic responses under simulated dynamic control conditions.

## REFERENCES


Abdel Azim, M.S. (1975), "Modelling of the myoelectric source", M.Eng. Thesis, McMaster University.

Abdel Azim, M.S. and Della Torre, E. (1975) "A detailed physical model of the EMG source", Proc. Sixth Ann. Pittsburgh Conf. on Modeling and Simulation, pp. 357-362.

Ashby, P. and Burke, D. (1971), "Stretch reflexes in the upper limb of spastic man", J. Neurol., Neurosurg., and Psychiat., vol. 34, pp. 765-771.

Basmajian, J.V. (1974), Muscles Alive : Their functions revealed by electromyography, ed. 3, Williams & Wilkins.

Bendat, J.S. and Piersol, A.G. (1968), Measurement and Analysis of Random Data, J. Wiley and Sons.

Bergland, G.D. (1969), "A guided tour of the Fast Fourier Transform", IEEE Spectrum, vol. 6, pp. 41-52.

Bottomley, A.H., Kinnier-Wilson, A.B. and Nightingale, A. (1963), "Muscle substitutes and myoelectric control", J. Brit. Inst. of Radio Engg., vol. 26, pp. 439-448.

Bousso, D. and Ishai, G. (1969), "Report on the use of myo-electric signals for multiple degree-of-freedom or in prosthesis control", TDM 69-7, Technion-Israel Institute of Technology, Dept. of Mechanics.

Brody, G., Scott, R.N. and Balasubramanian, R. (1974), "A model for myoelectric signal generation", Med. and Biol. Engg., vol. 12, pp. 29-41.

Brown, B.H. (1968), "Theoretical and experimental waveform analysis of human compound nerve action potentials using surface electrodes", Med. and Biol. Engg., vol. 6, pp. 375-386.

Buchthal, F., Guld, C. and Rosenfalck, P. (1955), "Innervation zone and propagation velocity in human muscle", Acta Physiologica Scandinavica, vol. 35, pp. 174-190.

Buchthal, F. and Rosenfalck, P. (1955), "Action potential parameters in different human muscles", Acta Psychiat. et Neurol. Scand., vol. 30, pp. 125-131.

Burke, D., Andrews, C.J. and Lance, J.W. (1972), "Tonic vibration reflex in spasticity, Parkinson's disease, and normal subjects", J. Neurol., Neurosurg., and Psychiat., vol. 35, pp. 477-486.

Chusid, J.G. (1973), Correlative Neuroanatomy and Functional Neurology, Chapter 7, Lange Medical Publications.

Clamann, H.P. (1969), "Statistical analysis of motor unit firing patterns in a human skeletal muscle", Biophysical Journal, vol. 9, pp. 1233-1251.

Close, J.R., Nickel, E.D. and Todd, F.N. (1960), "Motor-unit action-potential counts", J. of Bone and Joint Surgery, vol. 42-A, pp. 1207-1222.

Cochran, W.T., Cooley, J.W. et al. (1967), "What is the Fast Fourier Transform?", Proc. of the IEEE, vol. 55, pp. 1664-1674.

Cooley, J.W., Lewis, P.A.W. and Welch, P.D. (1969), "The Fast Fourier Transform and its applications", IEEE Trans. on Education, vol. 12, pp. 27-34.

Cox, D.R. and Smith, W.L. (1954), "On the superposition of renewal processes", Biometrika, vol. 41, pp. 91-99.

de Bruin, H. and Della Torre, E. (1975), "Real-time simulation of EMG signals", Proc. Sixth Ann. Pittsburgh Conf. on Modeling and Simulation, pp. 363-367.

de Bruin, H. and Della Torre, E. (1976), "Derivation of control information from electromyographic patterns", accepted for presentation at the Eleventh Int. Conf. on Med. and Biol. Engg., Ottawa.

Dorcas, D.S., Dunfield, V.A. and Scott, R.N. (1970), "Improved myo-electric control system", Med. and Biol. Engg., vol. 8, pp. 333-341.

Freund, H.-J., Dietz, V., Wita, C.W. and Kapp, H. (1973), "Discharge characteristics of single motor units in normal subjects and patients with supraspinal motor disturbances", New Devel. in Electromyography and Clin. Neurophys., vol. 3, pp. 242-250.

Friedlander, G.D. (1971), "Electricity in hospitals : elimination of lethal hazards", IEEE Spectrum, vol. 8, no. 9, pp. 40-51.

Fryer, T.B. (1970), "Implantable biotelemetry systems", NASA SP-5094, Technology Utilization Division, NASA, Washington, D.C.

Furnée, H. and Wijnschenk, M.J. (1968), "The control of artificial arms", Prosthetic Control Lab. 68-01, Delft University of Technology, Netherlands.

Garland, H., Angel, R.W. and Melen, R.D. (1972), "A state variable averaging filter for electromyogram processing", Med. and Biol. Engg., vol. 10, pp. 559-560.

Geddes, L.A., Steinberg, R. and Wise, G. (1973), "Dry electrodes and holder for electrooculography", Med. and Biol. Engg., vol. 11, pp. 69-72.

George, R. E. (1970), "The summation of muscle fibre action potentials", Med. and Biol. Engg., vol. 8, pp. 357-365.

Grimby, L. and Hannerz, J. (1968), "Recruitment order of motor units on voluntary contraction : changes induced by proprioceptive afferent activity", J. Neurol., Neurosurg., and Psychiat., vol. 31, pp. 565-573.

Henneman, E., Somjen, G. and Carpenter, D.O. (1965), "Excitability and inhibitability of motoneurons of different sizes" , J. Neurophysiology, vol. 28, pp. 599-620.

Herberts, P., Hirsch, C., Kadefors, R., Kaiser, E., Lindström, L., Magnusson, R. and Petersén, I. (1970), "Implantation of microcircuits for myoelectric control of prostheses", Proc. of First Nordic Meeting on Med. and Biol. Engg., Otaniemi, pp. 57-62.

Hirose, K. and Sobue, I. (1972), "Quantitative electromyography - a method by computer analysis", Electromyography and Clin. Neurophysiology, vol. 12, pp. 421-429.

Hogan, N. (1976), "A review of the methods of processing EMG for use as a proportional control signal", Biomedical Engineering, vol. 11, pp. 81-86.

Hollinshead, W.H. (1963), Functional Anatomy of the Limbs and Back, ed. 2, Saunders.

Horn, G.W. (1972), "Electro-control : an EMG-controlled A/K prosthesis", Med. and Biol. Engg., vol. 10, pp. 61-73.

Kadefors, R. (1970), "The voluntary EMG in prosthetics", Res. Lab. of Med. Electronics Rept. 1:70, Chalmers University of Technology, Gothenburg, Sweden.

Kadefors, R. and Olson, T. (1972), "Electrical impedance as a source of information in man-machine systems", Proc. IEEE, vol. 60, pp. 724-725.

Katz, B. (1966), Nerve, Muscle, and Synapse, McGraw-Hill.

Kreifeldt, J.G. (1971), "Signal versus noise characteristics of filtered EMG used as a control source", IEEE Trans. on Biomed. Engg., vol. BME-18, pp. 16-22.

Kreifeldt, J.G. and Yao, S. (1974), "A signal-to-noise investigation of nonlinear electromyographic processors", IEEE Trans. on Biomed. Engg., vol. BME-21, pp. 298-308.

Kwatny, E., Thomas, D.H. and Kwatny, H.G. (1970), "An application of signal processing techniques to the study of myoelectric signals", IEEE Trans. on Biomed. Engg., vol. BME-17, pp. 303-312.

Long, C. (1970), "Normal and abnormal motor control in the upper extremities", Final Report, Ampersand Research Group for Medical Engg., Case Western Reserve University, Cleveland, Ohio.

Magnusson, R. and Petersén, I. (1971), "Vocational electromyography", Proc. of Second Nordic Meeting on Med. and Biol. Engg., Oslo, pp. 174-176.

Micheelsen, V.W. (1966), Attempts to New Ways and Technical Aids for Education of the Cerebral Palsied Child, C.P.'s Publisher, Copenhagen.

Milner, M., Quanbury, A.O., Edwards, E.P. and Basmajian, J.V. (1969-1970), "Human locomotion by ordered electrostimulation of the available musculature", Lab. Tech. Reports LTR-CS-6, 11, 26, 33, National Research Council, Ottawa.

Mortimer, J.T., Magnusson, R. and Petersén, I. (1970), "Isometric contraction, muscle blood flow, and the frequency spectrum of the electromyogram", Proc. of First Nordic Meeting on Med. and Biol. Engg., Otaniemi, Finland, pp. 142-144.

NASA (1970), "Advancements in teleoperator systems", NASA SP-508, Technology Utilization Division, NASA, Washington, D.C., pp. 87.

NASA (no date), Medical Benefits from Space Research : NASA Contributions in the Field of Rehabilitation, Technology Utilization Division, NASA, Washington, D.C.

Nirenberg, L.M., Hanley, J. and Stear, E.B. (1971), "A new approach to prosthetic control : EEG motor signal tracking with an adaptively designed phase-locked loop", IEEE Trans. on Biomed. Engg., vol. BME-18, pp. 389-398.

Norris, F. H. Jr. and Gasteiger, E.L. (1955), "Action potentials of single motor units in normal muscles", Electroenceph. and Clinical Neurophysiology, vol. 7, pp. 115-126.

Ontario Crippled Children's Centre (1974), Symbol Communication Research Project - 100, 200, and 400 Vocabulary, Ontario Crippled Children's Centre, Toronto.

Parker, P.A. and Scott, R.N. (1973), "Statistics of the myoelectric signal from monopolar and bipolar electrodes", Med. and Biol. Engg., vol. 11, pp. 591-596.

Person, R.S. and Kudina, L.P. (1972), "Discharge frequency and discharge pattern of human motor units during voluntary contraction of muscle", Electroenceph. and Clin. Neurophysiol., vol. 32, pp. 471-483.

Person, R.S. and Libkind, M.S. (1970), "Simulation of electromyograms showing interference patterns", Electroenceph. and Clin. Neurophysiology, vol. 28, pp. 625-632.

Petersén, I. and Kugelberg, E. (1949), "Duration and form of action potential in the normal human muscle", J. Neurol. Neurosurg. and Psychiat., vol. 12, pp. 124-128.

Plonsey, R. (1969), Bioelectric Phenomena, Chapter 5, McGraw-Hill.

Pollak, V. (1971), "The waveshape of action potentials recorded with different types of electromyographic needles", Med. and Biol. Engg., vol. 9, pp. 657-664.

Ruch, T.C. and Patton, H.D. (1965), Physiology and Biophysics, ed. 19, Chapter 5, Saunders.

Schwartz, M. (1959), Information Transmission, Modulation, and Noise, McGraw-Hill.

Scott, R.N. (Principal Author, 1969-1971), "Myo-electric control systems, gait studies, muscle function, electrode studies", Bioengineering Institute Progress Reports 8-11, University of New Brunswick, Fredericton, N.B.

Stalberg, E. and Thiele, B. (1973), "Discharge pattern of motoneurons in humans", New Devel. in Electromyography and Clin. Neurophysiol., vol. 3, pp. 234-241.

Vodovnik, L., Long, C., Reswick, J.B., Lippay, A. and Starbuck, D. (1965), "Myoelectric control of paralyzed muscles", IEEE Trans. on Biomed. Engg., vol. BME-12, pp. 169-172.

Wani, A.M. and Guha, S.K. (1974), "Summation of fibre potentials and the EMG-force relationship during voluntary movement of a forearm", Med. and Biol. Engg., vol. 12, pp. 174-180.

# APPENDIX A

## DESCRIPTION OF THE EMG TRAINER

This appendix gives a description of the electromyographic trainer discussed in Chapter 2 and shown in Fig. 2.2. As shown by this figure, the device is separated into a processing and control module and a display module. The appendix describes each of these modules and the performance characteristics of the differential amplifier portion of the first module.

### A.1 The Processing and Control Module

The processing and control circuitry and its power supply are enclosed in a phenolic instrument case with all controls mounted either flush with the surface or on the side away from the patient as shown in Fig. 2.2. The processing and control circuits are mounted on a p.c. board and are shown in Fig. A.1. They can be conveniently separated into three functional blocks : A- the differential amplifier; B- the full-wave rectifier and averager; and C- the control circuit. The following is a description of each circuit and the power supply.

#### A Differential Amplifier

Since the skin/electrode impedance can vary from a few to tens of kilohms, depending on the electrodes, paste and skin preparation (Scott[Principal Author],1969-1971), the differential mode input impe-

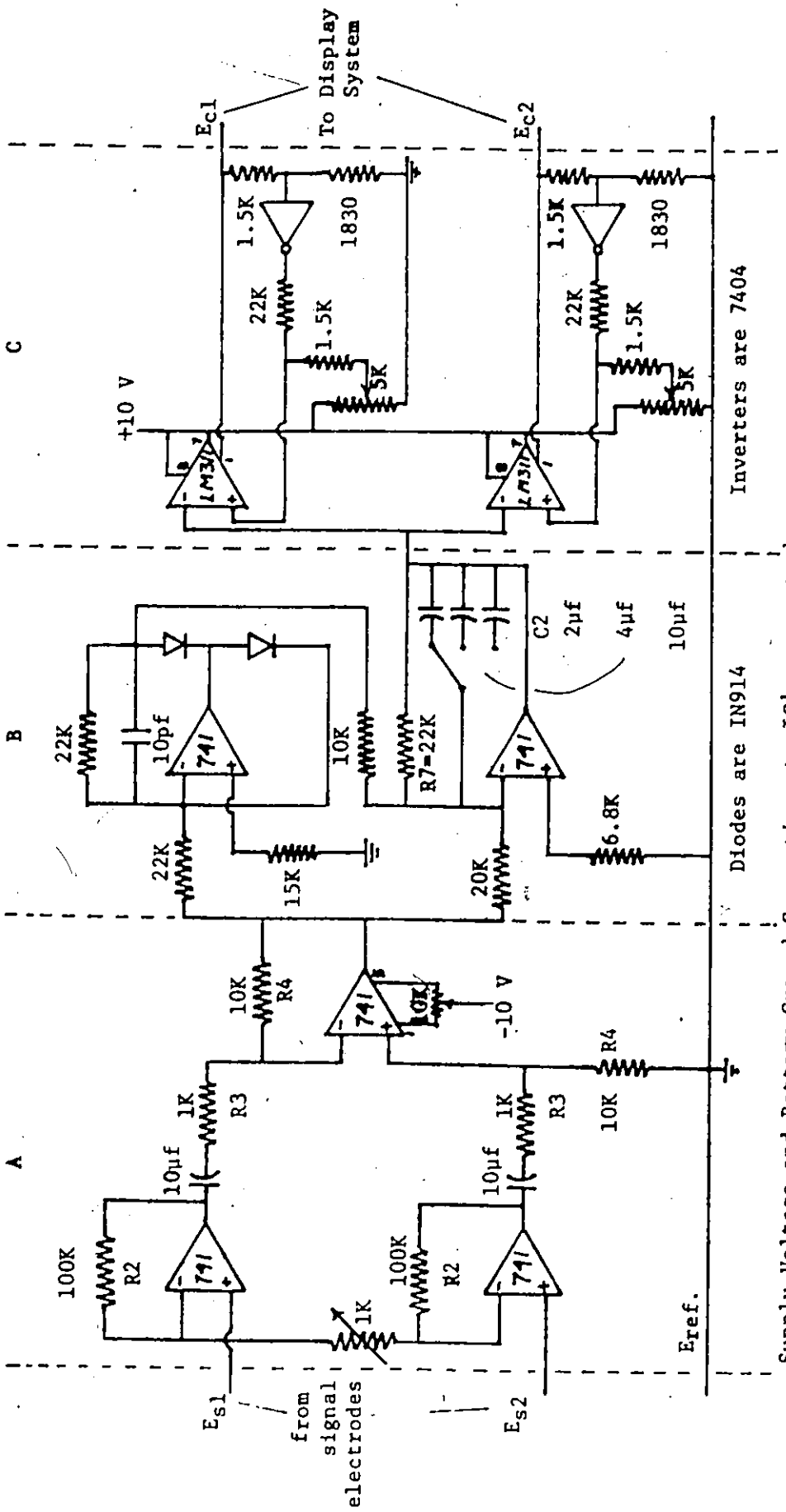


Figure A.1 Processing and Control Circuits

dance of the amplifier should be at least 100 kohm. The amplifier configuration used is a standard design which allows the electrodes to be connected directly to the high impedance (300 kohm. minimum) non-inverting inputs of the operational amplifiers. As a result of electrode interface polarization, there is a possibility of several millivolts d.c. appearing at the amplifier inputs in addition to the a.c. electromyographic signal which is usually less than 1 millivolt. However, the normal gain of the first stage (200 - 1000) is not large enough to cause this stage to saturate, and any d.c. signal component including the d.c. offset of the first stage amplifiers is decoupled by the 10μf. capacitors.

By carefully matching the feedback resistors R2 of the first stage and the ratios R4/R3 of the second stage the common mode rejection ratio (CMRR) can be maximized. The overall gain of the differential amplifier can vary from 1000 to about 10,000 and the CMRR and bandwidth as shown in Section A.3, make it suitable for EMG applications. Even though inexpensive operational amplifiers are used, this configuration has a high input impedance relative to the electrode impedances.

## B Full-Wave Rectifier and Averager

Since amplitude discrimination is used in most myo-electric controls (see Section 2.1.3), it was decided to use a rectifier followed by a low pass filter (averager) to process the amplified EMG signal. The full-wave rectifier-averager used (National Semiconductor Appn. Note LB-8) contains a precision rectifier which avoids the diode offset of a conventional half-wave diode rectifier or full-wave diode rectifier

bridge. If these simple diode rectifiers were used, the output would be zero if the EMG amplitude fell below the diode offset voltage resulting in a loss of amplitude information. This circuit, therefore, produces a better estimate of the average of the rectified signal.

The averager and rectifier gain is nominally 1 and the filter time constant given by $2\pi R7C2$ can be switch-selected to be nominally .25, .6 and 1.2 seconds. These values were determined empirically to be suitable for both normal and cerebral palsied subjects.

C Control Circuit

Since the patient had only minimal control of the biceps, it was decided that the initial training unit should employ only a three-state control system "off-low-high". We would consider it most fortunate if, after training, he could reliably control such a three-state system. The control circuit, therefore, consists of two parallel voltage threshold detectors which generate "on-off" control signals for the display system. The LM311 voltage comparators were chosen because of their high voltage and current switching capabilities, compatibility with TTL circuits, and insensitivity to supply voltage variation. Although this comparator can switch currents driving LED's or small relays, more reliable switching was achieved at the 10 V supply voltage by having it drive a switching transistor.

The threshold levels, being adjustable, can be set for the most efficient control of the device. These levels may have to be changed from day to day, depending on the amount of control exhibited by the subject.

The EMG average consists of a low-frequency ripple superimposed on a d.c. level. A hysteresis loop has therefore been added to the control circuit in order to avoid the generation of multiple "on-off" control signals caused by this ripple as the d.c. level approaches the threshold. As the EMG average increases and crosses the threshold, the comparator output turns on and the hysteresis loop causes the threshold to decrease by an offset. As the average decreases and crosses this new lower threshold, the comparator output turns off and the threshold increases again to its initial level. The amount of offset is dependent on the threshold level and increases or decreases with it. The hysteresis loop was constructed using a TTL digital inverter, rather than discrete components even though a 5 V supply is required for this IC. Since it is envisaged that a later, more complex control system will employ additional digital circuitry, this supply will be required in any case.

With the addition of a line-powered display system, isolation has to be provided between the high line voltage and the processing and control circuitry and power supply. This isolation circuitry has been mounted in the display case to avoid the presence of line voltages in the signal processing case. If these were present, a large 60 Hz interference signal would be superimposed on the amplified EMG. The output of the processing and control circuits, which control the display, are then two signals which are +10 V when "on" and 0 V when "off".

Power Supply and Battery Charger

The power supply for the processing and control circuitry is made up of 16 Nicad "AA" batteries connected in series and arranged in four groups of four to give +10, +5 and -10 volt supply voltages. These batteries were chosen because they are readily replaceable in the event of failure and their 500 mah. rating ensured continuous use of the communication device for one day without recharging. A battery charger was also designed and constructed which allows recharging of the batteries overnight without removing them from the case. This charger consists of a step-down transformer, a full-wave diode rectifier bridge and a series resistor leading to each group of 4 batteries. The battery charger plugs into the 5-pin DIN socket used for the electrodes and recharges the batteries when the power switch is in the "off" position.

## A.2 The Display Module

The display system is powered from the line voltage and is enclosed in a phenolic instrument case. The display which is shown in Fig. 2.2 consists of two 2.3 cm. diameter jewelled lights and a two-tone buzzer which are activated by the two "on-off" control signals. The buzzer can be turned off if desired.

The isolation between the display line voltage and the battery-powered processing and control circuit is provided by two sets of cascaded reed relays as shown in Fig. A.2. The $\pm$10 V battery supply voltages and the control signals are brought into the display case to drive a switching transistor and the coils of the two relays. It is felt that

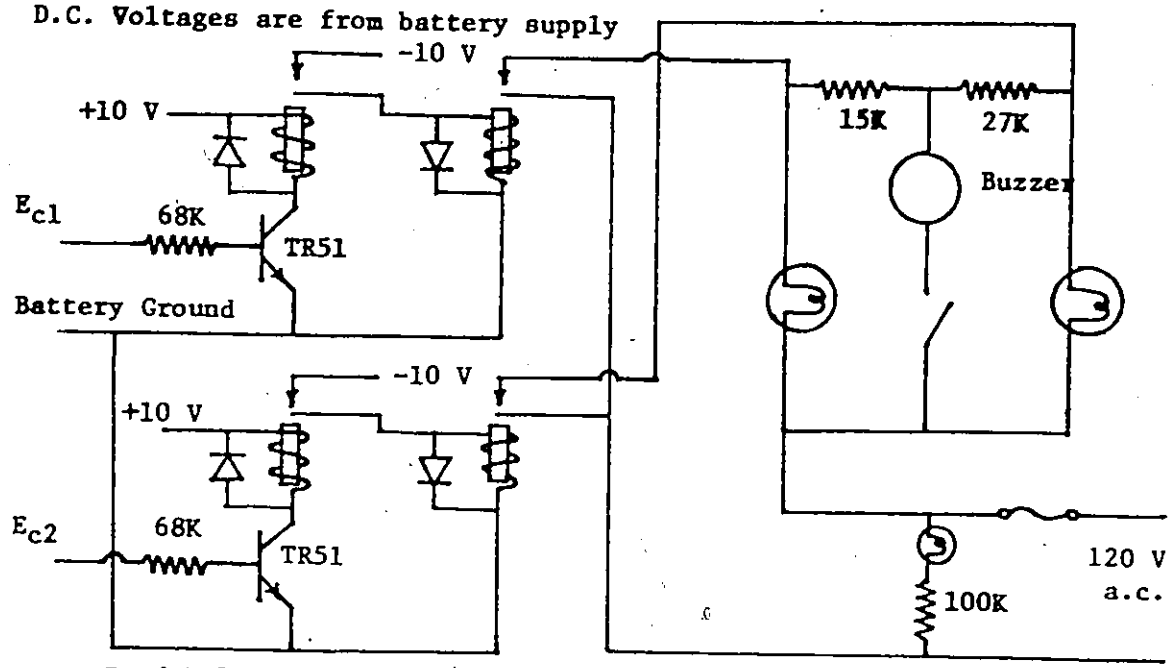


Figure A.2 Display and Isolation Circuits

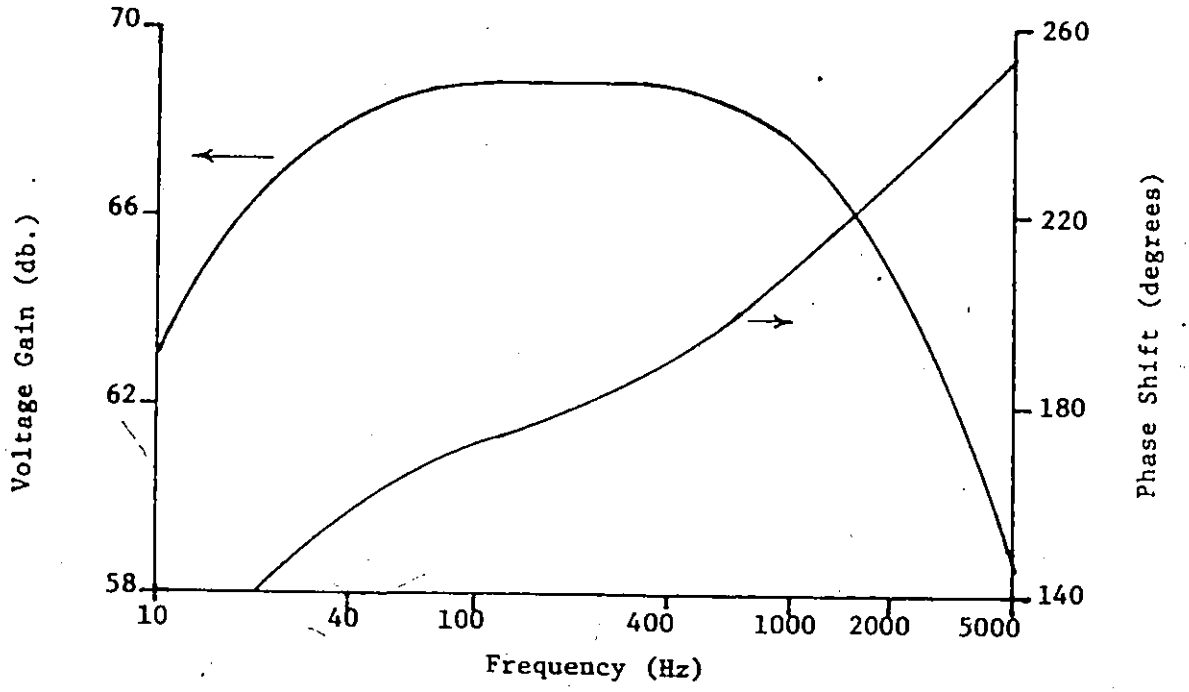


Figure A.3 Performance of the Differential Amplifier

these relays provide a reasonable margin of safety.

## A.3 Performance Characteristics of the Differential Amplifier

The trainer has been tested to determine if the performance of the differential amplifier meets the gain, bandwidth and common mode rejection requirements for surface recording of EMG signals. The bandwidth and phase shift of the differential amplifier were determined using sinusoidal inputs of .6 mV and 1.9 mV R.M.S. and a typical gain setting. The gain and phase performance of the amplifier is shown in Fig. A.3. The 3 db. pass band of the amplifier is from 18 Hz to 1600 Hz and the gain exhibits $\pm 1\%$ or .7 db. flatness in the band 29 Hz to 1100 Hz. As expected, at this gain the frequency performance of the 741 operational amplifiers is poor above 2 kHz. Since the bandwidth of surface recorded EMG is certainly less than 2 kHz, the frequency performance of the amplifier is quite adequate.

The common mode rejection ratio (CMRR) was also measured for the frequency range 20 Hz to 2 kHz and was found to be 81.3 $\pm 1.3$ db. in that range. This ratio was achieved by carefully matching the appropriate resistors as stated in Section A.1. Since 60 Hz power line interference is the main common mode signal, this rejection ratio should ensure a clean amplified EMG signal. The performance characteristics of the differential amplifier make it an adequate instrumentation amplifier for low-impedance surface electrode recorded EMG signals.

# APPENDIX B

## THE SIGNAL ACQUISITION AND ANALYSIS SYSTEM

A PDP 11/45 minicomputer operating under the DOS Monitor system was used for all EMG signal acquisition, implementation of the simulation algorithm described in Chapter 4 and analysis of real and simulated EMG signals. A hardware and software system was therefore designed and implemented by the author to accomplish these various tasks. This appendix describes the various facets of this system and the experimental set-up used to record and store the EMG signals.

### B.1 The Recording and Display of EMG Signals

Figure B.1 shows the equipment arrangement used to record and display the EMG signals. The contraction force indicator consisted of a simple 20 lb., 2-turn spring scale, which the subject activated by grasping a handle attached to a lever and flexing the forearm as shown in Fig. B.1. Although this method of force indication is inaccurate and ignores the gravitational force exerted on the forearm, it was felt that the accuracy was sufficient to indicate .45 kg. increments of muscle force. As outlined in Section 6.0, there will be considerable inaccuracy in the force-EMG correlation for the biceps brachii anyway since two muscles normally contribute to maintenance of isometric flexion of the supine forearm.

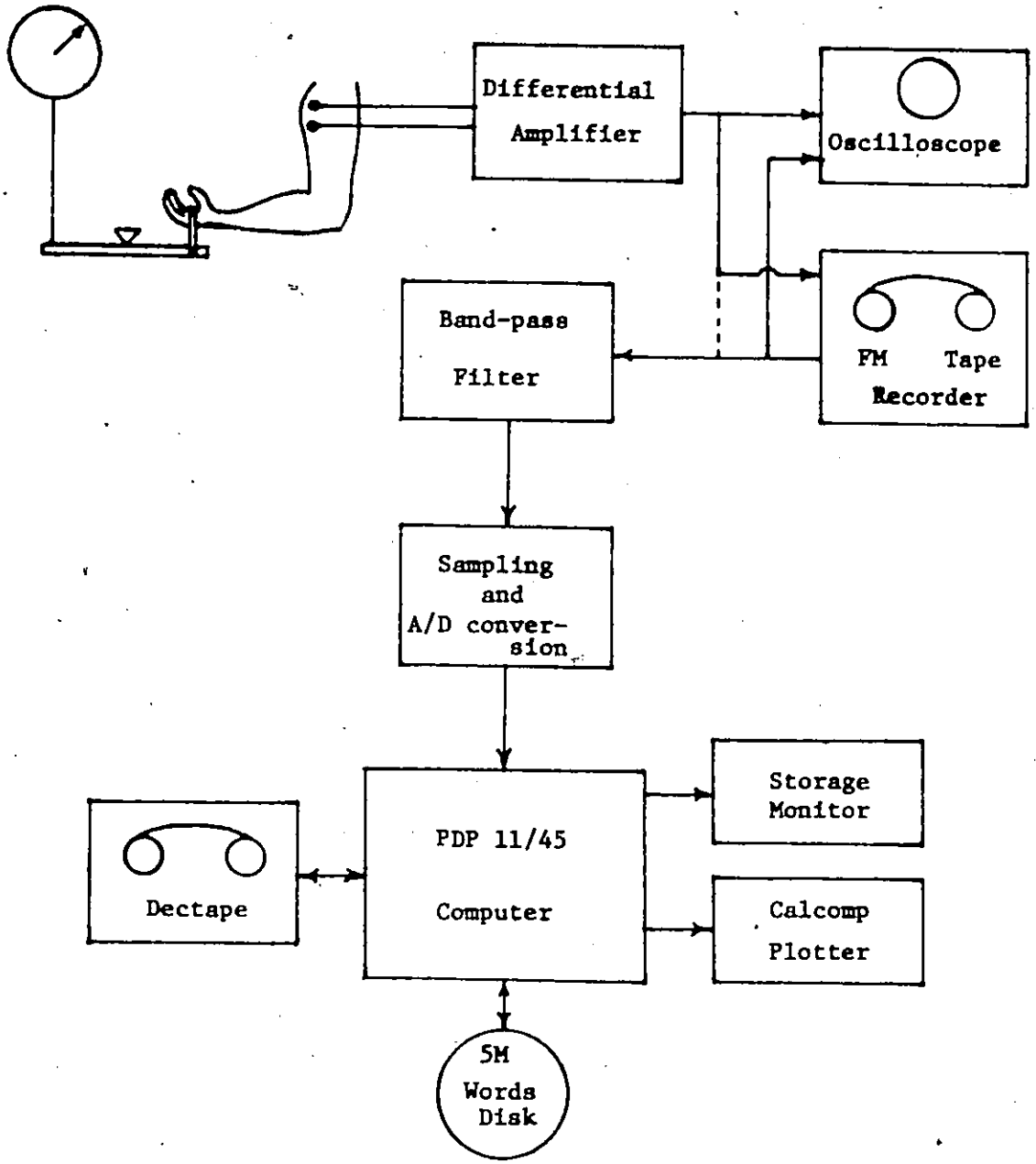


Figure B.1 EMG Signal Acquisition and Display

The EMG signals recorded using surface or needle electrodes were amplified by an a.c.-coupled Princeton Applied Research 113 differential amplifier. This amplifier incorporates a band-pass filter with 6 db./oct. roll-off whose passband was set from 3 Hz to 10 kHz to remove cable motion artifact and high frequency noise. The analog signals were stored on magnetic tape by a Hewlett Packard 3955 FM tape recorder at a speed of 15 inches per second. The signals for different force levels were then passed through a Krohn-Hite band-pass filter (24 db./oct. roll-off), sampled and digitized at the required rate by the analog to digital interface of the computer and stored on magnetic tape or disk. The passband of the filter was set from 3 Hz to one-half of the sampling frequency to avoid frequency aliasing effects. Alternatively, the FM tape recorder could be bypassed and the EMG signals directly sampled and stored by the computer. For both methods the amplifier EMG signal was monitored on an oscilloscope to detect obvious recording errors such as 60 Hz power line interference.

An assembly language data acquisition program was written which can obtain a maximum of 10 signal records (e.g. one record for each force level) of up to 10,000 samples each and store them in a file on magnetic tape or disk. After the data acquisition is complete, this program can display, under operator control, each record in 512 sample increments on a Tektronix 603 storage monitor allowing rejection of any record containing obvious errors. This program therefore also provides a facility for rapid visual examination of EMG signals. A Fortran IV program was also written which can display selected segments of each record on the storage monitor or the Calcomp incremental plotter. The data acquisition program,

which utilizes all facets of the interface described in Section B.2, can sample and store the signals at a maximum rate of 20 kHz allowing accurate visual representation even of needle recorded EMG signals.

## B.2 Signal Acquisition and Display Interface

A general signal acquisition and display interface was designed and implemented by the author to provide the necessary facilities for processing EMG signals. This interface is connected to the PDP 11/45 "unibus" through a DEC DR11-C General Device Interface which provides three addressable registers : a 16-bit read-only data register; a 16-bit read-write general register; and a 4-bit control and status register. In order to satisfy the various signal processing requirements, the interface was designed to provide the following facilities : multi-channel sampling and analog-to-digital conversion under real-time clock control, of bipolar signals; two channels of digital-to-analog conversion to provide X-Y displays on a storage monitor or output bipolar analog signals from the computer; program control of a storage monitor; and real-time clock control of program execution.

The general schematic of the interface is shown in Figure B.2. The interface has been designed so that only one program instruction is required for each of the following operations : selecting an analog channel and starting the A/D conversion; converting an "X" or "Y" digital sample and sending it to the monitor with or without intensification; reading the output of the A/D converter; and erasing or controlling storage of the monitor. In addition, the clock signal combined with the end-of-conversion signal, or the monitor erase complete signal can generate

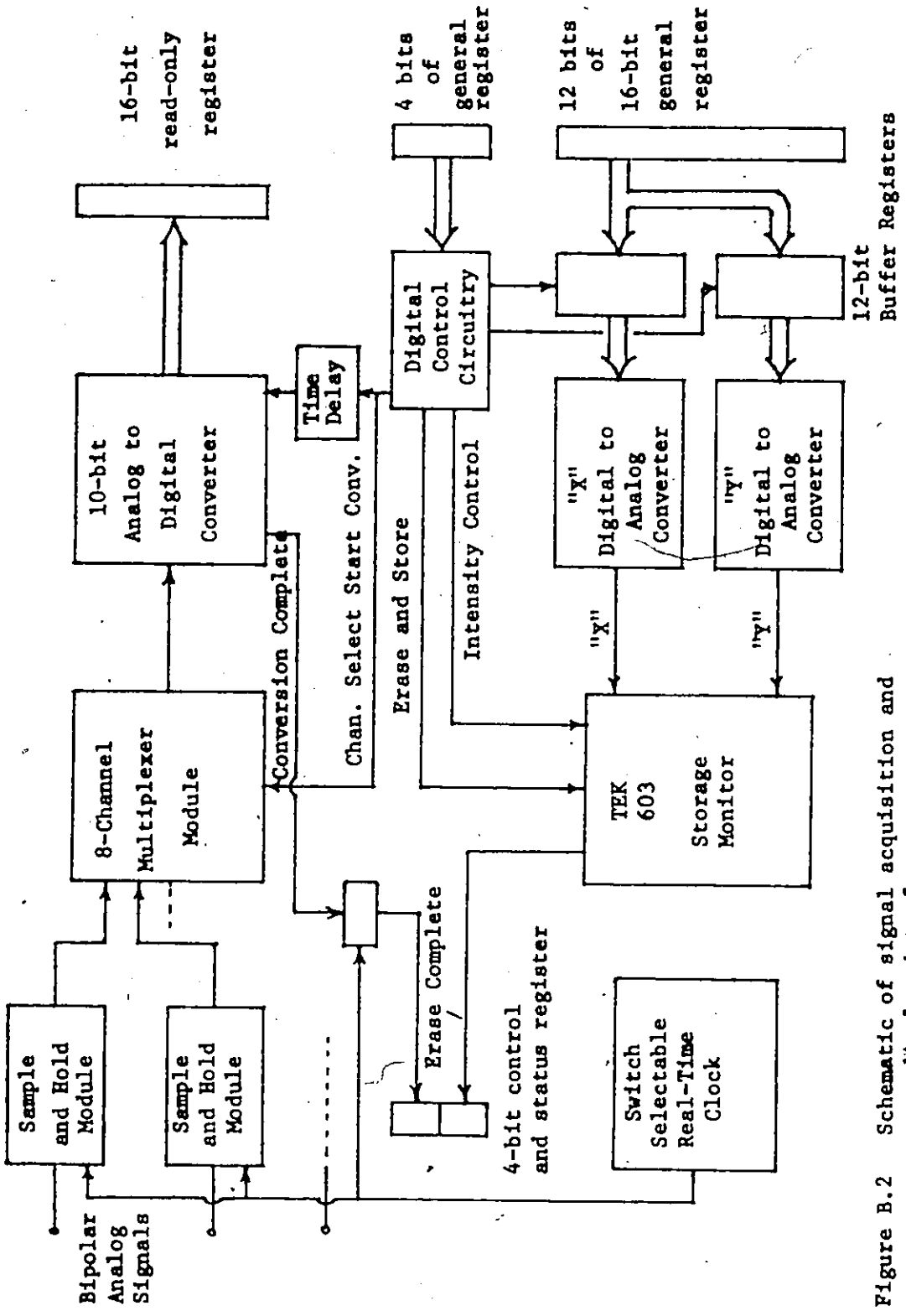


Figure B.2 Schematic of signal acquisition and display interface.

hardware interrupts allowing simultaneous data acquisition and processing of previously acquired data (e.g. for real-time control applications). The interface can consequently be easily programmed for a wide variety of signal processing and control tasks.

The following is a brief description of each of the modules of Fig. B.2.

Real-Time Clock

The real-time clock is composed of a 10 MHz crystal clock followed by seven cascaded multi-mode counters - hence allowing a range of accurate, stable frequencies. Fifteen discrete frequencies (50 kHz, 20 kHz, 10 kHz, ..., 1 Hz) are front panel switch-selectable. Since the clock signals are primarily used to control the sample and hold modules, the clock period has been chosen so that the hold-time to sample-time is in a ratio of 9 or 4 to 1 depending on the selected frequency.

Sample and Hold Module

The two sample and hold modules are Burr-Brown 12-bit compatible bipolar ($\pm$ 10 V) modules with an acquisition time of 4 μsec. This arrangement of multiple sample and holds followed by a multiplexer rather than the more common multiplexer followed by a single sample and hold arrangement allows accurate cross correlation measurements of higher frequency signals. The number of analog channels can be expanded to 8 by the addition of more sample and hold circuits.

Multiplexer

The 8-channel multiplexer is a Burr-Brown module with a settling time of 3 μsec. - hence the time delay in the start-conversion signal.

Analog to Digital Converter

The A/D converter is a 10-bit bipolar Datel module with 2's complement or 2's offset digital output and requires a conversion time of approximately 10 μsec. The digital output can be read directly as a 16-bit read-only register (the most significant bit of the A/D converter is connected to the 7 most significant bits of the data-read lines, resulting in a 2's complement 16-bit data word).

Digital to Analog Converter

The "X"-channel D/A converter is a 12-bit Analogic unipolar (+10V) module with a 3 μsec settling time. The "Y"-channel D/A converter is a 12-bit Analogic bipolar (± 10V) module with 2's complement input and a 3 μsec. settling time. The frequency response of the TEK 603 storage monitor signal channels and the storage writing characteristics are such that no time delay is required between loading a D/A converter buffer register and beam intensification.

Although the interface described above was designed specifically for EMG signal processing, its hardware characteristics allow the acquisition of signals at rates of from less than 1 Hz to 50 kHz. It can therefore function adequately as a general signal processing and display interface.

## B.3 Analysis of EMG Signals

All analysis of the simulated and real EMG signals was accomplished using the PDP 11/45 or 11/10 minicomputers. A number of Fortran IV programs were written which read the records of EMG signals, collected by the data acquisition program of Section B.1, 2500 samples at a time, processed them, and displayed the graphical results on the storage monitor or Calcomp plotter and the numerical results on a teletype or CRT interface. The simulated signals were also processed by these programs.

Due to the similarity of functions, these programs could be organized as short main programs with many common processing and display subroutines. The computation algorithms for the mean absolute value, the mean roots, and higher-order moments are very simple and were therefore included in their main program. The pattern recognition algorithm was also included as part of its main program because of the number of parameters involved and its unique application. The autocorrelation algorithm and the Fast Fourier Transform with its associated unshuffling routine were written as general Fortran IV compatible subroutines because of their complexity and wide applicability. The plotter subroutines were available from a standard software library supplied by the Digital Equipment Corp. A family of Fortran IV compatible assembly language and Fortran IV subroutines were written which can accept one or a number of floating point or integer data vectors, scale them, provide linear interpolation, and display them on the storage monitor in a choice of curves (i.e. continuous, short-dashed, long-dashed).

The autocorrelation and power spectral density functions were calculated in order to characterize the EMG signal and to determine if

consistent changes occurred in the time and frequency domain for changes in the muscle force. The autocorrelation function was therefore calculated for the full 2500 sample record. The power spectral density function was calculated for 1024 or 2048 samples of the record because of the algorithm requirement that the number of samples be a power of 2. Using less samples would lead to additional estimation errors while a consideration of more samples (i.e. 4096 for FFT) was impossible due to computer core limitations. On the other hand, the mean absolute value, mean root, higher-order moment and pattern recognition algorithms were tested as possible real-time processors. This necessitated calculating these parameters for short, discrete windows of the total record. For a 500 sample window, this would result in 5 estimates of the parameter or control function for a 2500 sample record. Whereas the autocorrelation and power spectral density programs gave one curve for each record, these programs calculated a number of estimates of the variable depending on the window length.

Each processing program was made operator-interactive through the CRT interface. Such parameters as data file, record number and length, window length, sampling frequency and muscle force, in addition to display decisions could be entered during program execution time. The large number of signal records obtained from different subjects, for a range of forces, using several sampling rates, could therefore be efficiently analyzed using this software system.